U.S. DEPARTMENT OF COMMERCE
National Technical Information Service
PB80-130222

Devolatilization Kinetics and Elemental Release in the Pyrolysis of Pulverized Coal

North Carolina State Univ at Raleigh

Prepared for

Industrial Environmental Research Lab, Research Triangle Park, NC

Nov 79

United States
Environmental Protection
Agency

Industrial Environmental Research
Laboratory
Research Triangle Park NC 27711

EPA-600/7-79-241
November 1979

PB80-130222

EPA

Devolatilization Kinetics and Elemental Release in the Pyrolysis of Pulverized Coal

Interagency Energy/Environment R&D Program Report

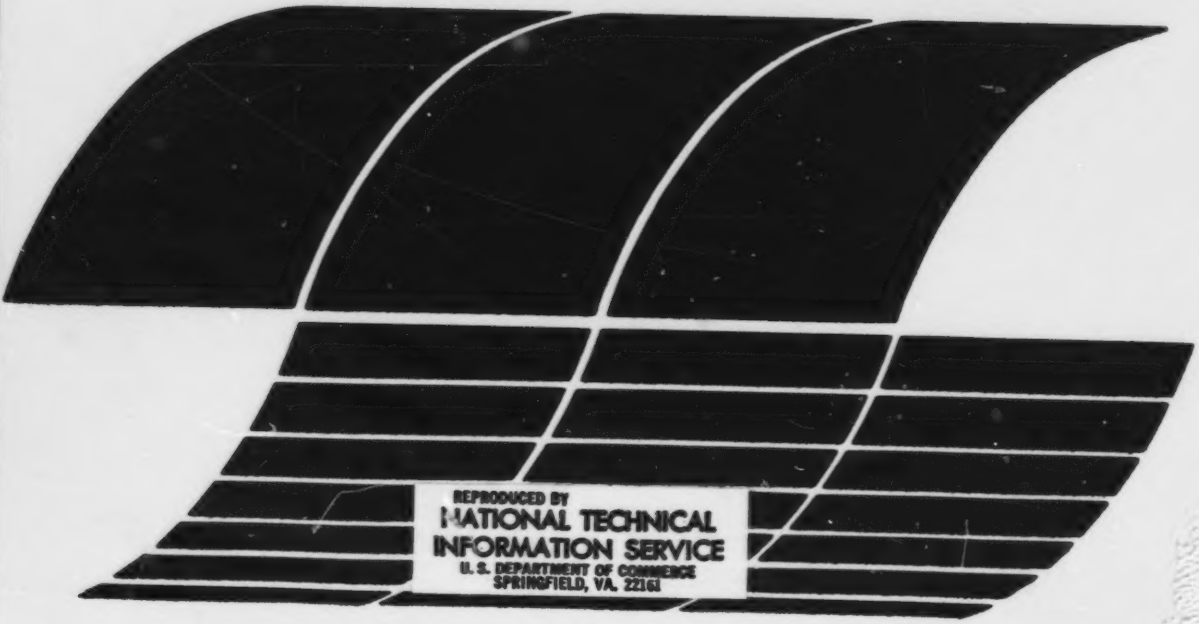

REPRODUCED BY
NATIONAL TECHNICAL
INFORMATION SERVICE
U. S. DEPARTMENT OF COMMERCE
SPRINGFIELD, VA. 22161

RESEARCH REPORTING SERIES

Research reports of the Office of Research and Development, U.S. Environmental Protection Agency, have been grouped into nine series. These nine broad categories were established to facilitate further development and application of environmental technology. Elimination of traditional grouping was consciously planned to foster technology transfer and a maximum interface in related fields. The nine series are:

1. Environmental Health Effects Research
2. Environmental Protection Technology
3. Ecological Research
4. Environmental Monitoring
5. Socioeconomic Environmental Studies
6. Scientific and Technical Assessment Reports (STAR)
7. Interagency Energy-Environment Research and Development
8. "Special" Reports
9. Miscellaneous Reports

This report has been assigned to the INTERAGENCY ENERGY-ENVIRONMENT RESEARCH AND DEVELOPMENT series. Reports in this series result from the effort funded under the 17-agency Federal Energy/Environment Research and Development Program. These studies relate to EPA's mission to protect the public health and welfare from adverse effects of pollutants associated with energy systems. The goal of the Program is to assure the rapid development of domestic energy supplies in an environmentally-compatible manner by providing the necessary environmental data and control technology. Investigations include analyses of the transport of energy-related pollutants and their health and ecological effects; assessments of, and development of, control technologies for energy systems; and integrated assessments of a wide range of energy-related environmental issues.

EPA REVIEW NOTICE

This report has been reviewed by the participating Federal Agencies, and approved for publication. Approval does not signify that the contents necessarily reflect the views and policies of the Government, nor does mention of trade names or commercial products constitute endorsement or recommendation for use.

This document is available to the public through the National Technical Information Service, Springfield, Virginia 22161.

F

TECHNICAL REPORT DATA

(Please read Instructions on the reverse before completing)

1. REPORT NO. EPA-600/7-79-241	2.	3. RECIPIENT'S ACCESSION NO. PB 80 130222
4. TITLE AND SUBTITLE Devolatilization Kinetics and Elemental Release in the Pyrolysis of Pulverized Coal		5. REPORT DATE November 1979 6. PERFORMING ORGANIZATION CODE
7. AUTHOR(S) V. H. Agreda, R. M. Felder, and J. K. Ferrell		8. PERFORMING ORGANIZATION REPORT NO.
9. PERFORMING ORGANIZATION NAME AND ADDRESS North Carolina State University Department of Chemical Engineering Raleigh, North Carolina 27650		10. PROGRAM ELEMENT NO. EHE623A 11. CONTRACT/GRANT NO. Grant R804811
12. SPONSORING AGENCY NAME AND ADDRESS EPA, Office of Research and Development Industrial Environmental Research Laboratory Research Triangle Park, NC 27711		13. TYPE OF REPORT AND PERIOD COVERED Final; 9/77 - 9/79 14. SPONSORING AGENCY CODE EPA/600/13

15. SUPPLEMENTARY NOTES IERL-RTP project officer is N. Dean Smith, Mail Drop 61, 919/541-2708.

16. ABSTRACT The report gives results of a study of the evolution of volatile matter and trace elements from pulverized coal during pyrolysis in an inert atmosphere, using batch and laminar flow furnace reactors. Five coals were used, ranging in rank from lignite to anthracite. Ash losses significantly affected calculated extents of devolatilization at any pyrolysis temperature, making the commonly used ash tracer technique a potential source of error in all experimental pyrolysis studies. Estimated weight losses can be corrected for this effect. Data on transient and equilibrium elemental release and volatile yields were obtained in a batch furnace reactor, under slow heating rates, over a wide range of temperatures and residence times. Weight losses of all coals increased significantly with temperature. Sm, Cr, Th, Sc, Fe, and Co were retained completely in the chars; As and Se showed intermediate volatility; and S, Pb, Hg, and Cl showed high volatility. An empirical mathematical model correlates the equilibrium release of Hg, Pb, As, Cl, and Se, as a function of temperature, for the five coals. The same model correlates S release data for coals with rank up to bituminous. Devolatilization kinetics data were obtained in a laminar flow reactor for two lignites and a subbituminous coal, with rapid heating, low to intermediate temperatures, rapid quenching, and 150-1500 msec residence.

17. KEY WORDS AND DOCUMENT ANALYSIS

a. DESCRIPTORS		b. IDENTIFIERS/OPEN ENDED TERMS	c. COSATI Field/Group	
Pollution	Elements	Pollution Control	13B	14B
Coal	Coal Gasification	Stationary Sources	21D	13H
Pulverized Fuels		Devolatilization		
Pyrolysis		Elemental Release	07D	
Volatility			20M	
Kinetics			20K	

18. DISTRIBUTION STATEMENT Release to Public	19. SECURITY CLASS (This Report) Unclassified	21. NO. OF PAGES 304
	20. SECURITY CLASS (This page) Unclassified	22. PRICE A14- A01

EPA Form 2220-1 (9-73)

EPA-600/7-79-241
November 1979

Devolatilization Kinetics and Elemental Release in the Pyrolysis of Pulverized Coal

by

V.H. Agreda, R.M. Felder, and J.K. Ferrell

North Carolina State University
Department of Chemical Engineering
Raleigh, North Carolina 27650

Grant No. R804811
Program Element No. EHE623A

EPA Project Officer: N. Dean Smith

Industrial Environmental Research Laboratory
Office of Environmental Engineering and Technology
Research Triangle Park, NC 27711

Prepared for

U.S. ENVIRONMENTAL PROTECTION AGENCY
Office of Research and Development
Washington, DC 20460

ia

ABSTRACT

The evolution of volatile matter and trace elements from pulverized coal during pyrolysis in an inert atmosphere has been studied in batch and laminar flow furnace reactors. Five coals were investigated, ranging in rank from lignitic to anthracitic.

It was determined that at any pyrolysis temperature ash losses may have a significant effect on calculated extents of devolatilization, making the commonly used ash tracer technique a potential source of error in all experimental pyrolysis studies. A technique to correct estimated weight losses for this effect has been developed.

Data on transient and equilibrium elemental release and volatile yields were obtained in a batch furnace reactor, under slow heating rates (5-45^{0}C/sec), over a wide range of temperatures (100-1200^{0}C) and residence times (1-20 minutes). Weight losses of all coals increased significantly with temperature. Sm, Cr, Th, Sc, Fe, and Co were retained completely in the chars; As and Se showed intermediate volatility (<50% release at 1200^{0}C); and S, Pb, Hg, and Cl were found to be highly volatile (>50% release at 800^{0}C).

An empirical mathematical model has been developed to correlate the equilibrium release of Hg, Pb, Cl, As, and Se, as a function of temperature, for the five coals studied. The same model was found to correlate sulfur release data for coals with rank up to bituminous.

Data on devolatilization kinetics were obtained in a laminar flow reactor for two lignites and a subbituminous coal, under rapid heating conditions (3×10^3-10^4 °C/sec), over a low to intermediate range of temperatures (300 to 900°C) and rapid quenching ($\sim10^5$ °C/sec) conditions, at residence times between 150 and 1500 msec. Weight losses of the three coals increased significantly with time and temperature and approached different final asymptotic values at different temperatures. Hg, Pb, S, As, Se, and La were found to be evolved in significant quantities in these experiments. The rate at which sulfur is released from coal was found to be directly proportional to the rate of dry ash-free weight loss under all pyrolysis conditions (including transient and equilibrium batch pyrolysis).

A minor and trace element balance was carried out around a steam oxygen coal gasification pilot plant.

TABLE OF CONTENTS

ABSTRACT ii

LIST OF FIGURES vii

LIST OF TABLES x

ACKNOWLEDGMENTS xii

1. SUMMARY 1

2. INTRODUCTION 5

- 2.1 Background 5
- 2.2 Literature Review 7
  - 2.2.1 Coal Petrography and Chemistry 7
  - 2.2.2 Coal Pyrolysis 12
  - 2.2.3 Experimental Methods and Results 15
  - 2.2.4 Pyrolysis Models 21
  - 2.2.5 Elemental Release During Gasification . . . 29
  - 2.2.6 Elemental Release During Pyrolysis 37
  - 2.2.7 Chemistry of Elemental Release During Pyrolysis 49
  - 2.2.8 Conclusions from Literature Review 53

3. DEVOLATILIZATION APPARATUS AND PROCEDURE 56

- 3.1 Selection of Apparatus 56
- 3.2 Description of Batch Reactor System 63
- 3.3 Experimental Procedure for Batch Reactor Experiments 66
- 3.4 Description of Laminar Flow Reactor System 67
  - 3.4.1 Gas Supply and Utilities Subsystem 70
  - 3.4.2 Feeder Subsystem 71
  - 3.4.3 Furnace Reactor and Gas Heaters 72
  - 3.4.4 Char Collection Apparatus 74
  - 3.4.5 Exhaust and Suction Subsystem 75
- 3.5 Experimental Procedure for Laminar Flow Reactor Experiments 76
- 3.6 Coals and Sample Preparation 77

4. DESIGN CALCULATIONS AND DATA REDUCTION EQUATIONS 83

- 4.1 Design Calculations for Batch Reactor System 83

4.2 Design Calculations for Laminar Flow Reactor 86
4.2.1 Particle Velocities and Residence Times 87
4.2.2 Heating and Cooling of the Coal Particles 96
4.3 Coal Composition and Weight Loss Variables 109
4.4 Determination of Weight Loss 113

5. ANALYSIS OF RESULTS FROM BATCH EXPERIMENTS 122

5.1 Preliminary Experiments 122
5.2 Equilibrium Batch Experiments 129
5.2.1 Analysis of Weight Loss Results 129
5.2.2 Analysis of Elemental Release Results 136

6. ANALYSIS OF RESULTS FROM LAMINAR FLOW REACTOR EXPERIMENTS 164

6.1 Weight Loss Estimation Errors 168
6.1.1 Precision and Accuracy of Weight Loss Estimations 179
6.1.2 Particle Classification Errors 182
6.1.3 Chemical and Physical Ash Losses 190
6.1.4 Mechanical Ash Losses 191
6.1.5 Tar Condensation 192
6.1.6 Effects of Coal and Gas Feed Rates and Residence Time Effect 193
6.2 Calculational Procedure for Estimation of Weight Loss 195
6.3 Modeling of Coal Pyrolysis 206
6.4 Analysis of Elemental Release Results 220

7. APPLICABILITY OF RESULTS TO A PILOT PLANT GASIFIER 248

7.1 Plant Description 248
7.2 Elemental Balances 250
7.3 Evaluation of Data 257

8. CONCLUSIONS 264

8.1 Trace and Minor Element Release 264
8.2 Volatile Yields and Kinetics of Devolatilization. . 266
8.3 Experimental Methodology 267

9. RECOMMENDATIONS 269

LITERATURE CITATIONS 272

APPENDIX: CHEMICAL ANALYSES 282

C.1 Proximate Analysis 282
C.2 Ultimate Analysis 283
C.3 Trace/Minor Element Analyses 284
    C.3.1 Neutron Activation Analysis 284
    C.3.2 Atomic Absorption Analysis 285
    C.3.3 Assessment of Trace Analyses 290

LIST OF FIGURES

2.1 Major Elements Retained In Montana Lignite Chars From Kobayashi (1976) 40

2.2 Major Elements Retained In Pittsburg Seam No. 8 Chars From Kobayashi (1976) 41

2.3 Comparison of Char Compositions from Pyrolysis and Hydro-pyrolysis of Litnite From Suuberg et al. (1978) 43

3.1 Batch Reactor System 64

3.2 Laminar Flow Reactor System 68

4.1 Temperature-Time Histories of Batch Samples . 84

5.1 Weight Loss in Transient Batch Experiments . 124

5.2 Sulfur Loss in Transient Batch Experiments . 126

5.3 Correlation Between Sulfur and A.R. Weight Loss in Transient Batch Experiments 128

5.4 A.R. Weight Loss in Equilibrium Batch Experiments 132

5.5 Weight Loss of Partially Dried Montana Lignite From Suuberg et al. (1978) 133

5.6 Comparison of D.A.F. Weight Loss Data for MRS Coal 135

5.7 Iron Mass Fraction in Batch Chars 142

5.8 Scandium Mass Fraction in Batch Chars 143

5.9 Sulfur Mass Fraction in Batch Chars 144

5.10 Lead Mass Fraction in Batch Chars 145

5.11 Mercury Mass Fraction in Batch Chars 146

5.12 Chlorine Mass Fraction in Batch Chars 147

5.13 Arsenic Retention in Batch Chars 153

5.14 Sulfur Retention in Batch Chars 154

5.15 Lead Retention in Batch Chars 155

5.16 Mercury Retention in Batch Chars 156

5.17 Comparison of Experimental Data With Sulfur Release Model 158

6.1 D.A.F. Weight Loss by Ash Tracer Method - MRS Coal 169

6.2 Mass Fractions in LFR Chars, MRS 800°C Runs 172

6.3 Mass Fractions in LFR 800°C MRS Chars - Volatile Elements 175

6.4 Mass Fractions in LFR 800° MRS Chars - Nonvolatile Elements 177

6.5 Rosin Rammier Plot of Montana Rosebud Coal 184

6.6 Ash Content of MRS Size Fractions 185

6.7 D.A.F. Weight Loss of MRS Coal 201

6.8 D.A.F. Weight Loss of NB8 Coal 202

6.9 D.A.F. Weight Loss of BZN Coal 203

6.10 D.A.F. Weight Loss of Texas Lignite From Nsakala (1976) 205

6.11 Comparison of Isothermal Models' Predictions 208

6.12 Comparison of Non-Isothermal models' Predictions 211

6.13 Comparison of LFR Asymptotic D.A.F. Weight Losses with Batch D.A.F. Weight Losses 213

6.14 Comparison of Wire-Screen and LFR Quasi-Equilibrium D.A.F. Weight Loss Data 216

6.15 Iron Mass Fraction in Chars 232

6.16 ASTM VM, C and H Retentions in MRS Chars . . 234

6.17 Lanthanum Retention in LFR Chars 235

6.18 Arsenic Retention in LFR Chars 236

6.19 Selenium Retention in LFR Chars 237

6.20 Sulfur Retention in LFR Chars 238

6.21 Lead Retention in LFR Chars 239

6.22 Mercury Retention in LFR Chars 240

7.1 Gasifier and Particulate, Condensables and Solubles (PCS) Removal System Showing Process Variable Monitoring Points 249

7.2 GO-15 Run Summary 253

LIST OF TABLES

2.1 Weight Loss During Pyrolysis (From Kuhn *et al.*, 1977) 45

2.2 Preliminary XES Data For Pyrolysis of Six Coals (From Kuhn *et al.*, 1977) 45

2.3 Results of Analysis River King (From Kuhn *et al.*, 1979) 47

2.4 Results of Analysis Crown No. 2 (From Kuhn *et al.*, 1979) 48

3.1 Coal Characterization Data 79

3.2 Elemental concentrations and Organic Affinity of Elements in The Rosebud Coal From Montana (From Fiene *et al.*, 1978) 80

5.1 Moisture and ash content of batch coals . . . 123

5.2 Equilibrium Batch Weight Loss Experiments . . 130

5.3 Significant Element - Temperature Correlations for Batch Pyrolysis 138

5.4 Equilibrium Elemental Release Model Parameters 152

5.5 Significant Element - Element Correlations - Batch Experiments 161

5.6 Significant Element - Element Correlations - Batch Experiments 162

5.7 Significant Element - Element Correlations - Batch Experiments 163

6.1 Summary of LFR Run Conditions 165

6.2 Room Temperature LFR Runs with MRS Coal . . . 186

6.3 Comparison of CY-1 to CY-2 A.R. Char Compositions 189

6.4 Weight Loss Estimates and Bounds 199

6.5 Significant Correlations in MRS - LFR Chars 223

6.6 Significant Correlations in NBB - LFR Chars 225

6.7 Significant Correlations in BZN - LFR Chars 226

6.8 Significant Element - Time Correlations at 800°C - MRS Runs 25, 27, and 29 227

6.9 Significant D.A.F. Weight Loss-Element Correlations 244

6.10 Significant Element - Element Correlations MRS Coal - LFR 800°C Runs 247

7.1 Operating Variables for GO-15 251

7.2 Summary of Solid Sample Analyses 255

7.3 Summary of Trace Element Analyses 256

7.4 Trace Element Mass Balance 258

7.5 ψ_A^+ Values in Spent Char 263

C.1 Percent Error (Instrumental) NAA in Coals . . 412

C.2 Summary of Atomic Absorption Analysis Parameters 415

ACKNOWLEDGMENTS

This report is a modified version of the Ph.D. dissertation of Dr. V. H. Agreda. The research was performed at North Carolina State University, under the direction of Professor R. M. Felder, and the dissertation was published in 1979.

The dissertation author (VHA) expresses his appreciation to all persons who have contributed advice and assistance in the research, notably the members of his advisory committee, Professors Felder, J. K. Ferrell, R. W. Rousseau, and W. L. Switzer. Special gratitude is expressed to Ms. K. Steinsberger and Mr. L. Hamel, who assisted in the chemical analyses. Finally, the author expresses his thanks to his wife, Carla, for her assistance in the preparation of the thesis, and to his son, Vic, for his patience and sacrifice during the course of this study.

1. SUMMARY

The evolution of volatile matter and minor and trace element constituents was studied for five coals under inert gas pyrolysis conditions in a batch-crucible reactor and a laminar flow reactor. The specific objectives of this project were as follows:

a. To design and build an experimental apparatus to study the devolatilization of coals at thermal equilibrium, i.e., at long residence times at a given temperature.

b. To design and build an experimental apparatus to study the kinetics of devolatilization during coal pyrolysis with high heating rates and small residence times.

c. To extend to low temperatures the study by Kobayashi (1976) of the problems involved in the use of ash as a tracer for the estimation of weight loss in laminar flow reactors.

d. To determine the rates at which total volatile matter is released (i.e., d.a.f. weight is lost) as a function of temperature and residence time during the pyrolysis of three coals.

e. To compare measured devolatilization rates with existing models of pyrolysis kinetics, and to modify the models or propose new models, as the results may dictate.

f. To determine which trace and minor elemental constituents of a given coal are evolved to a measurable extent.

g. To determine the equilibrium extent to which volatile trace and minor elements are evolved as a function of temperature.

h. To attempt the development of a mathematical model to describe the extent of elemental release at thermal equilibrium.

i. To measure and describe in a qualitative manner, the extent and rate at which minor and trace elements are evolved as a function of temperature and residence time during pyrolysis.

j. To carry out a trace element balance around a steam-oxygen coal gasification pilot plant, and to use the results of the pyrolysis studies in the analysis of the elemental balance.

A batch tube furnace and a laminar flow furnace were used for the experiments. Nitrogen was used as the bulk reactor gas for all the experimental runs with both reactors. Particles of only one average particle size, 41.5 microns, were pyrolyzed in the laminar flow reactor. Residence times in the batch reactor ranged up to 20 minutes, and reaction times in the laminar flow reactor ranged from 170 to 1500 msec. Temperatures ranged from 300 to 1200°C in the batch reactor and from 300 to 900°C in the laminar flow reactor. The following results and conclusions were reached:

a. Volatile material yields and devolatilization rates agreed reasonably well with those found in other studies. Kobayashi's two first-order parallel reactions model has been found to predict fast pyrolysis dry ash-free weight loss reasonably well in the 300 to 900°C temperature range.

b. It was determined that at any pyrolysis temperature ash losses may have a significant effect on calculated extents of devolatilization, making the commonly used ash tracer technique a potential source of error in all experimental pyrolysis studies. A technique to correct estimated weight losses for this effect has been developed.

c. Equilibrium yields of volatile matter and volatile trace elements generally increase with temperature. Sm, Cr, Th, Sc, Fe, and Co are retained completely in the chars up to 1200°C. As and Se exhibit intermediate volatility (<50% release at 1200°C), and S, Pb, Hg, and Cl are highly volatile (>50% release at 800°C).

d. The rate at which sulfur is released from coal is directly proportional to the rate of dry ash-free weight loss under all pyrolysis conditions studied.

e. Hg, Pb, S, As , Se, and La are evolved in significant quantities during fast pyrolysis.

f. There appear to be three modes of trace-minor element release from coal during pyrolysis in an inert gas: some elements (e.g., sulfur) are released together with the volatile matter; others appear to be released with the ash (e.g., Sm); and a third group of elements appear to be released at a much faster rate than either volatile matter or ash (e.g., Hg).

g. Several pyrolysis models, including a first-order model featuring temperature dependent asymptotic weight loss, were tested and found to provide reasonable correlations of the experimental data.

h. An empirical mathematical model has been developed to correlate the release of Hg, Pb, Cl, As, and Se, as a function of temperature, for coals ranging in rank from lignitic to anthracitic. The same model was found to correlate sulfur release data for coals with rank up to bituminous.

i. A minor and trace element balance was carried out around a steam-oxygen coal gasification pilot plant. The pyrolysis studies proved useful in analyzing the results of the mass balance, and they may be more useful when the plant is operated with New Mexico No. 8 coal instead of Western Kentucky No. 11 chemical grade coke.

2. INTRODUCTION

2.1 Background

The main approaches to the conversion of coal to gaseous fuels are steam-oxidant coal gasification, hydrocarbonization of coals, and coal pyrolysis. In all three processes, coal devolatilization or pyrolysis plays an important role. When coal is heated in any atmosphere it begins to release volatile products as the temperature and/or reaction time increase. This release can be very rapid and violent when the coal is heated rapidly to high temperatures. This is the case during flash pyrolysis in entrained bed gasifiers. When coal is subjected to very high heating rates, most of the volatile matter must be released before reactant gases, if there are any, begin to enter the pores of the coal particle and start to react.

In addition to the organic gases and vapors that constitute the principal products of pyrolysis, measurable quantities of minor and trace elements present in coal are evolved. Some of these species, such as sulfur, arsenic, and mercury, pose health hazards or are catalyst poisons which render the evolved gas unsuitable for subsequent catalytic combustion or synthetic fuel production. It is difficult to measure the extent to which such pollutants are emitted as pyrolysis effluents since they are present at low concentrations, and it is even more difficult to determine the rates at which they are evolved, since the pyrolysis process is complete in times typically on the order of tens to hundreds of milliseconds, depending on the temperatures. Nevertheless, an understanding of the kinetics and thermodynamics of trace element evolution is an essential step in the development of the technology needed to control emissions of these species from coal conversion plants.

Many trace element studies have been carried out on entire plants and on particular reactors. Studies have been carried out on the occurrence and distribution of trace elements in different coals (Gluskoter *et al.*, 1977), trace element measurements at coal-fired steam plants (Lyon, 1977), and trace and minor element balances around coal gasification plants (Forney *et al.*, 1975; Gasior *et al.*, 1978). The data obtained in these studies provide a good qualitative picture of the behavior and fate of trace and minor element constituents of coal during gasification; however, they do not provide the detailed information about reactor conditions needed to model the behavior and predict the fate of those elements during coal gasification operations. Some of the problems arise because of the difficulty of obtaining representative samples during steady state operation of a coal gasifier. However, the most serious problems appear to be posed by the need to obtain representative homogeneous samples and to analyze them precisely for trace elements. No trace element balances yet attempted appear to have been closed satisfactorily.

The purpose of this research was the quantitative determination of the extent and rate of evolution of selected minor and trace elements during the pyrolysis of coal. The results have relevance to processes based on the pyrolysis of coal and indirectly to all coal gasification processes.

2.2 Literature Review

2.2.1 Coal Petrography and Chemistry

The organic material in coal is a heterogeneous mixture of organic minerals known as macerals. Fourteen maceral groups have been identified (Spackman, 1975). The three principal groups of macerals, called microlythotypes are vitrinite, exinite, and inertinite. Exinite has the highest hydrogen content, volatile matter content, and heating value of the three microlythotypes, while inertinite has the least of all three. Inertinite has the highest density and the greatest degree of aromaticity, while exinite is the lowest in both properties. Vitrinite usually exhibits chemical and physical properties between those of the other two groups. The most abundant of the three microlythotypes is vitrinite. The different microlythotypes exhibit different behavior under pyrolysis: the total yield of volatiles is usually in the order exinite > vitrinite > inertinite. No information appears to be available on the trace and minor element content of the three microlythotypes.

Coal has a highly aromatic, cross linked micromolecular network structure. The aromatic rings form clusters; the number of rings per cluster, and therefore the aromaticity, increases with increasing rank of the coal (Hirsh, 1958), ultimately approaching a fully condensed graphitic structure. The aromaticity can be as low as 40% for subbituminous coals, which contain significant amounts of polycyclic aliphatic rings. The aromatic rings are thought to be linked by hydrocarbon and O - N - S chains of widely differing bond strengths.

Coals contain varying amounts of inorganic impurities, most of which are present in the form of ash. Ash, the inorganic mineral matter in coal, comprises about 5-20% of the mass of coal. The principal minerals found in coals include kaolite, pyrite, illite, calcite, and quartz. Mineral matter is distributed in coal more or less uniformly as small inclusions of variable composition and size. Typically, the ash inclusions appear to be about 1 μm; however, they can be as small as 0.1 μm and as large as the 20 to 60 μm pyritic particles observed in x-ray scans of coal (Solomon, 1977).

Because of its organic origin and its intimate conmixture with crustal formations, coal contains a large number of elements in major, minor, and trace quantities. The organic matter in coal consists primarily of carbon, hydrogen, oxygen, nitrogen, and sulfur. Minor and trace quantities of most other elements are also found in coal. Out of 92 known non-transuranic elements, only 14 have not yet been found in coal (Loran and O'Hara, 1977).

Gluskoter *et al.* (1977) have done extensive research on the occurrence and distribution of trace elements in coal. Their results show that the geometric mean concentrations of four of the elements that they investigated are greater by a factor of six or more than the geometric mean concentration of those elements in the earth's crust (Clarke values of the elements). Boron, chlorine, and selenium are enriched in coals of the Illinois Basin; arsenic, chlorine, and selenium are enriched in eastern coals; and selenium is the only element enriched in western coals. A larger number of elements are depleted in coals; that is, they are present at less than one-sixth of the Clarke value. The elements depleted in coals of the Illinois Basin are Al, Ca, Cr, F, Hf, Lu, Cu, Mg, Ma, P, Sc, Si, Sr, Ta, and Tl. All other elements were found to be within the range of one-sixth to six times the Clarke value.

Gluskoter *et al.* (1977) also reported that many elements are positively correlated with each other in coals.

The most highly correlated are Zn and Cd (correlation coefficient r = 0.94 for coals of the Illinois Basin). Chalcophile elements (As, Co, Ni, Pb, and Sb) are all mutually correlated, as are the lithophile elements (Si, Ti, Al, and K). Other significant correlations are Ca:Mn (r = 0.65) and Na:Cl (r = 0.48).

Van Krevelen and Schuyer (1957) have pointed out that virtually all of the nitrogen in coal exists as part of the organic coal substance. It is well known (Lowry, 1963) that sulfur occurs in coal in three forms: in organic combination as part of the coal substance, as pyrites or marcansite, and as sulfates. The amount of organic sulfur is normally not over 3%, but in exceptional cases it may be as much as 11%. The sulfates, mainly of calcium and iron, rarely exceed a few hundredths of a percent except in highly weathered or oxidized samples. It has been reported (Yurovskii, 1977) that in certain coals, elemental sulfur may be present in amounts up to 0.15%.

Duck and Himus (1951) concluded that most of the arsenic in coal occurs in the form of arsenopyrite. Horton and Aubrey (1950) found that phosphorus is associated with the inorganically-combined mineral matter in some coals, but the organic affinity of phosphorus seems to be rather high in other coals (Gluskoter _et_ _al_., 1977).

Goldschmidt (1935) developed the concept of organic and inorganic affinity for elements in coal. Gluskoter et al. (1977) produced an "organic affinity index" in an attempt to quantify the information presented in coal washability curves and histograms of washability data. Such curves and histograms are effective means of indicating whether the elements are associated with the organic or inorganic fractions of the coal. Values for the organic affinities of the elements were defined by normalizing the washability curves, removing from them a component that represents the contribution from the inseparable mineral matter, and then calculating the areas under the corrected curves. Values of this property range from 0.08 to 2.02 for the elements determined in the coals analyzed by Gluskoter et al. (1977). The variability in organic affinities between coals from different geographic locations is sufficiently large that a prediction of the value of organic affinity of an element in a sample is necessarily imprecise; however, it is safe to say that Ge, B, and Br generally are among the elements with the highest organic affinities, and As is among the elements with the lowest organic affinities. The organic affinities of 53 elements in several coals have been determined by Gluskoter et al. (1977).

A total separation of the mineral matter from the organic matter in coal cannot be made by gravimetric methods alone. Kuhn *et al.* (1977) have removed the mineral matter from cleaned coal by means of selective chemical dissolution in which the organic fraction of the coal was relatively unaltered. Their results show that Ge, Be, Sb, and Br have high organic association in coal; Ni, Cu, Cr, and Hg tend to be present in both organic and inorganic combination; and Zn, Cd, As, and Fe are primarily associated with coal mineral matter. It is apparent that correlation with organic sulfur is not an indicator of the organic association of other elements. Data in the same reference also imply that most of the organically bound elements are weakly bound; no more than a few parts per million can be considered an inherent part of the organic molecules.

2.2.2 Coal Pyrolysis

The pyrolysis of coal, variously termed thermal decomposition, carbonization, and devolatilization, is a chain of decomposition reactions wherein the linkages between aromatic clusters are broken and volatile decomposition products escape. Coals exhibit more or less definite decomposition temperatures, as indicated by melting and rapid evolution of volatile products, over a wide range in rank.

There are apparently five principal phases of devolatization (Suuberg *et al.*, 1978). The first occurs at very low temperatures, about 100°C, and is associated with moisture evolution. The second phase occurs between 350°C and 450°C and is associated with the evolution of a large amount of carbon dioxide and a small amount of tar. The third phase involves evolution of chemically formed water in the range 500-700°C. The only other significant product evolved in this phase is carbon dioxide. The fourth phase involves a final rapid evolution of carbon-containing species at temperatures from 700-900°C. Carbon oxides, tar, hydrogen, and hydrocarbon gases are rapidly evolved in this phase while little water is produced. The fifth phase is the high-temperature formation of carbon oxides.

Pyrolysis is extremely rapid. Equilibrium is reached in tens to hundreds of milliseconds, depending on the temperature, for most pyrolytic reactions. However, the nature of the equilibrium is complex; the process involves many parallel and series reactions with rates that vary by orders of magnitude. The study of those complex reactions is hampered by the fact that coal is not a homogeneous material; different portions (both microscopic and macroscopic) of a single coal sample exhibit widely differing chemical compositions and physical properties. In addition, samples from different portions of a mine are not identical.

Furthermore, there is a broad range of coal types, each of which decomposes in a slightly different manner. However, some useful (though sometimes contradictory) generalizations have been made.

The physical nature of coal devolatilization depends to a great extent on whether the coal is plastic or non-plastic. Plastic coals are also referred to as caking coals, since in the plastic state they are viscous liquid masses capable of coalescence and, upon resolidification, formation of a cake. The thermoplasticity of caking coals is manifested by softening, deformation, and resolidification upon heating. Plastic coals often devolatilize with the formation and eruption of bubbles, leaving a highly porous char containing entrapped bubbles. In extreme cases, the particles may swell to many times their original size, forming hollow char particles called cenospheres. The temperature limits on the region of plasticity depend on the heating rate: at low heating rates, the plastic region is typically 420 to 500°C with some variation among different coals, and at high heating rates, the plastic region extends to 2000°C or higher. The growth and escape of gas filled bubbles constitutes an important mode of volatiles transport in plastic coals.

2.2.3 Experimental Methods and Results

Variables known to be important to the pyrolysis process include coal type, composition, and source, particle size distribution, heating rate, final temperature, duration of heating, type and duration of the quenching process, and composition and pressure of the ambient gas.

Virtually all experimenters have relied upon the collection and analysis of quenched samples of the gas and/or char from a pyrolysis experiment. Measurements relevant to pulverized-coal pyrolysis have been obtained from four types of experiments.

In the first type of experiment, the coal dust is placed inside a crucible in a furnace and heated, and an inert gas flows past the crucible, sweeping the devolatilization products. Low heating rates and high residence times are obtained in this type of experiment. The largest uncertainty in the experiment is that the crucible must be heated first, thus giving rise to an unknown lag time and temperature difference.

In the second experiment type, the coal dust is embedded in the pores of a wire screen that is heated electrically. Heating rate, final temperature, and ambient atmosphere can be controlled and are not dependent on the pyrolysis process in this case. This approach is subject to the same problems as the first type.

The third type of experiment involves injecting the coal particles into a preheated gas. Thus, the ambient atmosphere, final temperature, and coal dust concentration are controlled. However, the heating rate of the particles is not known precisely because it is dependent on the ambient conditions experienced by the particle and the mixing of the carrier and main stream gas flows.

In the fourth type of experiment, coal dust is burned in a flame. The principal disadvantage of this experiment is that the only independent variables are those of the feed stream. Heating rate, final temperature, and ambient atmosphere are then all determined by the resultant flame; the reaction time is not known with any certainty because the reactions cannot be quenched simply by cooling.

Crucible experiments are usually carried out for the slow heating of coal (10-600°C/sec). Typically, this process is characterized by long residence times (minutes to hours) of the solids in the reactor zone. Experimental and theoretical studies of slow coal pyrolysis have focused on the plastic behavior of coals, optimization of coke yields, evolution of volatiles, mechanisms of primary decomposition, and, more recently, trace element studies.

Van Krevelen et al. (1961) observed two different stages of devolatilization undergone by coals being heated at 2°C/min: primary reactions which took place between 400 to 500°C, producing primarily tar, and secondary reactions (above 500°C) producing gases rich in hydrogen. Van Krevelen concluded that the two stages are governed by the amounts of aliphatic and aromatic hydrogen in coal. The primary devolatilization is a depolymerization process in which aliphatic bridges are ruptured with simultaneous transmission of hydrogen (disproportionation). The structural units to which this hydrogen is transmitted evaporate as tar, or recondense and yield semi-coke. The formation of tar terminates completely when the original aliphatic hydrogen atoms in the reaction mixture have been used up. Reactive oxygen groups such as OH groups, which are richer in low rank coals, decrease tar yield by consuming available hydrogen through dehydration, thus promoting condensation of aromatic nuclei. Low tar yields of high rank coals are explained in terms of the structural units being too large to evaporate.

Nsakala (1976) found that weight loss during batch pyrolysis decreased with increasing coal weight (i.e., increasing bed depth) for the pyrolysis of an HVA Ohio #5 coal. Kobayashi (1976) found the same effect (although to a fairly small extent) for an HVA Pittsburgh seam bituminous coal; however, he also found no bed depth effect for a Montana lignite. Therefore, it appears that the effect of bed depth decreases with decreasing coal rank.

The mechanism of rapid devolatilization in a dispersed phase was first investigated by Chukhanov (1952), and Shapatina *et al.* (1960). Augmentation of volatile yield under rapid heating conditions (greater than 10^3°C/sec) has been observed by different researchers using various experimental techniques. These include entrained flow reactors (Nsakala, 1976; Kobayashi, 1976; Coates *et al.*, 1974; Stickler *et al.*, 1974; Badzioch and Hawksley, 1970; Kimber and Gray, 1967; Eddinger *et al.*, 1966) and electrical screen heating (Suuberg *et al.* ,1978; Menster *et al.*, 1974; Anthony *et al.*, 1974; Loison and Chaubin, 1964).

At high heating rates (1,000 - 50,000°C/sec), such as those typically attained in continuous fluidized bed and entrained bed gasifiers, the yield of volatiles at a given temperature and the tar-to-gas ratio of the product are larger than at low to moderate heating rates (1-200°C/sec). This effect decreases with decreasing coal rank (Badzioch and Hawksley, 1970), becoming relatively small in the case of a lignite (Kobayashi, 1976). Furthermore, Kobayashi (1976) found that, for a bituminous coal and a lignite, little increases in volatile yields (above the ASTM volatile matter yield) could be expected by increasing the heating rate to peak temperatures below 1000°K.

Many different explanations have been given for the higher volatile yields from higher rank coals. However since only lower rank coals are used during the fast pyrolysis experiments in this study, the reader is referred to Kobayashi (1976) for a thorough review of the different proposed explanations, including his own which was based on his experimental results with crucible, free fall, and laminar flow reactors. In all cases, it was assumed that the ultimate volatile matter yield would be that measured during fast pyrolysis plus the ASTM volatile matter found in the chars. This implies a very fast set of reactions during fast pyrolysis and a much slower second set during the ASTM test. Typically, the residual volatiles in the char, as determined by proximate analysis, decrease exponentially with residence time in the reactor. The rate of pyrolysis is less at lower temperatures and heating rates, while the amount of residual volatiles decreases with increasing reactor temperature. As indicated above, both the rates of pyrolysis and the amount of residual volatiles also depend on coal type.

Anthony's (1974) results with coal particles suspended in a wiregrid show no discernable effect of heating rate on the volatile yield for a lignite, and only a 2% increase in volatile yield for bituminous coal, when the heating rate was increased from 600 to 10,000°C/sec for a final temperature of 1000°C. However, Kobayashi (1976) showed that the heating rates covered by Anthony were below the critical rates for the coals used, and so were in the range where little heating rate effect would be expected. An excellent discussion of the estimation and applicability of critical heating rates is given in Kobayashi (1976). For the purpose of this discussion, suffice it to say that if the characteristic heating time is much shorter than the characteristic reaction time during the heating period, only a small amount of reaction occurs during this period and the rest proceeds isothermally at the final temperature. Changes in heating rates in this range, therefore, should not make large differences in the devolatilization behavior.

It is generally agreed that rapid heating influences not only the amount of volatiles generated but also the product composition. The product distribution is a strong function of both the final reaction temperature and the heating rate. Depending on the reaction conditions, the volatiles may emerge as tars, repolymerize and deposit on the char, or crack to form low molecular weight hydrocarbons.

Anthony (1974) reported that a lower ambient pressure favors the liberation of a greater mass of volatiles for a Pittsburgh seam bituminous coal. He observed no effect of pressure for Montana lignite.

The effect of particle size on volatile yield and product distribution is unclear, as many contradictory results have been obtained by different researchers. Badzioch and Hawksley (1970) and several other researchers found no particle size effect, while Anthony *et al*. (1975) and others did find an effect, albeit a small one up to particle sizes of 1000 μm (Anthony *et al*., 1976). Nsakala (1976) found a very strong size effect between coal size fractions with average diameters of 64 μm, 86 μm, and 179 μm. However, the excellent theoretical analysis of that same data by Reidelbach and Algermissen (1978) shows that the results are due simply to the difference in heating rates between small and large particles.

2.2.4 Pyrolysis Models

The simplest and most commonly used model for correlating the kinetics of devolatilization entails treating coal pyrolysis as an equilibrium-limited first-order reaction occurring uniformly throughout the particle. The rate law is usually expressed as

$$\frac{dV}{dt} = Be^{-E/RT}(V_\infty - V) \qquad (2\text{-}1)$$

where

V = volatiles lost from the particle up to time t, expressed as a fraction or percentage of the original coal weight.

T = temperature

V_∞ = volatiles lost from particle up to t = ∞ (ultimate yield), approximated by extrapolation of measurements at long reaction times, expressed as a fraction or percentage of the original coal weight.

t = time

B = frequency factor

E = activation energy

The determination of the unknown parameters B, E, and V_∞ has been the focus of most kinetic studies. Discrepancies of as much as several orders of magnitude in rates are evident from the parameters obtained by different investigators, even when the same coal was studied (Kobayashi, 1976). Some of the discrepancies may be attributed to the differences in the structure of coal and physical factors; however, the extent of the discrepancies appears to be too large to be explained solely by these factors. It appears evident that the parameters obtained by different investigators are strongly dependent on the experimental apparatus employed and the manner in which the data were analyzed.

Kobayashi (1976) showed that differences between one bituminous coal and another can cause one to two orders of magnitude difference in the rates of devolatilization, and rate differences as large as four orders of magnitude may be observed if the coals differ widely in rank. Kobayashi also found that rates measured in a laminar flow experiment (reaction time 0-200 msec) were about one to two orders of magnitude larger than those in free fall experiments (reaction times of 1 sec to 10 min). He concluded from these observations that differences in the data reduction can cause as much as two orders of magnitude difference in the rates.

Many kinetic models have been tried, besides the simple single first-order scheme, ranging from series reaction schemes to complex series-parallel competing mechanisms, transport process-controlled reaction schemes, and empirically developed models. The most successful models developed to date are the empirical model of Badzioch and Kawksley (1970), the two first-order competing reactions model of Kobayashi (1972), the infinite parallel first-order reactions model of Anthony *et al*. (1976), and the ten reactions model of Reidelbach and Summerfield (1975 Badzioch and Hawksley (1970) used the following equations to correlate their data:

$$\Delta W^{*} = Q\ VM_{o}^{*}\ (1-C)\ (1-\exp\ \{-A|\exp(-B/T)|t_{I}\}) \qquad (2\text{-}2)$$

$$C = \exp\ [-K_{1}\ (T-K_{2})] \qquad (2\text{-}3)$$

where

VM_o = proximate volatile matter of coal

t_I = isothermal reaction time

Q, A, B, K_1, K_2 = empirically determined constants.

This model was also used by Nsakala (1976). In both cases, the model was used to correlate data from laminar flow reactors assuming isothermal reaction conditions. Excellent fit of high dry-ash-free (d.a.f.) weight loss data between 750 and 1000°C was obtained. However, Horton (1979) indicated that this model lacks the flexibility required to describe much of the experimental data available, and may even be inadequate to describe nonisothermal pyrolysis. Kobayashi (1972) proposed -- and later used successfully (1976) -- a model consisting of the following pair of parallel, first-order, irreversible reactions,

$$\begin{tikzcd} & \alpha_1 V_1 + (1-\alpha_1) R_1 \\ C \arrow[ur, "K1"] \arrow[dr, "K2"'] & \\ & \alpha_2 V_2 + (1-\alpha_2) R_2 \end{tikzcd} \tag{2-4}$$

where

α_1, α_2 = mass stoichiometric coefficients

V_1, V_2 = volatile yields

R_1, R_2 = char yields

K_1 and K_2 denote Arrhenius rate constants.

$$K_1 = B_1 e^{-E_1/RT} \tag{2-5}$$

$$K_2 = B_2 e^{-E_2/RT} \tag{2-6}$$

By assumption, $E_1 < E_2$.

At relatively low temperatures, the first reaction is assumed to be dominant, leading to an asymptotic volatile yield of α_1. At high temperatures the second reaction becomes faster than the first one, resulting in larger volatile yields. The rate equations are:

$$\frac{dC^*}{dt} = (K_1 + K_2)C^* \tag{2-7}$$

and

$$\frac{dV^*}{dt} = \frac{(dV_1^* + dV_2^*)}{C_o^*} \tag{2-8}$$

where

C^* = dry-ash-free mass of coal

V^* = dry-ash-free mass of volatiles

C_o^* = original d.a.f. mass of coal

Integration of equation (2-8) results in the following expression for the overall fraction d.a.f. weight loss, ΔW^*:

$$\Delta W^* = \frac{V_1^* + V_2^*}{C_o^*} = \int_o^t (\alpha_1 K_1 + \alpha_2 K_2) e^{-\int_o^t (K_1+K_2)dt} dt \tag{2-9}$$

where C_o^* = original d.a.f. mass of coal.

Under isothermal conditions, equation (2-9) can be integrated to give,

$$\Delta W^* = \frac{\alpha_1 K_1 + \alpha_2 K_2}{K_1 + K_2} \left(1 - e^{-(K_1 + K_2)t}\right) \quad . \qquad (2\text{-}10)$$

The asymptotic value of ΔW^* under isothermal conditions is given by

$$\Delta W^*_\infty = \frac{\alpha_1 K_1 + \alpha_2 K_2}{K_1 + K_2} \quad . \qquad (2\text{-}11)$$

This equation shows that the asymptotic weight loss is a weighted average of α_1 and α_2, the asymptotic values of weight loss at low and high temperatures, respectively. Hence, a value $\alpha_2=1$ may be assigned as complete weight loss is expected at extremely high temperatures, while α_1 may be approximated by the ASTM volatile matter or by a characteristic volatile yield at temperatures low enough for the second reaction to be considered negligible.

Kobayashi (1976) integrated equation (2-9) numerically using a simple empirical model to calculate the temperature rise of the coal particles. He obtained excellent correlations of data for a bituminous coal and a lignite in the temperature range between 1000°K and 2100°K, using the same parameters for both coals. The model is conceptually sound in that the variation in volatiles yield with temperature is explained by a second reaction rather than by a correlating parameter. One of the advantages of the model is that the competing reactions reduce to a single reaction when the second reaction is much slower than the first one, so that kinetic parameters obtained at relatively low temperatures could be utilized for the first reaction.

Perhaps the best approach developed to date for the modeling of the pyrolysis reactions of coal is based on the assumption of a large number of parallel decomposition reactions. The appearance of product i is modeled as a reaction first-order in the amount of i yet to be produced;

$$C \longrightarrow V_i + R \qquad (2\text{-}12)$$

$$\frac{dV_i}{dt} = K_i(V_{i_\infty} - V_i) \qquad (2\text{-}13)$$

$$K_i = B_i \exp(-E_i/RT) \ . \qquad (2\text{-}14)$$

Anthony (1974) noted that the single reaction model is applicable only to a single set of experimental conditions and therefore proposed this model with a Gaussian distribution of activation energies. The model is then expressed as;

$$\frac{V_\infty^* - V^*}{V_\infty^*} = \left[\sigma(2\pi)^{\frac{1}{2}}\right]^{-1} \left\{\int_0^t \exp\left[\left(-\int_0^t K dt\right) f(E) dE\right]\right\} \qquad (2\text{-}15)$$

with

$$f(E) = \left[\sigma(2\pi)^{\frac{1}{2}}\right]^{-1} \exp\left[-(E-E_o)^2/2\sigma^2\right] \qquad (2\text{-}16)$$

$$K = Be^{-E/RT} \qquad (2\text{-}17)$$

where E_o = mean activation energy

σ = standard deviation of the activation energy distribution.

For simplicity, Anthony (1974) assumed that the K_i's differed only in activation energy; therefore, a single preexponential factor can be used.

This approach provided an excellent correlation of the data from Anthony et al. (1975); however, Kobayashi (1976) argued that estimation based on Anthony's results suggested that the single reaction model may provide as good a correlation as the multiple reaction model in the experimental range in which the latter model was applied. Moreover, Horton (1979) indicated that probably this model cannot correlate certain types of fast pyrolysis data.

Nevertheless, the statistical model provides an explanation of a number of observed phenomena. Observed values of E in the range of 10-20 kcal/mole have been erroneously attributed to diffusion control of the observed rate. It can be shown that a distribution of activation energies in the range of 30-70 kcal/mole leads to an apparent single step activation energy of 10-20 kcal/mole.

Suuber et al. (1978) determined the kinetics of many pyrolysis reactions and then used the model proposed by Anthony to fit the data, allowing the preexponential factor, B, to assume a different value for each reaction. The distribution of activation energies obtained by Suuberg et al. (1978) from product composition was similar to that obtained by Anthony et al. (1976), whose results were based on weight loss. Both studies were made on the same lignitic coal.

Reidelbach and Summerfield (1975) proposed a complex reaction mechanism whereby a set of ten reactions was used to describe the process of pyrolysis. The model was later refined by Reidelbach and Algermissen (1976). As yet, only limited comparison has been made between this model and experimental data, but the results have been favorable. This is to be expected since the model also contains the reaction steps of Kobayashi's (1975) two parallel reactions model, which by itself quite successfully correlates much experimental data. Because of its complexity, only the first five reactions have usually been used (Reidelbach and Algermissen, 1978).

2.2.5 Elemental Release During Gasification

Many elemental mass balances have been made around production and pilot coal gasification plants. There appears to be no difficulty in closing major element balances: recoveries better than 95% are common for C, H, N, S, and O. Trace and minor element balances appear to be quite difficult to close, however, recoveries range from 4% (usually for Hg) to 1000%.

Trace element balances around the Synthane Process Development Unit (PDU) gasifier (Forney et al. 1975) point out the need for more precise sampling and analytical methods. Sixty-five elements were analyzed by spark source mass spectrometry in that study. The results show that the trace elements remained primarily in the chars and dusts emanating from the gasifier. Some elements, such as boron, chlorine, fluorine, and selenium were found in the water; others such as arsenic, lead, and cadmium, were in the tars. Most of the mercury appeared in the tar and water with little remaining in the char or dust.

A study on trace element disposition for the Sasol (South Africa) facility (Bennet, 1976) followed the partitioning between solid residues, liquid streams and gases. Lead, arsenic, and beryllium were found mainly in the ash, selenium and tellurium primarily in the liquid streams, fluorine two-thirds in the ash and one-third in the liquids. Mercury was found in all streams but concentrated mainly in the gas. The usual problems with data reliability were encountered; for example, 50% of the mercury could not be accounted for.

A coal hydrogasification study by Attari and Mensinger (1976) at the Institute of Gas Technology followed the concentrations of several trace elements in the feed and residue samples from the gasification of a Montana lignite and Illinois No. 6 coal. They found that the concentrations of several volatile trace elements (based on amounts fed) decreased appreciably in the residues of the different units of the process. It was also determined that under the same gasifier conditions, one coal suffered significant losses of one set of trace elements, but not of another set, while the other coal exhibited the reverse behavior. It was postulated that this behavior could be due to the chemical forms in which those elements occur in the coals studied having different tendencies to form hydrides in the reducing atmosphere of the hydrogasifier. Alternatively, it could simply be a case of different volatility of the compounds in the two coals. It was also pointed out that such behavior could be due to one of the coals having been pretreated, and therefore subjected to mild oxidation, prior to hydrogasification.

One of the better elemental balances available in the literature is that of Gasior _et_ _al_. (1978). Major, minor, and trace element balances were made for the Synthane PDU gasifier operating with Illinois No. 6 coal. A several-fold improvement in recovery and balance of a selected group of trace elements was achieved relative to the work of Forney _et_ _al_. (1975). The primary reasons for the improvement appeared to be that truly representative samples of the various solid, gas, and liquid streams were obtained, followed by meticulous care in preparing the samples to prevent contamination. Recoveries for minor elements appeared to be good except for chlorine (12% recovery). Most of the minor and trace elements were recovered in the char. However, in spite of all the sampling, sample preparation, and analysis improvements, the trace element balances were not closed satisfactorily. The worst case was, as expected, mercury for which only a 12.5% to 20% recovery was obtained. It was assumed that because of its volatility mercury leaves the process with the gas, the only stream that was not analyzed. Gasior et al. (1978) concluded that the trace element mass balances made were satisfactory within the degree of precision of the analytical methods used.

Trace element measurements at coal-fired power plants (Kaakinen, 1975; Klein, 1975) have shown that in general, the elemental constituents of coal can be divided into two groups: low volatility elements, which appear mainly in the bottom ash; and higher volatility elements, which appear in or with the fly ash. It has been shown (Lyon, 1977) that the most volatile elements, such as mercury and selenium, can actually escape in their elemental forms with the flue gas.

To summarize, environmental assessment studies on toxic elements have emphasized elemental material balances around the gasifier and quench system. For many elements, closing of the material balance is difficult since a significant fraction of the material may be part of the quenched product gas. Further, the analytical techniques often used for trace elements are not of high accuracy (Anderson _et al_., 1979). The problem is compounded by the imprecision introduced by the sampling of nonrepresentative materials, sample preservation problems, and the microscopic inhomogeneities of coal and char samples. In most cases, the trace element content of the quenched product gas is estimated by difference. Anderson _et al_. (1979) pointed out that trace element analysis in the gases is difficult because the form and approximate amounts of those elements in the gas are not known. However, as he points out, if one knew what compounds to look for and the approximate amount present, some of the analytical problems would be simplified.

The chemical reactions that C, H, and O undergo during gasification, particularly steam-oxidant gasification of coal, appear to be well understood. However, the chemistry and kinetics of N and S are less well understood, and virtually nothing is known about the chemistry and gasification kinetics of minor and trace elements.

Conversion of coal sulfur to gaseous species is thought to be a rate-limited phenomenon, generally promoted by conditions that lead to high carbon conversion. The products are principally H_2S and COS with some mercaptans and thiophenes. A study of the fate of sulfur species during the low Btu gasification of high volatile bituminous and lignite coals (Page, 1977) shows that approximately 97% of the bituminous coal sulfur was converted to H_2S and COS, while only 81% of the lignite sulfur was converted. The variation was attributed to the alkalinity of the lignite ash. The data indicate that the amount of COS formed during the gasification of coal is approximately four volume percent of the total gaseous sulfur species.

The gas-forming reactions involving sulfur are as follows (Vestal and Johnson, 1969):

$$2\ FeS + C \rightarrow 2\ Fe + CS_2 \qquad (2\text{-}18a)$$

$$CS_2 + H_2 \rightarrow CS + H_2S \qquad (2\text{-}18b)$$

$$CS_2 + CO \rightarrow CS + COS \qquad (2\text{-}18c)$$

$$CS + H_2 \rightarrow C + H_2S\ . \qquad (2\text{-}18d)$$

Vestal and Johnson (1969) present rate constants and activation energies for these and other desulfurization reactions in hydrogenous atmospheres. A study by Jensen and Austin (1977) gives plots of reaction rates vs. sulfur conversion and presents an analysis that suggests diffusion effects on the observed rates. Their work dealt with the steam gasification of coal minerals obtained from solvent refining of coal.

Stinett et al. (1974) applied the principle of thermodynamic free energy minimization to predict the effect of operating variables in fuel gasification processes on the equilibrium product gas , particularly with respect to sulfur-containing species. For steam-air (or oxygen) gasification of coal, they found that hydrogen sulfide is the predominant sulfur species. Small, but significant, amounts of carbonyl sulfide are also shown to be present.

Nitrogen is partially converted during gasification to ammonia, cyanide, and thiocyanate. Data for steam-air (or oxygen) systems (Page, 1977) show that there can be significant variation in the amount of ammonia formed during gasification of the same coal feedstock, depending on the amount of steam used to gasify the coal, the surface moisture content of the coal, and the time-temperature history of the coal particles in the gasifier. The first two parameters affect the hydrogen partial pressure inside the gasifier, which in turn directly governs the amount of NH_3 formed, and the third parameter affects the amount and characteristics of nitrogen intermediates formed in the gasifier. The average molar conversion of coal nitrogen to NH_3, is reported to be approximately 8%.

Anderson et al. (1979) performed a theoretical analysis of the formation and disposition of compounds containing As, Se, B, Pb, and Hg. Those elements were chosen because they were thought to be the elements most likely evolved from coal during gasification. This supposition agrees with the conclusions of Jahnig et al. (1975), based on low temperature gasification of Pittsburg seam coal, that the following percentages of volatile elements would be expected to devolatilize and appear in the gas cleaning section of a plant: Cl->90%; Hg->90%, Se-74%; As-65%; Pb-63%; and Cd-62%.

According to Loran and O'Hara (1977), highly volatile elements such as Be, Hg, and Pb, which do not form gaseous hydrides, condense on cooling and are likely to be removed in the aqueous condensates formed on gas cooling and/or purification. As, Sb, and Se are less volatile but can form covalent gaseous hydrides -- arsine, stibine, and hydrogen selenide. The authors point out, however, that these hydrides have stability characteristics which preclude their formation at the temperatures and pressures prevailing in some commercial gasifiers.

A serious problem may be posed by metal carbonyls formed by the reaction of carbon monoxide with free metals in the 40-300°C temperature range. Carbonyls form with all transition metals: higher pressures, of the order of 100 MPa (15,000 psi), and the presence of hydrogen favor their formation, while oxygen represses it. They decompose readily in air with half-lives estimated at 10-15 seconds for cobalt carbonyl, 10 minutes for nickel carbonyl, and a few hours for iron carbonyl.

The theoretical analysis performed by Anderson et al. (1979) suggests that the presence of arsine and its concentration in gasification process streams should be investigated further. Boric acid is projected to be the major product of boron removal from the feed coal. Volatile lead components should only exist in raw product gases from high temperature gasification processes, such as the Koppers-Totzek process. The thermodynamically preferred form of mercury in gasifier product gases has been found to be the gaseous element.

2.2.6 Elemental Release During Pyrolysis

Major, minor, and trace elements are evolved during the gasification of coal. The release is very rapid during the devolatilization stage, becoming slower later, as the coal continues to be heated or reacts with the surrounding gas. Therefore, it is important that the rate and extent to which different elements are evolved during the devolatilization of coal be determined.

Van Krevelen (1961) reported on the loss of C, H, and O during the slow pyrolysis of different coals at different total weight losses. For lignite, oxygen was more easily removed than hydrogen. For coals with carbon content around

82%, more oxygen was retained compared to hydrogen at small weight losses, but rapid loss of oxygen at the higher weight losses exceeded the hydrogen losses. For coals above 90% carbon content, relatively more oxygen was retained at all values of weight losses, which was interpreted to mean that oxygen becomes more strongly bonded as the rank increases.

Kobayashi (1976) determined the retention of C, H, N, S, and O in chars, following the pyrolysis of coal, in crucible, free fall, and laminar flow experiments, as a function of time and temperature. The retentions were calculated from the original compositions of the coals, measured overall weight losses, and the concentrations of the elements in the chars. Both rates and final losses were found to increase with temperature within the laminar flow range. The results for sulfur showed more scatter than those for the other elements. Kobayashi thought that such behavior might be due to some interactions of organic and inorganic sulfur; however, the scatter can also be explained by the fact that sulfur has the lowest concentration of the major elements in the coal, and its analysis is less precise than those of the other elements. The problem is compounded by the fact that calculation of elemental retention requires information on weight losses during the devolatilization. Therefore, the scatter in the data represents, in part, the errors associated with the weight loss measurements.

Among the elements studied by Kobayashi (1976), oxygen and hydrogen were most easily removed. Nitrogen behaved differently in the laminar flow runs: no appreciable loss was found until about 800°K, but more than 30% was retained even at the highest temperature (2200°K), which is in contrast to the results obtained for hydrogen, oxygen, and sulfur.

As shown in Figures 2-1 and 2-2, Kobayashi found that both a lignite and a bituminous coal show similar trends. At a given weight loss, more carbon, less hydrogen, and less oxygen were retained in chars from the crucible runs than in those from the laminar flow runs. Kobayashi indicated that nitrogen did not evolve measurably until about 30% weight loss, and then the retention fell rapidly to zero in the crucible runs. For the laminar flow runs, the nitrogen retentions above 50% weight loss appear to be close to those of carbon. The behavior of nitrogen suggests that most of the volatile matter up to 30% weight loss is aliphatic, since nitrogen is mainly incorporated in the heterocyclic ring structures in the original coal (Pohl, 1976), which are released in the latter stages of pyrolysis. For lignite, sulfur retentions in the crucible runs appeared to be higher on the average than those in the

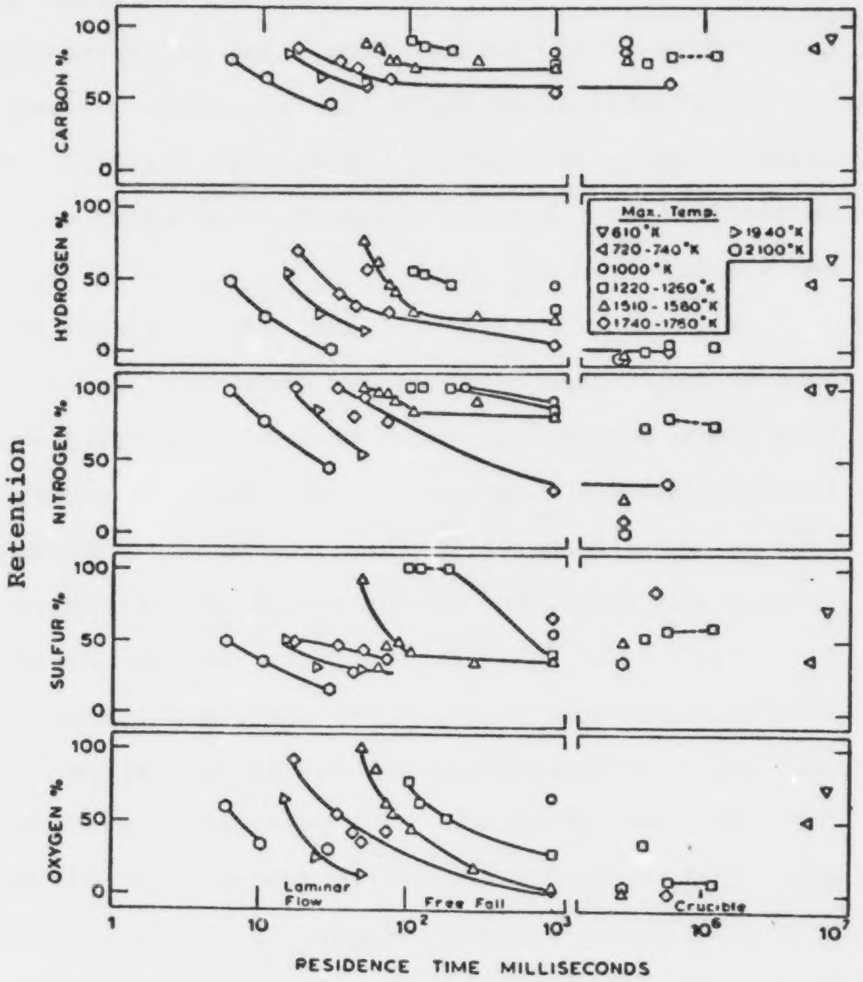

Figure 2.1 Major Elements Retained In Montana Lignite Chars From Kobayashi (1976)

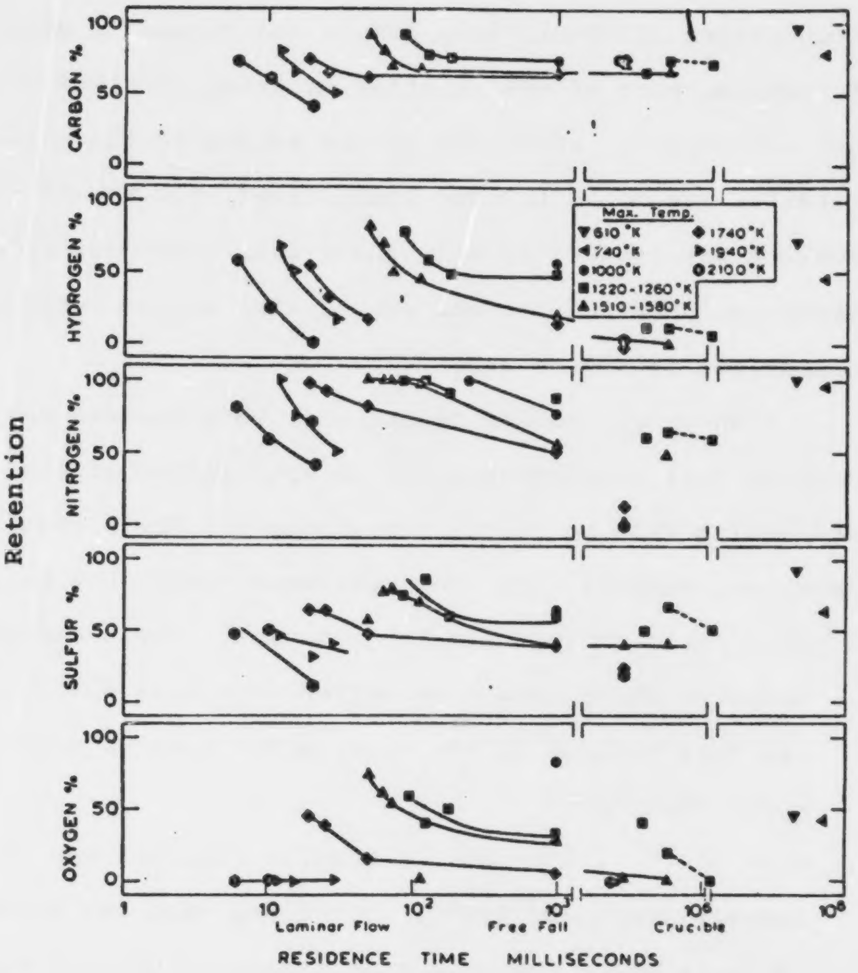

Figure 2.2 Major Elements Retained In Pittsburg Seam No. 8 Chars From Kobayashi (1976)

laminar flow runs. The opposite trend was found for bituminous coal.

Suuberg et al. (1978) found that although over 40% by weight of a lignite is volatilized at a relatively high temperature (1000°C), only 22% of the carbon is volatilized. Therefore, most of the volatile material consists of hydrogen and oxygen. About 70% of the sulfur in the solid material was found to have volatilized, but the nitrogen content was reduced by only about 25%. The data from this study, which were obtained with a wire screen furnace, are summarized in Figure 2-3.

Kuhn et al. (1977) report that both organic and inorganic coal constituents can be volatilized at low (≤250°C) and medium (250 to 650°C) temperatures. Their results from batch experiments with long residence times show that:

1. Most coals exhibit similar behavior. Coals heated in steps to 700°C show a reduction from 4.5% sulfur in the raw coal to 1.5% in the char, a 66% loss of sulfur on a whole coal basis.
2. Most of the sulfur was lost while the coal was heated between 300°C and 400°C, coinciding with the temperature range at which the coal char exhibited maximum Gieseler fluidity and minimum internal surface area. Only a small additional amount of sulfur was lost when the char was heated to 700°C.

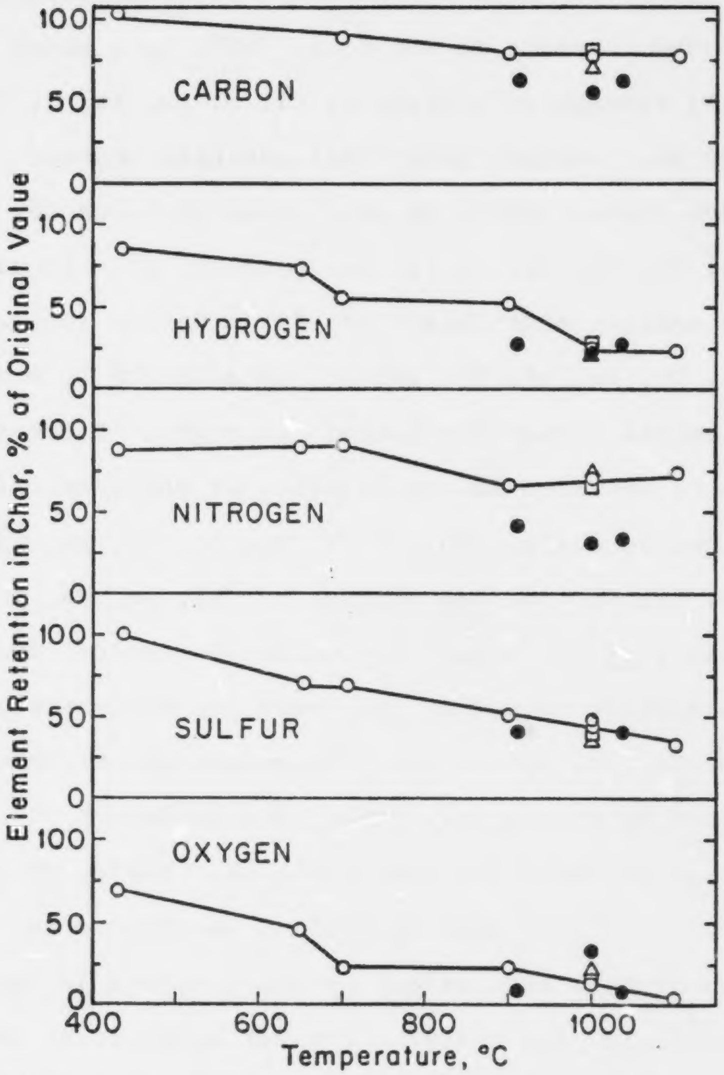

Figure 2.3 Comparison of Char Compositions from Pyrolysis and Hydropyrolysis of Lignite (o), 1 atm He, zero residence time at peak temperature; (Δ) 1 atm He, 5-20 sec. residence time; (□) 69 atm He, 5-10 sec residence time; (●) 69 atm H_2, residence time 2-30 sec. From Suuberg et al.(1978)

Shiley et al. (1978) report that elements which exhibit significant devolatilization (>30%) for bituminous coals heated in steps to 450°C and 700°C in a batch reactor under a N_2 atmosphere include P, Cl, S, As, Br, I, Pb, Se, Te, and Zn. Another group that exhibits moderate to significant losses (<30%) in some coals includes Cd, Cu, La, Li, Rb, Sb, Sm, Sr, U, Yb, and possibly Al. Lignite is reported to exhibit significant devolatilization losses of Si, K, Ti, Dy, Ga, Hf, Ni, and Sc, in addition to most of the elements listed for bituminous coals. Elements which appear to be retained in the majority of chars, except those from lignitic coals, include Si, Mg, Ca, Fe, Na, Ti, Ba, Ce, Co, Cr, Cs, Dy, Eu, Ga, Hf, Lu, Mn, Ni, Sc, Ta, Tb, Th, and V. Shiley et al. report inconclusive results, due to poor statistics caused by extremely low concentrations, for Ag, Au, In, Mo, W, and Sn. The weight and elemental losses found by Kuhn et al. (1977) and Shiley et al. (1978) are shown in Table 2-1 and Table 2-2. Shiley et al. (1978) emphasize that only volatility ranges can be given because the overall statistical errors involved in sampling, pyrolysis, and analysis reflect significant uncertainty. Percent relative standard deviation (%RSD) values for elements range from 5 to 10 in the case of minor elements to 20 to 40 for some trace elements. The %RSD includes cumulative errors due to inhomogeneous samples, poor counting

Table 2.1 Weight Loss During Pyrolysis (From Kuhn *et al*., 1977)

Sample number	Seam and State	Percentage weight loss at 450°	at 700°
C 18857	No. 6 Illinois	32.2	34.3
C 18571	No. 6 Illinois	27.5	21.5
C18571F	No. 6 Illinois	30.3	40.5
C 18440	Lignite North Dakota	33.9	44.1
C 18185	No. 5 Illinois	27.0	37.1
C 18847	Blue Creek Alaska	8.4	17.0

Table 2.2 Preliminary XES Data For Pyrolysis of Six Coals (From Kuhn *et al*., 1977)

	C-18440		C-18571		C-18571-F		C-18847		C-18857		C-18185	
Element	Raw Coal	450°C	Raw Coal	450°C[a]	Raw Coal	450°C	Raw Coal	450°C	Raw Coal	450°C	Raw Coal	450°C
Cd	2.3	2.3	3.3	1.6	1.8	0.8	1.4	0.9	1.9	0.75	7.0	7.0
In	2.6	0.72	1.7	0.10	1.9	<0.1	2.0	<0.1	0.9	<0.1	0.8	<0.1
Sn	5.0	1.0	6.9	0.18	5.1	0.8	3.9	<0.1	2.2	.68	1.4	<0.1
Sb	5.6	2.0	5.2	0.07	5.8	1.0	5.0	<0.1	1.9	<0.1	3.3	<0.1
Te	1.3	4.4	0.7	0.56	0.9	0.3	1.5	1.4	0.8	1.1	0.5	1.8
I	3.9	8.5	2.7	1.4	1.4	0.8	3.2	3.0	1.8	1.4	2.5	2.8
Cs	9.2	26.9[b]	2.7	3.8	2.9	2.0	8.6	8.4	3.3	3.3	2.4	8.9[b]
Ba	337	1205	44	48.5	34.3	35.1	202	241	51	53.8	40	302
La	8.1	10.7	8.8		6.3	4.9	13.5	13.9	10.8	8.9	4.9	8.1
Ce	8.7	13.6	9.2		9.7	7.0	20.4	24.7	10.0	11.5	8.9	12.3
Zn	3.7	14.3	84.5	48.3	21.8	18.3	13.7	12.1	35.3	45.7	323	246
Br	2.3	2.8	7.2	10.0	10.1	7.1	2.7	1.9	9.1	5.7	4.4	5.0
Rb	4.9	6.4	12.1	11.1	10.3	8.6	14.0	10.9	12.3	10.0	9.2	9.4
Sr	241.	245.1	27.5	30.4	21.7	19.6	68.2	59.3	29.8	26.4	22.0	27.5

NOTE: All values expressed as μgr/gr.

[a] Average of two determinations

[b] Interference from Ba

statistics (in neutron activation analysis), contamination, etc., for each coal or char.

Kuhn et al. (1978) and Shiley et al. (1977) used primarily energy dispersive and wavelength dispersive x-ray fluorescence, and instrumental neutron activation analysis. They carried out an extensive research effort to optimize the analytical conditions for the analysis of the coals and resulting chars to achieve the best detection sensitivity and to better quantify trace element losses.

More recently, Kuhn et al. (1979) have made a mass balance of elements mobilized during pyrolysis using the same bench scale pyrolysis system used in their earlier studies. Two coals were studied. The original coals, the chars, and the condensed volatile fraction were then sampled and analyzed by x-ray and neutron activation analyses. Each coal was pyrolyzed at 450°C and 600°C. The data thus obtained are shown in Tables 2-3 and 2-4. The actual values obtained for the materials are in one series of columns and calculated values normalizing the data to the original coal basis are presented in adjoining columns. The calculated values can then be added for each series. Kuhn et al. (1979) indicate that a mass balance within ± 20% is obtainable for many elements, a limit reported to be within the analytical methods and sampling errors for most of the elements studied.

Table 2.3 Results of Analysis River King
(From Kuhn *et al.*, 1979)

	Raw Coal	450°C Char		450°C Oil		600°C Char		600°C Oil	
		Wt= 71.5g		Wt= 13.83g		Wt= 62.2g		Wt= 12.71	
	C-20297	C-20300		C-20301		C-20321		C-20322	
Element	Actual	Actual	Calcd.	Actual	Calcd.	Actual	Calcd.	Actual	Calcd.
Fe	2.73%	2.53%	1.81%	38	5.25	2.30%	1.43%	7	0.89
K	0.20%	.28%	0.20%	5	0.69	0.25%	0.16%	8	1.02
Si	3.95%	5.76%	4.12%	LD	LD	6.33%	3.93%	LD	LD
Al	1.73%	2.39%	1.71%	LD	LD	2.65%	1.64%	LD	LD
Ca	.48%	.74%	.53%	LD	LD	1.00%	.62%	LD	LD
Ti	.11%	.09%	.06%	<2 ppm	<2 ppm	.09%	.06%	<2 ppm	<2 ppm
S	3.68%	3.40%	2.43%	2.22%	.30	2.75%	1.71%	2.61%	.33%
Cl	.03%	.01%	<.01%	37 ppm	5.1 ppm	.01%	.006%	39 ppm	5 ppm
Na	522	720	515	9	1.24	770	480	10	1.27
As	1.5	1.5	1.07	0.2	0.03	2.2	1.37	0.3	0.04
Ba	56	105	75.07	<10	<10	90	56.06	<10	<10
Br	2.0	2.5	1.79	3.2	0.44	2.2	1.37	6.0	0.76
Ce	7.0	14	10.01	<5	<5	11	6.85	<0.08	<0.08
Co	5.4	7.2	5.15	0.01	0.001	8	4.99	0.03	0.004
Cr	18	29	20.73	0.6	0.08	36	22.42	0.4	0.05
Cs	1.13	1.7	1.21	0.04	0.006	0.9	0.56	-	-
Eu	0.2	0.3	0.02	0.002	0.0003	0.3	.19	0.006	0.0008
Ga	3.2	4.6	3.29	<0.1	<0.1	5.3	3.30	0.1	0.01
Hf	0.6	1.0	0.71	<0.01	<0.01	0.8	0.50	<0.01	<0.01
La	5.0	7	5.00	0.006	0.0008	7	4.36	<0.01	<0.01
Lu	0.16	0.2	0.14	0.007	0.0009	0.12	0.075	<0.01	<0.0
Ni	14	30	21.45	<0.05	<0.5	25	15.57	<0.06	<0.6
Rb	21	27	19.3	0.2	0.05	22	13.70	<0.5	<0.5
Sb	0.30	0.3	0.21	0.1	0.014	0.5	0.31	0.5	0.06
Sc	3.0	4.2	3.00	0.002	0.0002	4.0	2.49	0.001	0.0001
Se	2.3	3.1	2.22	1.5	.21	2.5	1.56	1.7	0.22
Sm	1.0	1.4	1.00	<0.1	<.1	1.6	1.00	<0.1	<0.1
Sr	9	63	45.04	<1	<1	75	46.72	<1	<1
Ta	0.15	0.2	0.14	<0.01	<0.01	0.15	0.09	<0.01	<0.01
Tb	0.20	0.2	0.14	0.004	0.0006	0.19	0.12	<0.05	<0.05
Th	2.0	3	2.14	<0.1	<0.1	2.5	1.56	<0.1	<0.1
Yb	0.70	0.8	0.57	0.01	0.001	0.8	0.50	0.007	0.0009
Zn	32	78	55.77	2	0.28	100	62.5	2	0.25
Book No.		913-15		913-15A		913-17		913-17A	
Sn	3.0	<1.0	<1.0	2.4	.33	<1.0	<1.0	4.6	.60
I	1.6	1.5	1.1	2.0	.28	1.4	.87	2.6	.33
Zr	19.8	29	21	1.0	.14	32.2	20	2.4	.31
Mo	10.7	14.4	10.3	1.3	.18	16.3	10.1	5.3	.67

Elements at or below limit of detection in all phases for this coal
Pd, Ag, Cd, In, Te, Au, U, W. Mn, Dy, Nb, Y

Table 2.4 Results of Analysis Crown No. 2
(From Kuhn *et al.*, 1979)

	Raw Coal	450°C Char		450°C Oil		600°C Char		600°C Oil	
		Wt= 68.9g		Wt= 12.9g		Wt= 62.6g		Wt= 15.91g	
	C-20239	C-20317		C-20318		C-20319		C-20320	
Element	Actual	Actual	Calcd.	Actual	Calcd.	Actual	Calcd.	Actual	Calcd.
Fe	2.38%	3.6%	2.48%	7 ppm	0.90	3.8%	2.38%	4 ppm	0.63
K	0.17%	0.20%	0.14%	4 ppm	0.52	0.24%	0.15%	5 ppm	0.79
Si	2.43%	3.59%	2.47%	LD	LD	3.96%	2.47%	LD	LD
Al	1.62%	2.36%	1.63	LD	LD	2.53%	1.58%	LD	LD
Ca	.15%	.26%	.18%	LD	LD	.23%	.14%	LD	LD
Ti	.09%	.08%	.06%	<2 ppm	<2 ppm	.09%	.06%	<2 ppm	<2 ppm
S	3.43%	3.94%	2.71%	2.11%	.27%	3.84%	2.40%	2.48%	.39%
Cl	.07%	.02%	.01	61 ppm	8 ppm	.01%	.006%	149	24 ppm
Na	774	1000	689	6	0.77	1112	701	9	1.43
As	1.6	2.2	1.51	2	0.26	2.6	1.63	0.3	0.05
Ba	50	83	57.19	<10	<10	100	62.6	<10	<10
Br	3.6	4	2.75	6	0.77	3.1	1.94	7.2	1.14
Ce	12	14	9.64	<0.06	<0.08	14	8.76	<0.08	<0.08
Co	2.8	3.7	2.55	0.02	0.0026	4.0	2.50	0.01	0.001
Cr	13	20	13.78	1	0.129	21	13.14	0.3	0.05
Cs	1.2	1.1	0.76	-	-	1.1	0.69	-	-
Eu	0.18	0.3	0.21	0.007	0.0009	0.3	0.19	0.03	0.005
Ga	3.1	3.8	2.62	0.09	0.012	4.1	2.57	0.07	0.01
Hf	0.4	0.7	0.48	<0.1	<0.1	0.75	0.47	<0.1	<0.1
La	5.4	7	4.8	<0.1	<0.1	8.4	5.26	0.02	0.003
Lu	0.14	0.16	0.11	<0.01	<0.01	0.15	0.09	<10	<10
Ni	14.0	26	17.91	0.3	0.04	19	11.89	<0.5	<0.5
Rb	13	23	15.85	<1	<1	18	11.27	<0.5	<0.5
Sb	0.5	0.5	0.34	0.13	0.02	0.6	0.37	0.12	0.02
Sc	2.4	3.0	2.07	0.001	0.0001	3.1	1.94	0.001	0.0001
Se	2.3	2.8	1.93	1.2	0.15	2.7	1.69	1.6	0.25
Sm	1.0	1.4	0.96	0.002	0.0002	1.6	1.00	<0.01	<0.01
Sr	38	74	50.99	<1	<1	74	46.32	<1	<1
Ta	0.11	0.16	0.11	<0.01	<0.01	0.24	0.15	<0.01	<0.01
Tb	0.15	0.17	0.12	<0.01	<0.01	0.18	0.11	<0.01	<0.01
Th	1.7	2.1	1.45	<0.1	<0.01	2.1	1.31	<0.1	<0.1
Yb	0.6	0.84	0.58	0.007	0.0009	0.9	0.56	<0.01	<0.01
Zn	21	40	27.56	2	0.26	14	8.76	3	0.48
Book No.		913-14		913-14A		913-12		913-12A	
Sn	4.8	<1.0	<1.0	4.0	.51	<1.0	<1.0	4.8	.76
I	1.9	1.3	.90	2.1	.27	1.0	.63	3.2	.51
Zr	16.5	24.8	17	<1.0	<1.0	25.0	15.7	<1.0	<1.0
Mo	12.6	18.9	13.0	2.9	.37	17.7	11.1	3.7	.59

Elements at or below limit of detection in all phases for this coal
Pd, Ag, Cd, In, Te, Au, U, W, Mn, Dy, Nb, Y

2.2.7 Chemistry of Elemental Release During Pyrolysis

Relatively little information is available in the literature concerning the chemical mechanisms and kinetics of the release of sulfur and nitrogen from coal during devolatilization, and virtually no information is available on the chemical mechanisms and kinetics of the release of minor and trace elements during devolatilization.

The rates and extents of decomposition and volatilization of nitrogen compounds depend on the thermal environment of the coal particles. Low heating rates yield mainly ammonia and residual coke-nitrogen. As indicated earlier, nitrogen is evolved late in the particle heating sequence, indicating that most of the nitrogen is probably in the strongly bonded aromatic structures, and that at sufficiently high temperatures the relative yield of nitrogen exceeds the yield of total volatiles. Malte and Rees (1979) report that a rough, first-order fit of the data of Pohl and Sarofim (1977) gave a rate constant of (93×10^3) $[\exp(-11{,}400/T)]\,\text{sec}^{-1}$ for overall coal-nitrogen pyrolysis, with the reactant being the amount of the residual nitrogen. At 1500°K, this expression gives a characteristic pyrolysis time of 100 msec.

The behavior of sulfur in coal has been studied by several researchers. Kuhn _et_ _al_. (1977) report a greater loss of sulfur from the pyrite than from organic sulfur at low temperatures; whereas, the reverse was observed at temperatures above 450°C.

The dominant form of organic sulfur in the coal molecule is thought to be thiophene. Solomon (1977) indicates that as much as 60% of the organic sulfur resides in such heterocyclic rings. According to Attari et al. (1976), and sulfur side chains (-SH) and the linking sulfur chains (-S-) rupture first in the heating sequence during pulverized coal pyrolysis, leading to early volatile sulfur. The thiophene structure, however, is more stable and does not decompose until temperatures of about 1200°K are attained.

Through an x-ray scanning technique sensitive to S and Fe, Solomon (1977) was able to examine both inorganic and organic sulfur in coal char. He observed that the residual organic matter was depleted of sulfur, while the sulfur content of the inorganic ash was increased.

Padia (1976) indicated that pyrite is quite unstable at high temperatures. At 750°K, the oxidation of pyrite to hematite occurs as follows:

$$2\ FeS_2 + 5.5\ O_2 \longrightarrow Fe_2O_3 + 4\ SO_2\ . \qquad (2\text{-}19)$$

In a reducing environment, FeS_2 is transformed to FeS by the following reactions (Malte and Rees, 1979):

$$FeS_2 \longrightarrow FeS + \tfrac{1}{2} S_2 \text{ (gas)} \qquad (2\text{-}20a)$$

$$FeS \longrightarrow Fe + \tfrac{1}{2} S_2 \qquad (2\text{-}20b)$$

$$FeS_2 + H_2 \longrightarrow FeS + H_2S \qquad (2\text{-}20c)$$

$$FeS + H_2 \longrightarrow Fe + H_2S \ . \qquad (2\text{-}20d)$$

Solomon (1977) established the following experimental rate for the decomposition of FeS_2 to FeS

$$[\ell n(x-1)]/t = -480 \exp(-8400/T) \text{ sec}^{-1} \qquad (2\text{-}21)$$

where x pertains to FeS_x.

Kuhn *et al*. (1977) report that the pyrite contained in coal is converted to pyrrhotite and sulfur at 450°C or lower in a nitrogen atmosphere. Their chemical analyses also indicate a greater loss of sulfur from the pyrite than from organic sulfur at low temperatures, whereas, the reverse is true at high temperatures (>450°C).

As discussed in Section 2.2.1, minor and trace elements are present in coal in varying amounts and different degrees of association with the organic and inorganic matters of the coal. Most minor elements are generally associated with the discrete mineral matter. The principal minerals found in coals include kaolite, pyrite, illite, calcite, and quartz. Upon heat treatment of the coal to elevated temperatures, the minerals are changed chemically as described by Padia

(1976). At high enough temperatures ($>1300^{o}K$), the trace and minor elements associated with the mineral matter may be devolatilized and released from the coal, the extent of the evolution increasing with temperature.

The major form of arsenic in coal is thought to be arsenopyrite (Duck and Himus, 1951). When temperatures exceed $820^{o}K$, arsenopyrite begins to decompose into pyrrhotite (FeS) and metallic arsenic

$$\mathrm{FeAsS(s)} \xrightarrow{>820^{o}K} \mathrm{FeS(s)} + \mathrm{As(s)} \quad . \qquad (2\text{-}22)$$

The decomposition proceeds rapidly at temperatures greater than $1025^{o}K$ (Lukesh, 1940).

Anderson *et al.* (1979) suggest that selenium is initially present in coals as selenopyrite (FeSeS) which decomposes upon heating, releasing the element according to the reaction

$$\mathrm{FeSeS(s)} \xrightarrow{heat} \mathrm{FeS(s)} + \mathrm{Se(g)} \quad . \qquad (2\text{-}23)$$

Lead in coal is believed to exist initially as PbS (Anderson, 1979). However, it has been reported that lead is associated almost entirely with the organic fractions of coals. As indicated before, Horton and Aubrey (1950) found that phosphorus is associated with the inorganically combined matter in some coals, but the organic affinity of phosphorus seems to be rather high in other coals (Gluskoter et al., 1977). Anderson (1979) suggests that most of the boron in coal may be chelated. The chemical forms of mercury in coal are not known; however, evidence suggests that metallic mercury is released from coal during devolatilization.

Finally, Kuhn et al. (1977) concluded that the two most important temperatures for which volatility data need to be obtained are 450°C and 700°C. At 450°C, reactivity is highest, and most volatile products are released (over a very long period of time); at 700°C, virtually all volatile products are released but the coal structure is still intact. Heating above 750°C completely destroys the original coal structure, and the internal surface area decreases.

2.2.8 Conclusions from Literature Review

Significant progress has been made in the modeling of the pyrolysis of coal. Several models appear to provide fair correlations for weight loss as a function of time and temperature; however, much work still remains to be done to elucidate the actual mechanism of the pyrolysis reactions. Furthermore, all efforts in this direction are hampered by problems arising from the different behavior shown by different coals, inhomogeneities within a given coal, and problems in the interpretation of data obtained with different types of equipment. This last point was only discussed in the literature survey with regard to the disagreement in first-order kinetic parameters. Another extremely important problem, the interpretation of data obtained with similar equipment but with different operational assumptions, will be dealt with in the sections on the selection of experimental apparatus and design calculations.

Excellent mass balances around coal gasification plants can be made on major elements, but attempts to close mass balances on minor and trace elements are plagued with problems of irreproducibility and scatter of data. The causes of those problems are varied. They include coal and char inhomogeneity, sample contamination, low accuracy and precision of analytical techniques, and a lack of fundamental information regarding the mobility of trace elements of coal under gasification conditions.

Significant losses of major, minor, and trace elements occur during pyrolysis. It appears evident that the yield of a given element is a function of temperature. The pioneering work of Kuhn et al. (1979) has provided an excellent start to the determination of the mobility of trace elements during gasification. However, the pyrolysis data available has been obtained only in batch reactors with very long residence times, low heating rates, and at only two rather low temperatures. No studies have yet been reported in the literature on the release of trace and minor elements during fast devolatilization.

Finally, it should be pointed out that the foregoing was not an exhaustive review of the literature on coal pyrolysis, much less on coal gasification or on coal in general. Such literature is very extensive. Only information directly related to the work done in this research has been covered, and then only in summarized form. Excellent reviews and summaries of the literature on coal and coal gasification have been published by Lowry (1963), Gould (1967), and Massey (1974). The best reviews on the pyrolysis of coal are those of Kobayashi (1976), and Smoot and Pratt (1979). The subject of trace elements in fuel is reviewed by Babu (1975).

3. DEVOLATILIZATION APPARATUS AND PROCEDURE

3.1 Selection of Apparatus

Devolatilization has been shown to occur in a matter of a few hundred milliseconds at low temperatures, and within a few milliseconds at high temperatures. Therefore, it is required that the experimental apparatus be able to resolve times of this magnitude in order to observe the kinetics of devolatilization. At the same time, most coal gasification processes operate with residence times ranging from a few seconds, as in the Garret Flash Pyrolysis Process (Sass, 1974), to hours, as in fixed bed reactors. Furthermore, the analyses needed for the characterization of chars and the determination of their trace element content require reasonably large amounts of product char. Approximately 5 grams of sample are thought to be required. Even with the restrictions imposed in this research, namely, the study of the pyrolysis of pulverized coal in inert atmospheres, widely divergent requirements are evident.

A diversity of apparatus types have been used for the study of coal pyrolysis. Examples of equipment used are crucibles, retorts, different sizes of batch reactors with gas flow, differential scanning calorimeters , thermogravimetric balances, shock tubes, laser irradiation heating, wire screen furnaces, free fall reactors, and turbulent and laminar entrained flow reactors.

Most experimental techniques were ruled out for the present study because of inappropriate sample size, inadequate time resolution, or irrelevance to the conditions that are encountered in real gasification systems. It was decided that the use of a small bench scale batch reactor with gas flow and a laminar flow reactor would provide the information needed at long and short reaction times, and the required sample sizes. In addition, the laminar flow reactor provides high heating rates (10^3-10^5 °C/sec) comparable to those of entrained bed and fluidized bed commercial processes.

Small batch reactors have been used by many researchers, most recently by Kuhn _et al_. (1977, 1979). The equipment is simple and relatively easy to operate. However, the interpretation of the results may be subject to error when high rank coals are used. The volatile yields of high rank coals have been shown to be highly dependent on the heating rate and, to a lesser extent, on the bed depth in batch experiments.

The laminar flow reactor was initially developed by Sainsbury _et al_. (1966) and later used by many other researchers. Even though, in principle, this reactor is ideal for the study of coal pyrolysis, in practice its mechanical complexity makes it difficult to operate. Several parameters cannot be measured directly. Therefore, the reduction of the data has to be based on a mathematical model of the fluid and particle flow and heat transfer phenomena in the reactor.

Among the mechanical and physical problems and limitations of this type of reactor, the most important are the following:

1. Quantitative collection of the char is very difficult. A significant fraction of the char tends to miss water-cooled collectors, and another fraction tends to stick to the inner collector walls. For these reasons, weight losses have usually been estimated using the ASTM ash content of the coals and chars as a tracer.

Kobayashi (1976) and Padia (1976) showed that the use of ash as a tracer at high temperatures leads to significant errors. This study shows that the error is also quite significant at lower temperatues. Kobayashi (1976) solved this problem to an extent by using a sintered metal filter and collecting char at well above isokinetic suction flow rates. However, he had to use water jets to quench the pyrolysis. Besides increasing considerably the complexity of the system, the use of this type of collector gave rise to other problems. Ash and small coal particles were still lost through the pores of the filter; the data had to be corrected for the formation of soot, and the washing of the very hot chars may have caused chemical reactions between the water and the constituents of the char. Kobayashi's system has one more drawback, with respect to the purposes of the present research: the quenching water may change significantly the trace element content of the chars by washing and dissolving its inorganic minerals.

2. Water-cooled collectors cannot handle highly caking coals and quench adequately the pyrolysis reactions at the same time. Nsakala (1976) had to restrict his work to non-caking coals because of severe plugging problems in the collector. The inside diameter of the collector and the angle of the collector nozzle can be increased such that caking coals can be handled. However, doing so decreases the cooling rate of the particles in the collector. In addition, lower suction rates are necessary to obtain well defined laminar flow fields, which lead to lower particle collection efficiencies.

3. The heating of relatively large volumes of gas around water-cooled feeder probes is difficult. Nsakala (1976) had to restrict his work to temperatures below 808°C. Kobayashi was able to reach 2200°K using complex and expensive equipment which included an argon plasma gun and a graphite muffle tube.

4. The feeding of a small stream of coal dust well dispersed in a carrier gas at uniform rates is not a simple matter. However, it can be accomplished.

5. The high temperatures required and the large number of reactor internals and accessories make the materials requirements of this type of reactor quite stringent.

6. The heating rates of the particles are highly dependent on the heating of the cold carrier gas stream, which in turn is a function of the carrier gas flow rate, feeder geometry, and main stream gas flow rate. Estimation of the particle heating rate requires complex mathematical analysis of mass and heat transfer equations. The approaches taken have been: (a) to attempt to measure the heating rate of the carrier gas and (b) to solve simplifications of the mass, momentum, and heat transport equations. Nevertheless, in all cases the characteristic heating time of the coal particles ended up essentially as another fitted parameter.

This problem has been compounded by the different assumptions made by different researchers regarding the pyrolysis phenomena occurring during the heating period. Badzioch and Hawksley (1970) and Nsakala (1976) assumed that no reactions occurred during the heating of the coal particles and that the reactions are essentially isothermal. The empirical model that they used and their calculated kinetic parameters in essence reflect this assumption.

However, Kobayashi (1976) and Reidelbach (1978) have demonstrated that the heating period is indeed quite important.

7. The measurement of gas temperatures in the reactor is difficult because of complex radiative interactions between the measurement devices and the hot walls and cold spots of the reactor. Most researchers have resorted to measurements with suction pyrometers under simulated run conditions.

8. The residence times of the particles cannot be measured, but are calculated from their velocity and distance between the feeder and collector. However, the velocity of the coal particles is dependent on the reactor gas velocity and the particle size distribution. The gas velocity is, in turn, a function of the gas mass flow rate, reactor temperature, collector suction flow rate, and reactor geometry. Even though it is obvious that the main gas has a developing laminar flow velocity profile, fully developed laminar profiles have been assumed (Badzioch and Hawksley, 1970; Nsakala, 1976). In addition, most researchers regarded the free fall velocity of the particles as negligible (e.g., Badzioch and Kawksley, 1970; Nsakala, 1976). This assumption is obviously not correct in the case of particles larger than 100 μm such as some of those used by Nsakala (1976).

Kobayashi (1976) measured the velocities of the particles at a point in the reactor using a laser doppler anemometer. He then used the data to fit the parameters of a theoretical model of particle velocities and boundary layer development coupled with an empirical equation to describe the axial velocity of a developing laminar flow profile. Such an effort obviously involved considerable labor and added to the complexity of the apparatus.

9. Because of its complexity, control of the apparatus is difficult. Several gas feed and exhaust flows have to be maintained, coal feed rates must be reasonably uniform, and temperatures must be controlled and monitored.

It can be seen that the problems and drawbacks of laminar flow reactors are sufficiently serious that researchers (e.g., Tran, 1978) who could have built and used such equipment decided not to do so, giving as reasons the difficulties in the control and operation of the apparatus and the complex mathematical analysis of mass and heat transfer equations that are required for the data reduction. Nevertheless, this type of reactor can be quite useful if properly designed and if its limitations and the underlying assumptions made in the data analysis are carefully considered and appraised.

The following sections provide a description of the apparatus used, operating procedures, and the design calculations used in the analysis of the reactor parameters.

Of necessity, those descriptions and operating procedures are brief and presented in summarized form. Detailed operating procedures, calibration curves, and design drawings of the equipment are available in an internal technical report (Agreda, 1979) at the Chemical Engineering Department, North Carolina State University.

3.2 Description of Batch Reactor System

A schematic of the batch reactor system is shown in Figure 3.1. The system is built around a Lindberg Model 54032 single zone tube furnace and a Lindberg Model 59344 digital control console. The heating zone of the furnace is twelve inches long. The reactor temperature is measured with an Omega Model 2160A digital thermometer using a grounded chromel-alumel thermocouple with a 316 SS sheath. A quartz tube, 26 inches long and 1 inch in diameter is used as the reaction tube. The samples are introduced in porcelain boats. Two types of boats are used: glazed porcelain boats with a capacity of 2 grams of coal, and unglazed porcelain boats with a capacity of approximately 0.5 grams of coal.

The temperatures inside the furnace are determined by inserting the 1/16-inch thermocouple instead of a slide wire. The temperature controller's feedback loop uses a Platinel II thermocouple embedded in the heating element's

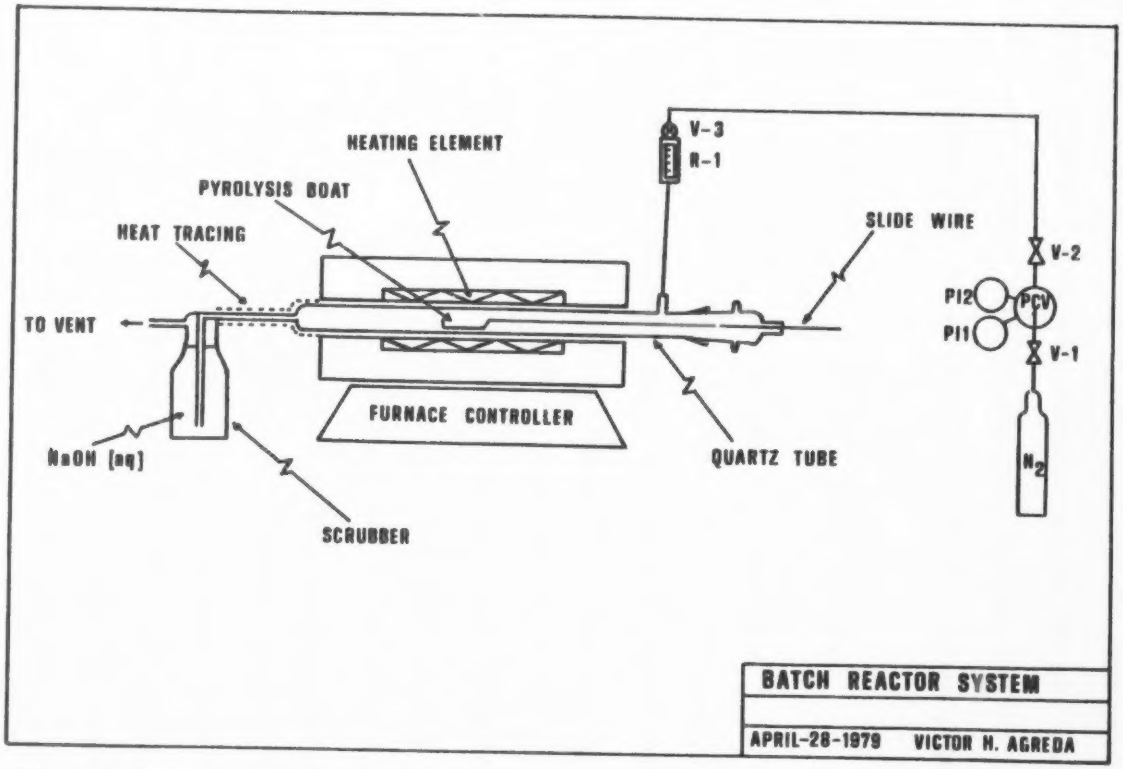
HEATING ELEMENT
PYROLYSIS BOAT
HEAT TRACING
TO VENT
NaOH (aq)
SCRUBBER
FURNACE CONTROLLER
V-3
R-1
SLIDE WIRE
QUARTZ TUBE
V-2
PI2
PCV
PI1
V-1
N_2
BATCH REACTOR SYSTEM
APRIL-28-1979
VICTOR H. AGREDA

Figure 3.1 Batch Reactor System

ceramic support. Therefore, it was necessary to calibrate the controller readings to the actual reaction zone temperature. The temperature profile of the furnace was determined experimentally. It was found that the peak temperature occurred close to the center of the furnace, and the profile is fairly flat in a 3-inch section at the center of the furnace. The pyrolysis boats were placed in this zone for the runs. Nitrogen was used as the sweep gas. The purpose of the gas flow was to remove the products of the pyrolysis without affecting the pyrolysis reactions. It was determined that the gas flow rate did not affect the reproducibility of the results, within experimental error, for all flow rates below 700 cc/min. The gas flow rate was kept at 300 cc/min in all runs.

Nitrogen flow to the pyrolysis tube is metered with an Air Products rotameter. The pyrolysis tube is connected to a scrubber bottle containing 70 ml of 10N sodium hydroxide. The partially cleaned exhaust gases are piped to a vent. All connections are made with Swagelock connectors with teflon ferrules. A 150 watt Fisher heating tape is used to heat-trace the tube exhaust. A 1/16-inch outer diameter (OD) stainless steel slide wire is used to insert the pyrolysis boats into the furnace. The slide wire holder is sealed with an O-ring.

Temperatures in this reactor can be varied between 200 and 1200°C. Residence times as low as 30 seconds can be achieved with fair reproducibility.

3.3 Experimental Procedure for Batch Reactor Experiments

The experimental procedure is as follows:

1. Select and set digital controller from temperature calibration curve.
2. Monitor reactor peak temperature and wait until digital temperature readout is at the desired level for at least 30 minutes. Usually at least 3 hours are needed for the reactor temperature to equilibrate.
3. Set gas flow at 300 cc/min.
4. Replace thermocouple with slide wire.
5. Turn heating tape on.
6. Weigh desired amount of coal in porcelain boat.
7. Place boat in mouth of tube. Connect slide wire in the boat's hook.
8. Close tube and seal gas-tight with the Swagelock fitting and the O-ring.
9. Purge with nitrogen for at least 5 minutes. The purpose of this step is to ensure that no air remains in the system, so that pyrolysis, not combustion, is studied.

10. Push boat, with slide wire, into the center of the reaction zone.
11. Keep boat in furnace for desired length of time.
12. Pull boat out of the reaction zone.
13. Allow boat to cool for 5 minutes before opening the tube to ensure that the coal does not combust.
14. Open mouth of pyrolysis tube and remove boat.
15. Place boat in desiccator. Wait until it cools completely (at least 15 minutes).
16. Weigh char and boat.
17. Empty boat into sample storage bottle.
18. Turn power off; cut gas flows off.
19. Clean pyrolysis tube after it has cooled to room temperature.

3.4 Description of Laminar Flow Reactor System

A detailed schematic diagram of the laminar flow reactor system is shown in Figure 3.2. The reactor design is similar to those of Badzioch and Hawksley (1970) and Nsakala (1976). It is not a replica of either, however, and can be operated over a wider range of conditions. The coal feeder-hopper is patterned after the miniature system used by Kobayashi (1976); it can be loaded with up to 25 grams of coal and reloaded as many times as necessary throughout the run.

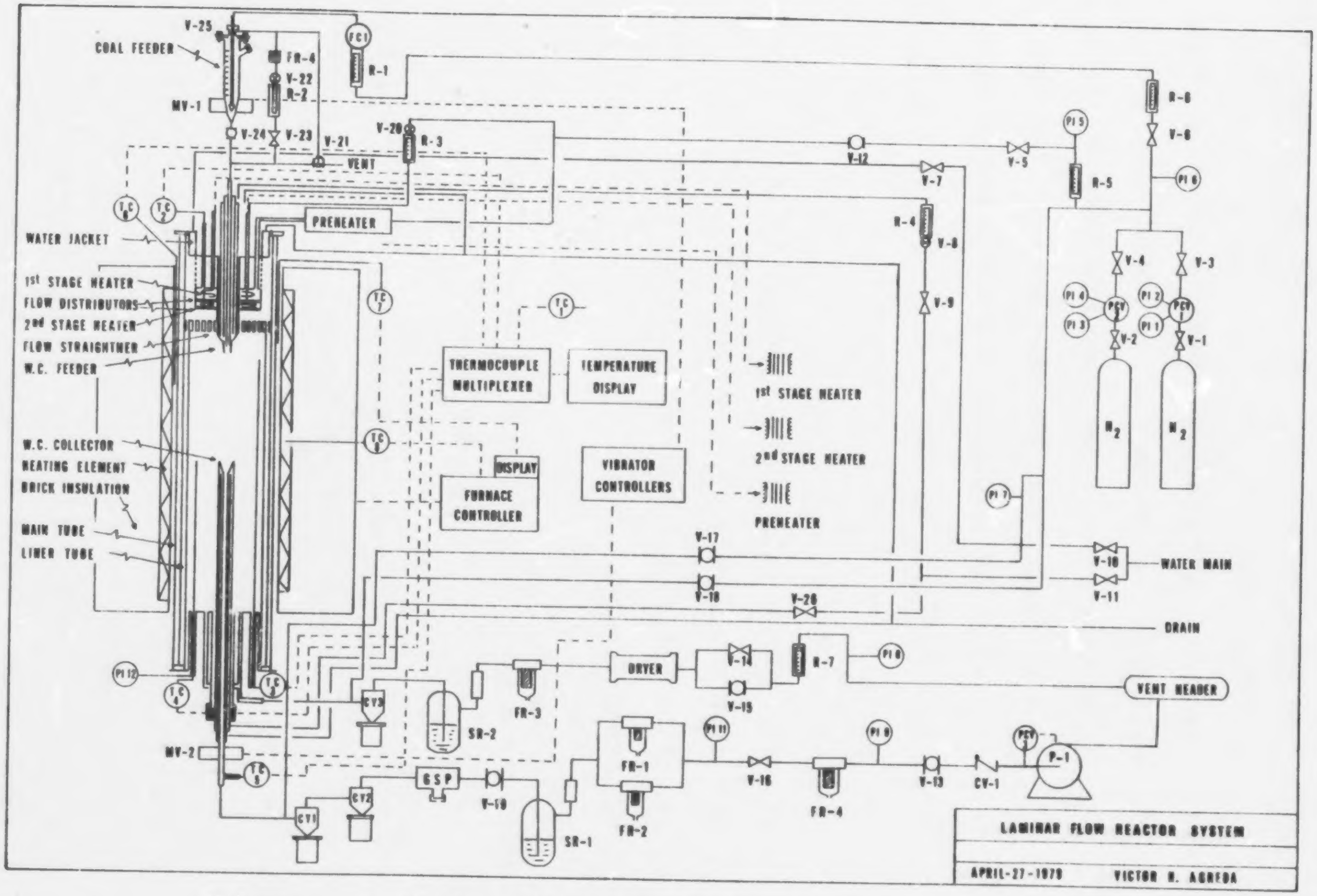
V-25
COAL FEEDER
MV-1
FR-4
V-22
R-2
V-24
V-23
V-21
VENT
FC1
R-1
V-20
R-3
V-12
V-7
V-5
PI 5
R-6
V-6
PI 6
R-5
R-4
V-8
V-9
V-4
V-3
PI 4
PCV
PI 3
PI 2
PI 1
V-2
V-1
N2
N2
PREHEATER
WATER JACKET
1st STAGE HEATER
FLOW DISTRIBUTORS
2nd STAGE HEATER
FLOW STRAIGHTNER
W.C. FEEDER
W.C. COLLECTOR
HEATING ELEMENT
BRICK INSULATION
MAIN TUBE
LINER TUBE
TC
THERMOCOUPLE MULTIPLEXER
TEMPERATURE DISPLAY
DISPLAY
FURNACE CONTROLLER
VIBRATOR CONTROLLERS
1st STAGE HEATER
2nd STAGE HEATER
PREHEATER
PI 7
V-17
V-18
V-28
V-10
V-11
WATER MAIN
DRAIN
PI 12
MV-2
CY3
CY2
CY1
SR-2
SR-1
FR-3
DRYER
V-14
V-15
R-7
PI 8
VENT HEADER
ESP
V-19
FR-1
FR-2
PI 11
V-16
FR-4
PI 9
V-13
CV-1
PCV
P-1
LAMINAR FLOW REACTOR SYSTEM
APRIL-27-1979
VICTOR H. AGREDA

Figure 3.2 Laminar Flow Reactor System

The basic principle of operation of the laminar flow reactor can be summarized as follows. Size-graded, finely ground coal particles are introduced into the water-cooled feeder tube from a partially fluidized vibrating hopper. The particles flow into a preheated stream of gas flowing downward through a vertical furnace tube at a Reynolds number low enough to ensure laminar flow. The furnace tube is held at the same temperature as the preheated gas. The small carrier flow of cold gas mixes rapidly with the hot gas stream, thus allowing the particles to be brought rapidly to the furnace temperature. Because the flow is laminar, the particles travel in a narrow streamline along the axis of the furnace and are aspirated into a water-cooled collector. The collector has a tapered entry so that the aspirated gases are accelerated to a high-velocity turbulent flow and thus are rapidly cooled. The cooling of the gases reduces the temperature of the suspended particles and quenches the decomposition. The transit time of the particles can be varied by changing the gas flow rate or by altering the distance between the feeder and the collector. Transit times in this reactor can be adjusted from 50 to 2,000 milliseconds. The temperature of the furnace and gas stream can be adjusted up to 1000°C. As indicated before, the pressure can be adjusted from atmospheric to 2.4 atm.

The operating ranges given are maximum obtainable limits. All the parameters cannot be varied independently within those limits, however, because they are interdependent. For example, the residence time is a function of gas flow rate, gas temperature, particle size and density, and feeder-collector distance. At very high temperatures, the gas velocity may be so fast that it cannot be compensated entirely by lowering the gas flow and increasing the feeder-collector distance. On the other hand, the minimum velocity that the particles can achieve is their free fall velocity in still gas. The pressure is a function of the main, exit, and suction gas flow rates.

The following sections provide details of the apparatus and equipment used.

3.4.1 Gas Supply and Utilities Subsystem

Nitrogen was used in all the experimental runs performed in this study. Other non-flammable gases can also be used, however. The gas supply consists of two A size nitrogen cylinders fitted with regulators (PCV1 and PCV2) and piped such that the supply can be switched from one cylinder to another during a run without disturbing the run parameters. City water is used for cooling in the feeder, water jacket, and collector. One 20 amp, 208 V line and one 20 amp, 110 V line are installed to provide electrical power for the equipment.

3.4.2 Feeder Subsystem

The coal feeder hopper is constructed of 38.1 mm OD lucite tube. It has a capacity of 25 grams of coal. A small amount of carrier gas is injected into the hopper (typically 1.0 ℓpm) through the hollow needle of the feed rate control valve, V-25. The tip of the valve has four small holes through which the gas is dispersed radially into the hopper. Approximately 50 cc/min of the feeder carrier gas rise through the hopper partially fluidizing the bed. The bed itself is continuously shaken by an electromagnetic vibrator (MV-1) to impede agglomeration. The remainder of the gas flows downwards through V-24 carrying the coal particles. The fluidizing gas joins the carrier gas stream through V-23. The feeder gas flow rate is controlled at the set point with FC1. The fluidizing gas is filtered through FR-4 and metered with R-2. V-21 is a three way valve used to equalize pressure across the hopper, which is necessary during start up or to stop the coal gas flow temporarily. V-21 is also used to purge the coal bed with nitrogen before a run. V-24 is closed and V-21 is set on the vent position for that purpose. For further details on the operation of the feeder system see Agreda (1979).

The coal particles, now well dispersed in the carrier gas, are injected into the reactor through a water-cooled feeder made of several concentric 316 stainless steel pipes.

The two outer shells have fiberfrax insulation between them to prevent excessive cooling of the main gas. The inner tube is 3.3 mm inner diameter (ID), and the outer shell is 2.54 cm OD. The end of the water-cooled feeder has a female thread such that alumina tips can be screwed in to connect with the 5 mm OD inner tube. Several feeder tips with orifice sizes ranging from 1.6 mm to 6.4 mm are available. The velocity of the feeder gas can therefore be controlled by increasing the gas flow, or, for a given gas flow, by changing the feeder tip bore size. The maximum bore size attainable is that of the thread itself which is 7 mm. The maximum bore size was used for all the runs reported in this thesis.

The coal feed rate can be adjusted by raising or lowering the needle of V-25, the electromagnetic vibrator power, and the ratio of fluidizing overflow gas to feeder gas. The primary means of control is the needle of V-25. Coal feed rates can be adjusted between 0.1 g/min to 2.0 g/min fairly reliably; however, the feed rate tends to vary slightly as the height of the bed decreases. Feeder gas flow rates can be adjusted from 0.1 to 2.0 ℓpm.

3.4.3 Furnace Reactor and Gas Heaters

The furnace tube is made of alumina with an inside diameter of 8 cm and a length of 1 meter. The liner tube is an alumina tube, 7 cm ID and 0.75 meters long. Heat is supplied by a three zone, 4000 watt, 230 volt Thermcraft furnace, with a heated length of 47 cm. The furnace temperature is controlled with a Lindberg Model 59344 digital control console which uses a Platinel II thermocouple as the sensing element. The furnace elements can be heated from 200 to 1200°C. The temperature profile of the heating elements is also monitored with a Pt-13% Rh thermocouple connected to a display (Omega Model 250) on the controller, and a chromel-alumel thermocouple multiplexed to the other system thermocouples.

The main gas is heated in three stages. The preheater consists of an 800 watt 19 mm Sylvania serpentine fluid heater. The heater itself is placed in the reactor head. It consists of two ARI 1000 watt heating coils separated by a 3.2 mm thick sintered stainless steel disk and encased in a stainless steel shell. The heaters are packed with stainless steel wool to improve the heat transfer efficiency to the gas. The power supplied to the preheater and heaters is controlled with three variable transformers. Another sintered stainless steel disc uniformly distributes the flow leaving the second stage of the gas heater. A 12.7 mm thick, 1.6 mm bore size alumina honeycomb disc placed 38 mm below the flow distributor, and resting on the liner tube, ensures that the gas enters the reactor in streamline flow. The feeder tip is 38 mm below the bottom of the honeycomb. The upper section of the gas heater-feeder reactor head has a water jacket, provided so that the viton gasket that seals the reactor against pressure leaks does not melt.

Two thermocouples are placed inside the reactor to monitor the reaction zone temperature. One is placed at the top of the reaction zone, close to the feeder tip, and the other is placed in the middle of the reactor. All chromel-alumel thermocouples are multiplexed to an Omega Model 2160A digital thermometer. The reactor pressure is monitored with an Air Products 0-30 psig (0-1600 mm Hg) gauge (PI 12).

3.4.4 Char Collection Apparatus

The pyrolysed chars are collected with a 30-inch long stainless steel collector made of concentric shells. The outer shell is 19 mm OD, and the inner tube is 0. 46 cm ID. The mouth of the collector is tapered, decreasing from 1.85 cm to 0.46 cm over a distance of 1.3 cm, so that the mouth makes a 62° angle with a horizontal line at the base. Two other collectors are available, which are designed to handle caking coals. Their inner tubes are wider and the collector angles with the base hroizontals are much larger.

The collector is fixed at the desired position and sealed pressure-tight with a packing gland. An electromagnetic vibrator (MV-2) prevents char particles from sticking to the collector walls. The exit gas temperature is monitored with a thermocouple (TC-5).

Most of the pyrolyzed chars are separated from the gas stream using two high efficiency cyclones placed in series. CY-1 is a 19 mm cyclone, and CY-2 is a 13 mm cyclone. Both are manufactured by the Air Correction Division of Universal Oil Products Company. The two cyclones ensure collection efficiencies greater than 99% for particles greater than 10 μm at the gas flow rates typically used in this system.

The char that misses the water-cooled collector exits the reactor through two ports located at the collector support base. This char is separated from the exit gas with an Air Correction 13 mm cyclone (CY-3).

3.4.5 Exhaust and Suction Subsystem

The collector suction line is connected to a high flow rate Lamert 03121 vacuum pump. Two water scrubbers and several large surface area filters are used to clean the gases exiting the cyclones. The water scrubbers were found to be necessary because of the large amount of tars produced in the pyrolysis of some coals. In addition, the main exhaust line has a Drierite drying column to remove the moisture before the gases enter the exhaust rotameter, R-7.

A gas sampling port (GSP) is provided in the suction line. The pressure at this point is usually close to the reactor pressure, thus providing a positive pressure sample which is obtained with a gas syringe. Preliminary work has shown that sulfur compounds can be detected in this sample using a Varian 3700 gas chromatograph with a dual flame photometric detector. Such work was barely begun; therefore, it is not reported here.

All primary gas flows throughout the entire reactor system are measured with wide-scale Fisher & Porter rotameters calibrated within 1% of full scale. Secondary flows, e.g., heater purge flows, are measured with small Air Products or Matheson rotameters.

The gas flow rate through the suction line is not measured directly, but is determined as the difference between the flows through R-7 and R-5. Before a run is made, V-13 is closed and a mass balance is made (R-5 and R-7 must measure the same flow) to ensure that there are no system leaks.

3.5 Experimental Procedure for Laminar Flow Reactor Experiments

As indicated previously, a detailed experimental procedure is available in an internal technical report (Agreda, 1979). For the purposes of this report, the following brief summary suffices.

1. Set up cooling water and gas supplies.
2. Start cooling water circulation.
3. Heat reactor to desired temperature as measured by T3.
4. Load coal in feed hopper and purge with nitrogen.
5. Start gas flows and suction system.
6. Start heaters and heat gas until T3 returns to the desired run temperature and reaches thermal equilibrium.
7. Start coal flow.
8. Maintain steady state operation by keeping reactor temperature, pressure, and flow rates constant.
9. Gather data on flows, pressures, temperatures, and levels every 10 minutes throughout the run.
10. Shut off feeder system when feed hopper is empty.
11. Turn heaters off.
12. Turn suction system off.
13. Stop all gas flows.
14. Collect chars from cyclone hoppers and weigh them.
15. Clean up and reset system.
16. When entire reactor system is below 50°C, turn cooling water off.

3.6 Coals and Sample Preparation

Five coals and one coke were used in this study. The coals used ranged in rank from lignite to anthracite. They are:

1. Beulah-Zap lignite from North Dakota.
2. North Barber No. 8 seam HVC coal, Navajo Mine, New Mexico.
3. Montana Rosebud subbituminous coal.
4. Western Kentucky No. 11 HVB coal.
5. Bottom Red Ash seam anthracite, Pennsylvania.
6. Chemical grade coke manufactured from Western Kentucky No. 11 HVB coal (at 1600 to 2000°F).

The sample names were codified using the initials of the coal names: BZN, NB8, MRS, WK11, and BRA.

Information about the coals was obtained from the North Carolina Research Triangle Institute, Pennsylvania State University - Coal Research Section, the U.S. Geological Survey, and the Illinois Geological Survey. The information obtained does not correspond necessarily to the specific samples used in this research; nevertheless, such information is useful in the interpretation of the findings of this study. A summary of the information is presented in Tables 3.1 and 3.2.

The coals were crushed to pass a No. 10 U.S. Standard sieve using a large mortar and pestle and pulverized using a Bico pulverizer with ceramic plates and a small porcelain ball mill. They were then size graded with U.S. Standard sieves and a mechanical sieve shaker.

Table 3.1 Coal Characterization Data (from several sources, see text)

As Received Analyses:				Proximate Analysis %			Ultimate Analysis %			Sulfur Forms %		
Coal	Code	Rank	FSI	Moist.	Ash	Vol. Matter	C	H	N	Pyritic	Sulfatic	Organic
Beulah Zap	BZN	Lig. A	0.0	29.63	6.39	28.57	46.82	6.56	0.73	<0.01	0.02	0.54
New Mexico No. 8	NB8	HVC	0.5	10.09	18.32	33.80	55.18	4.12*	1.21	0.31	0.00	0.42
Montana Rosebud	MRS	HVC	0.0	21.90	8.86	31.56	53.95	6.87	1.20	0.21	0.17	0.21
W. Kentucky No. 11	WK11	HVB	2.5	6.34	15.02	34.67	60.07	4.28*	1.75	2.63	0.14	1.87
Bottom Red Ash	BRA	Anthr.	0.5	4.68	5.71	4.90	84.33	1.71	0.81	0.15	0.00	0.58

*excludes moisture

Table 3.2 Elemental Concentrations and Organic Affinity of Elements in The Rosebud Coal From Montana (From Fiene *et al.*, 1978)

Element	Org. Aff.	Raw Coal	
		%	ppm
Al	.18	1.15	
Ca	.82	0.97	
Fe	.02	0.47	
K	.02	0.079	
Mg	.97	0.44	
Na	.88	0.019	
Ti	.15	0.05	
Si	.06	2.41	
LTA	.12		
HTA	.07	12.09	
Organic S	1.10	0.62	
Pyritic S	.02	0.22	
Sulfate S	.02	0.06	
Total S	.74	.90	
As	.03		0.69
B	1.24		100
Ba	.02		808
Be	.73		0.47
Br	.99		1.6
Cd	.06		0.22
Ce	.89		10.3
Co	.80		1.2
Cr	.09		6.2
Cs	.03		0.43
Cu	.44		8.8
Dy	.77		0.6
Eu	.89		
F	.76		
Ga	.76		3.3
Ge	.74		0.90
Hf	.39		1.2
Hg	.03		0.06
I	.02		0.3
La	.90		5.2
Li	.14		14.4
Lu	.68		0.06
Mn	.04		85

Table 3.2 continued

Element	Org. Aff.	Raw Coal	
		%	ppm
Mo	.83		7.1
Ni	.64		3.1
P	1.02		121
Pb	.04		4.6
Rb	.03		3.3
Sb	.95		
Sc	.78		1.6
Se	.05		0.93
Sm	.73		0.86
Sn	.04		8.1
Sr	.98		103
Ta	.61		0.13
Tb	.79		0.11
Te	-		<1
Th	.56		2.5
Tl	.11		0.46
U	.58		1.5
V	.60		10.6
W	1.15		0.70
Yb	.74		0.25
Zn	.02		4.3
Zr	.04		31

The 325x400 mesh size fractions of MRS, NB8, and BZN coals were used for the laminar flow reactor (LFR) runs, and the 200x325 mesh size fractions of all five coals were used for the batch runs. The particle size distribution of only one coal (MRS) was determined. The different size fractions of MRS coal were used to study the variation in moisture, ash, and sulfur content with particle size. The coke used in the pilot plant run was 10x80 mesh.

Kobayashi (1976) pointed out that particle size distribution is highly dependent on the pulverization method. Reidelbach and Algermissen (1978) showed that the size of the coal particles has a strong influence on the pyrolysis time and recommended that pulverized coal not be characterized only by a single mean particle size. Nevertheless, for the sake of simplicity and because of the screening procedure used in this study, an average particle size of 41.5 μm was used for the three coals used in the laminar flow reactor experiments.

No physical properties were determined for the different coals used. Average particle properties, also used by Kobayashi (1976), were used. They are:

heat capacity - $C_p = 0.25$ cal/gm $^{\circ}$K
density - $\rho_p = 1.25$ gm/cm^2
emissivity - $\varepsilon_p = 0.9$
thermal conducivity - $\lambda_p = 3.0 \times 10^{-3}$ cal/cm·sec·$^{\circ}$K.

4. DESIGN CALCULATIONS AND DATA REDUCTION EQUATIONS

4.1 Design Calculations for Batch Reactor System

There are only two controlled variables in the batch system: the furnace temperature, and the residence time of the coal in the furnace. The coal heating rate is a function of the furnace temperature and the heat capacity of the coal and boat.

The primary modes of heat transfer from the heating elements to the coal are most likely radiation from the top of the furnace and conduction from the heated boat at the bottom and sides of the coal bed. The temperature-time history of the coal was estimated in a crude manner. It was assumed that the heating and cooling rates of the coal were approximately the same as those of the surface of the heated boat. Therefore, an empty boat with a 1/16 inch grounded chromel-alumel thermocouple touching its surface was introduced into the reaction zone of the furnace. The temperature rise was monitored as a function of time. The heating and cooling curves are shown in Figure 4.1.

The heating rate is estimated by the equation:

$$m = \frac{0.95\ T_f - T_o}{t_h} \qquad (4\text{-}1)$$

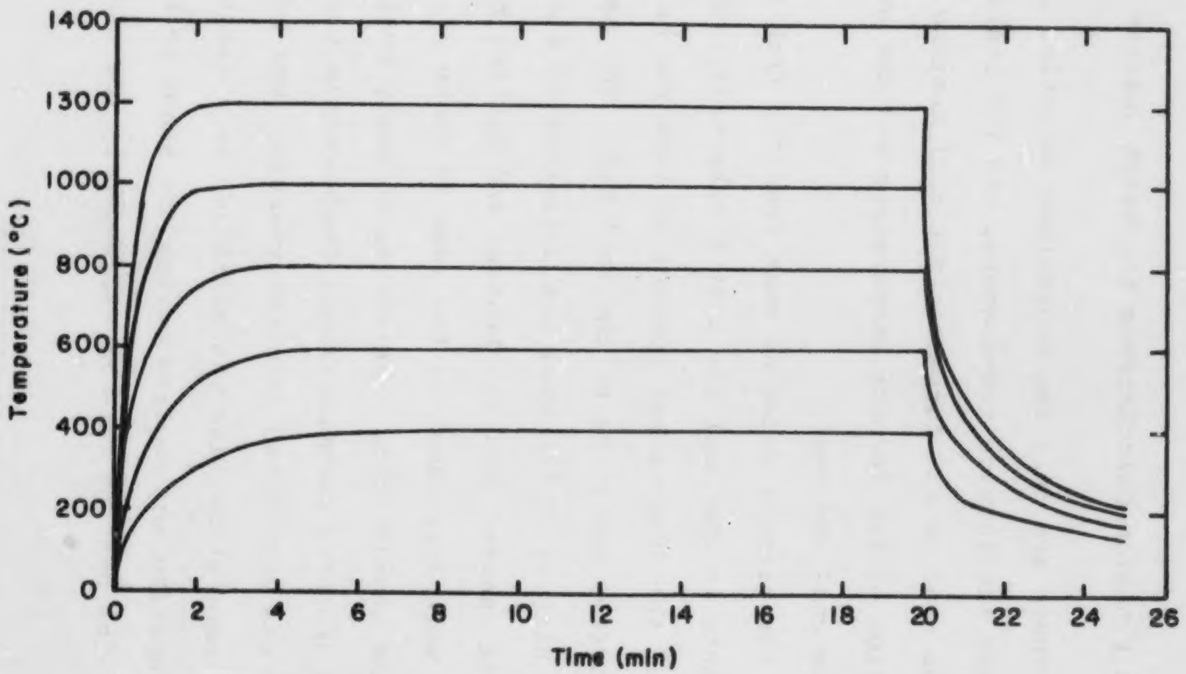

Figure 4.I Temperature-Time Histories of Batch Samples

where T_f = final temperature

T_o = initial temperature

t_h = time for heating to 95% of T_f.

Using this equation, the heating rates were found to range from 5°C/sec at 300°C to 45°C/sec at 1200°C.

The time constant for the heating of the coal and boat is estimated using the equation:

$$t = \tau_B\left[-\ell n\left(1 - \frac{T - T_o}{R_f - T_o}\right)\right] \qquad (4\text{-}2)$$

where t = time

T = temperature

T_o = initial temperature

T_f = final temperature

τ_B = boat heating time constant.

Linear regression of t vs. the bracketed term yields τ_B as the slope.

The gas velocity through the reaction tube is a function of the furnace temperature, but the flow was laminar in all runs. The Reynolds numbers ranged from 2.5 at 300°C to 1.6 at 1200°C.

4.2 Design Calculations for Laminar Flow Reactor

In order to obtain kinetic information on the devolatilization reactions from the laminar flow experiments, temperature-time histories of the injected coal particles must be known accurately. However, introduction of coal particles through a water-cooled injector makes actual temperature and velocity fields quite complicated.

Boundary layers grow near the walls of the muffle tube and injector. However, since the gas and muffle tube wall temperatures are the same, the thermal boundary layer develops only along the injector. Overisokinetic gas suction rates in the collector increase the gas velocity, therefore reducing the particle residence time. In addition, for larger particle sizes, the free fall velocities of the particles may be significant. In view of these considerations, the common assumptions that the particles move at the axial velocity of a fully developed laminar flow profile and that the reactor can be considered isothermal are inadequate.

The following sections describe the approach taken in the analysis of the laminar flow reactor. A compromise has been made between the simple assumptions made by Badzioch and Hawksley (1970) and Nsakala (1976) and the mathematical rigor, coupled with experimental realism, used by Kobayashi (1976).

4.2.1 Particle Velocities and Residence Times

Accurate knowledge of the velocity profile across the entire furnace tube is not necessary, since the particles are largely confined to a narrow streamline on the axis.

Because of the two sintered stainless steel disks and steel wool used in the gas heater, the velocity profile leaving the second distributor should be flat. The flow in each hole of the flow straightener has a parabolic velocity profile, since the maximum Reynolds number in each hole, for the experimental conditions used, is about 5. Since the voidage ratio of the honeycomb is approximately 0.5, the maximum velocity of the parabolic honeycomb flow is about four times as fast as the average main flow velocity. The characteristic decay time of the parabolic flows may be approximated by (Kobayashi, 1976)

$$t_{decay} = \ell^2/\nu \qquad (4\text{-}3)$$

where

ℓ = spacing of the holes

ν = kinematic viscosity of the gas .

At 800°C, this equation yields 0.1 msec as an order of magnitude estimate of the decay time. The injector tip was positioned 1.5 inches below the honeycomb to ensure flat velocity profiles under all experimental conditions.

The discussion that follows is intended to show that a flat velocity profile may be assumed at the feeder tip position in the reactor. The velocity of the coal feed carrier gas at the feeder tip is given by

$$u_f = \frac{4\overset{o}{m}_f}{\rho_f \pi d_f^2} \tag{4-4}$$

where $\overset{o}{m}_f$ = feeder gas mass flow rate

ρ_f = feeder gas density at room temperature and reactor pressure

d_f = feeder tip inside diameter.

Typically, the velocity of the cold feeder gas is set to be greater than that of the main gas stream at the feeder tip. Therefore, the coal particles enter at a velocity greater than the main gas centerline velocity; however, the theory of the fluid dynamics of jets indicates that the core of the jet emerging from the feeder tip should disappear within five feeder-tip bore diameters (Goldstein, 1965), i.e., the annular mixing region occupies the whole jet.

Another factor that must be taken into account is the density change due to the increase in temperature of the entering feeder gas stream. The axial velocity of an isothermal round jet in a uniform stream is given by (Pai, 1954)

$$\frac{u_x - u_m}{u_f - u_m} = \frac{6.5\ d_f/x}{1-0.6(u_m/u_f)} \quad ; \quad x \le 30\ d_f \tag{4-5}$$

where u_x = axial gas velocity
u_m = main stream gas velocity
x = axial distance from feeder tip.

However, the velocity field near the feeder tip is complicated by the formation of a cold boundary layer on the surface of the water-cooled feeder. The velocity in this region should be considerably lower than the average main gas velocity.

In summary, there are three concentric annular regions at the tip of the feeder: the emerging jet, the cold boundary region, and the hot main gas. The boundary layer thickness at the injector tip may be approximated by that of forced convection over a flat plate.

$$\delta = \frac{5 \cdot \ell}{Re_\ell} \qquad (4\text{-}6)$$

where δ = boundary layer thickness
ℓ = length of injector below honeycomb
Re_ℓ = $\ell u_m \rho_g / \mu$, Reynolds number
ρ_g = gas density
μ = gas viscosity.

Temperature and velocity profiles in the boundary layer are approximated by the following equation (Kobayashi, 1976):

$$\frac{u}{um} = \frac{T - T_f}{T_m - T_f} = \sin(\frac{\pi}{2}) \frac{r - r_f}{\delta} \qquad (4-7)$$

where r_f = outer radius of feed injector tip

T_f = temperature at feeder tip

T_m = main gas temperature

u = velocity.

For the range of conditions used in this study, the average velocity in the boundary region is on the order of one tenth of the feeder gas velocity, and the average temperature is only about 100°C hotter than the feeder gas temperature.

For all the complexity of the system, when the thickness of the feeder tip walls are considered, the continuity equation applied, and the gas mixing effect due to the movement of the coal particles in the feeder gas stream accounted for, the conclusion is reached that the velocity profile across the entire furnace tube at the feeder tip may be considered flat and equal to the average main gas velocity. At any rate, the uncertainties involved in the full reactor analysis do not warrant a more complex mathematical analysis.

The time that it takes for the coal particles to decelerate from u_f to their terminal velocity u_t can be calculated by making a force balance:

$$\frac{du_p}{dt} = g - \frac{\rho_g\, g}{\rho_p} - \frac{C_D\, u_p^2\, \rho_g\, 4\pi d_p^2}{2\, m_p} \qquad (4\text{-}8)$$

where u_p = particle velocity

t = time

g = acceleration of gravity

m_p = particle mass

ρ_p = particle density

$C_D = \frac{24}{Re_p}$ = drag coefficient assuming Stoke's law

Re_p = particle Reynolds number

d_p = particle diameter.

Assuming that $\rho_g << \rho_p$, the differential equation is solved yielding:

$$t = \frac{1}{N} \ln \left(\frac{u_f - g/N}{u_p - g/N}\right) \qquad (4\text{-}9)$$

where $N = \frac{48\ \mu\pi}{m_p}$. (4-10)

From equation (4-9), it is estimated that the time necessary for the particles used in this study to decelerate to u_f is less than 5 msec and therefore can be assumed to be negligible compared to typical residence times.

In view of the above results, it is assumed that the velocity of the particles at any point from the feeder to the collector is given by

$$u_p = u_t + u_x \qquad (4\text{-}11)$$

where u_p = particle velocity

u_t = terminal velocity of particle falling freely

u_x = main gas axial velocity.

The velocity distribution of the main gas across the reactor is that of a developing laminar flow. Kobayashi (1976) curve-fitted the numerical results of Langhaar (1942), yielding the following equations:

$$\frac{u_x}{\bar{u}_m} = 1 + 0.34Y^{0.45} \ , \quad 0 \leq Y \leq 6 \qquad (4.12)$$

$$\frac{u_x}{\bar{u}_m} = 2 - 3.48Y^{-1.47} \ , \ Y > 6 \qquad (4\text{-}13)$$

$$y = 400 \, \frac{x}{D_T} \, \frac{1}{Re_D} \qquad (4\text{-}14)$$

where u_x = centerline velocity of developing laminar flow

$\bar{u}_x$ = average main gas velocity

x = distance from feeder ti½

D_T = tube diameter.

Therefore, to calculate the residence time of the particles,

$$t_R' = \frac{z}{u_t + \bar{u}_x} \qquad (4\text{-}15)$$

where t'_R = uncorrected particle residence time

$\bar{u}_x$ = distance-averaged axial gas velocity

z = feeder-collector distance plus collector mouth-to-throat length

it is necessary to calculate the average axial velocity from the feeder to the collector

$$\bar{u}_x = \frac{\int_o^z u_x(x)\,dx}{z} \tag{4-16}$$

or in terms of the dimensionless variable y defined in equation (4-14),

$$\bar{u}_x = \frac{\int_o^{y<6} u_x(y<6)\,dy + \int_6^{y>6} u_x(y>6)\,dy}{y(z)} \,. \tag{4-17}$$

Substituting from equations (4-12) and (4-13) yields

$$\bar{u}_x = \frac{\bar{u}_m}{y(z)} \left\{ 2y \Big|_o^{z>6} + 7.4043\, y^{-0.47} \Big|_6^{z>6} \right\} . \tag{4-18}$$

To calculate the terminal velocities of the coal particles, it is necessary to determine their flow regime. This is done by first calculating (McCabe and Smith, 1967)

$$K = d_p \left[\frac{g \ \rho_g (\rho_p - \rho_g)}{\mu^2} \right]^{1/3} . \qquad (4\text{-}19)$$

If $K < 3.3$, Stoke's law applies, and

$$u_t = \frac{g \ d_p^2 (\rho_p - \rho_g)}{18\mu} . \qquad (4\text{-}20)$$

If $3.3 < K < 43.6$, the intermediate law applies, and

$$u_t = \frac{0.153 \ g^{0.71} \ d_p^{1.14} \ (\rho_p - \rho_g)^{0.71}}{\rho_g^{0.29} \ \mu^{0.43}} . \qquad (4\text{-}21)$$

However, the gas is accelerated by the overisokinetic suction rate at the collector (necessary to obtain good char collection efficiencies), so that a correction is necessary. The following equations are used for this purpose (Kobayashi, 1976):

$$\Delta t = \frac{(\tan\alpha)(r_1 - r_0)}{u_e} - \frac{r_1}{\tan \alpha} \{1 - (\frac{r_0}{r_1})^3\} \qquad (4\text{-}22)$$

$$r_1 = \sqrt{\frac{\overset{\circ}{m}_s}{\pi \rho_g \ u_e}} \qquad (4\text{-}23)$$

where Δt = decrease in residence time due to acceleration
$\overset{\circ}{m}_s$ = mass flow rate of suction stream at collector
ρ_g = density of main gas

u_e = axial main gas velocity at collector mouth entrance

r_o = radius of collector throat

α = acute angle that the collector nozzle makes with a horizontal line passing through its throat.

In these equations, r_1 is the radius of a hypothetical extension of the collector mouth entrance, obtained by assuming that the mass flow rate entering the extension at reactor conditions is the same as the true suction mass flow rate. Under this assumption, integration of the mass conservation equation yields equation (4-22), and the particle residence time is

$$t_R = \frac{z}{u_t + \bar{u}_x} - \Delta t \quad . \tag{4-24}$$

The gas flow and particle velocity calculations are carried out for each experimental run with the computer subprograms shown in Appendix B.1. Subroutine GASPR calculates the gas properties as a function of temperature and pressure; subroutine VTER calculates the terminal velocity (u_t) of the coal particles; subroutine VAXL calculates the average axial gas velocity ($\bar{u}_x$) and the gas velocity at the collector mouth (u_e); and finally, subroutine CORR calculates the time correction (Δt) due to the overisokinetic suction rate.

4.2.2 Heating and Cooling of the Coal Particles

The coal particles are heated in the furnace by radiation from the furnace walls and by convection from the gas. The mathematical representation of the unsteady heating of a coal particle suddenly plunged into hot gas leads to the following partial differential equation, assuming spherical symmetry (Reidelbach and Algermissen, 1978):

$$\frac{\partial T_{pi}}{\partial t} = \frac{1}{C_p \rho_p r^2} \cdot \frac{\partial}{\partial r} \left(r^2 \cdot \lambda_p \frac{\partial T_{pi}}{\partial r} \right) \qquad (4\text{-}25)$$

with boundary conditions

$$\frac{\partial T_{pi}}{\partial r} = 0 \quad \text{for } r = 0 \qquad (4\text{-}26)$$

$$\frac{\partial T_{pi}}{\partial r} = \frac{Nu\ \lambda_g}{\partial_p\ \lambda_p} (T_g - T_{pi}) + \frac{s_\sigma \varepsilon_p}{\lambda_p} (T_w^4 - T_{pi}^4) \qquad (4\text{-}27)$$

$$\text{for } r = R_i$$

where Nu = Nusselt number with respect to the diameter

T_{pi} = particle temperature

T_w = reactor wall temperature

T_g = gas temperature

λ_g = gas thermal conductivity

r = radial position

R_i = average radius of i^{th} particle size fraction

s = view factor

σ = Boltzmann constant

ε_p = particle emissivity

λ_p = particle thermal conductivity.

It is assumed that the coal is homogeneous and isotropic and does not swell or shrink during the decomposition process.

Rapid devolatilization is probably endothermic; however, no heat generation term appears in the above equations. Kobayashi (1976) pointed out that such an effect could be accounted for, if necessary, by increasing the specific heat of the coal particle. Furthermore, the enthalpy required to heat the feeder gas is much larger than the reaction enthalpy effect, thus making the later effect negligible.

It has been shown (Badzioch and Hawksley, 1970; Kobayashi, 1976; Nsakala, 1976; Reidelbach and Algermissen, 1978) that heat transfer through the particle boundary layer is the rate-determining step compared to thermal conduction inside the particle for particles in the pulverized particle size range (<200 μm). Hence, the particles can be treated as spatially isothermal. Kobayashi (1976) found that radiation heat transfer becomes dominant for particles larger than ∿100 μm, especially at high temperatures, while convection is dominant for small particles ($\sim 100\ \mu m$). Thus equation (4-25) may be replaced by an ordinary differential equation, obtained by substituting $(4\pi R_i{}^3/3)C_p \rho dT_{pi}/dt$ for $\partial T_{pi}/\partial r$ in equation (4-27), and multiplying the right-hand side by $4\pi R_i{}^2$.

Particles of different sizes are heated at different rates in the laminar flow reactor. Furthermore, due to convective heat transfer, the temperature of the gas surrounding the particles also varies in time and has to be calculated. Therefore, we have as the governing heat transfer equations (Reidelbach and Algermissen, 1978):

$$\frac{dT_{pi}}{dt} = \frac{3}{\rho_p C_p} \frac{Nu\lambda_g}{2} \frac{1}{R_i{}^2} (T_g - T_{pi}) + \frac{s\sigma\varepsilon_p}{R_i} (T_g - T_{pi}) \qquad (4\text{-}28)$$

and

$$\frac{dT_g}{dt} = - \frac{1}{\overset{o}{m} C_g} \sum_{i=1}^{n} \frac{3\overset{o}{m}_{pi}}{R_i \rho_p} \frac{N_u \lambda_g}{2} (T_g - T_{pi}) \qquad (4\text{-}29)$$

where $i=1,2,\ldots,n$ = particle size class

C_g = gas heat capacity

$\overset{o}{m}_p$ = coal mass flow rate

$\overset{o}{m}_g$ = gas mass flow rate.

Three thermodynamic parameters are important in this analysis: reactor wall temperature, initial surrounding gas temperature, and mass flow ratio of coal to gas. Each of these parameters has a distinct influence on the temperature history of a coal particle. The final temperature that can be reached is the reactor wall temperature. Reidelbach and Algermissen (1978) found that when the initial gas temperature is not too low compared to the wall temperature, the convective heat flow is higher than the radiative flow. The particle temperature at first rises rapidly until thermal equilibrium with the gas is approached, after which a slower temperature rise up to the wall temperature is observed.

As has been shown, the analysis of the heat transfer phenomena occurring when a coal particle is suddenly plunged into hot gas in a reactor is fairly straightforward. In the laminar flow reactor, however, the coal particles are injected with cold feeder gas through a water-cooled tube. The gas temperature near the particles increases at a rate controlled by the mixing and diffusion between the carrier gas and the hot main stream.

It has been shown by Kobayashi (1976), and implicitly assumed by Badzioch and Hawksley (1970) and Nsakala (1976), that the heating of the coal particles as they leave the feeder is controlled by the mixing of the feeder gas and main gas. The characteristic gas mixing time is much larger than the characteristic convection time to the particles.

This implies that detailed analysis of the temperature fields in the furnace is necessary in order to get an accurate temperature history of the injected coal particles.

Different approaches have been taken to solve, or get around, the problem of estimating the temperature history of the coal particles. Badzioch and Hawksley (1970) defined an isothermal reaction time

$$t_I = t_R - t_H \tag{4-30}$$

where t_I = isothermal reaction time
t_R = residence or transit time
t_H = heating time.

They assumed that no reactions take place during t_H. The best value of t_H which allowed correlation of the data with their model was found from statistical analysis of the data. Nsakala (1976) used a similar approach. He concluded that, under certain assumptions such as the pyrolysis activation energy being greater than 55 kcal/mole, the extent of pyrolysis during the heating time is negligible. The analysis of Badzioch and Hawksley's (1970) and Nsakala's (1976) data by Reidelbach and Algermissen (1978) shows that such a conclusion is very likely invalid. Furthermore, there is not one coal pyrolysis reaction, but a very large number of complex simultaneous reactions with many different activation energies. Data analysis by the infinite parallel reactions model (Anthony, 1975) typically yields mean activation energies of 48.7 to 56.3 kcal/mole with standard deviations ranging from 9.38 to 11.5 kcal/mole (Suuberg, 1978). For purposes of comparison with other researchers' data, t_H in this study is defined as 95% of the particle's heating time constant.

Kobayashi (1975) carried out a fairly rigorous analysis of the temperature and velocity fields in his laminar flow reactor. Three concentric regions -- the center region, boundary region, and main stream -- were considered. All the coal particles were assumed to remain in the center region, and the local velocities and temperatures of gas and particles were assumed to be the same. The momentum, energy, and mass conservation equations were then solved with appropriate boundary conditions and assumptions concerning the coal particles and their properties, shape and size of the flow regions, and velocity and temperature gradients at the interfaces. An approximate integral method was used to simplify the analysis, which then yielded a family of curves describing particle temperature as a function of distance from the feeder, time, and the ratio of the momentum shape factor to the energy shape factor (for a given set of reactor conditions)

$$\theta = \frac{K_M}{K_E} \qquad (4\text{-}31)$$

where K_M = momentum shape factor

K_E = energy shape factor.

A theoretical analysis showed that θ should lie between 1 and 3. Kobayashi (1976) used an indirect method based on the observed weight losses at different temperatures to determine the proper value. If a coal shows a given asymptotic weight loss at a given temperature, it is assumed that when the particle reaches this weight loss while being heated to a higher temperature, the particle temperature at that time is the same as the temperature at which the initial asymptotic weight loss was determined. Thus the coal weight loss itself provides the required temperature measurements. The appropriate value of θ was found to be 3.

Kobayashi (1976) pointed out that for practical purposes, the temperature-time histories of the coal particles may be approximated by the following exponential curve

$$\frac{T_p - T_f}{T_R - T_f} = 1 - e^{-t/\tau_H} \qquad (4\text{-}32)$$

where T_f = feeder gas temperature

T_R = reactor temperature

τ_H = heating time constant.

He then used his mathematical analysis to generate values of τ_H, for $\theta=3$, as a function of temperature, main gas velocity, and carrier gas velocity. The calculated values of τ_H were then used with equation (4-32) to calculate the temperature rise of the coal particles.

Examination of Kobayashi's data for τ_H suggests a strong correlation between τ_H, reactor temperature and feeder gas velocity, whereas the main gas velocity does not appear to influence τ_H appreciably. Least squares multiple linear regression yields the following empirical fit between τ_H, T, and u_f:

$$\tau_H = \exp\left[5.67238 - \frac{4.04814\ T_R}{10000} - 0.5348\ \ln(u_f)\right] \quad (4\text{-}33)$$

where τ_H = particle heating time constant in milliseconds

T_R = reactor temperature in degrees Kelvin

u_f = feeder gas velocity, at feeder tip, in cm/sec.

The coefficient of determination for this fit is $r^2=0.9941$. Equation (4-33) is used to calculate τ_H in the subsequent analysis. The finding that u_m does not have an appreciable effect on τ_H may be a consequence of the shielding effect of the annular boundary region that develops around the feeder, as discussed in Section 4.2.1.

Equation (4-29) shows that the coal mass flow rate affects the heating of coal particles by increasing the enthalpy requirement. Furthermore, if large clouds of coal are fed, the view factor S is reduced. Both effects tend to reduce the heating rate of the coal particles and therefore the rate of devolatilization. On the other hand, large numbers of particles in the laminar jet leaving the feeder tend to make the flow turbulent. A turbulent jet exiting the feeder could disturb the boundary region, leading to faster mixing of the cold feeder gas with the hot main gas and correspondingly faster heating rates, and hence to higher devolatilization rates. Badzioch and Hawksley (1970) found experimentally that the rate of devolatilization is independent of coal feed rate up to 0.5 g/min. The feed rates employed in their experiments ranged from 0.25 to 0.5 g/min for feeder gas flow rates of 1 to 2 ℓ/min. Kobayashi (1976) used coal feed rates ranging from 0.01 to 0.38 g/min for carrier gas flow rates ranging from 15 to 608 cc/min. Nsakala (1976) used coal feed rates ranging from 0.5 to 0.6 g/min for a feeder gas flow rate of 1.98 ℓ/min. Coal feed rates used in this study range from 0.3 to 3 g/min for a feeder gas flow rate of 1.0 ℓ/min.

The theoretical analysis of Reidelbach and Algermissen (1978) shows that a single particle size cannot be assumed for large size fractions of pulverized coal but that equations (4-28) and (4-29) should be used. However, for the size fraction used in the present study (325x400 mesh), their analysis suggests that the average particle size for the fraction may be used as representative of the entire size fraction.

In the reactor system used in this research, the pyrolysis reactions are quenched with a water-cooled collector. Heat is removed from the coal particles by convection to the gas, radiation to the collector wall, and, to a smaller extent, conduction by collision with the collector wall.

The gas temperature decrease in the collector is calculated by an iterative procedure (Howard, 1965). For a small section, Δx, in the collector

$$\overline{T} = T_w + (T_1 - T_2)\{\ell n[(T_1 - T_w)/(T_2 - T_w)]\}^{-1} \tag{4-34}$$

$$\frac{h}{C_g} = [\frac{\overset{\circ}{m}_g d_c}{4}(\Delta x)]\ell n[(T_1 - T_w)/(T_2 - T_w)] \tag{4-35}$$

$$\Delta x = (\frac{\overset{\circ}{m}\, d_c C_g}{4h})\ell n[(T_1 - T_w)/(T_2 - T_w)] \tag{4-36}$$

where $\overline{T}$ = average gas temperature in Δx

T_w = collector wall temperature

T_1 = temperature at beginning of Δx

T_2 = temperature at end of Δx

h = heat transfer coefficient

d_c = collector diameter.

The procedure is as follows:

1. Choose T_1 and T_2, one of which must be at a known point (e.g., $T_1 = T_m$ at probe entrance).
2. Calculate $\bar{T}$.
3. Calculate h/C_g.
4. Calculate Δx to locate interval
5. Use previous T_2 as the new T_1 and repeat the procedure.

It has already been indicated that the rate-determining step in the heating or cooling of coal particles is the heating or cooling of the carrier gas. The high velocity, turbulent flow in the collector leads to high heat transfer rates between the gas and the particles. The particle cooling rate calculated with the equations given above for the collector probe and suction rates used in this study is greater than 10^5 °C/sec. The quenching of the pyrolysis reactions within a few milliseconds is thus ensured. These conclusions are consistent with the findings of Badzioch and Hawksley (1970) and Nsakala (1976).

Finally, the reactor temperature must be measured. Suction pyrometers are typically used to measure gas temperatures. Badzioch and Hawksley (1970) and Nsakala (1976) measured the axial temperature profile of the gas in their reactors with such a probe. However, heat is transferred to the coal particles by convection from the gas and by radiation from the wall. To avoid ambiguity, the gas temperature and the reactor wall temperature should be the same. This may not have been the case for the reactor used by Nsakala (1976), in which the reactor walls were at a higher temperature (about 100°C higher) than the measured gas temperature. Reidelbach and Algermissen (1978) have shown that radiation heat transfer may be more important than previously thought because of the large specific surface of small coal particles. Therefore, if the gas and wall temperatures are not the same, the temperature that should be associated with the experiment becomes uncertain.

The energy balance on a thermocouple in the laminar flow reactor is

$$q_T = h_T A_T (T_m - T_T) + \varepsilon_T \sigma A_T (T_W^4 - T_T^4) \qquad (4\text{-}37)$$

where q_T = heat flow to the thermocouple
h_T = convective heat transfer coefficient
A_T = surface area of thermocouple
T_T = thermocouple temperature
ε_T = thermocouple emissivity
σ = Boltzman constant
T_m = main gas temperature.

Assuming that the grounded tip of a 1/16 inch thermocouple can be treated as a small sphere, the following correlation can be used (McAdams, 1953)

$$h_T = \frac{\lambda_g}{d_r}\ 0.37\ (Re)^{0.6} \quad ; \quad 25 < Re < 10^5 \qquad (4\text{-}38)$$

where $Re = \dfrac{\rho_g u_m d_T}{\mu}$

d_T = thermocouple characteristic diameter.

Therefore, assuming thermal equilibrium ($q_T=0$), equation (4-37) becomes:

$$T_m = T_T + (\varepsilon_T \sigma d_T/0.37\lambda_g)(T_T^4 - T_w^4)(\mu/\rho u_m d_t)^{0.6} \ . \qquad (4\text{-}37)$$

The thermocouple emissivity may be assumed to have a value of 0.22 (Kaskan, 1956). Therefore, if T_w and u_m are known, the reactor gas temperature (T_m) can be estimated.

The procedure followed during most of the runs in this study (also followed by Badzioch and Hawksley, 1970 and Kobayashi, 1976) was to set $T_w = T_T$ with no gas flow, assuming that h_T was small and T_m for the still gas inside the furnace was close to T_w. Hence, when the gas flows are started, T_T drops to some intermediate temperature between T_w and T_m. Heat is added to the gas until T_T returns to the original T_w reading. At that point, T_m should equal

T_W (i.e., $q_T = 0$). This may not be exactly true because some spots in the cold ends of the reactor may change in temperature, relative to the original measurements, as the heated gas passes by them.

Sainsbury et al. (1966) studied this problem. Their experimental results show that, when the procedure outlined above is followed, the difference in the readings obtained with a thermocouple and a suction pyrometer differ from 10 to 25°C, with the thermocouple always having the higher temperature. Their study did not account for the heat transfer between the reactor walls and the water-cooled collector as a function of feeder-collector distance, however, this is a phenomenon that can cause the temperature profile of the furnace walls to vary appreciably. Hence, it is clear that there is at least a 5 to 12.5°C uncertainty in the reactor temperature, under the best circumstances.

4.3 Coal Composition and Weight Loss Variables

For the purposes of this study, coal is taken to contain three major fractions: moisture (M), ash (A), and volatiles (V). V should not be confused with the ASTM volatile matter (VM). Each coal element is expressed as a fraction, by weight, of the coal according to the following equation:

$$X^{+} = \frac{\text{weight of element in char}}{\text{as-received weight of char}} \ . \qquad (4\text{-}39)$$

Different samples of a given type of coal may have slightly different moisture and ash contents; furthermore, the moisture content of a coal sample may change depending on the environmental conditions to which the sample is subjected. Therefore, it is sometimes advantageous to express the weight fractions of coal components on moisture-free (m.f.) and dry-ash-free (d.a.f.) bases, in addition to the as-received (a.r.) basis. For the sake of simplicity, the following nomenclature is used: superscript "+" denotes as-received mass fraction (i.e., including moisture and ash); superscript "‡" denotes moisture-free mass fraction; and superscript "*" denotes dry-ash-free mass fraction. The mass fractions calculated on different bases are related to one another as follows:

$$X^{\ddagger} = \frac{X^{+}}{1-M^{+}} \quad ; \frac{\text{weight of element}}{\text{weight of dry char}} \qquad (4\text{-}40)$$

$$X^{*} = \frac{X^{+}}{1-A^{+}-M^{+}} \ ; \frac{\text{weight of element}}{\text{weight of dry ash free char}} \qquad (4\text{-}41)$$

and $$X^{*} = \frac{X^{\ddagger}}{1-A^{\ddagger}} \quad ; \frac{\text{weight of element}}{\text{weight of dry ash free char}} \ . \qquad (4\text{-}42)$$

Throughout this report, subscripts are used as follows: "C" denotes feed coal, "H" denotes char, "V" denotes volatiles, and "A" denotes ash (e.g. X_H^* , X_V^* , etc.).

When W_C mass units of coal are pyrolyzed, W_H mass units of char are produced. Each has its own moisture, ash, and volatiles fractional content. The fractional a.r. weight loss is given by:

$$\Delta W^+ = \frac{W_C^+ - W_H^+}{W_C^+} \tag{4-43}$$

The fractional m.f. weight loss is given by

$$\Delta W^\ddagger = \frac{(W_C^+ - M_C^+ W_C^+) - (W_C^+ - M_C^+ W_C^+)}{(W_C^+ - M_C^+ W_C^+)} \tag{4-44}$$

or

$$\Delta W^\ddagger = 1 - \frac{W_H}{W_C^+} \left[\frac{1 - M_H^+}{1 - M_C^+}\right] \tag{4-45}$$

In the same manner, the d.a.f. fractional weight loss is calculated as

$$\Delta W^* = \frac{W_C^+(1 - M_C^+ - A_C^+) - W_H^+(1 - M_H^+ - A_H^+)}{W_C^+(1 - M_C^+ - A_C^+)} \tag{4-46}$$

or

$$\Delta W^* = 1 - \frac{W_H^+}{W_C^+} \left[\frac{1 - M_H^+ - A_H^+}{1 - M_C^+ - A_C^+}\right] \tag{4-47}$$

All mass fractions can be expressed as percentages simply by multiplying by 100. Throughout this thesis, mass fractions and weight losses expressed as percentages will be preceded by the symbol "%" (e.g., $\%A_C^*$, $\%\Delta W^{\ddagger}$, etc.).

The extent to which an element is retained in the char can be expressed in different ways. Chemical analyses yield the mass fractions of an element in the feed coal (X_C) and in the char (X_H). The mass fraction of that element in the char is normalized to mass of element in char per unit mass of feed coal with the following equation:

$$\psi_H = X_H(1-\Delta W) \quad ; \quad \left(\frac{\text{weight of element in char}}{\text{weight of feed coal}}\right) \qquad (4\text{-}48)$$

The fraction of that element retained in the pyrolyzed coal is therefore:

$$\phi_H = \psi_H / X_C \quad ; \quad \left(\frac{\text{weight of element in char}}{\text{weight of element in feed coal}}\right) \qquad (4\text{-}49)$$

where ϕ_H = fractional retention of element in char.

The elemental loss expressed as a fraction of its initial weight in the feed coal is

$$\Delta\Omega_H = (X_C - \psi_H)/X_C \quad ; \quad \left(\frac{\text{weight loss of element}}{\text{weight of element in feed coal}}\right) \qquad (4\text{-}50)$$

One advantage of ϕ_H and $\Delta\Omega_H$ is that they do not depend on the basis, a.r., m.f., or d.a.f., in which X_C and ψ_H are expressed (X_C and ψ_H must be in the same basis, of course). A disadvantage is that they do not show the actual mass fractions upon which they are based. This makes it difficult to compare intelligently the relative retentions in two coals which have very different mass fractions of a given element.

4.4 Determination of Weight Loss

Weight loss can be determined directly by weighing the feed coal and the resultant char, and using equation (4-43). This procedure is used for the batch runs.

The determination of weight loss by direct weight measurements is usually not feasible in laminar flow reactors with water-cooled collectors, since a significant fraction of the char tends to miss the collector mouth or stick to the collector walls. Therefore, an indirect method is required.

If a coal component is not released from the coal particles during devolatilization, it can be used as a tracer for the indirect calculation of weight loss. The tracer balance on an a.r. basis is:

$$\gamma_C^+ W_C^+ = \gamma_H^+ W_H^+ \qquad (4\text{-}51)$$

where

γ_C^+ = a.r. tracer mass fraction in coal

γ_H^+ = a.r. tracer mass fraction in char

Combining with equation (4-43) yields

$$\Delta W^{+} = 1 - \frac{\gamma_C^{+}}{\gamma_H^{+}} \quad . \qquad (4\text{-}52)$$

It follows that

$$\Delta W^{\ddagger} = 1 - \frac{\gamma_C^{+}}{\gamma_H^{+}} \left[\frac{1-M_H^{+}}{1-M_C^{+}}\right] \qquad (4\text{-}53)$$

or

$$\Delta W^{\ddagger} = 1 - \frac{\gamma_C^{\ddagger}}{\gamma_H^{\ddagger}} \qquad (4\text{-}54)$$

and

$$\Delta W^{*} = 1 - \frac{\gamma_C^{+}}{\gamma_H^{+}} \left[\frac{1-M_H^{+}-A_H^{+}}{1-M_C^{+}-A_C^{+}}\right] \qquad (4\text{-}55)$$

or

$$\Delta W^{*} = 1 - \frac{\gamma_C^{\ddagger}}{\gamma_H^{\ddagger}} \left[\frac{1-A_H^{\ddagger}}{1-A_C^{\ddagger}}\right] \qquad (4\text{-}56)$$

or

$$\Delta W^{*} = 1 - \frac{\gamma_C^{*}}{\gamma_H^{*}} \quad . \qquad (4\text{-}57)$$

It is obvious that, for the tracer method to be effective, the tracer must have certain properties:

1. It must have zero volatility during pyrolysis.
2. It must be homogeneously dispersed throughout the coal and char samples.
3. It must be amenable to highly accurate analysis.

The first requirement rules out all major elements and many volatile trace and minor elements. The third requirement probably rules out all trace and most minor elements. Among the major fractional components of coal, moisture and volatiles are immediately ruled out again by the first requirement. This leaves the inorganic mineral matter in the coal, or the ash.

Many investigators have used ash as a tracer in determining weight losses of pulverized coals (Nsakala, 1976; Kobayashi, 1976; Stickler _et al_., 1974; Badzioch and Hawksley, 1970; Howard and Essenhigh, 1967). When ash is used as the tracer, equation (4-56) reduces to

$$\Delta W^{*} = 1 - \frac{A^{\ddagger}}{A_H^{\ddagger}} \left[\frac{1-A_H^{\ddagger}}{1-A^{\ddagger}}\right] \quad . \qquad (4\text{-}58)$$

All researchers in the field have used the residue left after ignition of the coals and chars at 700 to 750°C (as in the ASTM ash test or its European equivalent) as the measure of the ash. All researchers except Kobayashi (1976) used the ash content (on an m.f. basis) to estimate the d.a.f. weight loss using equation (4-58).

O'Gorman and Walker (1969) found from their studies of mineral matter characteristics of American coals of various rank that there is a significant loss of CO_2 from calcite ($CaCO_3$) at temperatures between 800 and 900°C, and of H_2O

from clay [specifically kaolinite ($Al_2O_3 \cdot 2SiO_2 \cdot 2H_2O$)] at 500°C. Since most laminar flow reactors are operated at temperatures in the range 800-1500°C, it is possible that ash determinations of the feed and chars done at 750°C could lead to errors if ash is used as a tracer. For this reason, in the present study, ash content has been determined at 950°C which is 50°C higher than the highest temperature in any laminar flow reactor run.

The raw data of Badzioch et al. (1968) show consistently negative d.a.f. weight losses (i.e., they show d.a.f. weight gains) at low temperatures for most of the coals in their study. Particularly in the case of low rank coals, there appears to be a pattern whereby the weight gain decreases as the temperature increases for a given residence time. They indicated that such results were due to analytical errors in the determination of ash and to the scatter that occurs because the ash particles are, to a great extent, discrete from coal and tend to segregate on handling, e.g., in the vibrating feeder. Thus, samples collected after passing through the furnace inevitably have a more widely scattered ash yield than replicate samples of the feed coal.

Of all the investigators that have used ash as a tracer, only Kobayashi (1976) examined in depth the accuracy of the ash tracer method. However, his study covered only the high temperature range of coal devolatilization (1000 to 2100°K). Good particle recoveries, achieved as a consequence of the well-designed collector and short residence times studied, enabled Kobayashi to compare weight loss directly measured with that calculated by the use of ash as a tracer. His results, coupled with an extensive study by Padia (1976) on the behavior of coal ash under high temperature conditions, enabled him to make a quantitative determination of the extent of the error caused by the use of ash as a tracer.

According to Kobayashi (1976), possible problems associated with the method are:

1. The percentages of ash in different size fractions of pulverized coals vary in a manner that depends on the method of classification.
2. Some of the ash particles are not embedded in the coal particles but exist as separate entities.
3. The original mineral matter undergo different chemical reactions upon heating. Hence, pretreatments of coal at temperatures even lower than the ashing temperature could cause errors in estimating weight losses.
4. Significant loss of ash occurs at high temperatures due to vaporization and decomposition. Furthermore, interactions between ash and carbon could contribute to some of the weight losses of coal.

The first and second points are important in relation to the sampling techniques used for char. Inertial separation devices such as cyclones preferentially collect larger and heavier particles, which may have different ash contents compared to the average ash content of the original coal. Such problems become more serious when a significant fraction of the ash exists as separate particles, as has been observed by Littlejohn (1966).

Kobayashi (1976) used a bronze filter to collect the char particles, and water jets at the collector mouth to quench the reactions. Nevertheless, ash losses were still significant because the high flow of quenching water appeared to have forced some of the fine particles through the bronze filters, which resulted in a significant underestimation of weight losses by the ash tracer method at low decomposition rates. However, Kobayashi also reports that even though the coals used in his research were size-graded, under microscopic observation they showed some smaller particles than the size grade should have. Therefore, the direct measurement weight loss determinations could have been biased (probably only slightly) towards higher weight losses since small coal particles could also have been lost through the filter.

Separate tests done by Kobayashi under simulated flow conditions at room temperature revealed that the fraction of ash in the coal samples from the test experiment was about 15% lower than that of the original ash content. Therefore, it was recommended that the ash fraction of coal used in the ash tracer method should be that of coal particles which have experienced the same sampling process at room temperature as they would in the real experiment.

Kobayashi attempted to explain the experimental observations that weight losses of a lignite by the ash tracer method were about 5% lower than those measured directly, even when the devolatilization temperatures were lower than the ashing temperature. He postulated (based on the work of Padia, 1976) that this phenomenon was the result of differences in $CaSO_4$ formation between ashes that are produced from coals preheated in an inert atmosphere and those obtained without devolatilization. Padia (1976) conducted an extensive study of the behavior of ash under pyrolysis and combustion conditions, and he concluded that the ash produced by the ASTM method from chars pyrolyzed in an inert atmosphere should weigh 4.75% less than the ash produced from raw coal.

The fourth point does not pertain to the range of temperatures used in this research. Kobayashi observed significant ash losses due to vaporization and decomposition only for temperatures above 1250°K.

Kobayashi found that in addition to ash losses, other important sources of error or bias in weight loss determinations in laminar flow and free fall reactors are particle losses (due to particles missing collectors or going through filters and cyclones) and the formation of soot and tar. Particle losses cause high direct weight loss determinations, while soot and tar formation on the particles themselves or on the collection devices cause low direct weight loss determinations and compound the problem of ash losses by "diluting" the ash. The following equation was proposed to calculate the fractional a.r. weight loss of coal during pyrolysis:

$$\Delta W^{*} = \frac{W_C^{+} - W_R^{+} - W_{PL}^{+} - W_{AL}^{+} - W_{ST}^{+}}{W_C^{+} - W_{PL}^{+}} \qquad (4\text{-}59)$$

$$W_R^{+} = W_H^{+} + W_{ST}^{+} \qquad (4\text{-}60)$$

where W_R^{+} = weight of collected residue

W_{PL}^{+} = weight of particle losses

W_{AL}^{+} = weight of ash losses

W_{ST}^{+} = weight of soot and tar.

Thus, if particle losses, ash losses, and the deposition of soot and tar on the coal particles can be quantified, the true weight loss can be calculated. Kobayashi (1976) had to use W_R rather than W_H. He could not quantify W_{AL} and W_{ST}, and assumed that W_{PL} was negligible in his laminar flow and free fall experiments.

In conclusion, it is to be expected that weight loss determinations by the ash tracer method are biased low. A systematic examination of the effect of the ash content of the coal and errors in the ash analysis on the accuracy of the method, coupled with an experimental study of the problem, could be quite useful. Experiments at low temperatures would complement the work of Kobayashi (1976).

5. ANALYSIS OF RESULTS FROM BATCH EXPERIMENTS

The results presented and discussed in this section provide information pertaining to the devolatilization behavior of five different coals at or near thermal equilibrium. The five coals, described and characterized in Section 3.6, range in rank from a lignite to an anthracite.

5.1 Preliminary Experiments

Data from batch experiments with extremely long reaction times (hours or days) may not be applicable as a direct extension of laminar flow reactor experimental data. The objectives of these experiments were to determine the minimum time required for devolatilization reactions and elemental release to reach equilibrium in the batch reactor and to qualitatively assess observed pyrolysis phenomena in the same reactor.

Two parameters were monitored during each run - ΔW^+ and ΔS (see equations (4-43) and (4-50)). The runs were performed using small unglazed porcelain boats loaded with 100 mg of the 200x325 mesh size fractions of the coals studied. The moisture and ash content of these coals are shown in Table 5.1. The weight loss curves obtained are shown in Figure 5.1. Comparison of this figure with Figure 4.1 suggests that there is a significant lag between

Table 5.1 Moisture and ash content of batch coals

Mesh = 200x325

Coal	% M^+	%A^+
BZN	28.14	5.55
NB8	10.33	19.60
MRS	15.90	7.64
WK11	5.07	5.59
BRA	2.22	9.14

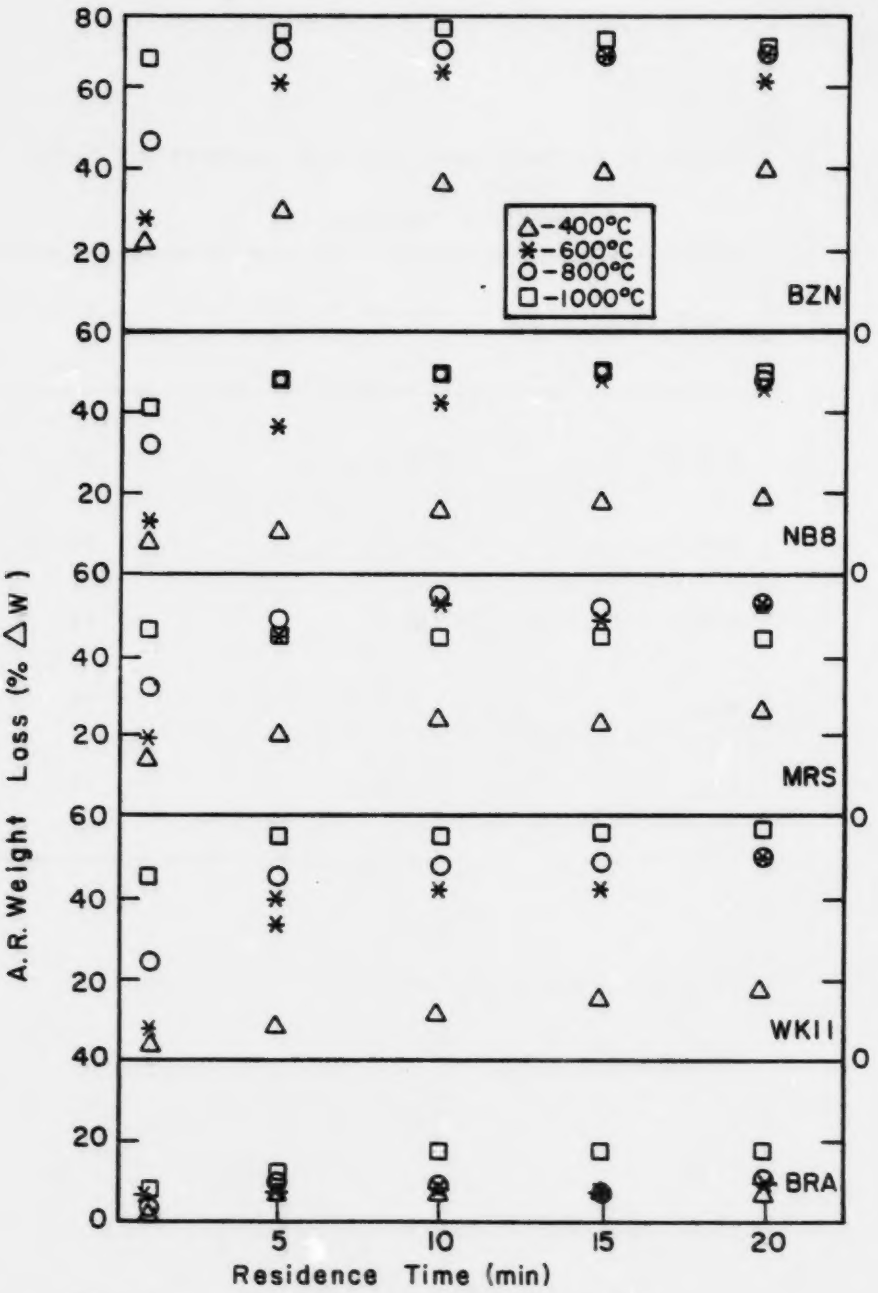

Figure 5.1 Weight Loss in Transient Batch Experiments

weight losses and the estimated temperature rise of the coal beds. First-order pyrolysis time constants can be estimated using the following equation:

$$t = \tau_{\Delta W^+}\left[-\ell n\left(1- \frac{\Delta W^+}{\Delta W^+_\infty}\right)\right] \qquad (5\text{-}1)$$

where ΔW^+_∞ = a.r. weight loss as $t \to \infty$

$\tau_{\Delta W^+}$ = devolatilization time constant.

Typical values of $\tau_{\Delta W^+}$ are 22 sec (NB8, 600°C) and 63 sec (WK11), 1000°C) which may be compared with typical τ_B values (calculated using equation (4-2)) of 0.4 sec at 600°C and 0.1 sec at 1000°C. The comparison suggests that the actual temperature rise of the coal bed may have been slower than was estimated. Furthermore, the reaction times reported in this section do not include the cooling time. Because of these uncertainties, no attempt was made to establish any kinetic parameters from these data.

Nevertheless, qualitative analysis of the data yields interesting results. All coals exhibit a dramatic increase in ΔW^+ between 400 and 600°C. Furthermore, it appears that equilibrium is reached much more rapidly at the higher temperatures. These observations are consistent with the data of Kobayashi (1976) and other researchers.

The results of the transient sulfur analyses are shown in Figure 5.2. ΔS was calculated using equation (4-50).

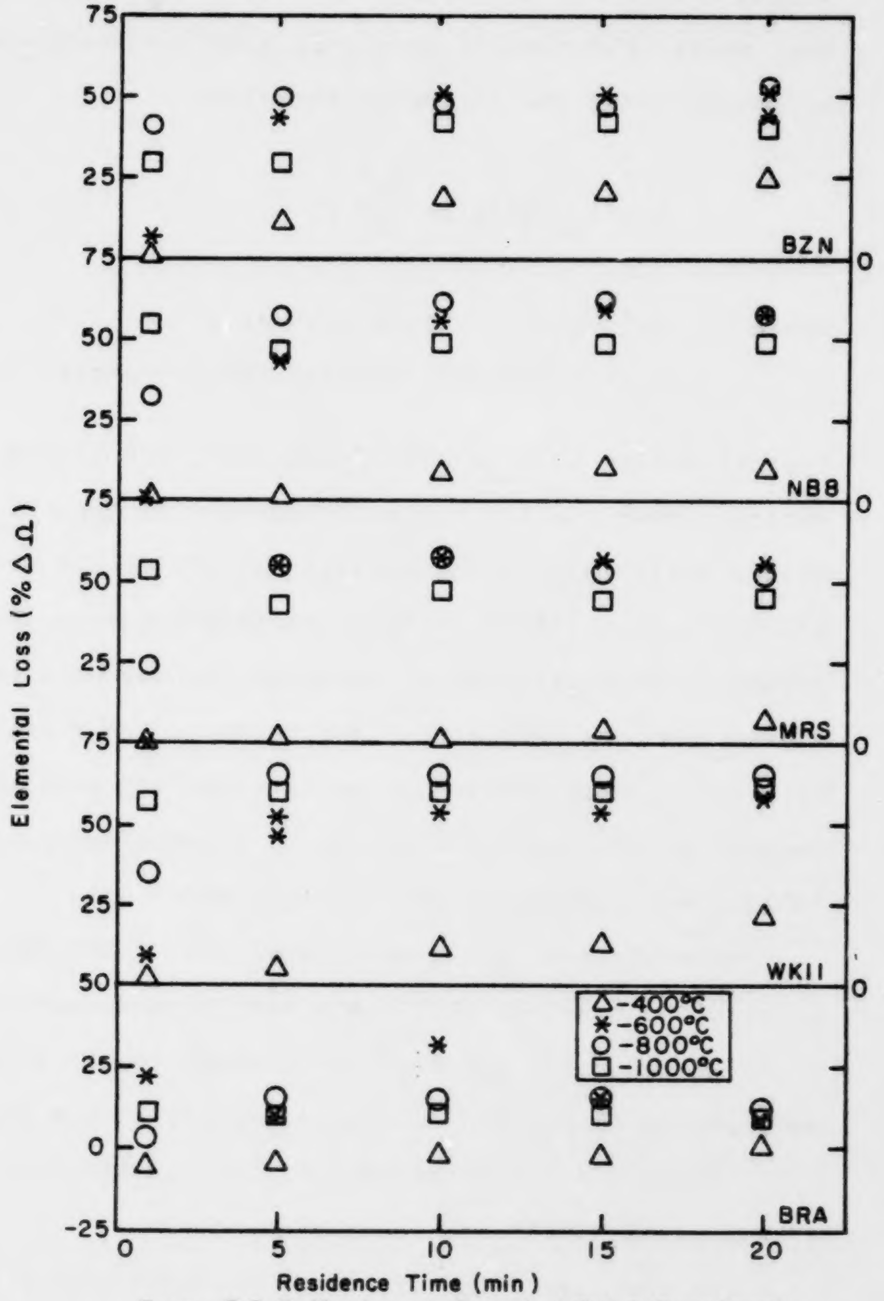

Figure 5.2 Sulfur Loss in Transient Batch Experiments

The plots show clearly the same trends as do those of ΔW^+, indicating that during the devolatilization stage of coal gasification, the rate of sulfur release is proportional to the rate of volatiles released. The high correlation between ΔS and ΔW^+ shown in Figure 5.3, holds for all coals studied. The intercept at the abscissa is close in each case to the moisture content of the feed coal ($\%M^+$), indicating that little or no sulfur evolves until the coal moisture has been driven off.

An unexpected result is shown in Figure 5.2. For each coal, the sulfur losses at 1000°C are lower than those at 800°C and in some cases at 600°C. This finding might be attributable to systematic experimental error, but its consistency from coal to coal and the rapid initial sulfur loss shown during the transient heating period appear to indicate the contrary.

The data for BRA coal are consistently scattered and erratic. However, BRA is an anthracitic coal, and it shows small devolatilization and sulfur losses. Because of the small changes observed, the errors inherent in the experiments and the chemical analyses are likely to propagate, yielding the observed scatter in the data.

Finally, a reaction time of 20 minutes was chosen for subsequent experiments. After 20 minutes, devolatilization and sulfur losses appear to have reached equilibrium at

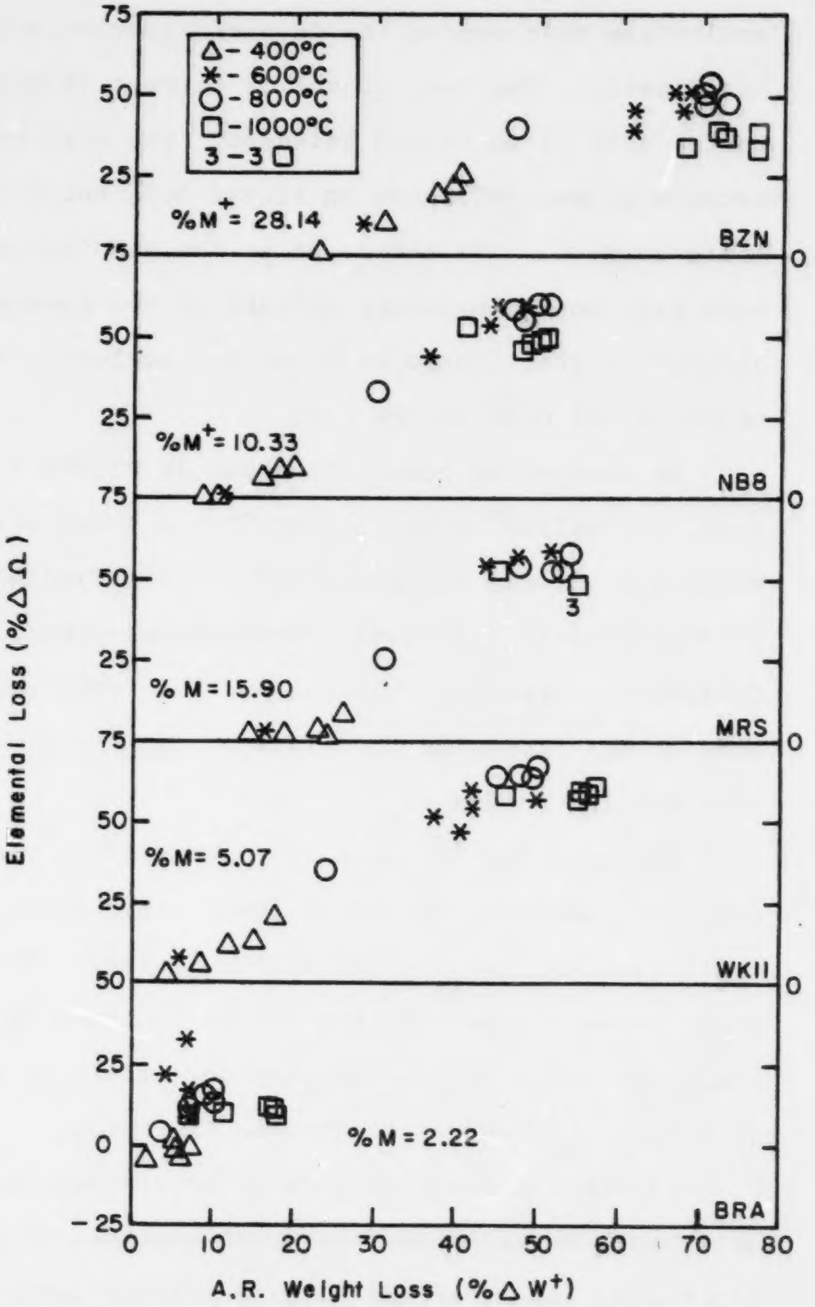

Figure 5.3 Correlation Between Sulfur and A.R. Weight Loss in Transient Batch Experiments

temperatures greater than or equal to 600°C and to closely approach equilibrium at 400°C.

The data from the experiments described above and some statistical analyses are given in Appendix B.1.

5.2 Equilibrium Batch Experiments

All equilibrium batch runs were performed with pyrolysis times of 20 minutes, using the 200x325 mesh size fractions of five feed coals. The moisture and ash contents of the feed coals are given in Table 5.1. Glazed porcelain boats were loaded with 2.0 grams of coal for each experiment. Each experiment was repeated as many times as was necessary to obtain the minimum amount of char (3 grams) required for analysis. Typically, three coal batches were pyrolyzed at each temperature. The exceptions were the 300°C runs where only one batch of each coal was pyrolyzed (the chars from these runs were analyzed only for Pb, Hg, and S). Weight losses and elemental retentions were determined as functions of temperature at essentially thermal equilibrium conditions. The results are analyzed in the following sections.

5.2.1 Analysis of Weight Loss Results

A summary of run conditions and a.r. weight loss (ΔW^{+}) results is given in Table 5.2. The reproducibility of the

Table 5.2 Equilibrium Batch Weight Loss Experiments

Run No.	Coal	T ^{o}C	$\%\Delta W^{+}$	$S_{\%\Delta W^{+}}$
B-1	BZN	400	40.81	0.25
B-2	WK11	400	16.63	0.36
B-3	NB8	400	18.15	0.14
B-4	BRA	400	2.77	0.03
B-5	MRS	400	24.79	0.89
B-6	BRA	600	3.34	0.08
B-7	NB8	600	36.36	0.15
B-8	MRS	600	41.45	0.03
B-9	BZN	600	52.68	0.07
B-10	WK11	600	39.70	0.47
B-11	BRA	800	4.45	0.21
B-12	NB8	800	41.34	0.23
B-13	MRS	800	47.81	0.70
B-14	BZN	800	63.57	1.78
B-15	WK11	800	44.98	0.25
B-16	BRA	1000	6.11	0.02
B-17	NB8	1000	44.93	0.35
B-18	MRS	1000	51.72	0.84
B-19	BZN	1000	76.19	2.63
B-20	WK11	1000	47.73	0.08
B-21	BRA	1200	7.04	0.02
B-22	NB8	1200	51.29	0.85
B-23	BZN	1200	89.87	2.62
B-24	MRS	1200	64.27	0.76
B-25	WK11	1200	49.29	0.11
B-26	BRA	300	2.66	no reps
B-27	NB8	300	11.66	no reps
B-28	BZN	300	31.32	no reps
B-29	WK11	300	6.55	no reps
B-30	MRS	300	18.40	no reps

weight loss data was extremely good, as evidenced by the standard deviations shown in the table. The average devolatilization a.r. weight losses are shown in Figure 5.4. Weight losses calculated in m.f. and d.a.f. bases are listed in Appendix B.1.

The weight loss data shown in Figure 5.4 depict the characteristic devolatilization bahavior of coals pyrolyzed in batch reactors. Moisture evolution occurs at 100°C, devolatilization begins at about 350°C, and most of the weight loss occurs between 400 and 750°C. The lignite (BZN) exhibits the largest devolatilization weight loss, and the anthracite (BRA) exhibits the smallest. Subbituminous and bituminous coals (NB8, MRS, and WK11) exhibit intermediate weight losses.

Data obtained by Suuberg _et_ _al_. (1978) for the pyrolysis of Montana lignite in a strip wire-screen batch reactor are shown in Figure 5.5. These data are quite similar to the a.r. weight loss data of the MRS coal shown in Figure 5.4. The same pattern is apparent: moisture evolution occurs first, devolatilization begins at about 350°C, and most of the weight loss occurs between 400 and 750°C. However, quantitative comparison of a.r. weight losses is difficult because of the differing moisture and ash contents of the feed coals used in the two studies. Dry ash-free weight losses calculated from the data of Suuberg _et_ _al_.

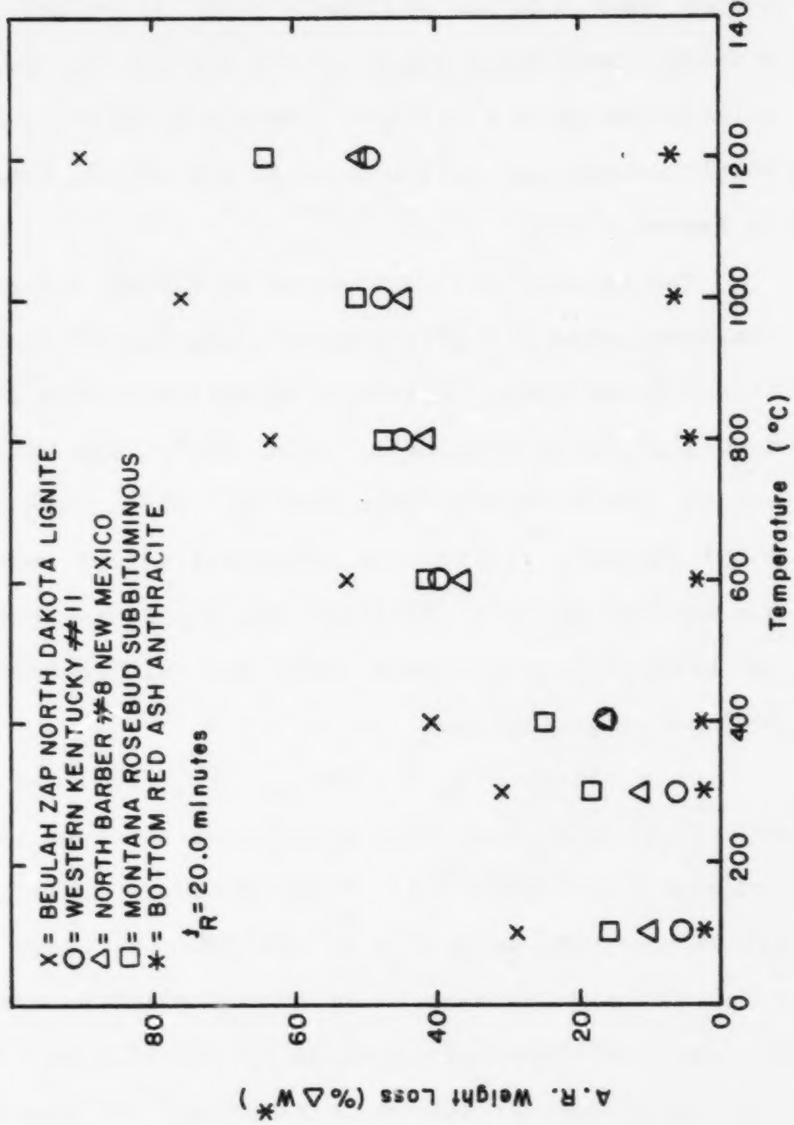

Figure 5.4 A.R. Weight Loss in Equilibrium Batch Experiments

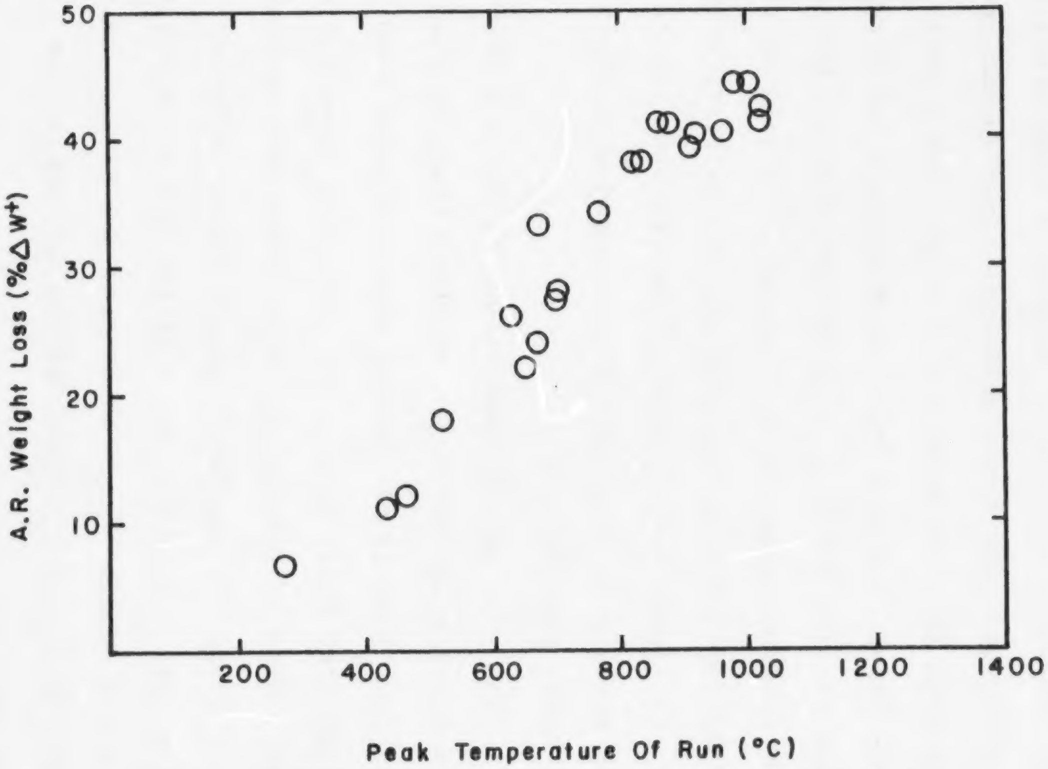

Figure 5.5 Weight Loss of Partially Dried Montana Lignite From Suuberg *et al.* (1978)

(1978) and from this study are compared in Figure 5.6. The agreement is good considering that the two experiments are fundamentally different. Suuberg's experiments were carried out with short residence times (about one second) and high heating rates (10^3 °C/sec) (i.e., fast pyrolysis in a batch reactor), while this study's batch experiments were carried out with long residence times (20 minutes) and low heating rates (5 to 45°C/sec). It will be shown in a later section that the lower batch fast pyrolysis values of ΔW^* in Figure 5.6 are consistent with the LFR fast pyrolysis results of this investigation and with the findings of other researchers.

The a.r. weight loss values at 450 and 700°C in Figure 5.4 agree qualitatively with those found by Kuhn _et_ _al_. (1977) for coals of similar ranks as those used in this study (see Table 2.1). The residence times and heating rates used by Kuhn _et_ _al_. were comparable to those used in this study for the batch experiments. Unfortunately, Kuhn _et_ _al_. do not report the moisture and ash content of the coals in their study: therefore, the precise calculation of their d.a.f. weight loss values for comparison purposes is not possible.

Comparison of the batch equilibrium a.r. weight losses with the asymptotic weight losses at each temperature in the transient batch experiments reveals that WK11 and BRA

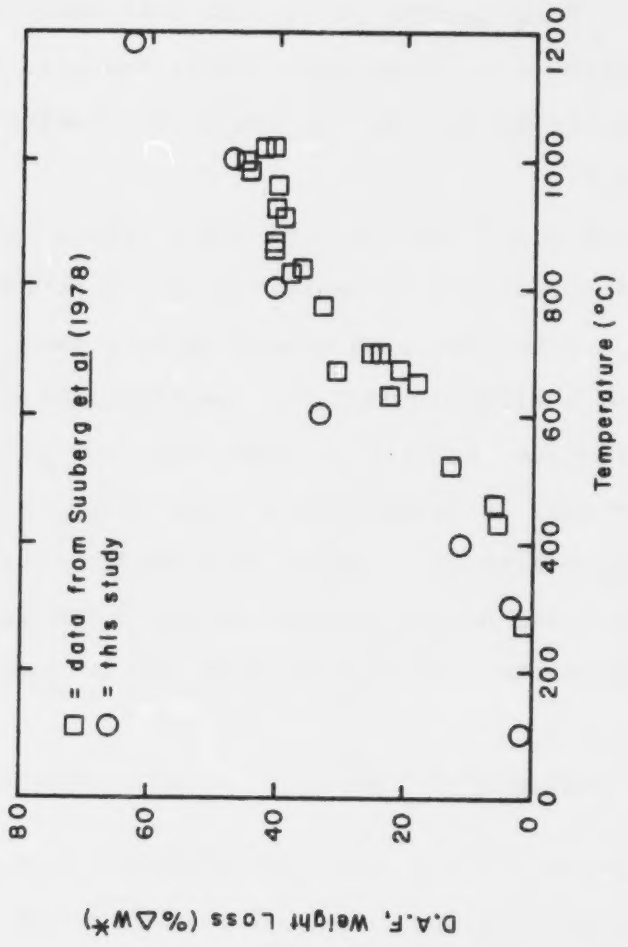

Figure 5.6 Comparison of D.A.F. Weight Loss Data for MRS Coal

coals had larger weight losses in the transient experiments. This effect is probably due in part to the change in bed depth from several millimeters in the transient experiments to over one centimeter in the equilibrium experiments. This is consistent with that observed by many researchers (e.g., Kobayashi, 1976; Nsakala, 1976) for coals with ranks higher than or equal to bituminous (such as WK11 and BRA).

The d.a.f. weight loss (ΔW^*) versus temperature curve for each coal was curve-fitted with a fourth-order polynomial. The resulting equations were used in the development of a kinetic model for devolatilization in the laminar flow reactor, as will be described in a later section. The Statistical Analysis System (SAS) computer program used for the curve-fitting is given in Appendix A.1. The statistical analysis of the regression and comparisons of the curve-fits with the experimental data are in Appendix B.1.

5.2.2 Analysis of Elemental Release Results

Fifteen trace and minor elements were analyzed in the feed coals and chars produced in these experiments. In order to determine the behavior of trace elements as a function of temperature, a simple statistical analysis was carried out. The quantities X_H, ψ_H, ϕ_H, and $\Delta\Omega_H$ on as-received and moisture free bases (see Section 4.3) were calculated for each coal and char elemental mass fraction, and were then linearly regressed against T. Coefficients of determination and Student's-t values (used to determine whether the slope is significantly different from zero) were also calculated. All calculations were done with computer program BATCH, shown in Appendix A.1. The calculated data are given in Appendix B.1.

The significant element-temperature correlations are summarized in Table 5.3. The variations of the different parameters (X_H, ψ_H, and ϕ_H) with T can be used to infer certain types of elemental devolatilization behavior. The interpretation of the regression results are as follows:

1. If $X_H^{\ddagger}$ versus T has a slope significantly greater than zero (indicating that the char is becoming progressively enriched in the element), and $\psi_H^{\ddagger}$ versus T has a slope equal to zero (indicating that the absolute amount of element in the char is remaining constant), it is deduced that the element is completely retained in the char.
2. If the slope of $X_H^{\ddagger}$ versus T is greater than zero, and that of $\psi_H^{\ddagger}$ versus T is less than zero, the element's release from the coal is significant. Furthermore, the element is released at a proportionately lower rate than the total volatile matter.

Table 5.3 Significant Element-Temperature Correlations for Batch Pyrolysis

Coal	NB8			WKII			BZN			BRA			MRS		
Parameter Element	$X^{\ddagger}$	$\Psi^{\ddagger}$	$\emptyset_H$	$X^{\ddagger}$	$\Psi^{\ddagger}$	$\emptyset_H$	$X^{\ddagger}$	$\Psi^{\ddagger}$	$\emptyset_H$	$X^{\ddagger}$	$\Psi^{\ddagger}$	$\emptyset_H$	$X^{\ddagger}$	$\Psi^{\ddagger}$	$\emptyset_H$
Sm	+ **			+ *	− *		+ *						+ *		
Sb															
As			− Δ			− Δ	+ *		− Δ			− Δ			
Se			− Δ			− Δ			− Δ			− Δ	+ *		
V													+ *		
Cl			− Δ			− Δ	− *	− **	− **	− *	− *	− *		− *	− x
La	+ *			+ *		− Δ	− *		− Δ				+ *	− *	− *
Th	+ **			+ *									+ *		
Cr				+ *											
Sc	+ *			+ **			+ **						+ *		
Fe	+ **			+ **			+ *						+ *		
Co	+ **			+ *				− *	− *						
Hg	− *	− *	− *		− *	− *		− *	− *			− Δ			− Δ
Pb	− **	− **	− **		− **	− **		− **	− **			− Δ	− **	− **	− **
S	− *	− **	− **	− **	− **	− **		− **	− **	− *	− **	− **		− **	− **

* = significant@ 95%C.L.
** = significant@ 99%C.L.
Δ = undetected trend
+ = positively correlated (slope >0)
− = negatively correlated (slope < 0)

3. If the slope of $X_H^{\ddagger}$ versus T is equal to zero, and that of $\psi_H^{\ddagger}$ versus T is less than zero, the element's release is significant and occurs at the same rate as ΔW versus T.
4. If the slope of $X_H^{\ddagger}$ versus T is less than zero, and that of $\psi_H^{\ddagger}$ versus T is also less than zero, the element's release from the coal is significant and the element is released at a higher proportional rate than the total volatile matter.
5. If the slope of ϕ_H versus temperature is equal to zero (indicating that no appreciable amounts of that element have been released), the element is not volatile. If it is less than zero, the element is volatile. The behavior of ϕ_H simply mirrors that of ψ_H, but, more importantly, it allows easy visual examination of the data. Since ϕ_H must range from 1.0 (complete retention) to 0.0 (no retention), its value quickly indicates whether the element is retained entirely in the char or not. This is useful because the linear regression analyses only detect consistent trends. If a retention (ϕ_H) drops at low temperatures and then remains at a constant value, no linear trend would be found; nevertheless, it would be obvious that the element had been released from the coal.
6. If no significant correlations are found for a given element, it must be concluded that the scatter in the

data is too large for any trend to be detected with the statistical analyses used. A conservative statistical criterion based on the two-tailed Student's t-test was used to determine the significance level of the trends.

The statistical analyses must be used with caution, however, as they only detect consistent trends. As indicated above, if a retention (ϕ_H) drops to low values at low temperatures, no linear trend would be found. Another problem may be caused by the presence of clear outliers, which may force rejection of clearly significant trends. Cases where the linear regression analyses missed a drop in ϕ_H have been marked as such in Table 5.3. Visual inspection of the reduced data (shown in Appendix B.1.) showed that rapid decreases in ϕ_H for Hg, As, La, Cl, and Se were not detected in a few cases. In general, however, the statistical analyses proved to be accurate.

Reproducibility problems were encountered in all batch experiments with Bottom Red Ash anthracite. The extreme scatter in the data made it possible to detect only the most obvious trends, and the precision problems due to the low weight and elemental losses of the anthracite were compounded by chemical analysis problems. Because of the problems encountered with BRA, some of the following generalizations may not apply to this particular coal.

It has been established that Sm, Cr, Th, Sc, Fe, and Co are retained completely in the chars produced in the batch pyrolysis experiments with nitrogen over a temperature range of 25 to 1200^{o}C. As illustrations, the mass fractions (X_{II}^{+} and ψ_{II}^{+}) of Fe and Sc are plotted versus temperature in Figures 5.7 and 5.8. La, Se, and As exhibit intermediate volatility (<40% release); however, the scatter in the data for La make this conclusion suspect, as will be discussed later. Finally, S, Pb, Hg, and Cl are highly volatile (>50% release). Mercury and chlorine show losses greater than 70% at temperatures below 700^{o}C, and more than 75% of the lead is released at temperatures above 1000^{o}C. Figures 5.9 to 5.12 show mass fractions (X_{II}^{+} and ψ_{II}^{+}) of S, Pb, Hg, and Cl as functions of temperature. The mass fractions of chlorine were found to be below the neutron activation analysis detection limit in some chars. The estimated upper limits for those mass fractions are shown in Figure 5.12. The data for V and Sb were too scattered for any conclusions to be reached.

The results found in this research agree to a substantial extent with the findings of Kuhn et al. (1978), who analyzed the chars produced during the pyrolysis of several coals heated in steps to 450 and 700^{o}C in a nitrogen atmosphere (see Section 2.6.6). Kuhn's results for the elements investigated in this study were: 1. Cr, Th, Sc,

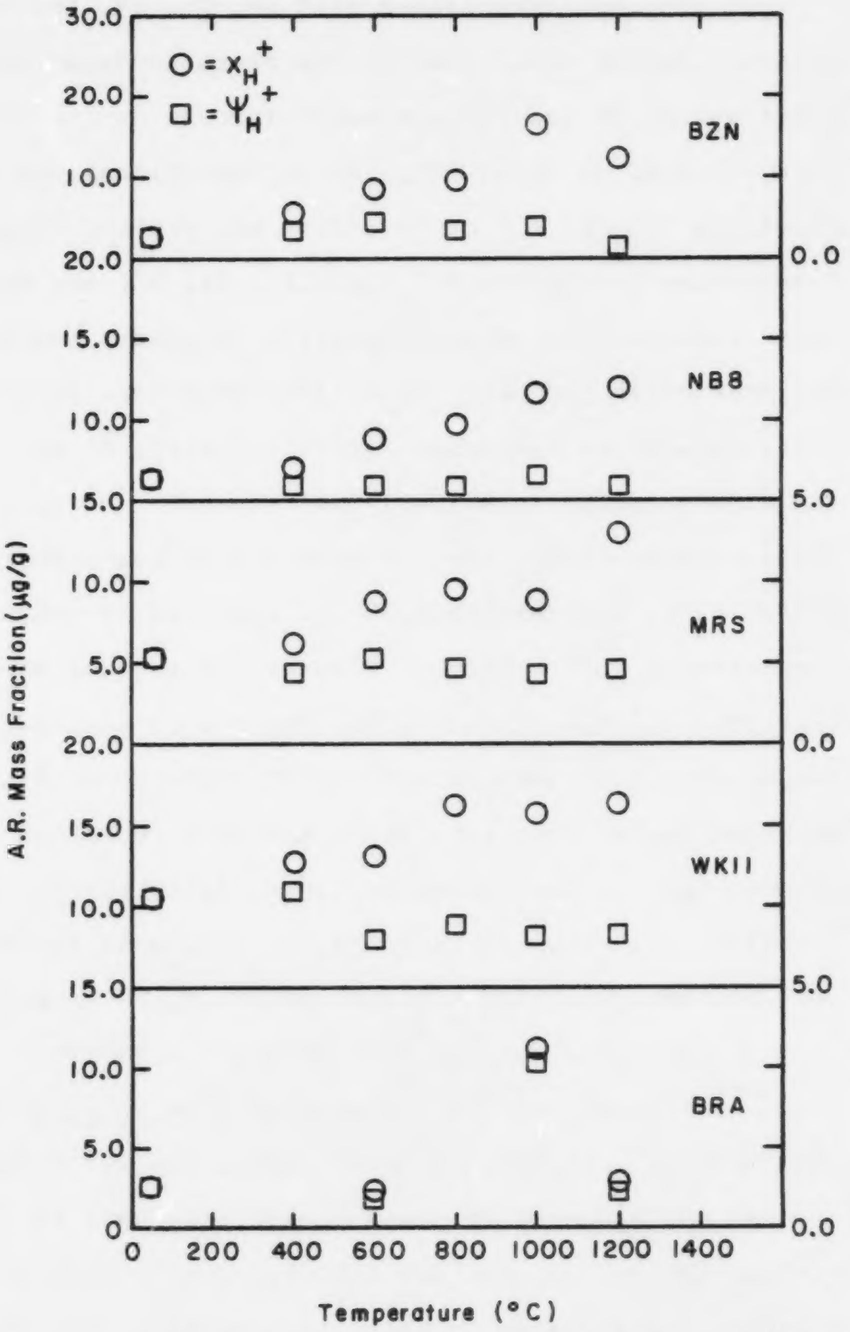

Figure 5.7 Iron Mass Fraction in Batch Chars

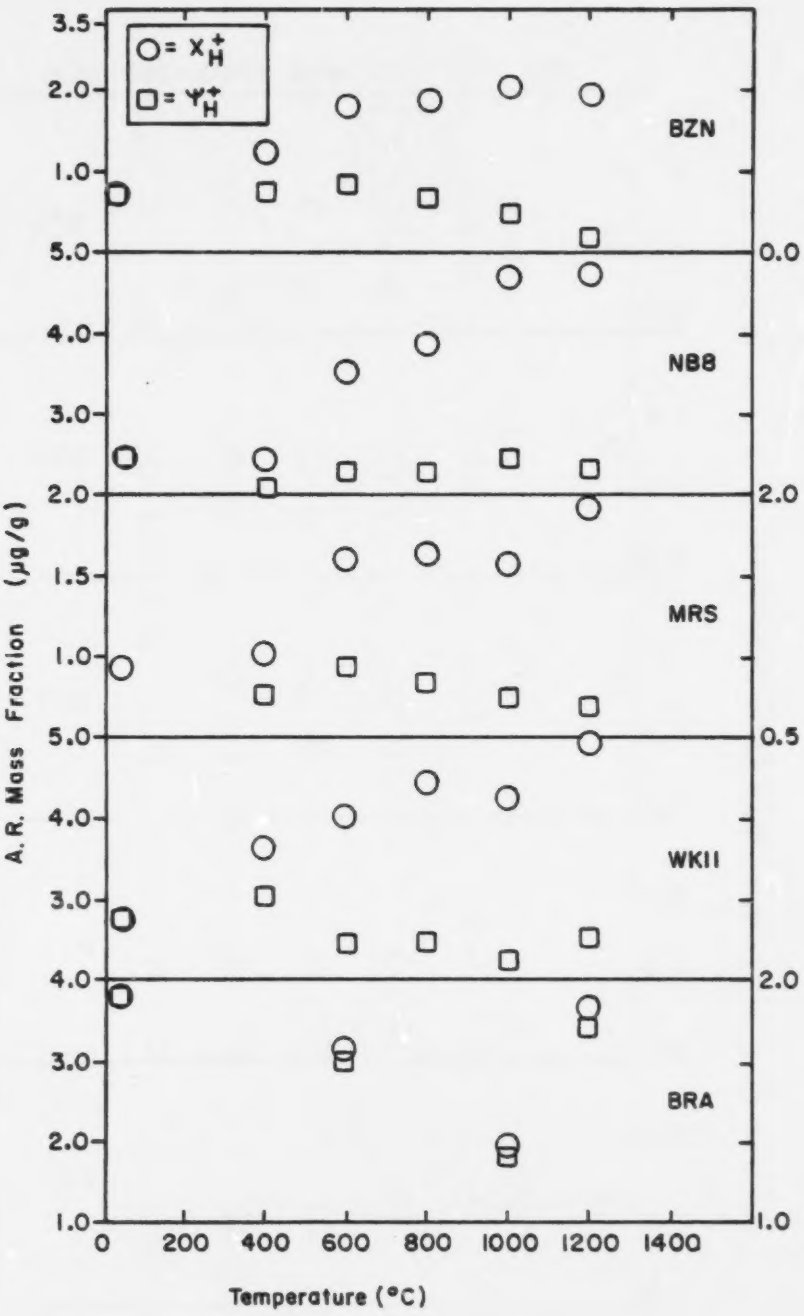

Figure 5.8 Scandium Mass Fraction in Batch Chars

F

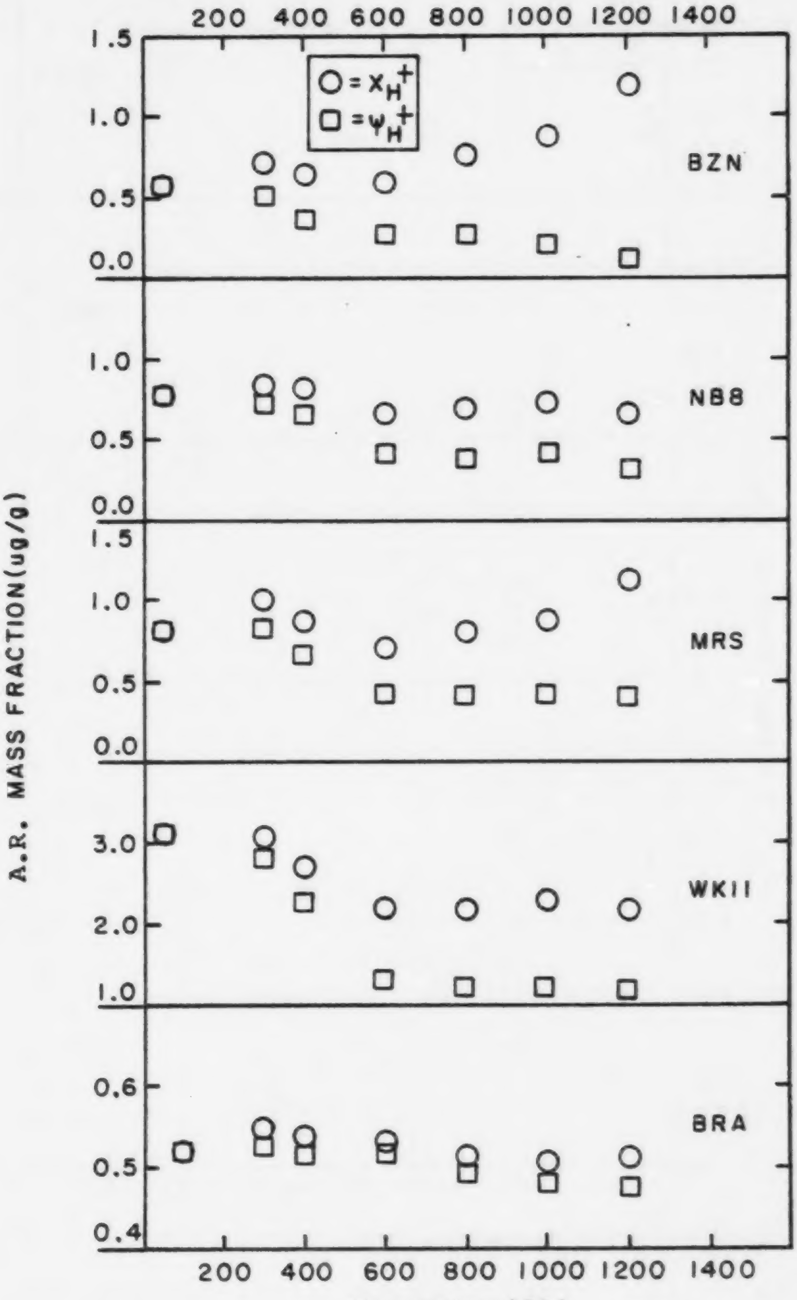

Figure 5.9 Sulfur Mass Fraction in Batch Chars

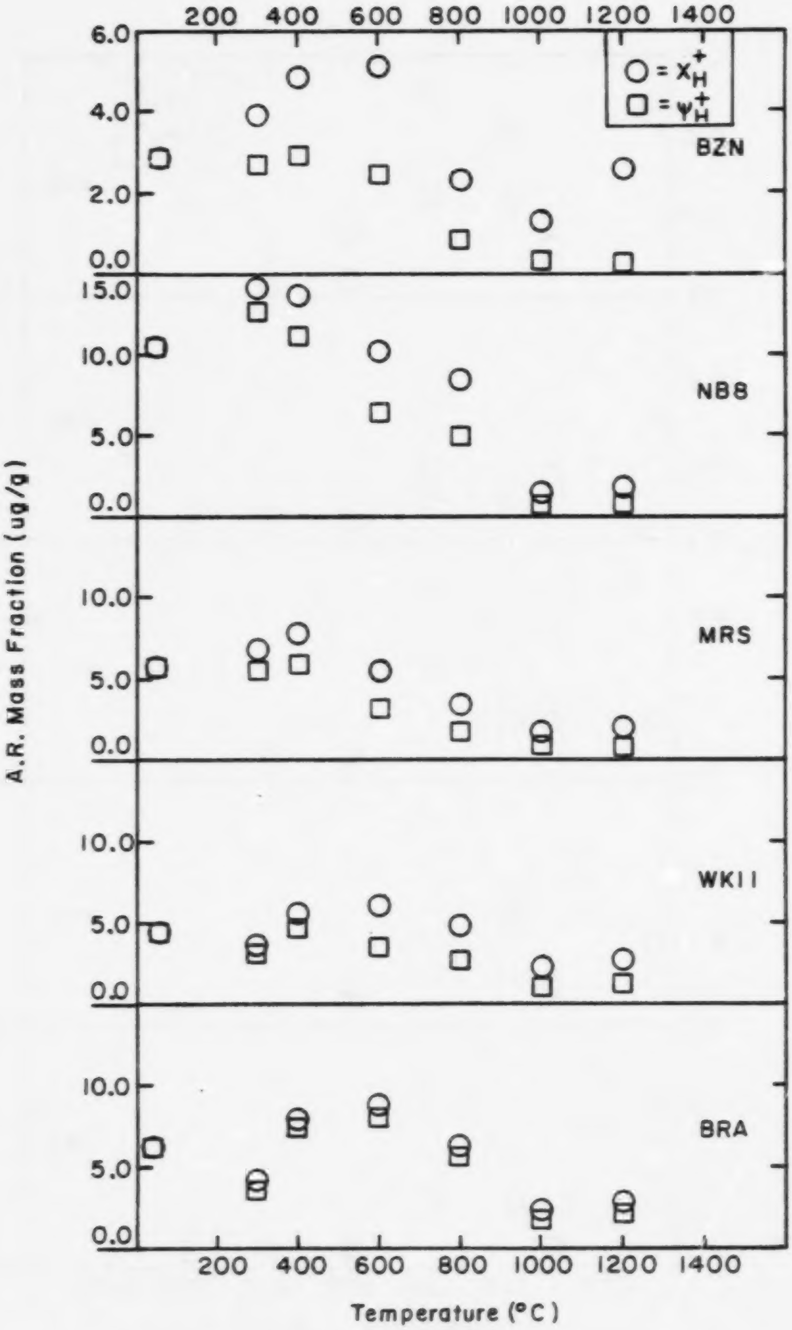

Figure 5.10 Lead Mass Fraction in Batch Chars

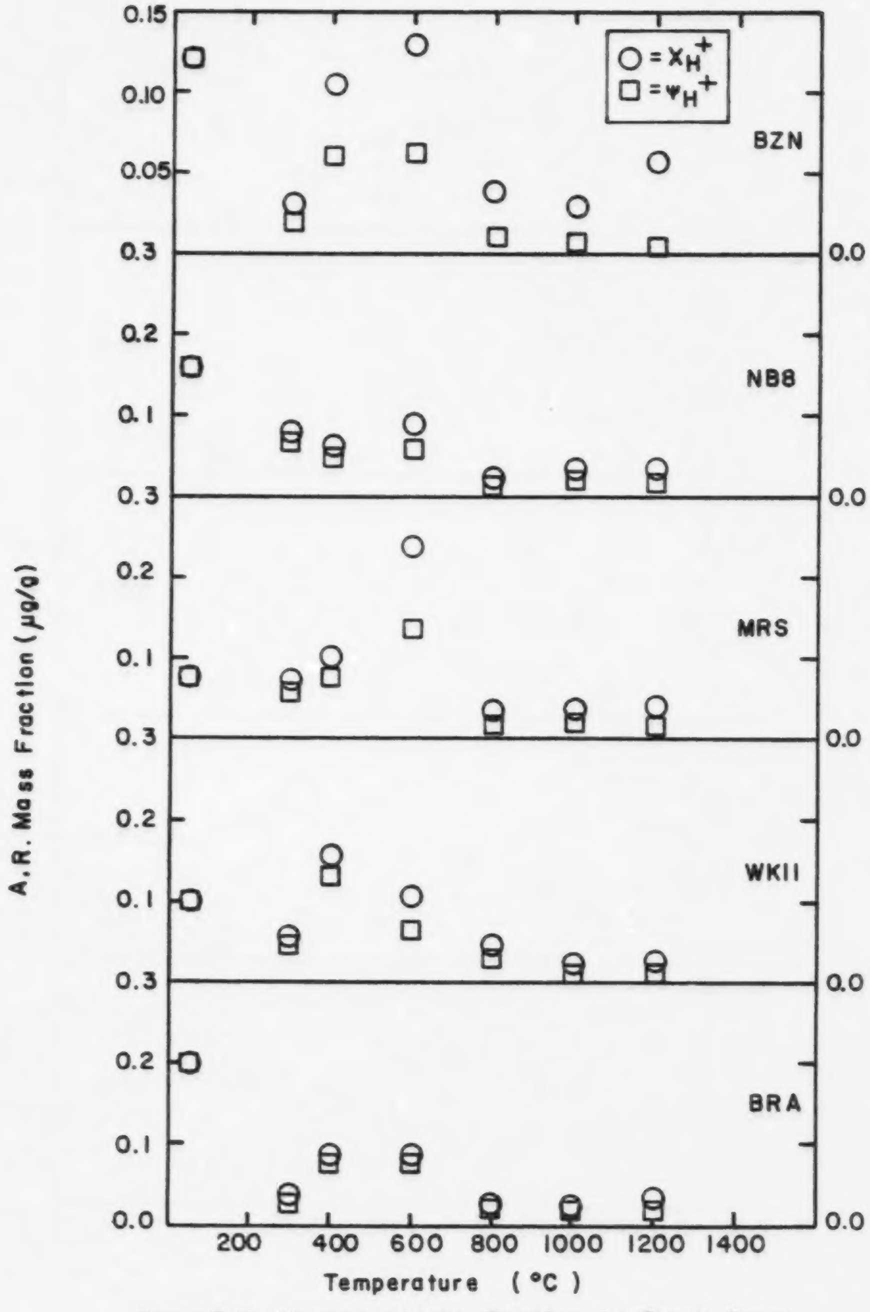

Figure 5.11 Mercury Mass Fraction in Batch Chars

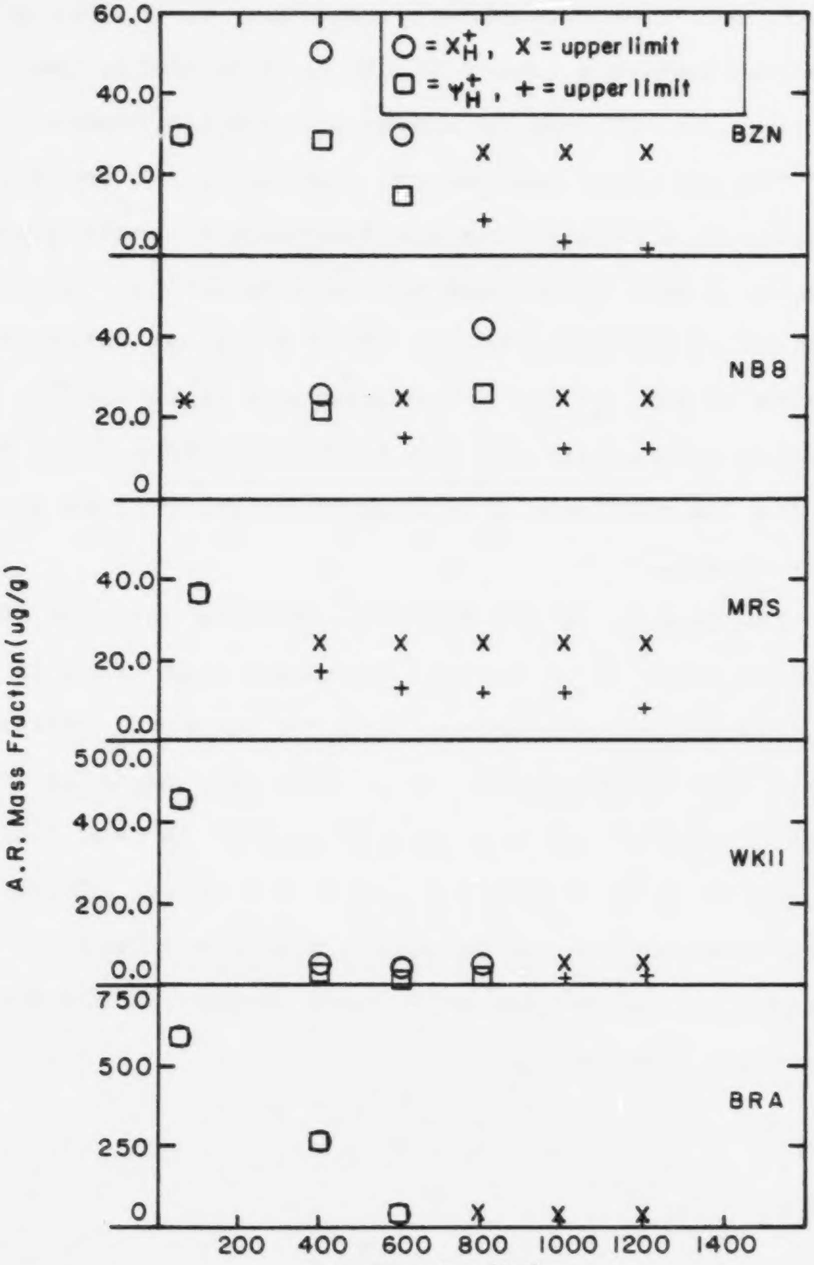

Figure 5.12 Chlorine Mass Fraction in Batch Chars

Fe, Co, and V were completely retained; 2. La, Sb, and Sm showed moderate losses (<30%) in some coals, and 3. Cl, S, As, Pb, and Se showed significant losses (>30%).

The agreement between the results of the two studies is gratifying considering the diversity of coals studied. It appears that trace elements tend to exhibit the same behavior in different coals. This study has extended the results of Kuhn et al. to temperatures up to 1200°C, and provides enough data for the development of a model describing the equilibrium release of volatile trace and minor elements.

Examination of the elemental release data for the elements found to be volatile suggests that there is a critical temperature above which the elemental release begins. Once this temperature is reached, the value of ψ_H (mass of element in char/mass of element in feed coal) decreases until an asymptotic limit is reached. These observations suggest the following simple mathematical model to describe the release of a given element from a coal undergoing pyrolysis.

$$\psi_H = \begin{cases} X_C , & T<T_C \\ X_C f(T) , & T \geq T_C \end{cases} \tag{5-2}$$

where X_C = mass fraction of element in feed coal

ψ_H = mass of element in char per unit mass of feed coal

T_C = critical temperature at which elemental release begins

or in terms of the fractional retention ϕ_H (mass of element in char/mass of element in feed coal)

$$\phi_H = 1 + H(T - T_C)\cdot\{f(T-T_C) - 1\} \qquad (5\text{-}3)$$

where

$H(T - T_C)$ = unit step function

$$\phi_H = \psi_H / X_C \, . \qquad (4\text{-}49)$$

An equation capable of correlating the data for all elements with intermediate and high volatility is:

$$f(T-T_C) = 1 - \Delta\Omega_e\left[1-e^{-b(T-T_C)}\right] \qquad (5\text{-}4)$$

where

$\Delta\Omega_e$ = asymptotic fractional elemental release

b = constant .

The asymptotic fractional elemental release ($\Delta\Omega_e$) was estimated by linear regression of the equation

$$\Delta\Omega_H = \frac{d}{T} + \Delta\Omega_e \, , \quad \Delta\Omega_H \geq 0.67\Delta\Omega_e \qquad (5\text{-}5)$$

where

d = constant

$\Delta\Omega_e = \Delta\Omega_H$, $T \rightarrow \infty$.

Duhne (1977) has shown that estimates of asymptotic equilibrium values for physical and chemical processes can be obtained from linear regression of an equation of the form of equation (5-5). If the highest value of $\Delta\Omega_H$ for each element is assumed to be very close to $\Delta\Omega_e$, the requirement that the data lie within 33% of the equilibrium point (relative to a total range between zero and equilibrium) is usually satisfied if the highest three points for each element and coal are used.

Least squares estimation of b and T_C in equation (5-4) tends to yield values of T_C below room temperature for Se and Hg. The following equation was found to correlate the data close to T_C for all elements with data close to T_C, and so provided a basis for estimating this parameter:

$$\phi_H = a_1 + a_2 \ln(T) \quad , \quad \phi_H < 1.0 \qquad (5-6)$$

where

a_1, a_2 = constants

The constants a_1 and a_2 were determined from least squares regression of ϕ_H and $\ln(T)$ for experimental values of $\phi_H < 1.0$. The critical temperature was then calculated by setting $\phi_H(T_C) = 1.0$. This projection of the decay of ϕ_H to the critical temperature is not influenced by the value of the asymptotic retention $(1-\Delta\Omega_e)$.

This procedure was used to determine T_C for H_g, Cl, Pb, and S. However, it could not be used to determine T_C

for As and Se because of lack of data at 300°C. Because of the chemical similarity between those two elements and sulfur, the value of T_C determined for sulfur was also used for As and Se.

Marquardt's (1963) algorithm for nonlinear regression was used to estimate the parameter b of equation (5-4). Clear outliers (e.g., large negative values of $\Delta\Omega_{II}$), mass fractions below the detection limit (e.g., chlorine data at high temperature), and the data for sulfur in the anthracite (BRA coal) (which was markedly different from that for the lower rank coals) were not used in the regression. The parameter b could have been obtained from simple linear regression; Marquardt's algorithm was used only as a matter of convenience since data plots and statistical analysis of the regression could be obtained with a SAS program used extensively in this study. This program (BMOD) is listed in Appendix A.1; a listing of the data used and the statistical analysis of the regression are in Appendix B.1.

The parameters of the elemental retention model (equations (5-3) and (5-4)) are listed in Table 5.4. Comparisons between the model predictions and the experimental data for As, S, Pb, and Hg are shown in Figures 5.13 to 5.16. The model provides a good description of the experimental data for five coals with a single set of parameters for each element (except for sulfur in BRA). This result by

Table 5.4 Equilibrium Elemental Release Model Parameters

Element	T_C °C	$\Delta\Omega_e$ %	b 1/°C
As	223	66.3	8.83×10^{-4}
Se	223	55.4	48.21×10^{-4}
Pb	499	100.0	26.57×10^{-4}
S	223	77.1	20.08×10^{-4}
Cl	234	100.0	39.42×10^{-4}
Hg	110	97.3	25.81×10^{-4}

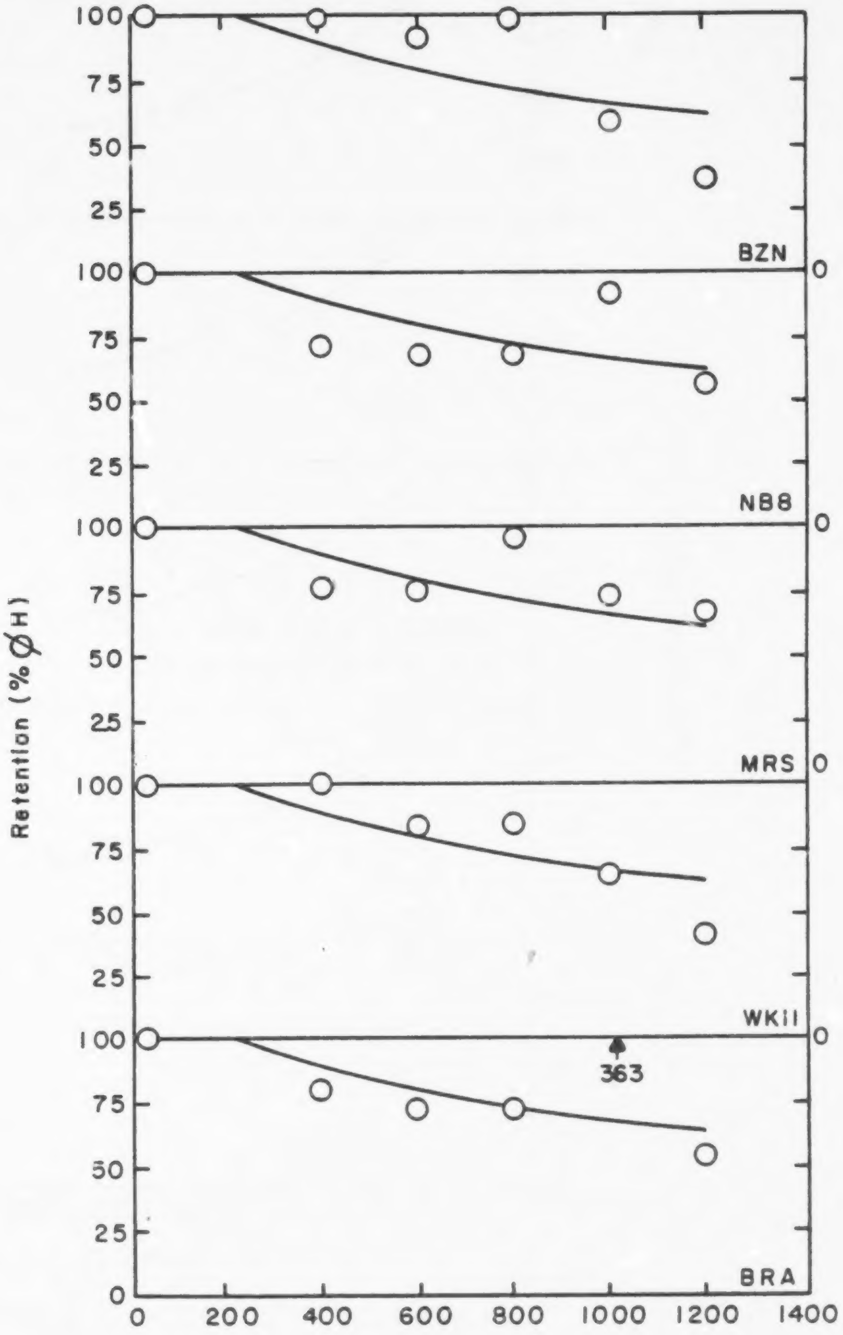

Figure 5.13 Arsenic Retention in Batch Chars

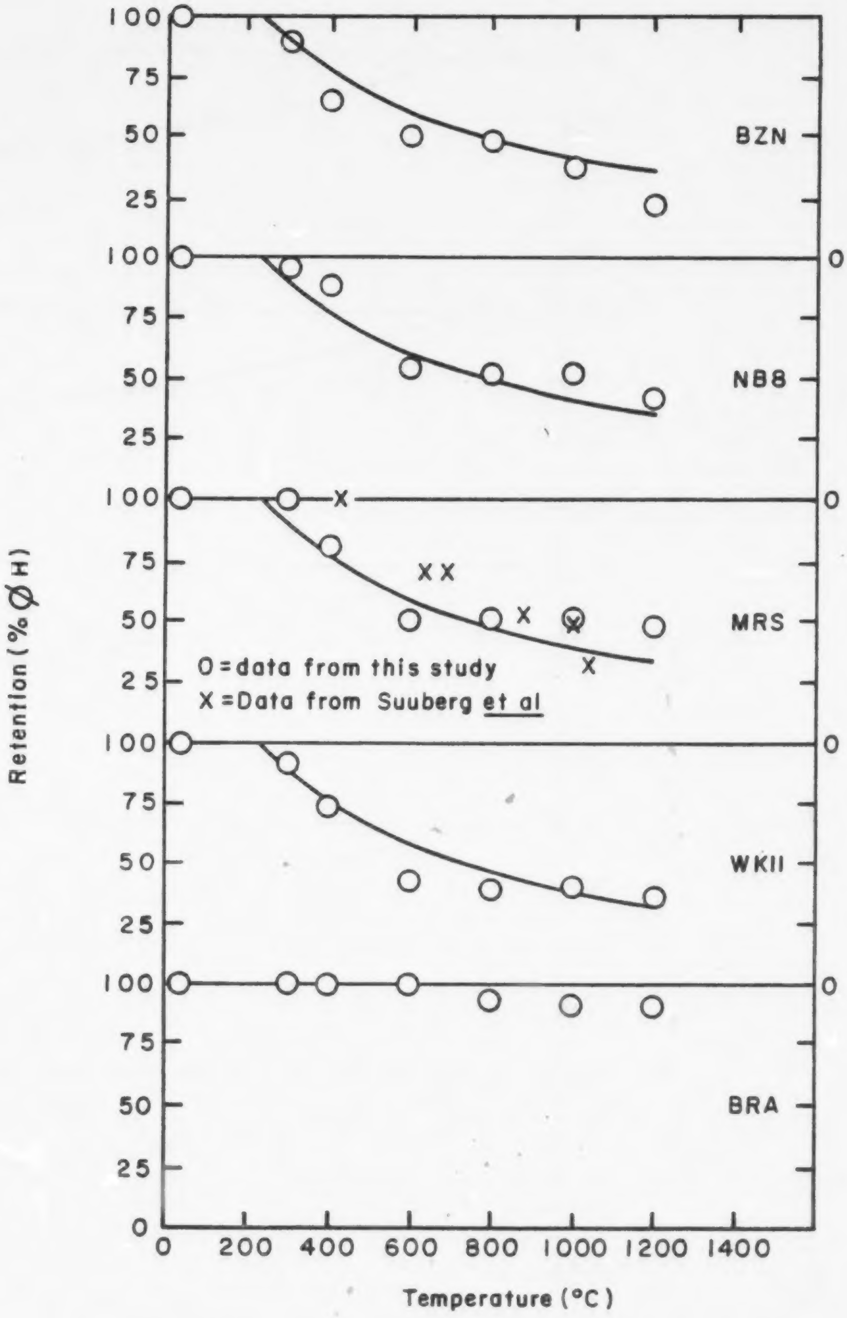

Figure 5.14 Sulfur Retention in Batch Chars

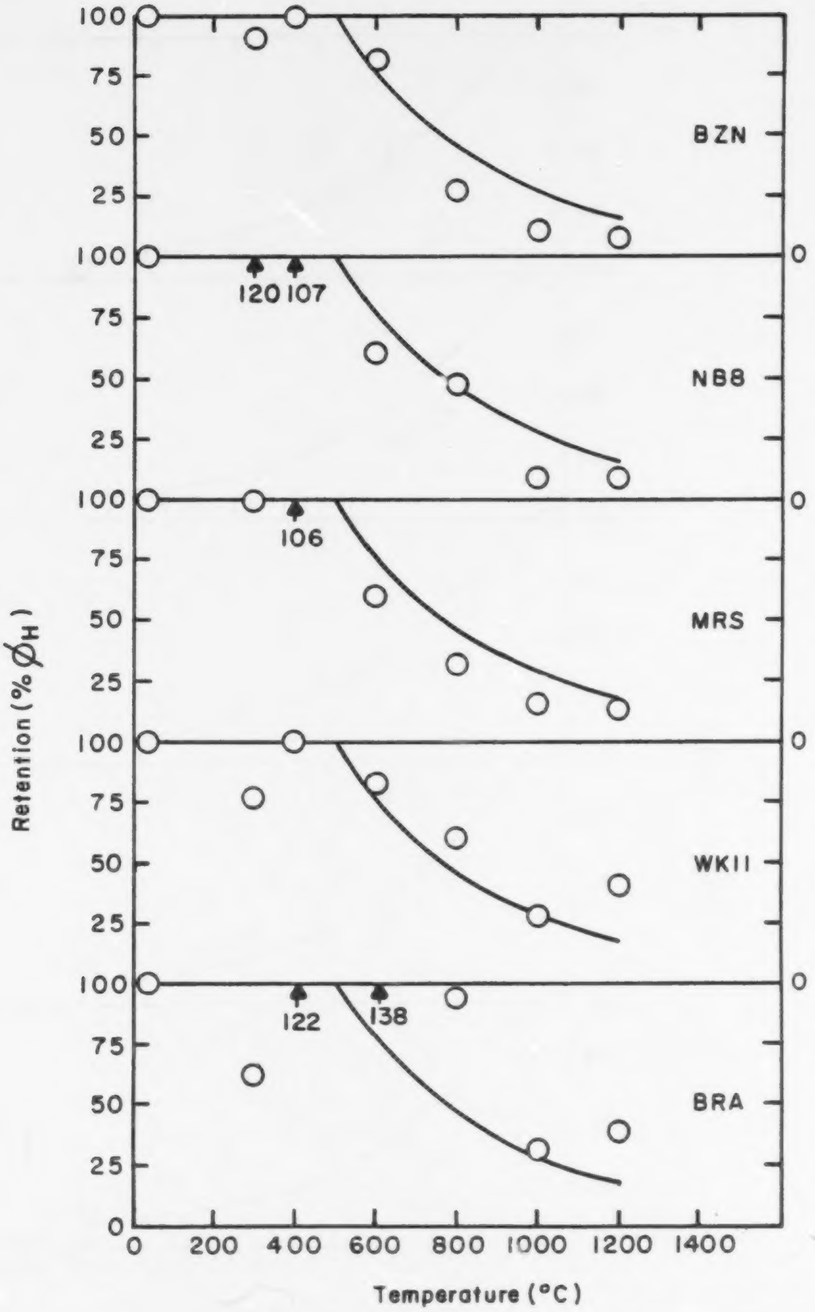

Figure 5.15 Lead Retention in Batch Chars

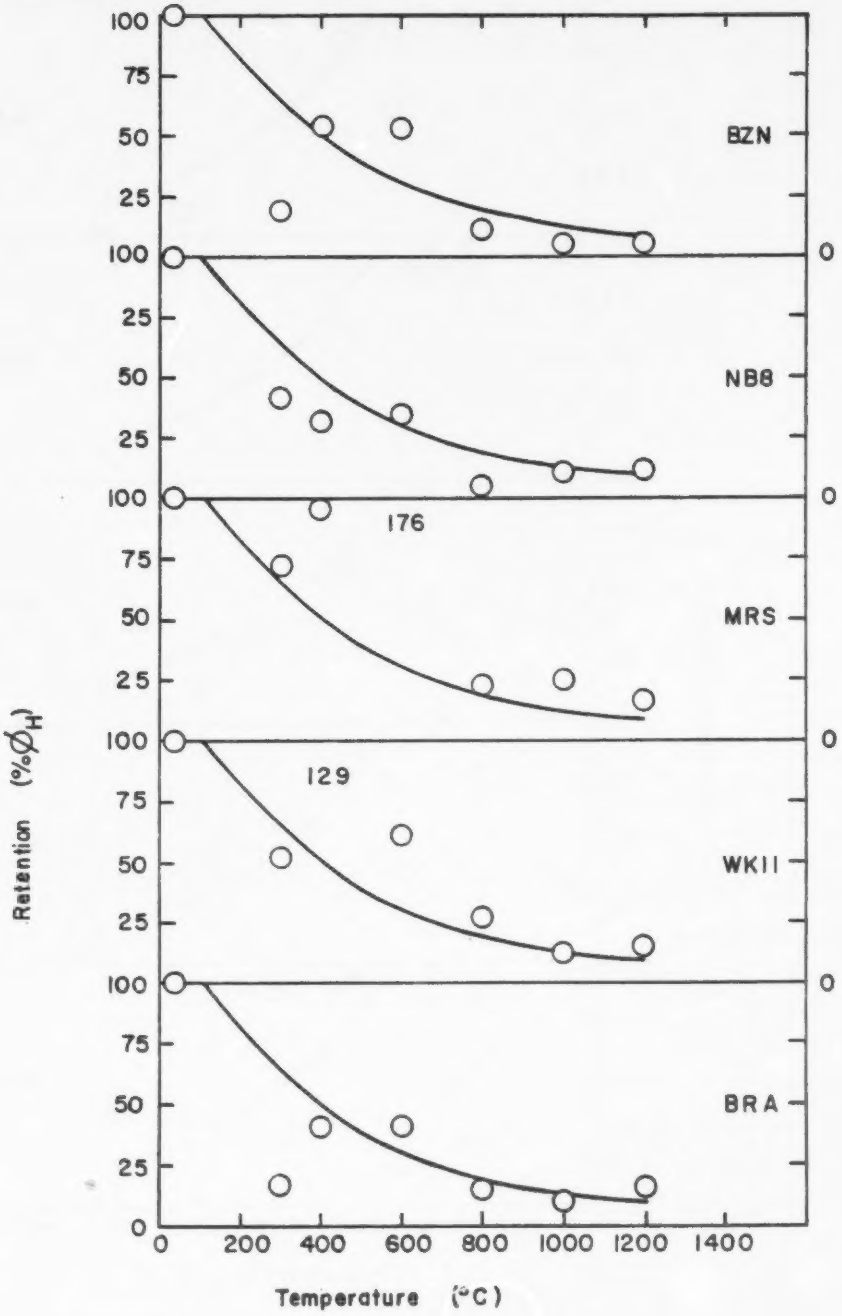

Figure 5.16 Mercury Retention in Batch Chars

itself constitutes a significant finding, in that it indicates that trace elements tend to behave in the same manner during the pyrolysis of coals regardless of their rank, with the exception of sulfur in anthracite. Therefore, the model should provide excellent engineering estimates of the extent of volatile trace and minor element release as a function of temperature during the devolatilization stage of any gasification process.

Figure 5.14 shows the similarity between the data obtained in this study and that obtained by Suuberg et al. (1978) for Montana lignite during wire screen batch experiments. The model developed in this study provides a fair description of such data. The arsenic retention data obtained in this study agree closely with the arsenic retentions determined by Duck and Himus (1951) for four coals carbonized at eight temperatures (ranging from 290 to 1050°C).

The sulfur release determined in this study agrees with the findings of Kuhn et al. (1977) who reported that most of the sulfur is lost between 300 and 400°C. They report a 66% loss of sulfur at 700°C. Kuhn et al. indicated that most of the coals in their study showed similar behavior; however, the results of this study indicate that sulfur is evolved to a much lesser extent, at a given temperature, in anthracite. The weight and sulfur loss data from the transient experiments (shown in Figure 5.3) and the equilibrium batch experiments (Figure 5.17) suggest that the following equation holds for all ranks of coal:

F

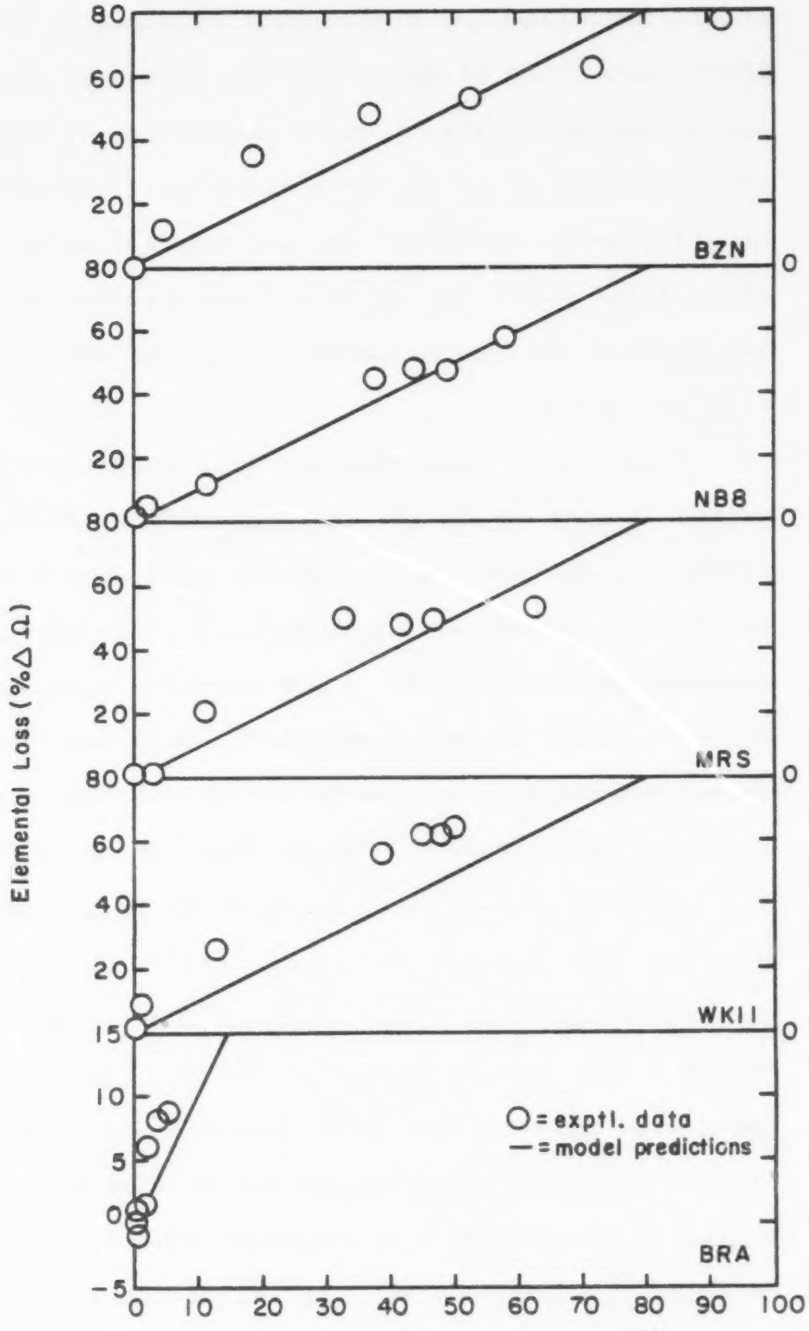

Figure 5.17 Comparison of Experimental Data With Sulfur Release Model

$$\Delta S = \Delta W^{*}. \qquad (5\text{-}7)$$

It will be shown in later sections that this relation is also valid for fast pyrolysis, and it might apply as well to the steam-oxygen gasification of WK11 coke. The reason for such behavior is not clear since sulfur exists in at least three primary forms in coal (pyrites, sulfates, and organically bound sulfur). A possible explanation could be inferred from the findings of Kuhn et al. (1977); they report that the pyrite contained in coal is converted to pyrrhotite and sulfur at 450°C or lower in nitrogen atmosphere. Their chemical analyses also indicate a greater loss of sulfur from the pyrites than from organic sulfur at low temperatures, whereas the reverse was found to be true at high temperatures (>450°C). Furthermore, as discussed in Sections 2.2.5 and 2.2.7, pyrites react with carbon to form carbonyl sulfide and decompose releasing sulfur in gaseous form.

The degree to which equation (5-7) correlates the sulfur loss data of the equilibrium experiments is shown in Figure 5.17. The relationship appears to hold fairly well for all the coals studied, although better agreement is obtained for the lower rank coals (BZN, NB8, and MRS).

In addition to examining the trends with temperature shown by the mass fractions of individual elements, it is useful to determine whether the rates of evolution of certain elements show high correlations. Element-to-element correlations of $X_H^{\ddagger}$ were tested for significance with computer program BATCH (Appendix A.1). The calculated slopes and coefficients of determination are shown in Appendix B.1. Those found to be significant at the 95% and 99% confidence levels using a table of correlation coefficients (Snedecor and Cochran, 1967) are shown in Tables 5.5 to 5.7. It is apparent that low volatility elements tend to be highly correlated, while high volatility elements do not. This is to be expected, since elements retained completely in the chars are enriched at a rate inversely proportional to the decrease in char weight, while very volatile elements tend to be depleted at different rates.

The following low volatility elements: Sm, Th, Sc, La, Fe, and Co are positively correlated in at least four of the five coals studied. The only unexpected element in this list is lanthanum. This result appears to indicate that the previous classification of lanthanum as a medium volatility element may have been due to scatter in the data. As shown in Tables 5.5 to 5.7, volatile elements tend to be negatively correlated with nonvolatile elements. A possible application of such correlations is, therefore, to estimate the volatility of elements whose mass fractions cannot be determined by finding whether they are positively or negatively correlated with readily measured low volatility elements.

Table 5.5 Significant Element-Element Correlations-Batch Experiments

NB8 Coal

Element	Sm	Sb	As	Se	V	Cl	La	Th	Cr	Sc	Fe	Co	Hg	Pb	S
Sm			+ *				+ **	+ **		+ **	+ **	+ **		— *	— *
Sb								+ *				+ *			
As								+ *		+ * *	+ **			— **	
Se															
V		+ *													
Cl															
La								+ **	+ *	+ *	+ *	+ *			— *
Th	+ **								+ *	+ **	+ **	+ **		— *	
Cr	+ *						+ *	+ *		+ *					— *
Sc	+ *							+ *	+ **		+ **	+ **		— **	
Fe	+ *						+ *	+ **	+ **	+ **		+ **		— **	
Co	+ **							+ **	+ **	+ *	+ **			— *	
Hg											+ *	+ *			
Pb							— *						— *		
S	— *					+ *		— *		— *	— *	— *			

WKII COAL

* = significant @ 95 % C. L.
** = significant @ 99% C. L.
+ = positively correlated
— = negatively correlated

Table 5.6 Significant Element-Element Correlations—
Batch Experiments

BZN COAL

Element	Sm	Sb	As	Se	V	Cl	La	Th	Cr	Sc	Fe	Co	Hg	Pb	S
Sm							+ **	+ **		+ *	+ **	+ *	− **		
Sb															
As		+ **													+ *
Se					+ *				+ *			+ *			+ *
V															+ *
Cl				+ **			− **			− *					
La	+ *	− *	− *							+ **	+ **		− *	− *	
Th	+ **						+ *				+ **	+ *	− *		
Cr	+ *	− **	− **				+ **	+ *				+ *			+ *
Sc		− *					+ *		+ *		+ *		− *		
Fe		+ **	+ **						− *			+ *	− *		
Co		− **	− *				+ *		+ **	+ *	− *		− *	− **	
Hg				+ *		+ **									
Pb															
S															

BRA COAL

* = significant at 95% C.L.
** = significant at 99% C.L.
+ = positively correlated
− = negatively correlated

Table 5.7 Significant Element - Element Correlations - Batch Experiments

Element	Sm	Sb	As	Se	V	Cl	La	Th	Cr	Sc	Fe	Co	Hg	Pb	S
Sm															
Sb															
As															
Se	+ *														
V			+ *												
Cl															
La	+ **														
Th	+ **			+ *			+ **								
Cr			+ *	+ *											
Sc	+ **						+ **	+ **							
Fe	+ *						+ **	+ *		+ **					
Co	+ *							+ *							
Hg			− *												
Pb	− *			− *	− *		− **	− **		− *	− *	− *			
S															

MRS COAL

* = Significant at 95% C.L.
** = Significant at 99% C.L.
+ = positively correlated
− = negatively correlated

6. ANALYSIS OF RESULTS FROM LAMINAR FLOW REACTOR EXPERIMENTS

The purpose of these experiments was to study the devolatilization and elemental release of three coals (MRS, NB8, and BZN) as functions of temperature and time. As indicated previously, a laminar flow reactor was chosen to carry out the experiments. Thus, rapid heating conditions (10^3 - 10^4 °C/sec) and small residence times (170 - 1500 msec) were attained.

Fifty-two runs were carried out. The first fourteen runs were made with WK11 and MRS , and were intended primarily to shake down the reactor system. The results obtained in these runs are not reported in this thesis. Twenty-six runs were made with MRS coal, at temperatures ranging from 25 to 900°C. Nine runs were made with NB8 coal, five at 800°C and four at 900°C. Finally, three runs were made with BZN coal, all at 800°C.

A summary of run conditions is shown in Table 6.1 The residence times calculated using Subroutine RESTIM in computer program MODLLS are shown in Appendix A.2. The isothermal reaction time t_I (as used in equation (4-30), Section 4.2.2) is defined here as t_R minus three times the coal heating constant τ_T. This is done only for the purpose of allowing comparison of the results with the work of other researchers (e.g., Badzioch and Hawksley, 1970; Nsakala, 1976).

Table 6.1 Summary of LFR Run Conditions

Run No.	Coal	T ^oC	t_R msec	t_I msec	Coal Feed Rate g/min	Char Recovery %	CY3 Recovery %	Comments
15	MRS	294	1523	1416	0.45	44.50	24.72	
16	MRS	395	482	380	0.42	68.00	3.92	
17	MRS	398	714	612	0.47	54.50	24.77	
18	MRS	398	976	874	0.54	-	-	
19	MRS	402	1233	1131	0.37	52.00	31.73	
20	MRS	600	172	78	0.79	74.00	0.00	
21	MRS	600	285	191	1.44	75.00	0.00	
22	MRS	598	522	427	1.10	68.67	0.97	
23	MRS	597	774	679	0.51	63.50	5.83	
24	MRS	799	171	84	6.00	83.00	0.00	Bad run-discarded
25	MRS	800	270	183	0.43	69.17	0.00	
26	MRS	800	518	431	0.32	68.00	1.47	
27	MRS	800	770	683	0.43	45.00	1.56	
28	MRS	799	521	434	0.48	61.00	1.64	
29	MRS	799	519	432	0.36	73.50	0.68	
30	MRS	800	516	429	0.37	69.00	1.45	
31	MRS	801	825	738	0.36	26.00	55.36	
32	MRS	601	501	406	0.32	71.00	1.41	
33	MRS	870	557	472	0.32	-	-	
34	MRS	602	1017	923	14.50	-	-	Bad run-discarded
35	BZN	803	517	430	1.08	-	-	

Table 6.1 continued

Run No.	Coal	T ^{o}C	t_R msec	t_I msec	Coal Feed Rate g/min	Char Recovery %	CY3 Recovery %	Comments
36	BZN	804	816	727	1.20	51.00	0.00	
37	BZN	808	268	181	2.85	74.67	0.00	
38	NB8	801	518	431	0.79	-	-	
39	NB8	802	818	731	0.53	54.50	0.00	
40	NB8	805	269	182	0.32	77.33	0.00	
41	NB8	803	397	310	0.42	81.33	0.00	
42	NB8	802	670	583	0.51	64.00	0.00	
43	NB8	900	613	527	0.41	59.33	0.00	
44	NB8	900	255	172	0.40	73.00	0.00	
45	NB8	900	767	684	0.83	60.50	0.83	
46	NB8	900	441	358	0.41	62.50	0.00	
47	MRS	900	619	534	0.74	52.00	0.00	
48	MRS	900	254	170	1.05	76.00	0.00	
49	MRS	900	766	683	0.48	50.00	0.00	
50	MRS	900	443	360	0.96	57.50	0.00	
51	MRS	25	1428	1309	0.49	66.67	25.00	
52	MRS	25	488	272	0.25	92.00	2.90	

The sections that follow present the results obtained in the laminar flow reactor runs. The ash tracer technique is examined in detail; the results of the trace element analyses are used to aid in the determination of the extent of ash losses, and a procedure is developed to correct for such losses. The devolatilization results are presented and compared with the predictions of Kobayashi's (1976) parallel reactions model, a first-order model featuring temperature-dependent asymptotic weight loss, and two empirical models with parameters fitted by least squares regression.

Thirty trace and minor elements were analyzed in the chars produced in three 800°C runs (25, 27, and 29) with MRS coal. Special care and precautions were taken in the operation of the reactor system and the handling of the char samples for these runs. A detailed analysis of the results of these runs and a less detailed analysis of the results of the elemental analyses from the other runs were carried out. At least ten elemental analyses were performed for every char produced with the LFR. Finally, statistical trend analyses of elemental release were carried out, and an attempt was made to model the rate and extent of elemental release as a function of time and temperature.

6.1 Weight Loss Estimation Errors

The ideal way to conduct laminar flow experiments would be to feed a measured amount of coal, collect all of the char produced, and determine by difference how much of each analyte of interest was evolved. The difficulty in collecting 100% of the char has led to the use of a non-volatile material as a tracer. Ash is almost invariably used for this purpose.

Weight loss on dry ash-free basis in laminar flow reactor experiments is usually estimated with the equation

$$\Delta W_A^* + 1 - \frac{A_C^\ddagger}{A_H^\ddagger}\left[\frac{1 - A_H^\ddagger}{1 - A_C^\ddagger}\right] \qquad (4-58)$$

where $A_C^\ddagger$ = moisture-free ash fraction of feed coal
$A_H^\ddagger$ = moisture-free ash fraction of char.

The results obtained using this formula are shown in Figure 6.1 for MRS coal. NB8 and BZN exhibit similar behavior. As the data of Figure 6.1 show, low temperatures and low residence times consistently lead to negative values of ΔW_A^*. Since negative d.a.f. weight losses are a physical impossibility, it is clear that the ash tracer method leads to underestimation of ΔW^* and therefore of $\Delta W^\ddagger$ (m.f. weight loss) and ΔW^+ (a.r. weight loss). The

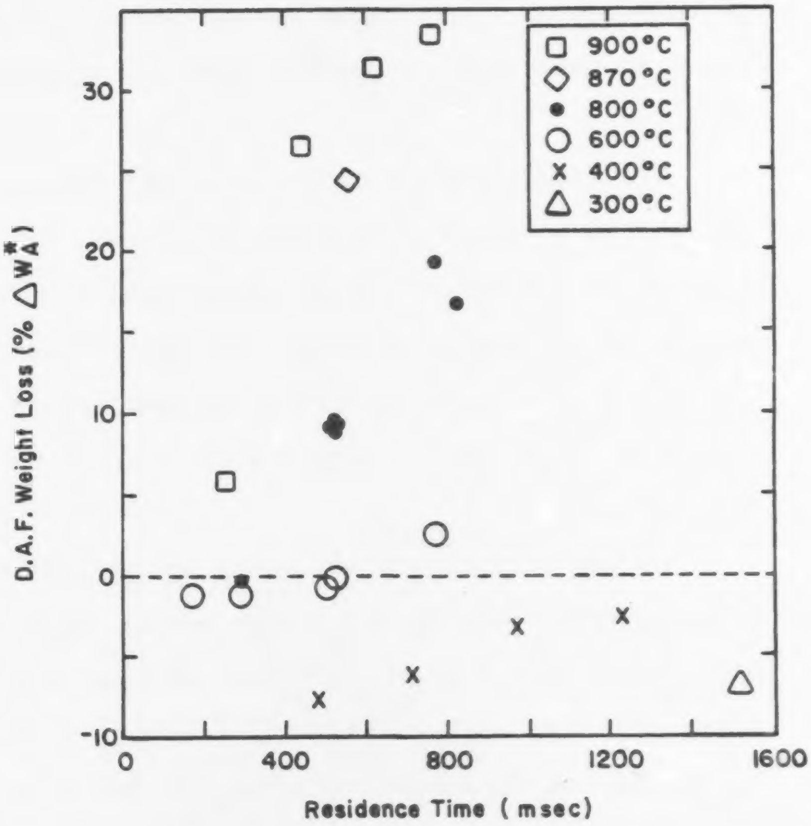

Figure 6.1 D.A.F. Weight Loss by Ash Tracer Method – MRS Coal

first two quantities are much more sensitive to this effect and to errors in the ash analyses as large moisture losses tend to make all values of ΔW_A^{+} (T, t_R) positive, hiding the ash-introduced error. Values of $\%\Delta W_A^{*}$, $\%\Delta W_A^{\ddagger}$, and $\%\Delta W_A^{+}$ determined by the ash tracer method are calculated with computer program LFRS1 (Appendix A.2) and tabulated in Appendix B.2.

The attainment of negative weight losses cannot be attributed to error in the ash analyses. All analyses were carried out in random order using blind samples, so that errors in the analyses would have led to random variations and not to the observed consistent pattern of decreasingly negative d.a.f. weight losses with increasing time and temperature.

It has been argued (Badzioch et al., 1968) that ash-induced errors have a very large effect only at low decomposition rates, i.e., at low temperatures and/or residence times and high coal ranks. This can be shown mathematically by taking the derivative of equation (4-58) with respect to $A_H^{\ddagger}$

$$\frac{d\Delta W_A^{*}}{dA_H^{\ddagger}} = \left[\frac{A_C^{\ddagger}}{1 - A_C^{\ddagger}}\right] \left[\frac{1}{(A_H^{\ddagger})^2}\right] . \qquad (6\text{-}1)$$

The rate of change of $\Delta W_A^{\ddagger}$ is higher for small values of $A_H^{\ddagger}$, so that underestimation of ΔW_A^{*} at low values of $A_H^{\ddagger}$ is larger than at high values of $A_H^{\ddagger}$ for the same net amount of ash loss.

However, the underestimation effect cannot be ignored at high temperatures. The mass fractions of several elements in MRS feed coal (X_C^{+}) and the chars (X_H^{+}) from runs 25, 27, and 29 are shown in Figure 6.2. It is evident that the chars are enriched in some of these elements, since X_H^{+} is greater than X_C^{+}. However, for three of the elements shown (P, As, and La), ψ_A^{+} (mass of element in char per unit mass of feed coal estimated using ash as a tracer) values are also larger than the feed values. Such behavior is physically impossible as the following argument demonstrates.

The mass balance for coal pyrolysis is

$$W_C = W_H + W_V \tag{6-2}$$

where W_C = feed coal weight
W_H = char weight
W_V = volatiles weight.

The species mass balance is

$$X_C W_C = X_H W_H + X_V W_V \, . \tag{6-3}$$

If ash is used as a tracer,

$$W_H = W_C \frac{A_C}{A_H} \tag{6-4}$$

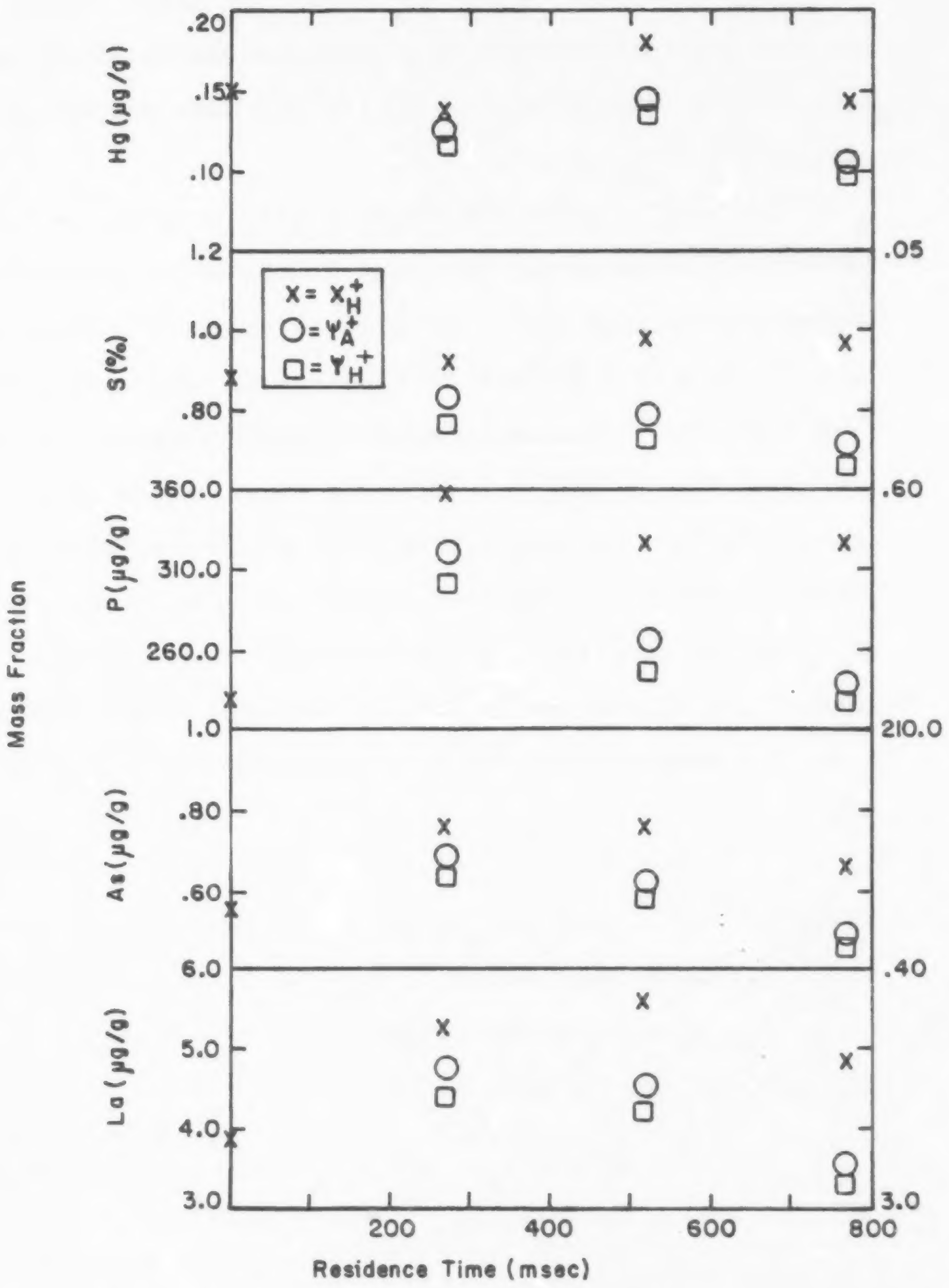

Figure 6.2 Mass Fractions in LFR Chars, MRS 800°C Runs

where A_C = ash content of feed coal

A_H = ash content of char.

These two equations combined with equations (4-43) and (4-48) yield

$$\psi_A = X_H \left(\frac{A_C}{A_H} \right) \tag{6-5}$$

where $\psi_A = \psi_H$ estimated using ash as a tracer.

These relationships are valid for all bases, a.r., m.f., and d.a.f., as long as all parameters are expressed on the same basis.

Combining equations (6-2) and (6-4) and substituting into equation (6-3),

$$X_H = \frac{X_C - X_V(1 - A_C/A_H)}{A_C/A_H} \quad . \tag{6-6}$$

Substituting into equation (6-5),

$$\psi_A = X_C - X_V(1 - A_C/A_H) \quad . \tag{6-7}$$

Since

$$A_H \geq A_C \tag{6-8}$$

it follows that

$$\psi_A \leq X_C \quad . \tag{6-9}$$

That is, the mass fractions of elements in the char, when normalized to feed coal weight, must be less than or equal to the feed coal mass fractions of those elements. The condition that underlies this inequality is that there have been no ash losses.

The contrary behavior of several elements (P, As, and La) is shown in Figure 6.2. The values of ψ_A^+ for the more volatile elements, Hg and S, do meet the criterion set by equation (6-9); however, this occurs at the conditions of the runs shown only because the high volatilities of these elements overcome the ash loss effect. The opposite result is obtained for sulfur at lower extents of devolatilization (i.e., lower T and/or t_R), as illustrated in Figure 6.3. Mercury is evolved too quickly under any conditions for the effect to be observed. Figures 6.2 and 6.3 also depict values of ψ_H^+ calculated by a corrected ash tracer method which will be discussed later.

If only one element had shown this behavior, it could have been attributed to sample contamination, or to analytical error. However, the result was obtained for several elements whose concentrations were determined by four different analytical techniques, so that the inadequacy of the ash tracer method must be regarded as genuine. The results shown in Figure 6.2 correspond to MRS runs 25, 27, and 29.

An interesting corollary of the above analysis is that elements which are entirely, or at least very strongly, associated with the ash should be lost from the coal in the

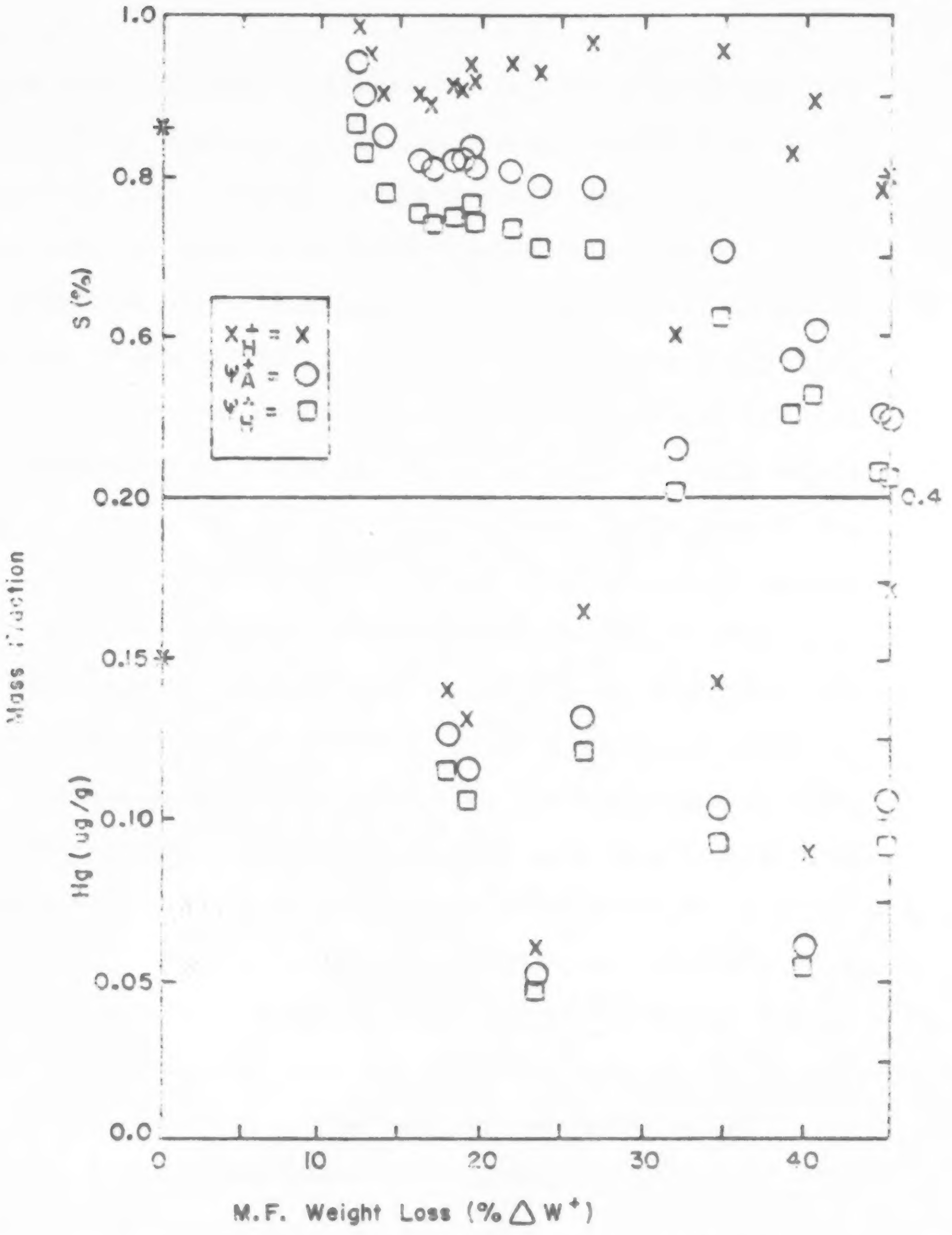

Figure 6.3 Mass Fractions in LFR 800°C MRS Chars - Volatile Elements

same proportion as the ash itself. Thus the mass fractions of those elements normalized using equation (6-5) should satisfy the equality of equation (6-9), i.e., $\psi_A = X_C$. Some nonvolatile trace elements were found to show such behavior in MRS coal. The results for four nonvolatile elements are shown in Figure 6.4. The chars of MRS runs 25, 27, and 29 show enrichment in the mass fractions of these elements (X_H^+) as the residence time increases, while the slopes of ψ_A^+ versus t_R for Sm and Mn are not significantly different from zero, indicating that $\psi_A^+ = X_C^+$ and thus that these two elements are released from the coal at the same rate as the ash. This finding suggests that significant amounts of trace elements may be released from coal as submicron ash particles during gasification. The statistical analyses discussed in later sections use this information to determine the mode of elemental transport from the coal particles to the gas stream.

A number of factors are potential sources of error in values of ΔW calculated by the ash tracer method. Among these factors are the following:

1. Measured ash contents of the feed coal and the char may be in error either due to analysis errors or to run-to-run variability.
2. The ash contents of coal and char particles vary with particle size. The cyclones used to collect the char

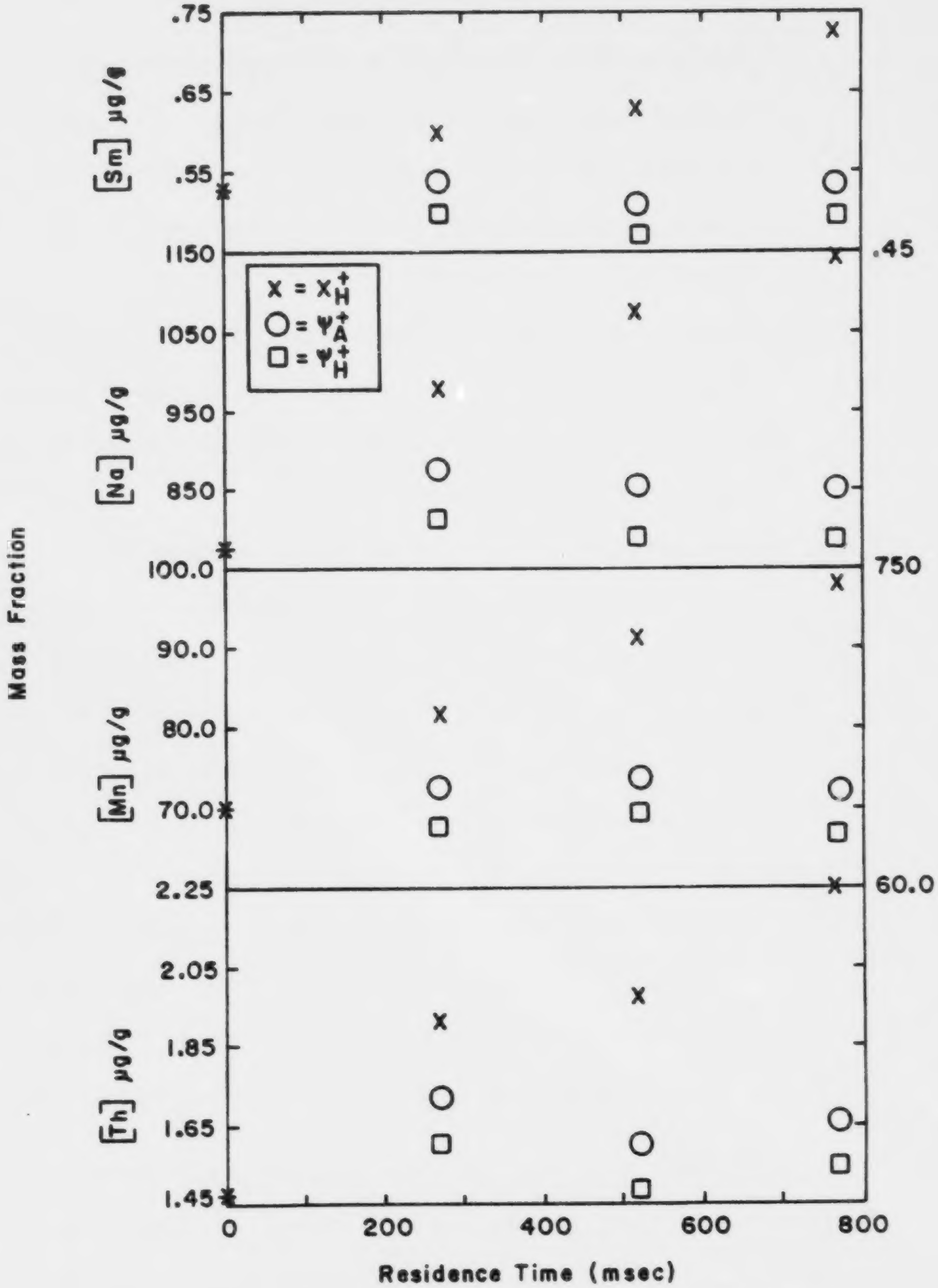

Figure 6.4 Mass Fractions in LFR 800° MRS Chars-Nonvolatile Elements

impose a size classification, and thereby bias the measured ash content of the product. If the cyclone contents are mixed to provide the product char, inhomogeneity and imperfect sampling constitutes another potential source of error.

3. There is a difference between the experimentally measured proximate ash content of an as-received coal and the same coal which has been subjected to predevolatilization.
4. Tars evolved in pyrolysis may condense in the collected char, thereby decreasing the apparent weight loss.
5. The rate of heating of the coal and hence the devolatilization rate may be a function of the coal feed and feeder gas rates, both of which influence mixing and heat transfer near the feed inlet.
6. Some of the material that constitutes what is termed "ash" in coal may in fact be lost during pyrolysis, either by being converted to gaseous species or by being expelled as particles too small to be collected by the devices employed in the experimental system.

The sections that follow explore each of these effects, quantifying them to the extent possible. The results of these studies are then used to formulate in Section 6.2 a weight loss calculation method that accounts in part for possible ash losses during pyrolysis.

6.1.1 Precision and Accuracy of Weight Loss Estimations

The magnitude of the d.a.f. weight losses cannot be explained by the variability in the moisture and ash analyses, as shown in the following discussion. The effects that errors in chemical analyses have on values of $\%\Delta W^*_A$ obtained using ash as the tracer may be estimated using the following equation:

$$S^2_{\Delta W^*_C} = \left(\frac{\partial \Delta W^*_A}{\partial A^+_C}\right)^2 S^2_{A^+_C} + \left(\frac{\partial \Delta W^*_A}{\partial A^+_H}\right)^2 S^2_{A^+_H} + \left(\frac{\partial \Delta W^*_A}{\partial M^+_C}\right)^2 S^2_{M^+_C} + \left(\frac{\partial \Delta W^*_A}{\partial M^+_H}\right)^2 S^2_{M^+_H} \qquad (6\text{-}10)$$

where S_i = standard deviation of ith parameter. From equation (4-58),

$$\frac{\partial \Delta W^*_A}{\partial A^+_C} = \frac{-1}{A^+_H}\left[\frac{1 - M^+_H - A^+_H}{1 - M^+_C - A^+_C}\right] - \frac{A^+_C}{A^+_H}\left[\frac{1 - M^+_H - A^+_H}{(1 - M^+_C - A^+_C)^2}\right] \qquad (6\text{-}11)$$

$$\frac{\partial \Delta W^*_A}{\partial A^+_H} = \frac{A^+_C}{(A^+_H)^2}\left[\frac{1 - M^+_H - A^+_H}{1 - M^+_C - A^+_C}\right] + \frac{A^+_C}{A^+_H}\left[\frac{1}{1 - M^+_C - A^+_C}\right] \qquad (6\text{-}12)$$

$$\frac{\partial \Delta W^*_A}{\partial M^+_C} = \frac{-A^+_C}{A^+_H}\left[\frac{1 - M^+_H - A^+_H}{(1 - M^+_C - A^+_C)^2}\right] \qquad (6\text{-}13)$$

$$\frac{\partial \Delta W_A^*}{\partial M_H^+} = \frac{A_C^+}{A_H^+}\left[\frac{1}{1 - M_C^+ - A_C^+}\right] . \qquad (6\text{-}14)$$

An intermediate temperature and residence time have been chosen to estimate the theoretical $S_{\Delta W_A^*}$ from the estimated errors in the chemical analyses. For run No. 29 (coal = MRS, T = 799°C, t_R = 519 msec, $\Delta W_A^* = 0.0884$), the variance components are estimated to be:

$$S^2_{A_C^+} = 1.089\text{x}10^{-6} \simeq S^2_{A_H^+}$$

$$S^2_{M_C^+} = 1.046\text{x}10^{-5} \simeq S^2_{M_H^+}$$

$$\left(\frac{\partial \Delta W_A^*}{\partial A_C^+}\right)^2 = 105.79$$

$$\left(\frac{\partial \Delta W_A^*}{\partial A_H^+}\right)^2 = 70.91$$

$$\left(\frac{\partial \Delta W_H^*}{\partial M_H^+}\right)^2 = 1.39$$

$$\left(\frac{\partial \Delta W_H^*}{\partial M_H^+}\right)^2 = 1.05 .$$

The variances of the average moisture and ash contents of the feed coal were determined from five replicate analyses. It is assumed that the moisture and ash analyses of the chars have the same variances as those of the feed. Therefore, the variances of the mean moisture and ash contents were used for $S^2_{M^+}$ and $S^2_{A^+}$. Equation (6-10) then yields $S_{\Delta W^*_A} = 0.0148$. However, this is not a good estimate of the expected run-to-run variability, because the same sample of feed coal was used for all the runs with a given coal (MRS in this case), and the average values of M^+_C and A^+_C were used for the computation of ΔW in all the runs with that coal. Consequently, $S^2_{M^+_C}$ and $S^2_{A^+_C}$ must be set equal to zero in order to obtain the expected run-to-run variability due to analytical error. Equation (6-10) then yields $S_{\Delta W^*_A} = 0.0093$. The largest contributors to the error estimates are the ash variance components, even though the value of S_{M^+} is an order of magnitude larger than the value of S_{A^+}. If only the second variance component in equation (6-10) were used, $S_{\Delta W^*_A} = 0.0087$. The conclusion is that the error in ΔW^*_A reflects almost entirely the error in the ash determination.

In order to determine the experimental variance between runs, four replicate runs were made. Run numbers 26, 28, 29, and 30 were made at the same experimental conditions. The average weight loss and standard deviation estimated from those four replicates are as follows:

$$\overline{\Delta W_A^*} = 0.0904 , \quad S_{\Delta W_A^*} = 0.0035.$$

Thus, the experimental variance of these four laminar flow experiments is smaller than the theoretical estimate. However, not all experiments were conducted under conditions as carefully controlled as in these runs.

Comparison of the theoretical and experimental standard deviations with the negative values of ΔW_A^* (see Figure 6.1) indicate that they are too large to have been caused by analysis error or run-to-run variability. Furthermore, as indicated before, random errors in the proximate analyses could not have caused the monotonic increases in negative ΔW_A^* values with increases in T and t_R.

Variances in chemical analyses and between runs are not large enough to explain the magnitude nor the trend of negative ΔW_A^* values. Therefore, if meaningful thermodynamic and kinetic parameters are to be obtained, it is imperative that the ash loss effect be accounted for.

6.1.2 Particle Classification Errors

Inertial separation devices, such as the cyclones used in this study, preferentially collect larger and heavier particles, which may have ash contents different from that of the original coal. Such problems become more serious when a significant fraction of the ash exists as separate particles, as has been observed by Littlejohn (1966).

The particle size distribution of MRS pulverized coal is shown in Figure 6.5. The ordinates are the percentages by weight of particles greater than and less than the particle size given in the abscissa. They were determined from the weights retained in different U.S. Standard Sieves during the size grading of the coal. The moisture and ash contents of the different size fractions were also determined; the results are shown in Figure 6.6. It is evident that the moisture-free ash content ($A^{\dagger}$) increases as the coal particle size decreases. The d.a.f. sulfur contents of the different size fractions (% S^{*}) do not show a statistically significant trend. This appears to indicate that sulfur in MRS coal is associated primarily with the coal's organic matter, in agreement with the findings of Fiene _et al_. (1978) shown in Table 3.2.

In an experiment suggested by the above results, two runs were carried out in the LFR at room temperature. The objective was to determine the moisture, ash and sulfur contents of the coal fractions collected in the three LFR system cyclones (depicted in Figure 3.2). The results are shown in Table 6.2. The coal fraction collected in the 3/4 inch cyclone (CY-1) clearly has a reduced ash content relative to the feed coal, while the fraction collected in the 1/2 inch cyclone (CY-2) is enriched in ash. The material

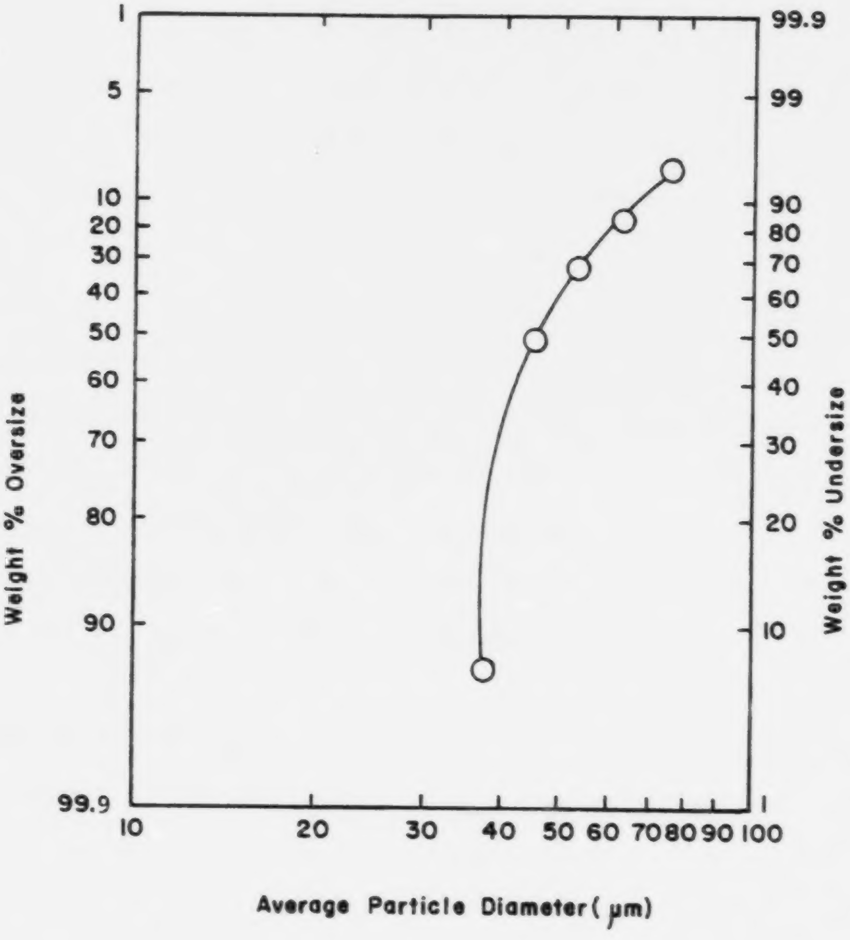

Figure 6.5 Rosin Rammler Plot of Montana Rosebud Coal

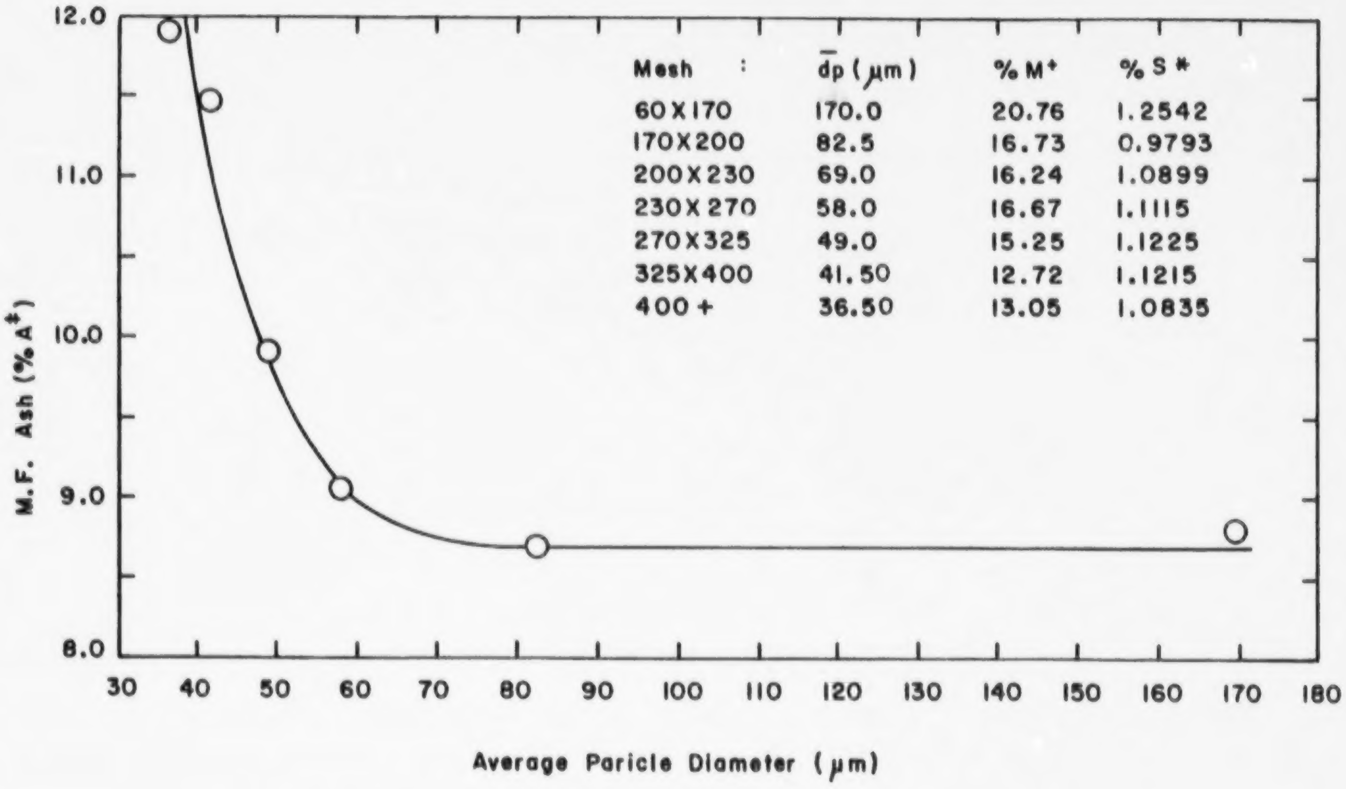

Figue 6.6 Ash Content of MRS Size Fractions

Table 6.2 Room Temperature LFR Runs with MRS Coal

Run No.	t_R	CY. No.	Recovery %	$\%M^+$	$\%A^‡$	$\%S^‡$	$\%AW_A^*$	$\%AW_W^*$
Feed		-	-	12.72	11.47	0.9929	0.0	-
51	1428	1	42.0	6.62	11.09	0.9612	-3.86	
		2	8.0	7.39	11.76	0.7047	+2.80	
		3	16.7	6.99	10.99	0.9753	-4.92	
		TOTAL	66.70					39.9
52	488	1	78.7	6.63	11.26	1.0184	-2.10	
		2	10.7	7.54	12.02	0.7115	5.18	
		3	2.7		not enough sample			
		TOTAL	92.10					14.11

in CY-3 (another 1/2 inch cyclone), which traps the coal particles that miss the collector, also shows a reduced ash content. The results of the ash analyses appear to be confirmed by the sulfur analyses. There is a sharp reduction in the sulfur content of the particles trapped in CY-2, indicating that the particles trapped in this cyclone have less organic matter.

Approximately a 6% a.r. weight loss (ΔW^+) is found, in runs 51 and 52, due to the drying effect of the nitrogen gas used (as evidenced by the reduction in moisture). However, the ash tracer method yields $\Delta W^+ \approx 3\%$ for the char collected in CY-1. Furthermore, d.a.f. weight loss values calculated by the ash tracer method (equation (4-58)) yield negative values for CY-1 and positive values for CY-2 in runs 51 and 52. Both sets of values are erroneous, since room temperature runs should not exhibit d.a.f. weight loss, much less d.a.f. weight gain.

The source of errors is of course the ash loss of the sample in CY-1 and the ash enrichment of the sample in CY-2. The weighted average ash content of CY-1 and CY-2 (i.e., that which would be calculated if the two samples had been mixed) is still much lower than the r.f. ash content of the feed (e.g., $\%A^{\ddagger} = 11.20$ in run 51). Therefore, it is clear that a significant amount of ash is not collected by either CY-1 or CY-2. The samples collected in CY-3 are depleted of ash in spite of the size of that cyclone (1/2 inch) quite likely because of the reduction in the collection efficiency due to the low flow rates of the gas stream passing through it.

Table 6.3 shows a comparison between the composition of CY-1 and CY-2 chars for several high temperature runs. It is obvious that the chars collected in the two cyclones are different. The lower sulfur contents of the chars in CY-2 indicate that they are enriched in ash as was the case in the room temperature runs. In addition, since the procedure followed in the sampling of the chars consisted of combining the chars collected in the hoppers of CY-1 and CY-2, incomplete mixing could have led to a large amount of scatter in the trace element analyses. Fortunately, most of the char was collected in CY-1 in the majority of runs. To minimize this potential inhomogeneity problem, each sample used for neutron activation analysis (NAA), atomic absorption analysis (AAA), and moisture analyses weighed 0.5 g, which was typically 4% of the total amount of collected char. Replicate sulfur analyses were carried out for all chars, because each analysis required only a 0.1 g sample.

Kobayashi (1976) suggested that the ash fraction of coal used in the ash tracer method should be that of coal particles which have experienced the same sampling process

Table 6.3 Comparison of CY-1 to CY-2 A.R. Char Compositions

Run No.	Feed Coal	%M$^+$		%A$^+$		%S$^+$	
		CY-1	CY-2	CY-1	CY-2	CY-1	CY-2
38	NB8					0.9459	0.7145
39	NB8					0.9506	0.6643
40	NB8	0.702	3.67	23.56	28.65	0.9152	0.7448
41	NB8					0.9686	0.7365
42	NB8					0.9707	0.6963
43	NB8					0.8582	0.7042
44	NB8					0.9952	0.7333
45	NB8	0.460	5.37	38.20	28.05	0.8713	0.7032
46	NB8					0.9784	0.6929
47	MRS					0.7860	0.6547
48	MRS					0.9330	0.6309
49	MRS					0.7923	0.6091
50	MRS					0.8947	0.5877

at room temperature as they would in the real experiment. Therefore, the d.a.f. ash content of CY-1 in the room temperature runs, 51 and 52 for MRS coal, was used. The char collected in CY-2 was not taken into account because the amount collected varied from run to run. Also, the amount of char collected in CY-2 was small in most of the runs. When the CY-1 d.a.f. ash content was used in the calculations, the magnitudes of the negative ΔW_A^* values of MRS chars (see Figure 6.1) were reduced by only about 10%. Therefore, it is evident that there are other sources of ash loss and/or bias of the data. No cold runs were made for NB8 and BZN coals. It was assumed, as an initial estimate, that the same percentage of ash was lost as in the runs with MRS, then these feed ashes were adjusted downward until they met the criteria developed in Section 6.2 for upper and lower bounds of weight loss estimates.

6.1.3 Chemical and Physical Ash Losses

The findings of Kobayashi (1976) show that ash losses due to vaporization are not significant up to 1250°K. However, Padia (1976) concluded, based on his studies of ash in coal, that the ash produced from pyrolyzed chars weighs 4.75 percent less than that produced from unpyrolyzed coal. Such behavior was said to be the result of differences in $CaSO_4$ formation during the ashing of coals preheated in an inert atmosphere and unpyrolyzed coals. This phenomenon will be referred to as Padia's effect in this report. Kobayashi (1976) confirmed Padia's findings: his results also show approximately a 5% difference in the ash produced from pyrolyzed and unpyrolyzed coals.

Padia's findings suggest that the ash-induced error can be minimized by increasing the ash content of the chars by about 5%. This correction, coupled with the use of the reactor at room temperature, should provide better weight loss estimates. This procedure was used in this study. The pertinent equations will be developed in Section 6.2.

6.1.4 Mechanical Ash Losses

As indicated in the previous section, ash losses due to vaporization are not significant up to 1250°K. Another potential source of ash loss is that during fast pyrolysis, the volatile components of coal escape at very high velocities, thus carrying with them solid particles which may be in their path. This hypothesis is supported by calculations made by Kobayashi (1976). From experimentally measured gas flow rates through discs of coal and pressure drops at room temperature (Karn et al., 1975), Kobayashi estimated coal particle internal pressures of 100 atmospheres. This estimate is not unreasonable considering the high volatile matter flow rates expected during devolatilization; it also agrees with Lewellen's (1975) prediction of a few hundred atmospheres of internal pressure when a 70 micron particle is heated to 1000°C at 10^4 °C/sec. Moreover, microscopic examinations of pyrolyzed coal particles usually reveal "blow holes" on the surface of the char particles (Horton and Smoot, 1975), indicating that volatiles (and probably ash particles) are released from coals. Inorganic mineral matter is known to be distributed in coal more or less uniformly as small inclusions of variable composition of approximately 2 μm mean size (Padia, 1976). Such small particles would probably pass through the cyclones used in this study. Unfortunately, this effect cannot be quantified.

6.1.5 Tar Condensation

Visual examination of the lucite cyclone hoppers during the LFR experiments clearly indicated that yellow-brown fumes of condensing tars deposited on the hopper walls. The coal particles would be expected to act as condensation nuclei for the tars. The extent of the error in weight loss and elemental evolution measurements that results from this phenomenon is unknown, but such an effect could be substantial for mercury and elements which are predominantly associated with the organic fraction of the coal. This effect could be reduced by lowering the cooling rate of the coal particles as they pass through the collector and the cyclones. As in the case of mechanical ash losses, this effect cannot be quantified.

6.1.6 Effects of Coal and Gas Feed Rates, and Residence Time Effect

As shown in Table 6.1, the coal feed rate varied significantly in many runs. The evidence suggests that increases in coal feed rate lead to increases in weight loss at a given temperature and residence time. This is very likely due to the turbulence caused by the higher particle loading at the feeder tip, leading to more rapid heating of the gas surrounding the coal particles and consequent decrease in the value of the particle heating time constant. This would not necessarily be true at very high coal loading ratios (as shown by Reidelbach and Algermissen, 1978) because of the increased enthalpy requirement.

An additional complicating factor is introduced by changes in feeder gas velocity, u_f. The laminar flow reactor was operated with a coal feeder gas velocity in a region where the coal particle heating time constant τ_H appears to be highly sensitive to changes in u_f. This effect is shown by taking the partial derivative of equation (4-33) with respect to u_f:

$$\frac{\partial \tau_H}{\partial U_f} = \frac{-0.5348}{U_f} \exp \left[5.67238 - \frac{4.0844T}{10000} - \ln(u_f) \right] \quad (6\text{-}15)$$

As u_f becomes small, $\partial \tau_H / \partial U_f$ becomes large. The value of u_f used in this research is lower than those used by all other researchers in the field, a consequence of an attempt to minimize the dispersion of the coal particles and thereby to maximize the particle collection efficiency. Furthermore, the flow controller used in the feeder gas line was oversized. This may have introduced variations in feeder gas flow rate that may not have been detected.

Nevertheless, neither changes in coal feed rate nor fluctuations in u_f could have caused the negative values of ΔW_A^*. Such changes can only perturb the extent of reaction at a given T and t_R, i.e., cause scatter in the data. The conclusion is that negative values of ΔW_A^* cannot be due to experimental error, but must be attributed to ash losses.

Another reason for carrying out runs 51 and 52 was to determine the effect of residence time on sample recovery. This was done by using CY-3 as a device to estimate the fraction of sample which missed the collector. The higher the sample recovery in CY-3, the larger the amount of coal that was not collected. The results shown in Table 6.2 indicate that smaller residence times lead to better collection efficiencies. Because of the design of the reactor collector base, total recovery of the char that misses the collector is not possible. If it were, the gravimetrically determined weight loss calculated with the following equations:

$$\Delta W_W^* = \frac{[1 - M_C^+ - A_C^+] - R_H \; [1 - M_H^+ - A_H^+]}{1 - M_C^+ - A_C^+} \qquad (6\text{-}16)$$

where

$$R_H = \frac{\text{weight of char recovered in CY-1, CY-2, and CY-3}}{\text{weight of feed coal}} \qquad (6\text{-}17)$$

would equal zero in runs 51 and 52. The data in Table 6.2 show that this is not the case. However, it is seen that the lower the char recovery in CY-3, the better does ΔW_W^* estimate ΔW^* (which should be zero for runs 51 and 52). Therefore, a negligible recovery in CY-3 would imply that ΔW_W^* is a good estimate of ΔW^*. Table 6.1 shows that several runs meet this criteria.

6.2 Calculational Procedure for Estimation of Weight Loss

It has been shown that ash losses bias weight loss estimates downward. In order to determine the behavior of volatile components of coal, and of its elemental constituents, it is imperative that the underestimation due to ash losses be corrected. The procedure that was used for the estimation of d.a.f. weight losses (ΔW^*), and upper and lower bounds on ΔW^* is presented in this section.

Dry ash-free weight losses were estimated with the following equation:

$$\Delta W^* = 1 - \frac{E_C^*}{E_H^*} \qquad (6\text{-}18)$$

where

E_C^* = d.a.f. ash fraction of particles collected during cold runs (see Section 6.1.2)

E_H^* = d.a.f. ash fraction of char particles corrected for Padia's effect

E_H^* is calculated from the equations

$$E_H^* = \frac{E_H^+}{1 - E_H^+ - N_H^+} \qquad (6\text{-}19)$$

where

$$E_H^+ = \frac{1.0475A_H^+}{1 + 0.0475A_H^+} \qquad (6\text{-}20)$$

and

$$N_H^+ = \frac{M_H^+}{1 + 0.0475A_H^+} \qquad (6\text{-}21$$

E_H^+ and N_H^+ are hypothetical quantities used only to estimate d.a.f. weight loss. They are the values that the a.r. char's ash and moisture would have if the yield of ash had not been reduced by the pyrolysis in inert gas (Padia's effect) as discussed in Section 6.1.3.

It should be noted that the values of E_C^* used are specific to the apparatus used in this study (e.g. cyclone sizes, etc.).

Actual moisture and ash contents of the feeds and chars are used to carry out all other calculations in the different bases. Once ΔW^* is calculated using equation (6-18) weight losses in a.r. and m.f. bases are calculated using equation (4-47) rearranged to the form

$$\frac{W_H^+}{W_C^+} = \frac{(1 - \Delta W^*)\ (1 - M_C^+ - A_C^+)}{1 - M_H^+ - A_H^+} \qquad (4\text{-}47)$$

and substituting into equations (4-43) and (4-45). Weight loss values on the three bases are calculated by computer program LFRS1 listed in Appendix A.2. The results are in Appendix B.2.

This method only provides estimates of the true weight losses, since it does not account for such phenomena as loss of ash in submicron particles and condensation of tars on the product char. An indication of the validity of the estimate could be obtained if upper and lower bounds on the value of ΔW^* were known; an estimated value of ΔW^* that did not fall within these bounds could then be rejected out of hand.

In fact, such bounds can be estimated from considerations presented in Section 6.1. The uncorrected value of ΔW_A^*, which does not account for ash losses, must be lower than the true weight loss. (This is easily shown mathematically, but the fact that in extreme cases ΔW_A^* is negative provides a convincing heuristic demonstration.) On the other hand, as was shown in Section 6.1.6, the values of ΔW^* determined gravimetrically from the weights of the chars collected in all three cyclones (ΔW_W^*) provides an upper bound on the pyrolysis weight loss, in that some material is inevitably not collected in the cyclones.

The weight loss estimates and bounds calculated in this manner are shown in Table 6.4. The bounds calculated for MRS coal indicate that the value of E_C^+ used for this coal provided good estimates of ΔW^*. However, the upper bounds for some NB8 and BZN runs (ΔW_W^*) were slightly lower than the ΔW^* estimates. Consequently, the E_C^* values for these coals were adjusted downward until the estimates of ΔW^* were between the bounds. This procedure is particularly sound in the case of NB8 coal because its high ash content allowed the calculation of good weight loss estimates by the ash tracer method for those runs where the extent of decomposition was high (e.g., run 45). In addition, most of the char passed through the water-cooled collector, as evidenced by the zero percent recoveries in CY-3 for the NB8 runs.

Table 6.4 Weight Loss Estimates and Bounds

Run No.	$\%\Delta W_A^*$ (Low Bound)[1]	$\%\Delta W^*$	$\%\Delta W_W^*$ (High Bound)
15	-7.19	0.64	-
16	-7.65	0.21	-
17	-6.27	1.48	-
18	-3.12	4.41	-
19	-2.58	4.90	-
20	-1.37	6.03	16.22
21	-1.41	5.99	14.75
22	-0.30	7.02	-
23	2.38	9.50	-
24	-2.32	5.14	6.42
25	-0.72	6.63	22.19
26	9.55	16.15	-
27	19.16	25.05	-
28	8.76	15.41	-
29	8.84	15.49	17.27
30	9.03	15.66	22.30
31	16.52	22.61	-
32	0.43	7.62	-
33	24.64	30.14	-
34	0.71	7.95	-
35	3.81	9.89	-
36	7.30	13.16	33.33
37	-1.60	4.82	4.91
38	5.06	3.02	-
39	23.95	22.31	44.47
40	-7.40	0.00	13.62
41	8.74	6.77	12.97
42	22.80	21.13	34.60
43	41.92	40.67	44.63
44	20.47	18.76	24.37
45	46.35	45.20	45.26
46	41.43	40.17	41.66
47	31.19	36.21	44.02
48	5.74	12.61	15.05
49	33.43	38.29	46.80
50	26.32	31.70	37.57

---

[1] The actual lower bound must be greater than zero

Dry ash-free weight losses calculated by the procedure developed above are shown in Figures 6.7 to 6.9 for MRS, MB8, and BZN respectively. The procedure used to estimate ΔW^* yielded positive values for all runs except run 40 (for which ΔW^* has been set equal to zero) while also indicating low d.a.f. weight losses at low temperatures and/or residence times (e.g., MRS coal at 300°C). In addition, ψ_{II}^+ values calculated using these estimates of ΔW^* approach the criteria of equation (6-9) as shown in Figure 6.2 to 6.4. Therefore, it is concluded that the procedure is basically sound.

Quantitative comparison of the data obtained in this study with data obtained by other researchers is quite difficult to obtain, for several reasons. The data obtained by each researcher reflects strongly the equipment design and run parameters used (e.g., feeder, main, and suction gas flow rates); residence time calculations and estimations of particle time-temperature histories depend on the model used and the assumptions made; and weight loss estimations by the ash tracer method are dependent on the efficiency of the devices used to collect the char. Some researchers simply ignored negative d.a.f. weight losses calculated by the ash tracer method (e.g., Badzioch and Hawksley, 1968), others carried out all their experiments at

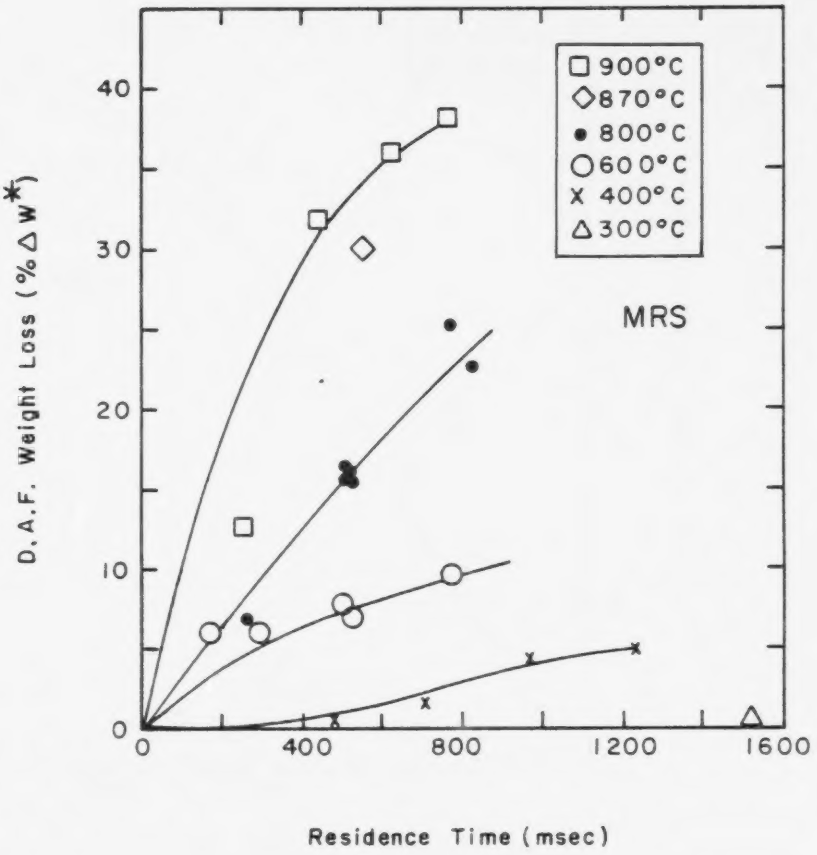

Figure 6.7 D.A.F. Weight Loss of MRS Coal

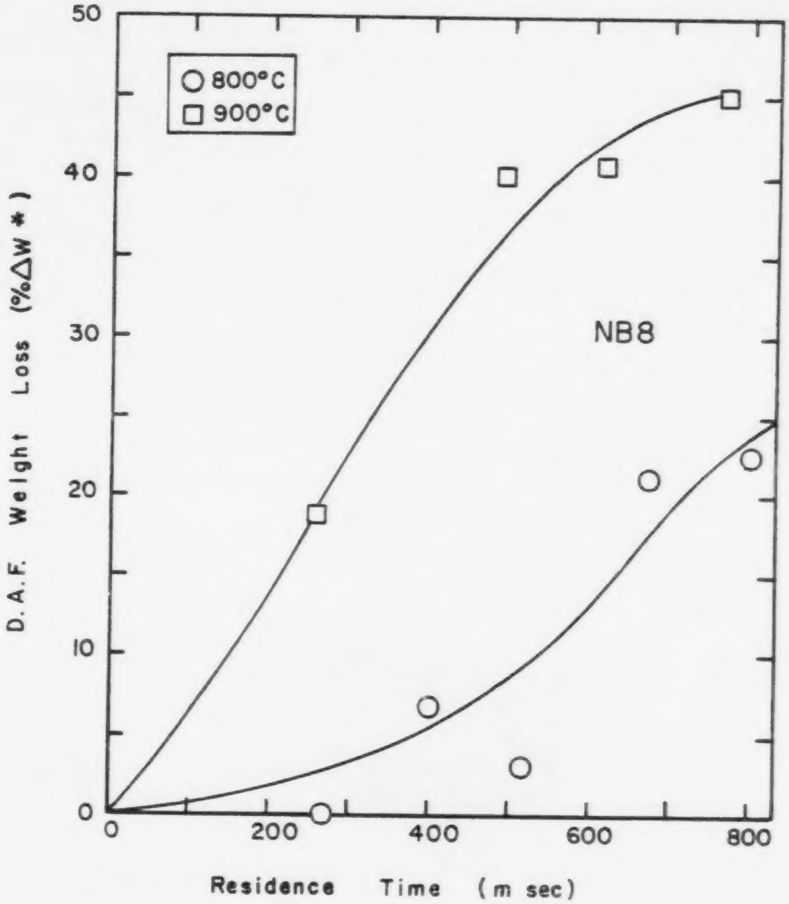

Figure 6.8 D.A.F. Weight Loss of NB8 Coal

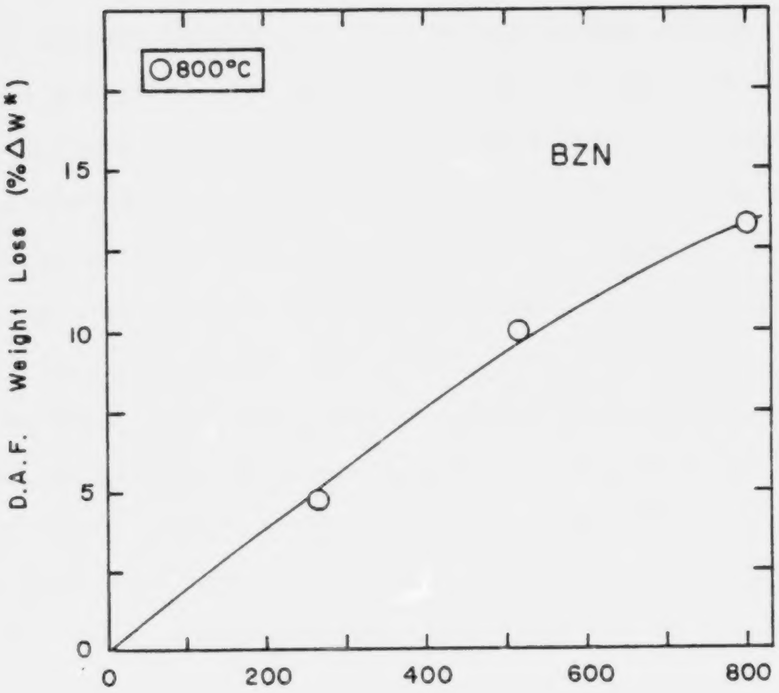

Figure 6.9 D.A.F. Weight Loss of BZN Coal

temperatures high enough for the ash loss effect to have been overcome by the weight loss (e.g., Nsakala, 1976).

Nevertheless, a qualitative comparison is instructive. The data of Nsakala for a Texas lignite is shown in Figure 6.10. Direct comparison of this figure and Figures 6.7 to 6.9 is not possible because the abscissa in Figure 6.10 corresponds to isothermal reaction times which are approximately 100 msec lower than the actual residence times. In addition, Nsakala used a simplistic model, which assumed a fully developed laminar profile in the reactor, to calculate residence times. Since such is not the case in reality, the actual residence times for those experiments should be still larger. Furthermore, Nsakala operated his reactor with a wall temperature approximately 100°C higher than the reactor main gas temperature which was reported to be 808°C in all his runs. Therefore, it is not clear whether such data should be associated with 800 or 900°C data in this study. Finally, differences in feeder gas velocities should have led to different particle temperature-time histories which, in turn, would have led to different weight losses for the same residence times. Nevertheless, qualitative comparison of the sample data from Nsakala's work and this study indicates that the same phenomena have been observed in both studies.

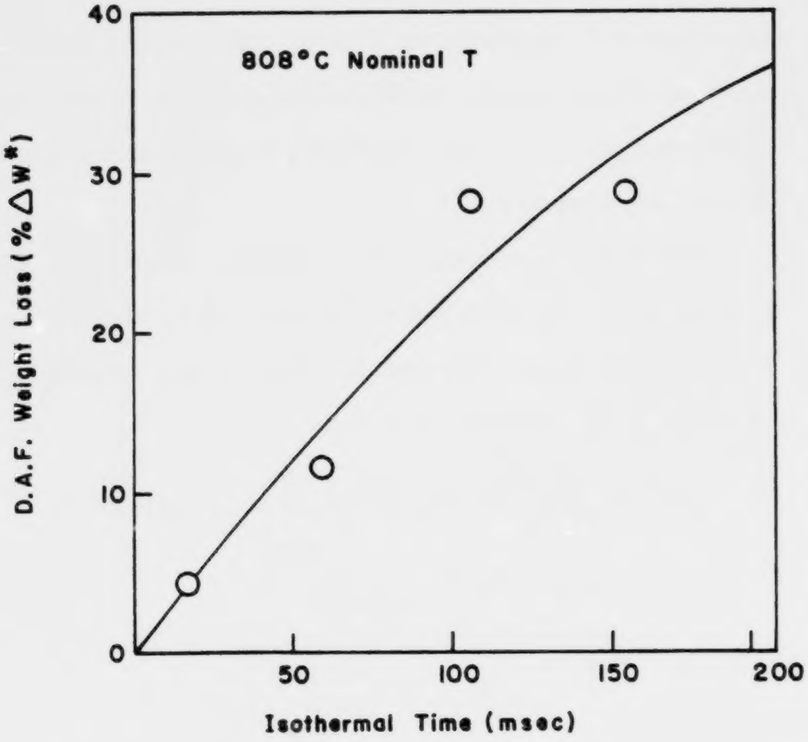

Figure 6.10 D.A.F. Weight Loss of Texas Lignite From Nsakala (1976).

6.3 Modeling of Coal Pyrolysis

The experimental weight loss data for MRS coal, described previously, have been correlated with four models: Badzioch and Hawksley's (1970) isothermal model, an isothermal first-order model, Kobayashi's (1976) nonisothermal first-order parallel reactions model, and a nonisothermal first-order model.

Badzioch and Hawksley's model parameters have been curvefitted with the LFR data for MRS coal, using Marquardt's (1963) nonlinear regression algorithm. The model equation presented in Section 2.2.4 is

$$\Delta W^* = Q(VM_o^*)(1-C)\ \left[1-\exp\{-At_I[\exp(-B/T)]\}\right] \qquad (2\text{-}2)$$

$$C = \exp\ [-K_1(T - K_2)] \qquad (2\text{-}3)$$

$$t_I = t_R - 3\tau_H \qquad (6\text{-}22)$$

where

VM_o^* = ASTM proximate volatile matter of coal on d.a.f. basis.

The value of VM_o^* was determined to be 44.1% for the MRS coal fraction used in the LFR experiments. Badzioch and Hawksley (1970) determined that C in their model was equal to 0.14 for all nonswelling coals. Nsakala (1976) used this value successfully to model the pyrolysis of Montana lignite. Since the free-swelling index of MRS coal is 0.0, C = 0.14 was used in the curvefit. The values of the other constants were found to be $Q = 1.77$, $A = 685.75\ \text{sec}^{-1}$, and $E = 7356.40\,^{o}K$. The statistical analysis of the regression is shown in Appendix B.2; the SAS program used to fit the data (program BADZ) is listed in Appendix A.2. Figure 6.11 shows reasonable agreement between this model and experimental weight loss values; the sum of squares of the error (or residuals), SSE, is also shown in this figure.

The following first-order isothermal model was fitted to the MRS-LFR data.

$$\Delta W^{*} = \Delta W^{*}_{\infty}\ (1 - e^{-Kt_{I}}) \qquad (6\text{-}23)$$

where

$$\Delta W^{*} = \beta_{o} + \beta_{2}T^{2} \qquad (6\text{-}24)$$

$$K = Be^{-E/RT} \qquad (6\text{-}25)$$

β_o, β_2 = constants

B = preexponential factor

E = activation energy

The model parameters were found to be $\beta_o = -3.75$, $\beta_2 = 4.47\times10^{-5}\ {}^{o}K^{-2}$, $B = 72.65\ \text{sec}^{-1}$, and $E = 8866$ cal/mole. A comparison of the model curvefit and the experimental data for MRS coal is shown in Figure 6.11. The SAS program MODL6A used to fit the data is in Appendix A.2. The statistical analysis of the regression, included in Appendix B.2, shows that the sum of squares of the error

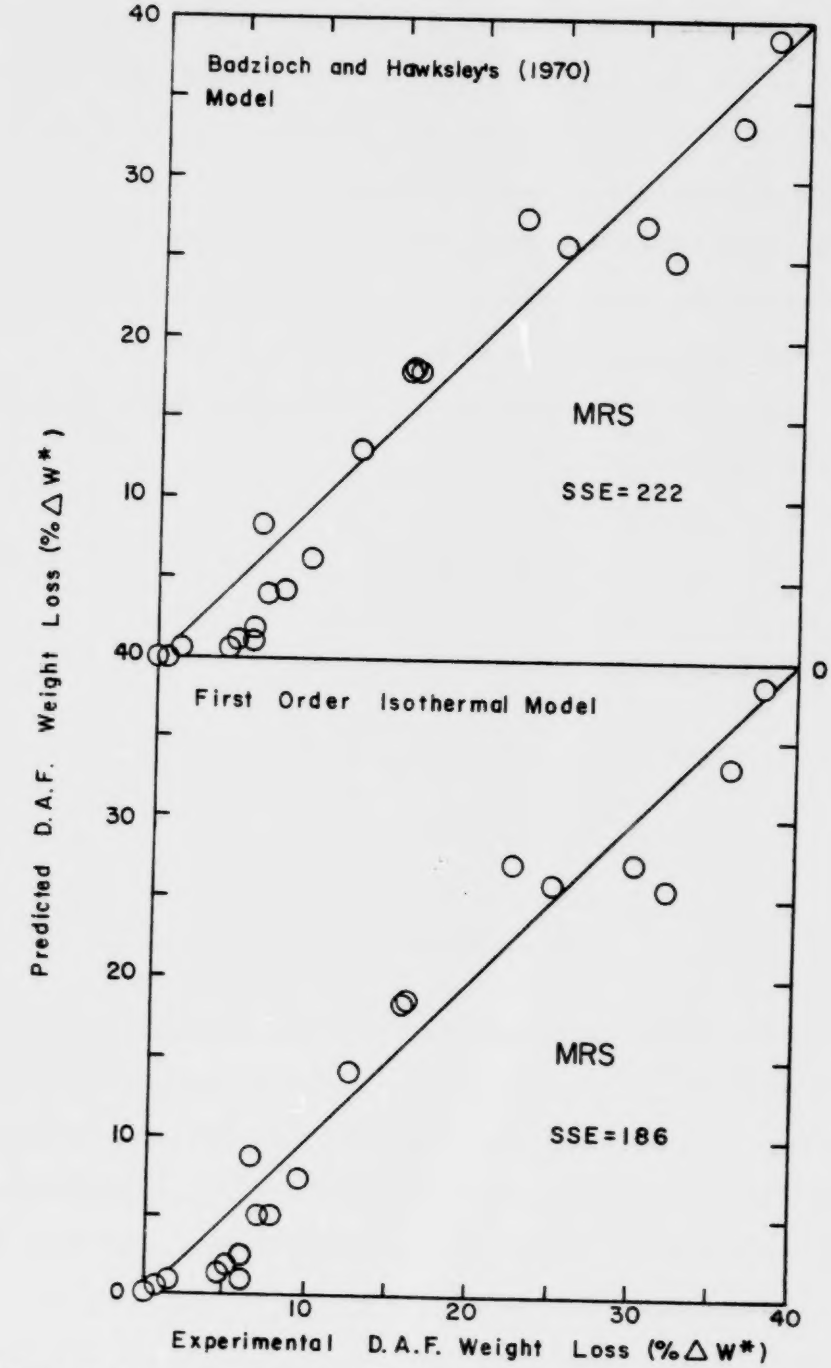

Figure 6.11 Comparison of Isothermal Models' Predictions

(SSE) for this model fit is smaller than that of Badzioch and Hawksley's model data regression.

Among the nonisothermal pyrolysis models available in the literature, Kobayashi's model was selected because of its simplicity and proven ability to correlate with a single set of parameters extensive amounts of devolatilization data for various coals (among them Montana lignite). This model was described in detail in Section 2.2.4. The expressions for the overall d.a.f. fractional weight loss are

$$\Delta W^{*} = \int_{0}^{t} (\alpha_1 K_1 + \alpha_2 K_2)\, e^{\int_{0}^{t} (K_1 + K_2) dt}\, dt \qquad (2\text{-}9)$$

where
$$K_1 = B_1 e^{-E_1/RT} \qquad (2\text{-}5)$$

$$K_2 = B_2 e^{-E_2/RT} . \qquad (2\text{-}6)$$

Values given by Kobayashi for the constants are $\alpha_1 = 0.3$, $\alpha_2 = 1.0$, $B_1 = 2x10^5$ sec $^{-1}$, $B_2 = 1.3x10^7$ sec $^{-1}$, E_1 = 25 kcal/mole, and E_2 = 40 kcal/mole. These values are used in subroutine PYROTH (Appendix A.2) to calculate ΔW^* for all the coals (MRS, BZN, and NB8) by integrating equation (2-9) numerically. Particle residence times and time-temperature histories are calculated as indicated in Sections 4.2.1 and 4.2.2. Values of ΔW^* predicted by this model for MRS coal are compared with experimental results in Figure 6.12. Overall, agreement between the model's *a priori* predictions and the experimental data is very good. The sum of squares of the residuals is smaller than those of the two isothermal models, indicating a better fit. It must be stressed that this model's parameters have not been fitted to the experimental data, as was done for the first two models presented in this section.

A first-order nonisothermal model has been developed. The rate equation (equation (2-1)) is expressed as:

$$\frac{d\Delta W^*}{dt} = K(\Delta W^*_\infty - \Delta W^*) \tag{6-26}$$

with boundary conditions

$$\Delta W^* \rightarrow \Delta W^*_\infty \text{ as } t \rightarrow \infty$$

$$\Delta W^* = 0 \text{ at } t = 0$$

where

$$K = Be^{-E/RT} \tag{6-25}$$

$$\Delta W^*_\infty = f(T).$$

ΔW^*_∞ is the equilibrium d.a.f. weight loss at a given temperature. Since K and ΔW^*_∞ are functions of particle temperature, which in turn is a function of time, equation (6-26) is a linear ordinary differential equation which is solved using an integrating factor, yielding:

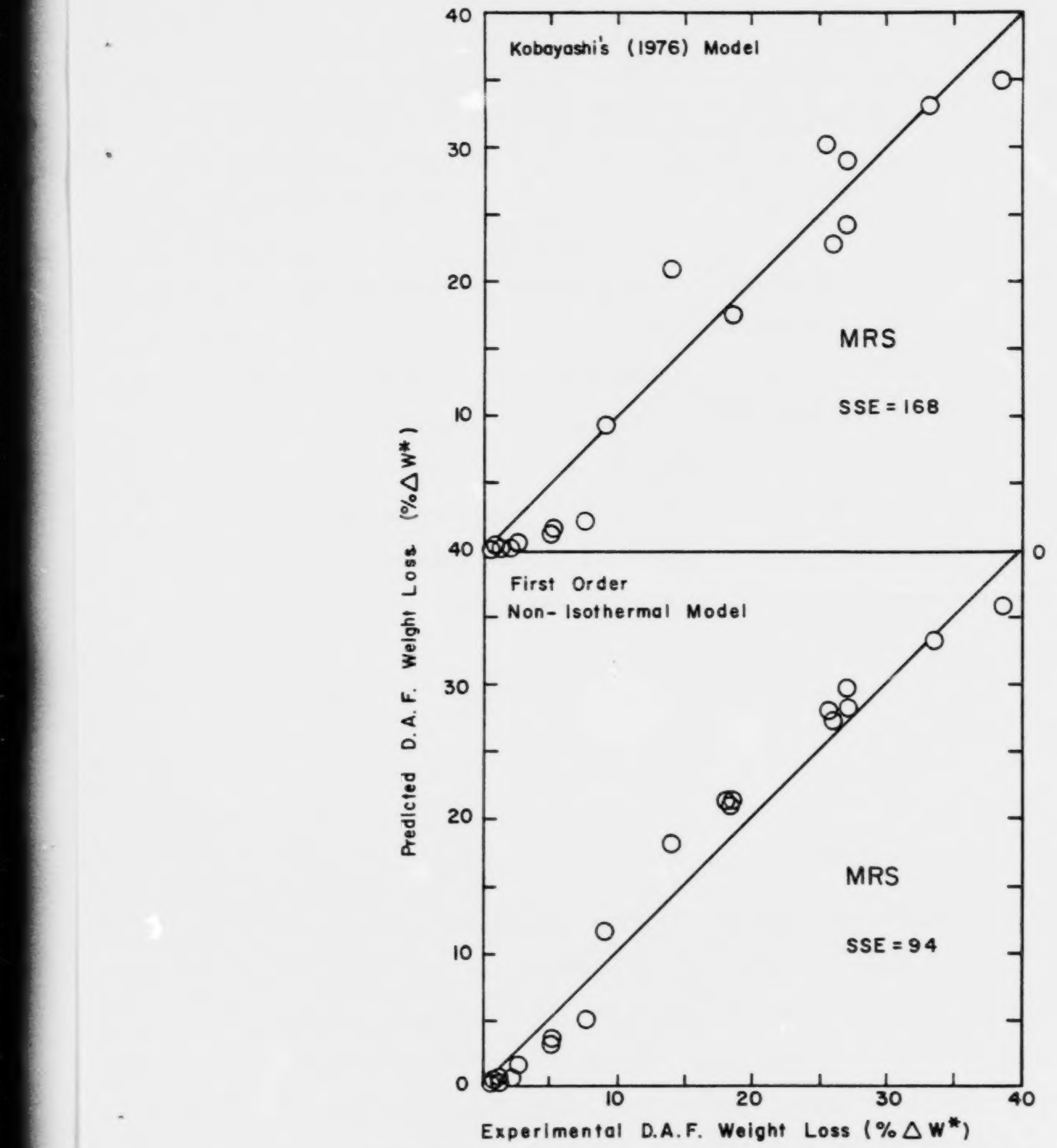

Figure 6.12 Comparison of Non-Isothermal Models' Predictions

$$\Delta W^{*} = \frac{\int_{o}^{t} K\Delta W_{\infty}^{*}\, e^{\int_{o}^{t} K\, dt}\, dt}{e^{\int_{o}^{t} K\, dt}} \quad . \qquad (6\text{-}27)$$

For isothermal conditions, this equation reduces to the familiar form of equation (6-23).

Values of ΔW_{∞}^{*} at each temperature can be obtained from estimates of the asymptotic d.a.f. weight losses in the LFR experiments. As discussed in Section 5, Duhne (1977) has shown that estimates of asymptotic equilibrium values for physical and chemical processes can be estimated from linear regression of an equation of the form:

$$\Delta W^{*} = \frac{d}{t_R} + \Delta W_{\infty}^{*} \quad , \ \Delta W^{*} \geq 0.67\Delta W_{\infty}^{*} \qquad (6\text{-}28)$$

where

d = constant

$\Delta W_{\infty}^{*} = \Delta W_{\infty}^{*}$ as $t_R \rightarrow \infty$.

If the highest value of ΔW^{*} at each temperature is assumed to be very close to ΔW_{∞}^{*}, the requirement that the data lie within 33% of the equilibrium point (relative to a total range between zero and equilibrium) is usually satisfied using the three highest ΔW^{*} points at each temperature.

Values of ΔW_{∞}^{*} estimated in this manner for NRS coal are compared with batch equilibrium d.a.f. weight loss values (ΔW_{E}^{*}) in Figure 6.13. The LFR asymptotic values of ΔW^{*} are

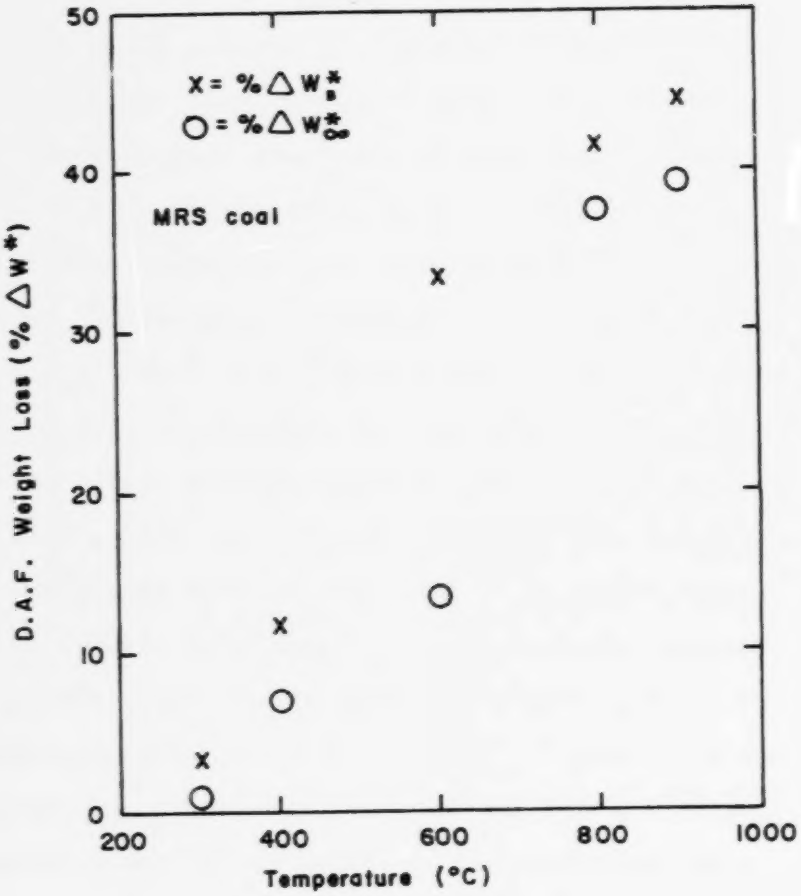

Figure 6.13 Comparison of LFR Asymptotic D.A.F. Weight Losses with Batch D.A.F. Weight Losses

consistently below the batch values. The implication of these findings is that high heating rates during fast pyrolysis (3×10^3-10^4 °C/sec) lead to lower asymptotic weight losses than do the lower heating rates (5-45°C/sec) that characterize batch pyrolysis.

These observations are consistent with findings by other researchers. Kobayashi observed the same effect under higher heating rate conditions (10^4-10^5 °C/sec). He found that, during laminar flow experiments with small residence times (5-220 msec), Montana lignite weight loss curves leveled off at significantly lower values than the asymptotic values of weight loss at long residence times. He determined that for this lignite at 1240°C, about 30% of its d.a.f. weight was lost in 100 msec, 45% in 1 sec, and 57% in about 10 minutes. Horton (1979) reviewed the fast pyrolysis data of several researchers and noted that a quasi-equilibrium is reached before the particles are quenched. He indicated that, judged by the reaction occurring during the experiments, the pyrolysis process appears complete; however, additional devolatilization occurs when the quenched char particles are reheated in a batch reactor. The implication is that if the particles had been maintained longer at the elevated temperature in the primary reactor (wire screen or laminar flow), the additional pyrolysis would have occurred there. In addition, the enhanced fast pyrolysis volatile yields reported in the literature usually include the weight loss during fast pyrolysis and the additional proximate furnace volatile matter loss. However, low rank coals have been found to show relatively small enhancement in volatile yields. Therefore, finding that fast pyrolysis quasi-equilibrium volatile yields are below slow pyrolysis equilibrium values is reasonable.

Comparison of the fast pyrolysis data obtained in this study for Montana Rosebud with that of Suuberg et al. (1978) for Montana lignite is shown in Figure 6.14. The agreement between the two sets of data obtained with two different heating rates (10^3 °C/sec in Suuberg et al.'s experiments and 3×10^3-10^4 °C/sec in this study) is entirely consistent with the discussion presented by Kobayashi (1976) regarding the effect of heating rates on volatile yields. He pointed out that there should not be any such effect for heating rates above the critical heating rate calculated with the equation

$$\left(\frac{\Delta T}{\Delta t}\right)_C = \frac{RT_\infty^2}{3E} \cdot Be^{-E/RT} \qquad (6\text{-}29)$$

where

E = first-order activation energy

T_∞ = temperature at t = ∞

B = preexponential factor

R = gas law constant

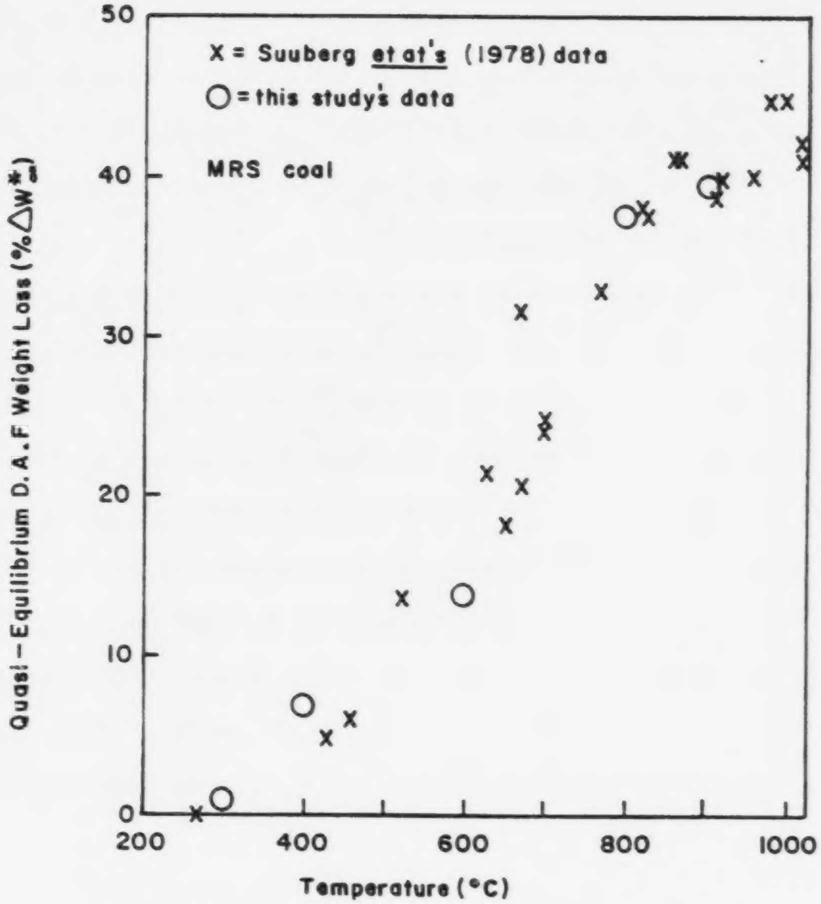

Figure 6.14 Comparison of Wire-Screen and LFR Quasi-Equilibriun D.A.F. Weight Loss Data

Kobayashi estimated that the critical heating rate of Montana lignite is 336°C/sec. Both Suuberg's and this study's heating rates are well above this value.

The values of ΔW^* calculated from the regression of equation (6-28) have been curvefitted with a fourth order polynomial

$$\Delta W^* = \beta_o + \beta_1 \left(\frac{T}{100}\right) + \beta_2\left(\frac{T}{100}\right)^2 + \beta_3\left(\frac{T}{100}\right)^3 + \beta_4\left(\frac{T}{100}\right)^4 \quad (6\text{-}30)$$

where

T = temperature, °K.

The values of this equation's parameters were found to be: $\beta_o = -1.78$, $\beta_1 = 1.14$, $\beta_2 = -0.259$, $\beta_3 = 2.48\text{x}10^{-2}$, $\beta_4 = -8.23\text{x}10^{-4}$. The SAS program used is listed in Appendix A.1. The statistical analysis of the regression is shown in Appendix B.2. This equation was then used in the first-order nonisothermal model (equation (6-28)) to calculate d.a.f. weight losses for MRS coal. Subprogram PYROTH in Appendix A.2 carried out the numerical integrations. The results of the calculations are in Appendix B.2. The activation energy and preexponential factors used were found by trial and error (E = 11.8 kcal/mole, B = 500 sec^{-1}). Because of the form of equation (6-27), a parameter search procedure would be necessary to determine the optimal values of E and B; however, the trial and error procedure was found to be satisfactory.

The agreement between the model predictions and the experimental data is shown in Figure 6.12. The sum of squares of the residuals (SSE in the figures) for this model is less than the values for all the other models tested.

The preceding discussion suggests that none of the fast pyrolysis models developed to date can be used in real gasification systems where the heating rates may be lower (e.g., because of particle size or bed depth) and typical residence times may be in the order of minutes. In order to provide a model which can be used to obtain engineering estimates of the weight loss of coal during the devolatilization stage in fluidized bed gasifiers , the equilibrium batch d.a.f. weight loss data for each of the five coals studied have been curvefitted with equation (6-29). The nonisothermal first-order model (equation (6-27)) will then yield asymptotic d.a.f. weight loss values in agreement with the results of 20 minute residence time batch experiments. Dry ash-free weight losses predicted by this method (using the same Arrhenius parameters) are shown in Appendix B.2. The sum of squares of the errors of this model fit for MRS coal to the fast pyrolysis data is 421.0 which is larger than that obtained with the LFR data; it is not unreasonable, however.

In order to allow prediction of ΔW^+ and $\Delta W^\ddagger$, the rate of moisture evolution must be modeled. The following equation is used as a rough estimate of the moisture release rate:

$$M = M_\infty \left[1 - \exp\left(- \int_o^t B_M e^{-\Delta H/RT} dt\right)\right] \qquad (6\text{-}31)$$

where

M_∞ = ASTM moisture content of coal

ΔH = enthalpy of vaporization of water plus sensible heat for 600°C steam (15943 cal/mole)

B_M = empirical constant evaluated using MRS-LFR data at 300°C (1.652×10^6 sec^{-1}).

Kobayashi's model and the first-order nonisothermal model with batch ΔW^* values, coupled with the above moisture evolution model, yield the predictions shown in Appendix A.2. The same appendix also contains the experimental data calculated in a.r., m.f., and d.a.f. bases. This model predicts very rapid evolution of moisture, which is what is observed experimentally. All of the runs except run 15 (the 300°C run) produced chars with less than 2% moisture. Such residual moisture is probably due to water condensation in the collector and cyclones, and to laboratory humidity absorption during sampling. This hypothesis is supported by the random variations in char moisture at a given T and t_R.

6.4 Analysis of Elemental Release Results

The results discussed in Section 5 show that several elements are evolved in significant quantities during batch pyrolysis. It is of interest to determine how fast the elemental release occurs. For this purpose, the chars produced in the laminar flow reactor (LFR) experiments were analyzed for several major, minor, and trace elements in addition to moisture, ash, and volatile matter. A listing of the results of the analyses of the coals and chars is shown in Appendix B.2.

The objectives of these experiments were to determine, in a qualitative manner, the behavior of the elemental components of coal during fast pyrolysis, and to develop and test a kinetic model for the elemental release. Sampling and analysis problems made determination of meaningful kinetic parameters difficult (modifications that might allow such determination will be discussed subsequently). Therefore, simple statistical trend analysis was used to determine whether different elements were retained completely in the chars, or whether they were evolved to a measurable extent. Order-of-magnitude estimates of the kinetic parameters for sulfur were obtained for a first-order, single reaction, elemental release model.

Different groups of chars were analyzed for different species, for a variety of reasons. Excellent data on the release of the major elements and volatile matter during fast pyrolysis is available (Kobayashi, 1976) for temperatures above 800°C (see Figures 2.1 and 2.2). Therefore, C, H, and ASTM proximate volatile matter were analyzed only for low temperature runs. Because of its importance in coal gasification, sulfur was analyzed in all chars. Most trace and minor elements studied were analyzed only for the higher temperature runs in order to diminish the effect of tracer-introduced bias. Three 800°C runs with MRS coal were analyzed for all the elements that the analytical capabilities permitted. These runs have been used primarily to find element-to-element correlations.

Values of ψ_H and ϕ_H were calculated using equations (4-48) and (4-49), and were also calculated using the ash tracer method without any corrections. Equation (6-5) was used for this purpose. To distinguish ψ and ϕ values determined using the best ΔW^* estimates from those determined using the uncorrected ash tracer method, the latter are subscripted with an "A" instead of an "H". The values of X_H^+, ψ_H^+, ψ_A^+, $X_H^\ddagger$, $\psi_H^\ddagger$, $\psi_A^\ddagger$, ϕ_H, and ϕ_A for all elements and coals were linearly regressed versus residence time and temperature. The computer program (LFRS1) used for this purpose is listed in Appendix A.2. The results of the data analysis are tabulated in Appendix B.2.

The mathematical analyses of the time-temperature histories of the coal particles and the pyrolysis modeling studies suggest that using linear regression to detect trends with time and temperature may be an oversimplification. However, in view of the scatter in the data and the uncertainties in the residence time, particle temperature, and weight loss estimations, a more complex approach is not justified. To allow for all these uncertainties, a less stringent criterion than in the batch data analysis was used to test for significance of the slopes with respect to time and temperature. Significance at the 80, 90, and 98 percent confidence levels was determined using a two-tailed t-test.

Tables 6.5 to 6.7 present the element-temperature and element-time correlations. Caution must be exercised in the interpretation of these tables. The uncertainties in the sampling, analysis, and weight loss estimations may have biased some results. In addition, the temperature and residence time ranges over which the chars were analyzed vary for different elements and coals. The reader is urged to refer to Appendix B.2 for the specific T and t_R values which were used in the multiple linear regression of a specific element. The conclusions shown in Tables 6.5 to 6.7 are valid only within the range of T and t_R values of the chars analyzed for each element.

The element-time correlations for the MRS coal runs (25, 27, and 29) are shown in Table 6.8. As indicated before, special precautions were taken in the LFR operation,

Table 6.5 Significant Correlations in MRS-LFR Chars

MRS Coal	Element-Temperature Correlations					Element-Time Correlations				
ELEMENT	$X_H^{\ddagger}$	$\Psi_A^{\ddagger}$	$\Psi_H^{\ddagger}$	$\emptyset_A$	$\emptyset_H$	$X_H^{\ddagger}$	$\Psi_A^{\ddagger}$	$\Psi_H^{\ddagger}$	$\emptyset_A$	$\emptyset_H$
Volatile Matter			— **		— **					
C	+ *	— **	— **	— **	— **					
H	— **	— **	— **	— **	— **					— △
S	— *	— **	— **	— **	— **			— ⊕		— ⊕
Mn	— *					+ **				
Cu										
Al			— *		— *	+ ⊕				
Ce	+ *	+ **	+ *	+ **	+ *	+ ⊕	— *	— *	— *	— *
Se	+ *	+ ⊕		+ ⊕	— △	— *	— *	— *	— *	— *
Th						+ ⊕				
Cr										
Sm						+ *				
U										
La					— △					— △
As	+ **	+ *	+ *	+ *	— △	— **	— **	— **	— **	— **
Sb (by NAA)										

⊕ = significant at 80% C.L.
* = significant at 90% C.L.
** = significant at 98% C.L.
△ = undetected trend
— = negatively correlated
+ = positively correlated

Table 6.5 (Continued)

MRS Coal	Element-Temperature Correlations					Element-Time Correlations				
ELEMENT	$X_H^{\pm}$	$\Psi_A^{\pm}$	$\Psi_H^{\pm}$	$\emptyset_A$	$\emptyset_H$	$X_H^{\pm}$	$\Psi_A^{\pm}$	$\Psi_H^{\pm}$	$\emptyset_A$	$\emptyset_H$
Br										
Na		+ ✱	+ ⊕	+ ✱	+ ⊕	+ ⊕		− ⊕		− ⊕
K										
Ti										
Sc						+ ✱				
Eu										
Ru										
Fe	+ ⊕	+ ⊕		+ ⊕			− ⊕	− ⊕	− ⊕	− ⊕
Co	+ ⊕	+ ✱	+ ✱	+ ✱	+ ✱					
Zn										
Cs										
P	+ ✱				− △					− △
Hg	− ✱	− ✱	− ✱	− ✱	− ✱	+ ⊕				
Pb	+ ✱					− ✱	− ✱	− ✱✱	− ✱	− ✱✱
V (by AA)	+ ⊕		− ⊕		− ⊕					
V (by NAA)								− ⊕		
Sb (by AA)	+ ✱	+ ⊕		+ ⊕						

⊕ = significant at 80% C.L.
✱ = significant at 90% C.L.
✱✱ = significant at 98% C.L.
△ = undetected trend
— = negatively correlated
+ = positively correlated

Table 6.6 Significant Correlations in NB8 –LFR Chars

NB8 Coal	Element- Temperature Correlations					Element-Time Correlations				
ELEMENT	$X^{\ddagger}_{H}$	$\Psi^{\ddagger}_{A}$	$\Psi^{\ddagger}_{H}$	$\varnothing_{A}$	$\varnothing_{H}$	$X^{\ddagger}_{H}$	$\Psi^{\ddagger}_{A}$	$\Psi^{\ddagger}_{H}$	$\varnothing_{A}$	$\varnothing_{H}$
S					− △		− ⊕		− ⊕	− △
Se					− △					− △
Sm										
La					− △					− △
As	+ ✱	+ ✱	+ ⊕	+ ✱	− △		− ✱	− ⊕	− ✱	− ⊕
Sb(by NAA)	+ ✱	+ ✱	+ ✱	+ ✱	+ ✱					
Hg	+ ✱				− △	− ✱	− ✱	− ⊕	− ✱	− ⊕
Pb					− △	+ ✱✱				
Fe										
Co	+ ✱	+ ✱	+ ⊕	+ ✱	+ ⊕		− ⊕		− ⊕	
Th										
Sc		+ ✱✱		+ ✱✱			− ✱✱		− ✱✱	
V (by NAA)										

⊕ = significant at 80% C.L.
✱ = significant at 90% C.L.
✱✱ = significant at 98% C.L.
△ = undetected trend
− = negatively correlated
+ = positively correlated

Table 6.7 Significant Correlations in BZN –LFR Chars

BZN Coal	Element- Temperature Correlations					Element- Time Correlations				
ELEMENT	$X_H^{\ddagger}$	$\Psi_A^{\ddagger}$	$\Psi_H^{\ddagger}$	ϕ_A	ϕ_H	$X_H^{\ddagger}$	$\Psi_A^{\ddagger}$	$\Psi_H^{\ddagger}$	ϕ_A	ϕ_H
S			$\overset{-}{\oplus}$		$\overset{-}{\oplus}$	$\overset{-}{\oplus}$	$\overset{-}{*}$	$\overset{-}{*}$	$\overset{-}{*}$	$\overset{-}{*}$
Se					$\overset{-}{\triangle}$					$\overset{-}{\triangle}$
Sm	$\overset{+}{\oplus}$	$\overset{+}{\oplus}$		$\overset{+}{\oplus}$						
Sb(by NAA)										
Hg										$\overset{-}{\triangle}$
Pb										$\overset{-}{\triangle}$
Sc										
Fe			$\overset{-}{*}$		$\overset{-}{*}$	$\overset{+}{*}$	$\overset{+}{*}$	$\overset{+}{*}$	$\overset{+}{*}$	$\overset{+}{*}$
Co										
La					$\overset{-}{\triangle}$		$\overset{-}{\oplus}$		$\overset{-}{\oplus}$	$\overset{-}{\triangle}$
Th										
As					$\overset{-}{\triangle}$					$\overset{-}{\triangle}$
V (by NAA)	$\overset{+}{*}$	$\overset{+}{**}$	$\overset{+}{**}$	$\overset{+}{**}$	$\overset{+}{**}$	$\overset{+}{*}$	$\overset{+}{**}$	$\overset{+}{**}$	$\overset{+}{**}$	$\overset{+}{**}$

⊕ = significant at 80% C.L.
* = significant at 90% C.L.
** = significant at 98% C.L.
△ = undetected trend
— = negatively correlated
+ = positively correlated

Table 6.8 Significant Element-Time Correlations at 800°C - MRS Runs 25, 27, and 29

Element	$\chi_H^{\ddagger}$	$\Psi_A^{\ddagger}$	$\Psi_H^{\ddagger}$	$\varnothing_A$	$\varnothing_H$
C	+ *	− ⊕	− **	− ⊕	− **
H	− *	− **	− *	− **	− *
S		− *	− **	− *	− **
Sm	+ ⊕		+ ⊕		− △
U	+ *	+ ⊕		− ⊕	+ ⊕
La					− △
As					− △
Sb(by NAA)	+ ⊕		− *		− *
Br					
Na	+ **				
K		− ⊕	− *	− ⊕	− *
Ti					
Mn	+ *		− ⊕		− ⊕
Cu					
V(by NAA)					
Al					

Element	$\chi_H^{\ddagger}$	$\Psi_A^{\ddagger}$	$\Psi_H^{\ddagger}$	$\varnothing_A$	$\varnothing_H$
Ce	+ *				
Se					− △
Th	+ *				
Cr					
Sc	+ **				
Eu					
Ru					
Fe	+ **				
Co	+ ⊕				
Zn					
Cs					
P					− △
Pb					
Hg					− △
Sb(by AA)					
V(by NAA)	+ *				

⊕ = significant at 80% C.L.
* = significant at 90% C.L.
** = significant at 98% C.L.
△ = undetected trend
− = negatively correlated
+ = positively correlated

char sampling, and chemical analyses for these runs. In addition, these chars were analyzed for all the elements which the analytical capabilities available allowed. Therefore, the results shown in Table 6.8 provide some additional information which becomes apparent with the improved precision in the results.

The most important interpretations of the information presented in Tables 6.5 to 6.8 are as follows:

1. If $X_H^{\ddagger}$ versus T has a slope significantly greater than zero, indicating that the char is becoming progressively enriched in the element as the temperature increases, and $\psi_H^{\ddagger}$ versus T also has a slope equal to or greater than zero (the latter due to underestimation of ΔW^*), indicating that the absolute amount of element in the char is remaining constant, it may be inferred that the element is not released from the particle in the temperature range investigated.
2. If the slope of $X_H^{\ddagger}$ versus T is greater than zero, and that of $\psi_H^{\ddagger}$ versus T is less than zero, the element release from the coal is significant, but its fractional release at a given temperature is less than that of total volatile matter.
3. If the slope of $X_H^{\ddagger}$ versus T is equal to zero, and that of $\psi_H^{\ddagger}$ versus T is less than zero, the element release is proportionally equal to the total volatile matter release.

4. If the slopes of $X_H^\ddagger$ and $\psi_H^\ddagger$ versus T are less than zero, the element release is proportionally greater than the total volatile matter release.
5. If the slope of ϕ_H versus T is equal to zero (indicating that no appreciable amounts of the element have been released), the element is not volatile. If it is less than zero, the element is released to an extent that increases with increasing temperature. The behavior of ϕ_H simply mirrors that of $\psi_H^\ddagger$, but, more importantly, it allows easy visual examination of the data. Since ϕ_H must range from 1.0 (complete retention) to 0.0 (no retention), its value quickly indicates whether the element is retained in the char or not. This is useful because the linear regression analyses only detect consistent trends. If a retention (ϕ_H) drops at low temperatures and then remains at a constant value, no linear trend would be found; nevertheless, it would be obvious that the element had been released from the coal.
6. Those elements for which the slope of $X_H^\ddagger$ versus T is positive, the slope of $\psi_A^\ddagger$ versus T is zero (indicating that the mass fraction normalized by the uncorrected ash tracer method meets the equality criterion of equation (6-15)), and the slope of $\psi_H^\ddagger$ versus T is negative, are released to the same extent (with respect to T) as the ash is lost from the particles.

7. If the slopes of $X_H^{\ddagger}$ and $\psi_A^{\ddagger}$ versus T are positive, and the slope of $\psi_H^{\ddagger}$ versus T is negative, the element is released to a lesser extent (as a function of T) than the ash.

8. If the slope of $X_H^{\ddagger}$ versus T is positive and that of $\psi_A^{\ddagger}$ versus T is negative, the element is released to an extent large enough to overcome the ash loss effect.

9. The interpretations of the slopes of $X_H^{\ddagger}$, $\psi_H^{\ddagger}$, and ϕ_H versus t_R are similar to those versus T. The rates of elemental release are compared with ΔW versus t_R instead of ΔW versus T, however.

10. If no slopes are found to be significantly different from zero for a given element, either the scatter in the data is too large for any significant trends to be detected, or the trends cannot be detected through linear regression. Obvious undetected trends have been marked as such in Tables 6.5 to 6.7.

Because of the large number of elements studied, an element-by-element interpretation of the results shown in Tables 6.5 to 6.7 is out of the question. However, since the most important information needed for the evaluation of the fate of trace elements in coal gasification processes concerns the release of volatile elements, only one non-volatile element will be examined as an example. The bulk of the discussion that follows concerns only elements which show significant release from the coals studied.

As was the case in the batch experiments, certain elements exhibit similar behavior in every coal. Furthermore, the elements found to be released in significant quantities during the batch experiments generally show the same behavior during LFR experiments. Nonvolatile elements are retained in the chars: $X_H^{\ddagger}$ for those elements increases with time and temperature, while $\psi_H^{\ddagger}$ remains at the feed value. As an example, the behavior of iron is shown in Figure 6.15. The slight increase in the ψ_H^{+} values in this figure suggest that weight losses are still being underestimated slightly. Other such elements include Co, Fe, Sc, Na, Ce, and V. Other elements are found to be released in significant quantities, as evidenced by the negative slope of $\psi_H^{\ddagger}$ or ϕ_H. Such elements include C, H, S, Pb, Hg, As, Se, and La. Sm and Mn appear to be released from some chars at the same rate as the ash.

Temperature appears to be a more important factor than residence time in determining the extent of elemental release during fast pyrolysis of the three coals studied over the temperature range (800 to 900°C for most elements) and residence times (250 to 800 msec for most elements) covered in this study. This is indicated by the larger number of significant trends with respect to temperature found in the multiple linear regressions.

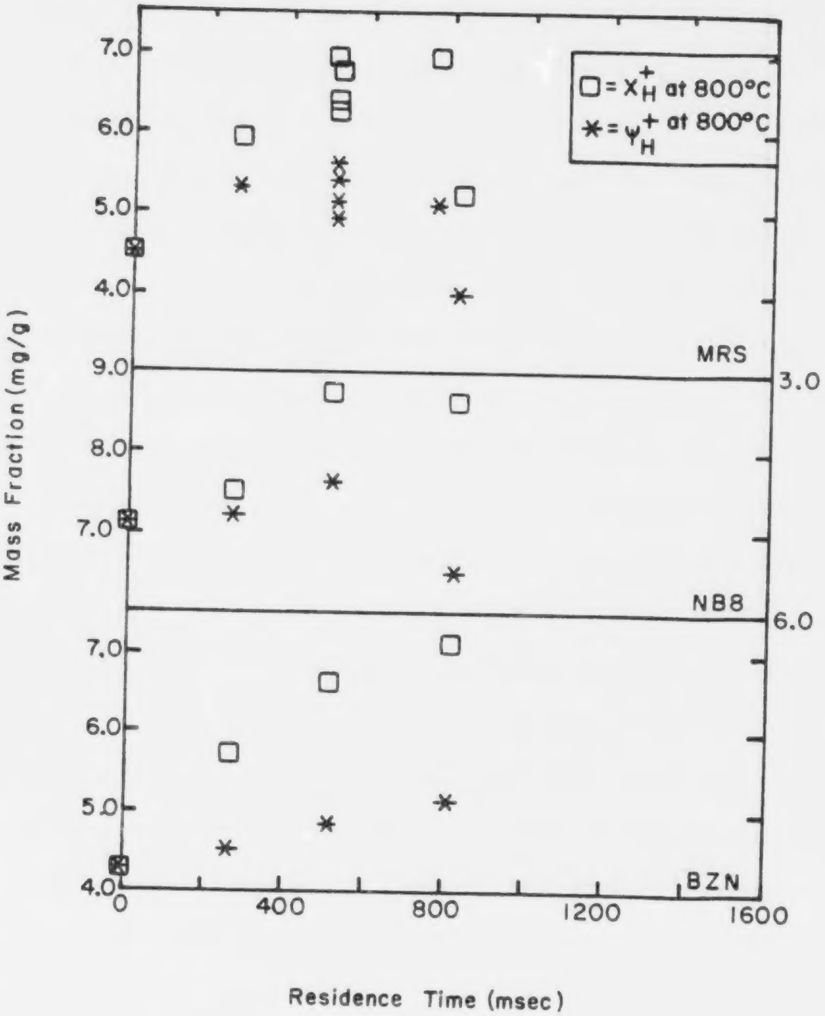

Figure 6.15 Iron Mass Fraction in Chars

The data presented in Figure 6.16 complement the findings of Kobayashi (1976) which were shown in Figures 2.1 and 2.2. Carbon, hydrogen, and ASTM volatile matter are shown to be released from the coal particles in measurable quantities during fast pyrolysis at low temperatures. Figures 6.17 to 6.22 show the decrease in retention (ϕ_H) of La, As, Se, S, Pb, and Hg as functions of T and t_R. The solid lines in Figure 6.20 are model predictions which will be discussed later. The trends are evident in all cases: ϕ_H decreases as T and/or t_R increase. However, it is also evident that the scatter in the data and the uncertainties in the manner in which the weight loss data had to be estimated would make the determination of meaningful kinetic parameters quite difficult.

Another problem, perhaps more important than random data scatter, is the consistent pattern of retention values greater than 100% at low temperatures and/or reaction times (i.e., low extents of devolatilization). This problem is severe in the case of the medium volatility elements (La, Se, and As). It appears that the weight loss estimations are still biased low, at least at low temperatures and/or residence times. As indicated before, other evidence that substantiates this observation is seen in Figure 6.15; the normalized iron mass fractions (ψ_H^+) are consistently above the feed mass fraction. They should have been equal to zero, within experimental error.

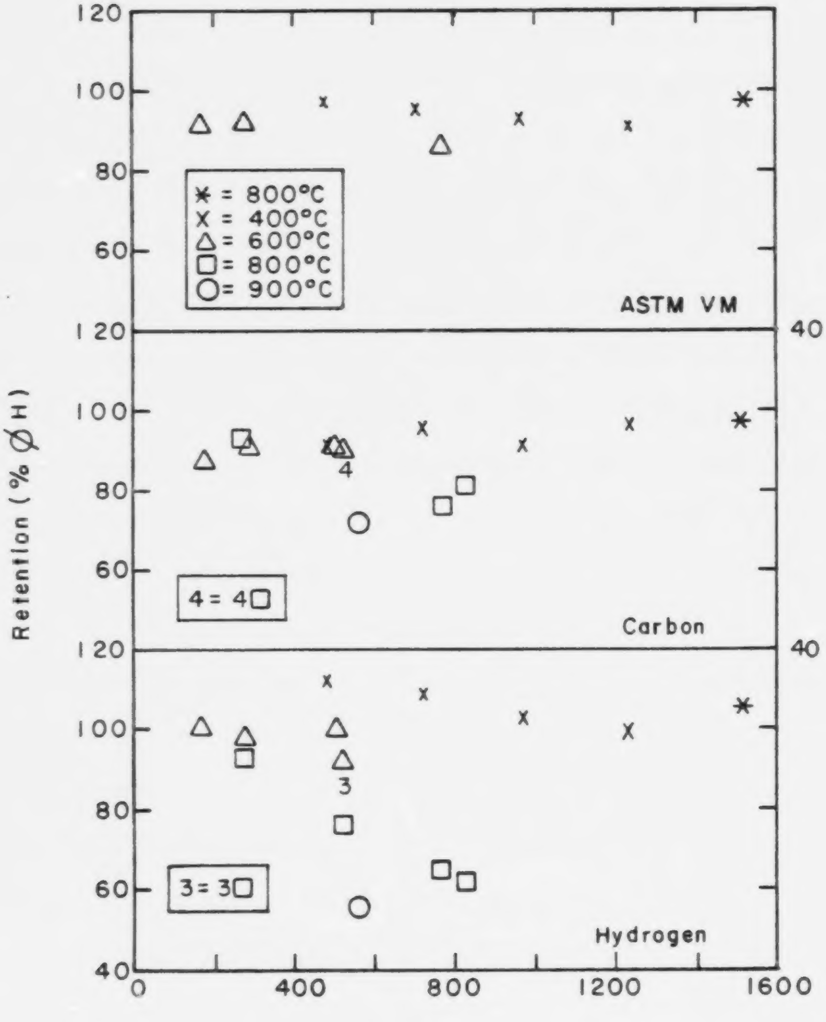

Figure 6.16 ASTM VM, C and H Retentions in MRS Chars

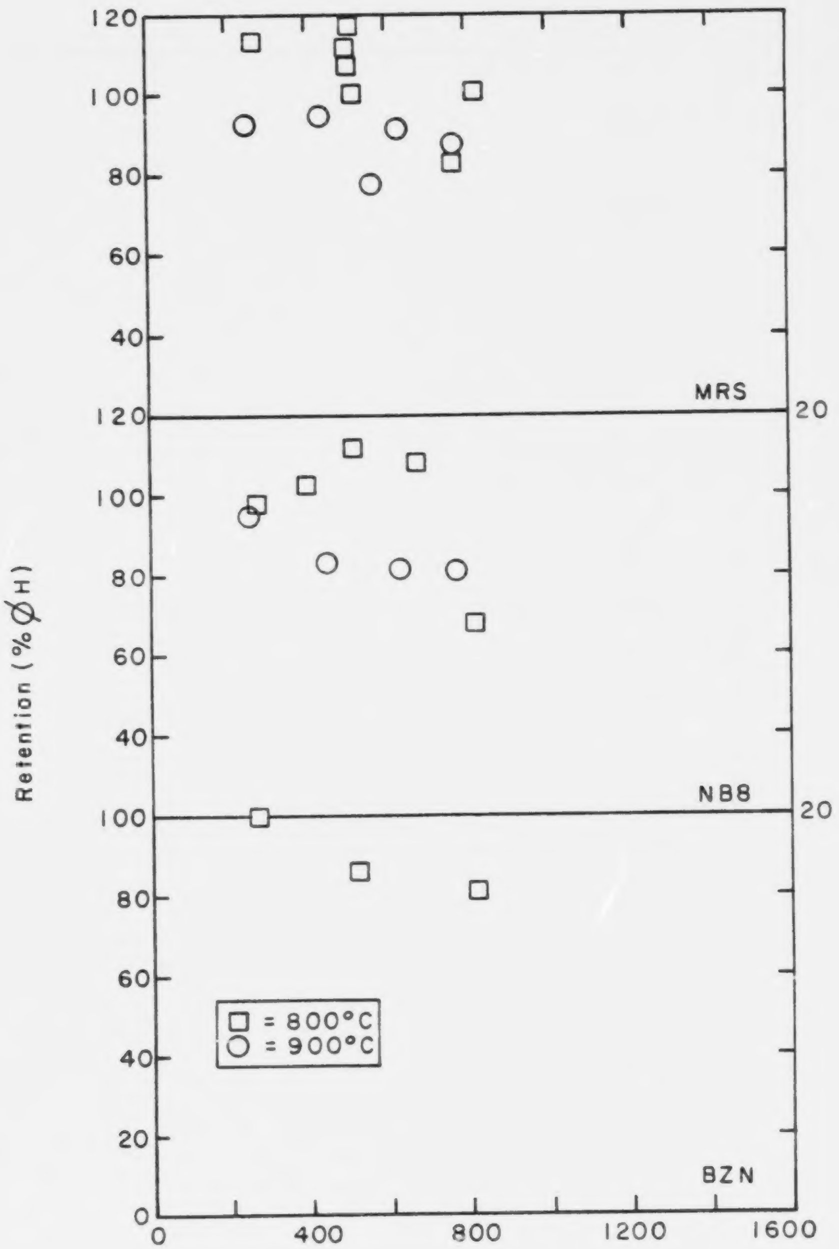

Figure 6.17 Lanthanum Retention in LFR Chars

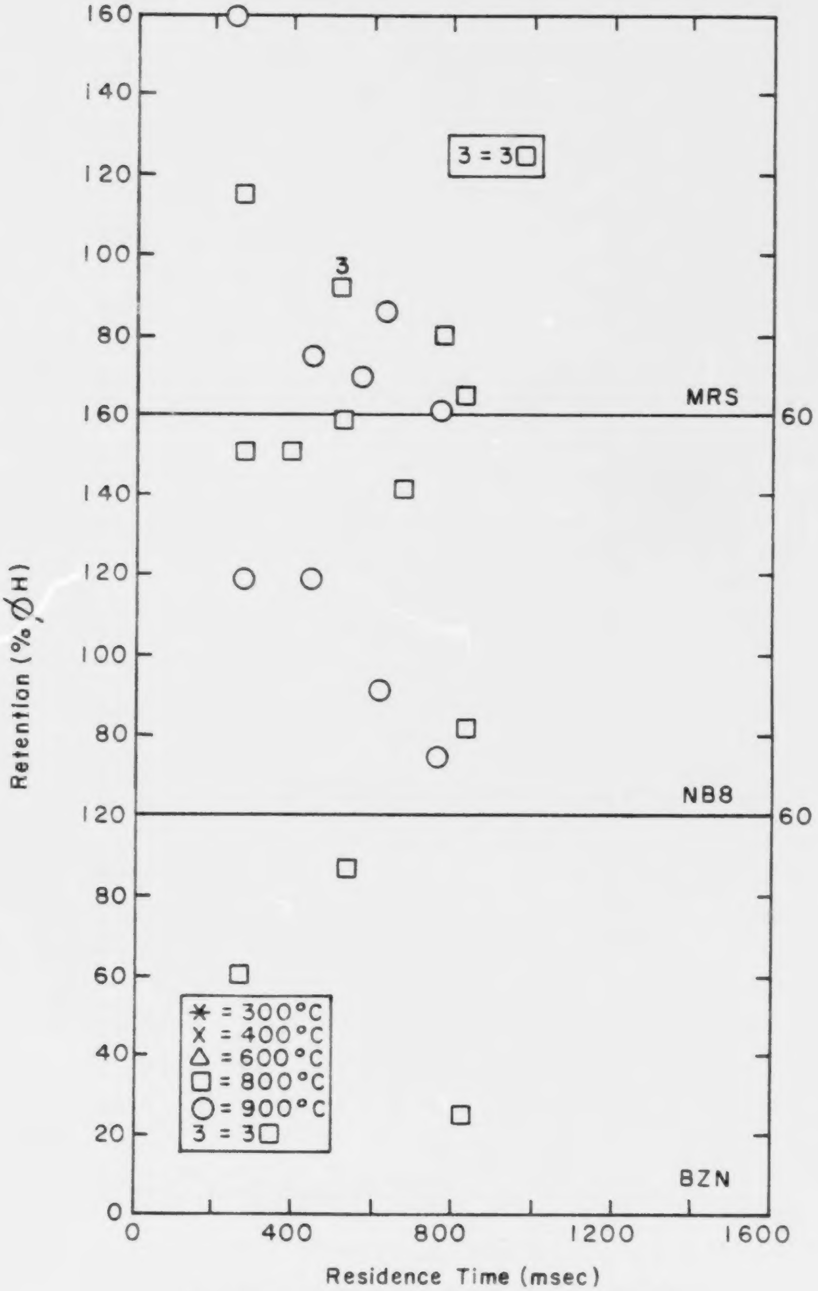

Figure 6.18 Arsenic Retention in LFR Chars

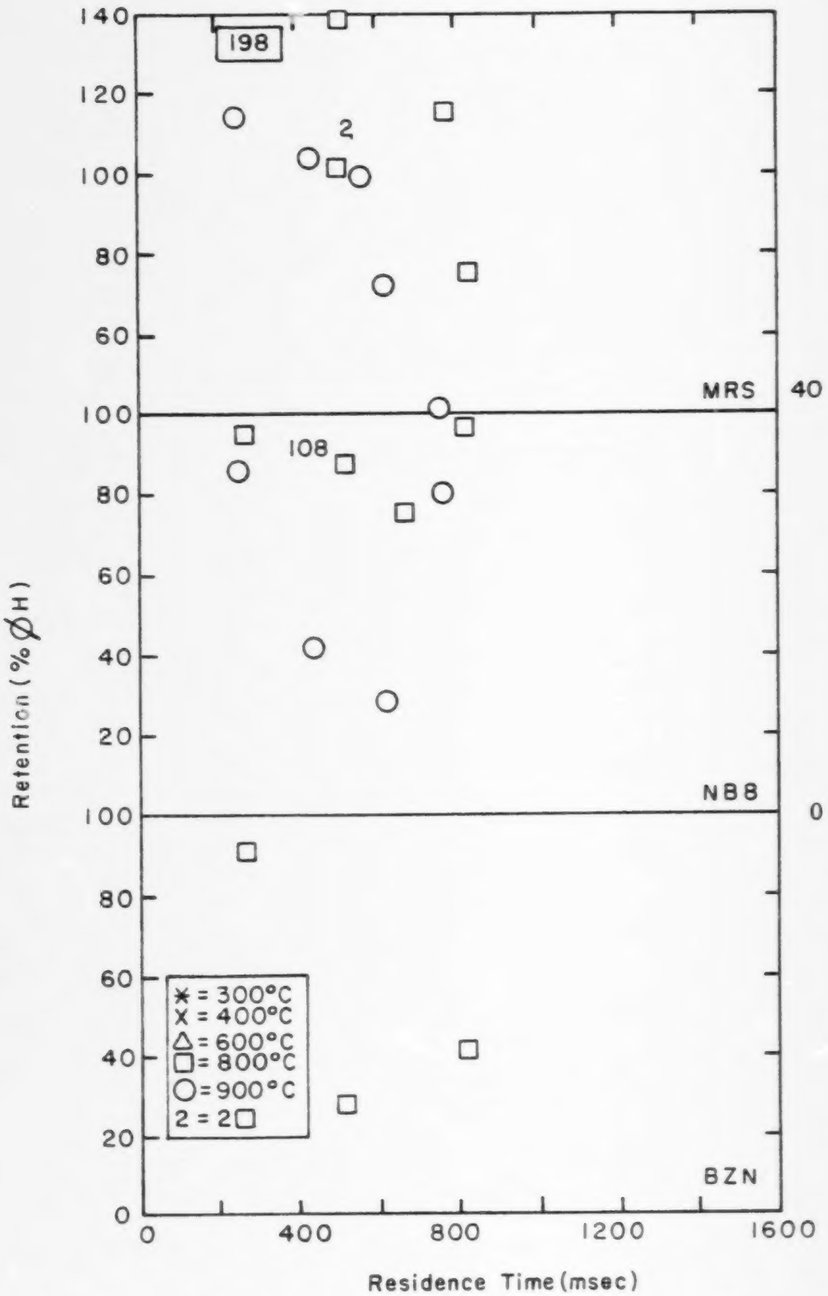

Figure 6.19 Selenium Retention in LFR Chars

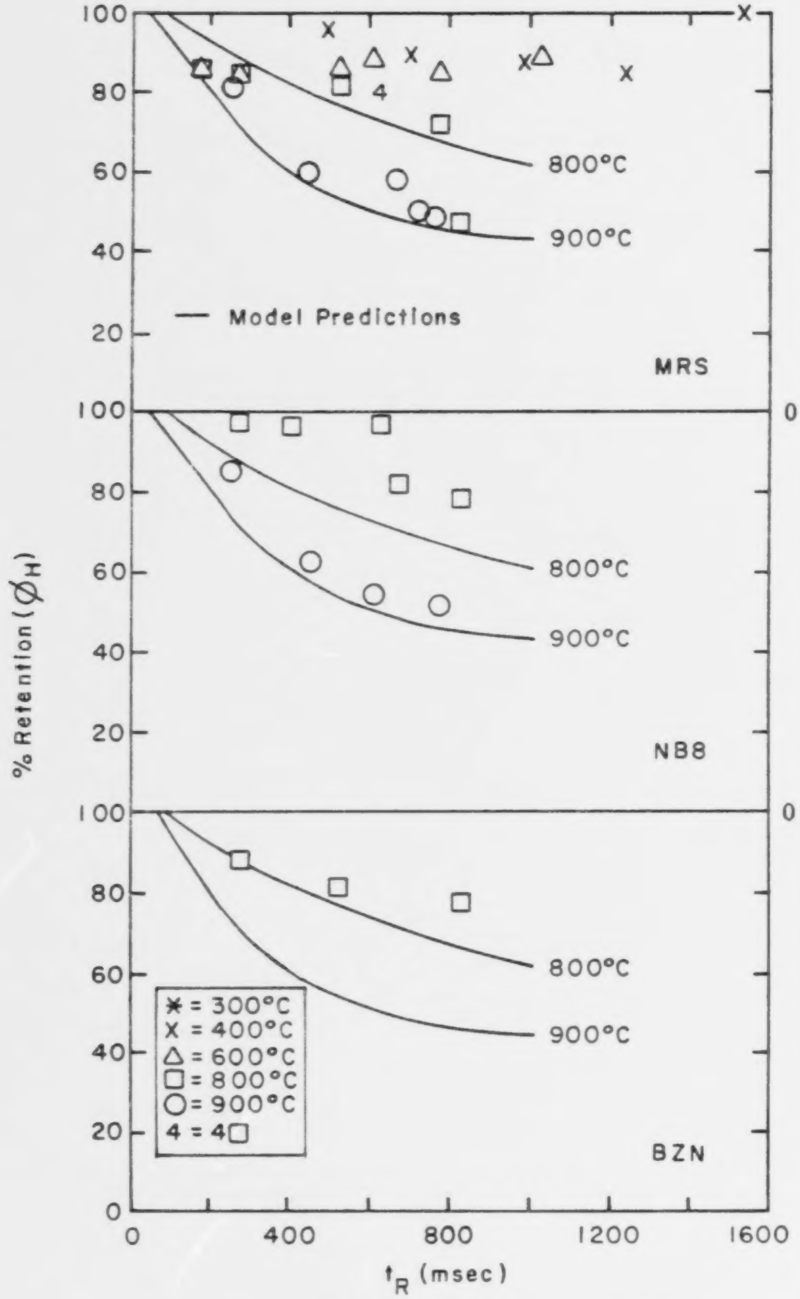

Figure 6.20 Sulfur Retention in LFR Chars

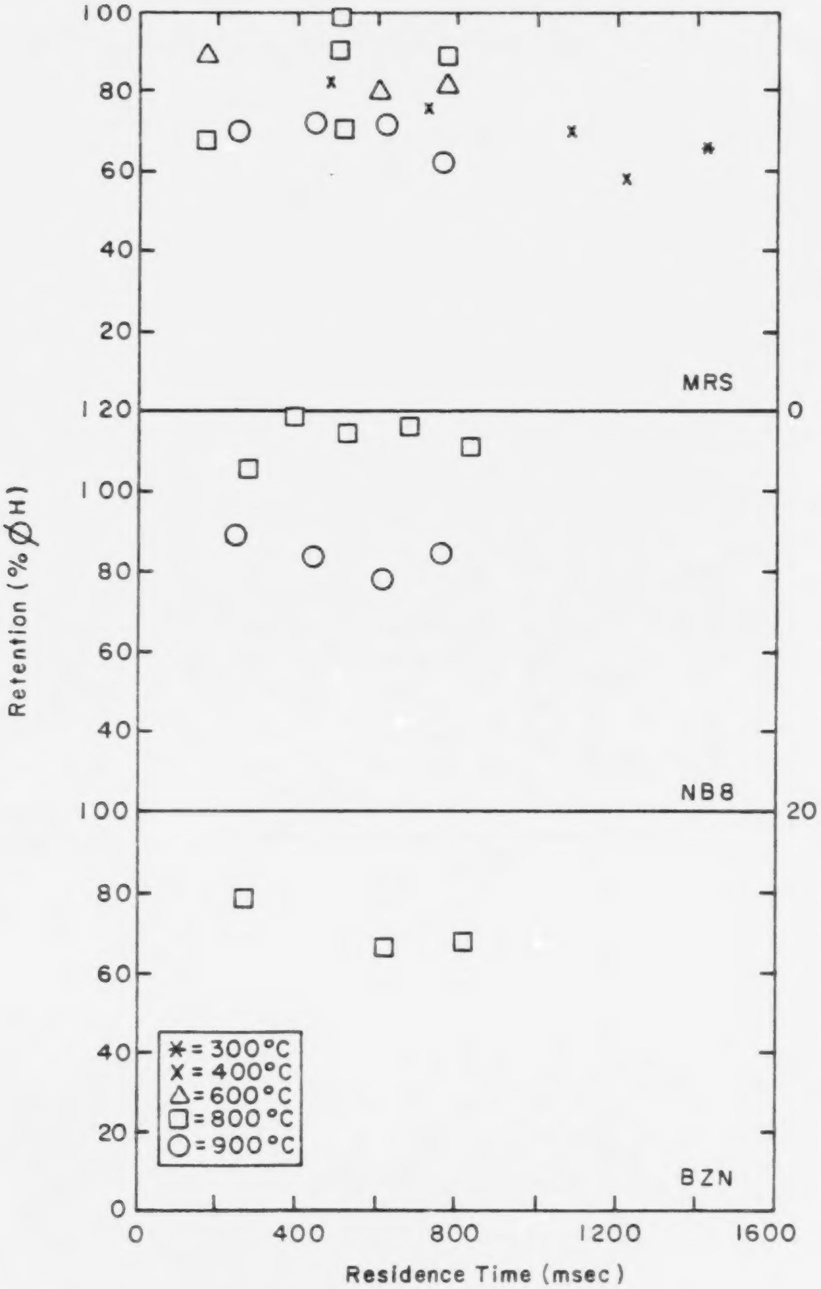

Figure 6.21 Lead Retention in LFR Chars

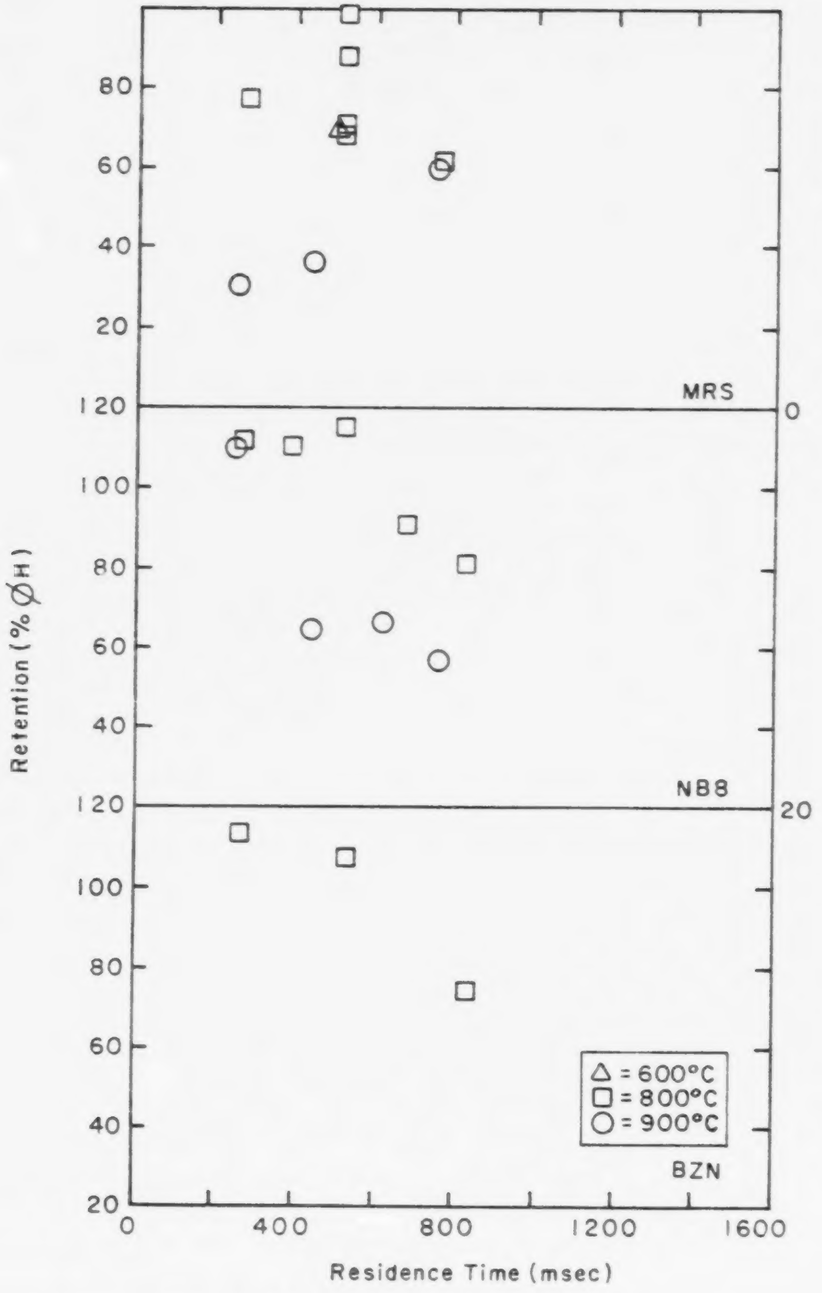

Figure 6.22 Mercury Retention in LFR Chars

Despite these problems, the trends shown by the retention curves of the volatile trace elements suggest that if the weight loss bias problem could be solved, the calculation of kinetic parameters would be possible. To that end, a first-order model is proposed for the evolution of trace elements in coal during fast pyrolysis. The rate equation is:

$$\frac{d\Delta\Omega_H}{dt} = K(\Delta\Omega_\infty - \Delta\Omega_H) \qquad (6\text{-}32)$$

with boundary conditions

$$\Delta\Omega_H \rightarrow \Delta\Omega_\infty \quad \text{as } t \rightarrow \infty$$

$$\Delta\Omega_H = 0 \text{ at } t = 0$$

where

$$K = Be^{-E/RT} \qquad (6\text{-}25)$$

$$\Delta\Omega_\infty = f(T) .$$

$\Delta\Omega_\infty$ is the equilibrium d.a.f. elemental release at a given temperature. Since K and $\Delta\Omega_\infty$ are functions of particle temperature, which in turn is a function of time, equation (6-32) is a linear ordinary differential equation which is solved using an integrating factor, yielding

$$\Delta\Omega_H = \frac{\int_0^t K\Delta\Omega_\infty e^{\int_0^t K\,dt}\,dt}{e^{\int_0^t K\,dt}} . \qquad (6\text{-}33)$$

Values of $\Delta\Omega_\infty$ at each temperature can be obtained using the batch model in the form

$$\Delta\Omega_\infty = H(T - T_C) \cdot \{\Delta\Omega_e[1 - e^{-b(T - T_C)}]\} \qquad (6\text{-}34)$$

Particle residence times and time-temperature histories are calculated as indicated in Sections 4.2.1 and 4.2.2.

The isothermal form of equation (6-33)

$$\Delta\Omega_H = \Delta\Omega_\infty(1 - e^{-Kt}) \qquad (6\text{-}35)$$

was used to determine model parameters for sulfur as a rough estimating procedure. Linear regression of t versus $\ell n[1 - \Delta\Omega_H/\Delta\Omega_\infty]$ yielded $-1/K$ as the slope; linear regression of $\ell n(K)$ versus $1/T$ yielded $\ell n(B)$ as the intercept and $-E/R$ as the slope. All the 800 and 900°C data for this element (in the three coals) was used for the regressions except for the $\Delta\Omega_H$ of run 31 which is an obvious outlier. The value of the frequency factor was found to be $B = 171.113$ sec^{-1} with a value of the activation energy $E = 2.502 \times 10^4$ cal/mole. No parameters could be obtained for the other volatile elements because of the high degree of scatter and/or bias of their $\Delta\Omega_H$ data.

Integration of equation (6-33) was carried out using Simpson's rule with program LTEMP listed in Appendix A.2. The model predictions (tabulated in Appendix B.2) are shown as the solid lines in Figure 6.20 (as $\phi_H = 1 - \Delta\Omega_H$). The model's predictions appear to be qualitatively correct. These results suggest that given the proper Arrhenius parameters the proposed model could predict the elemental release data reasonably well. Regardless of the precision of the kinetic parameters obtained, the model predictions must converge to the batch model values ($\Delta\Omega_\infty$) thus ensuring the model's accuracy at long residence times (on the order of minutes).

In the absence of good kinetic parameters for the elemental release model, the following findings may be used as rules of thumb to predict rates of elemental release. Several volatile species have been found to be highly correlated with ΔW^* (d.a.f. weight loss); they are shown in Table 6.9. ASTM volatile matter (VM), carbon, and hydrogen were expected to be highly correlated since they must be evolved for the coal to lose weight. The other volatile elements appear to be released at a rate proportional to the d.a.f. weight loss. Therefore, the proportionality constant (slope) may be used to predict the rate of elemental release through the equation

$$\Delta\Omega_H = K_S \Delta W^* \tag{6-36}$$

for

$$T > T_C$$

$$\Delta\Omega_H \leq \Delta\Omega_\infty(T)$$

Table 6.9 Significant D.A.F. Weight Loss-Element Correlations

Coal	MRS			NB8			BZN		
Element/ Analyte	Slope (K_s)	r^2		Slope (K_s)	r^2		Slope (K_s)	r^2	
VM	1.2	0.93	+ * *	NA			NA		
C	0.80	0.89	+ * *	NA			NA		
H	1.8	0.95	+ * *	NA			NA		
S	1.2	0.87	+ * *	1.1	0.97	+ * *	1.7	0.98	+ * *
Se	2.1	0.41	+ * *	1.1	0.55	+ * *	5.6	0.80	+ ⊕
As	1.6	0.44	+ * *	0.89	0.26	+ ⊕	2.7	0.33	
Sm	0.94	0.49	+ * *	0.72	0.86	+ * *	-0.90	0.33	
Hg	0.97	0.24	+ ⊕	1.2	0.86	+ * *	1.7	0.30	
Pb	0.37	0.05		0.66	0.54	+ * *	2.6	0.90	+ *

where

K_S = proportionality constant (slope).

This model presumes that an element is not released until T reaches T_C, and thereafter is released at a rate proportional to the rate of d.a.f. coal weight loss (calculated with a suitable model or determined experimentally). The proportionality constant was estimated from linear regression of $\Delta\Omega_H$ versus ΔW^* with program LFRS1 shown in Appendix A.2. The results of the regressions for all elements and coals are listed in Appendix B.2. This model should provide rough estimates for the release of S, Hg, Pb, As, and Se as functions of temperature and residence time, during the pyrolysis of pulverized coal. In the absence of better data, the model parameters should be useful for use with low rank and medium rank coals.

The finding that K_S for sulfur is roughly equal to one, determined during transient and equilibrium batch pyrolysis, is confirmed by the values shown in Table 6.9. Therefore, equation (5-7) is found to hold for all pyrolysis conditions.

As indicated previously, samples from MRS coal runs at 800°C were analyzed for all the elements that the analytical capabilities allowed. The mass fractions of these elements were correlated with one another. The reason for this data analysis (carried out with program LFRS2 listed in Appendix A.2) was to determine significant element-to-element correlations ($X_H^{\ddagger}$ to $X_H^{\ddagger}$). The significant correlations are shown in Table 6.10. These results are not as consistent as were those of the batch runs; however, the same general behavior is apparent. Low volatility elements tend to be positively correlated with one another; high volatility elements tend to be negatively correlated with low volatility elements; and high volatility elements tend not to be correlated with other high volatility elements.

Table 6.10 Significant Element- Element Correlations
MRS Coal-LFR 800°C Runs

$*$ = significant at 95% C.L.
$**$ = significant at 99% C.L.
$+$ = positively correlated
$-$ = negatively correlated
$\$$ − by NAA
$\#$ − by AA

ELEMENT	C	H	S	Sm	U	La	As	$\mathrm{Sb}^{\$}$	Br	Na	K	Ti	Mn	Cu	$\mathrm{V}^{\$}$	Al	Ce	Se	Th	Cr	Sc	Eu	Ru	Fe	Ca	Zn	Cs	P	Pb	Hg	$\mathrm{Sb}^{\#}$	$\mathrm{V}^{\#}$
C																																
H																																
S																																
Sm																																
U	+ *																															
La																																
As						+ **																										
$\mathrm{Sb}^{\$}$																																
Br																																
Na	+ *				+ **																											
K								− *																								
Ti			+ *																													
Mn										+ *																						
Cu																																
$\mathrm{V}^{\$}$						− *	− **																									
Al																																
Ce		− **																														
Se			− *																													
Th	+ **				+ **					+ *																						
Cr																		+ *														
Sc					+ *					+ **			+ **						+ *													
Eu																																
Ru												+ *				+ *																
Fe		− *			+ *					+ *							+ *		+ *		+ *											
Co		− *															+ **															
Zn												+ *											+ **									
Cs																+ *							+ *			+ *						
P																																
Pb																												+ **				
Hg														+ **																		
$\mathrm{Sb}^{\#}$						+ **	+ *								− *																	
$\mathrm{V}^{\#}$													+ *								+ *											

7. APPLICABILITY OF RESULTS TO A PILOT PLANT GASIFIER

An air/oxygen-steam fluidized bed gasifier is being operated at the Chemical Engineering Department at North Carolina State University. This facility would have provided an excellent pilot plant scale test of the elemental release model. Unfortunately, throughout the duration of this study, a chemical grade coke with very small volatile matter content was used as the feed stock. The coke was made from Western Kentucky No. 11 coal at a coking temperature range of 1600 to 2000°F. Since this study focused on the behavior of trace and minor elements during the devolatilization stage of coal gasification, its applicability to the elemental behavior of a predevolatilized coal is limited. Nevertheless, some useful comparisons can be made. In particular, the ash tracer technique can be used to gain useful insights on the behavior of trace and minor elements during the gasification process.

7.1 Plant Description

Descriptions of the pilot plant are contained in Ferrell et al. (1977a, b). A schematic diagram of the gasifier and the particulates, condensables, and solubles (PCS) removal system is shown in Figure 7.1. Solid samples are obtained from the coal feed hopper, char receiver, and cyclone;

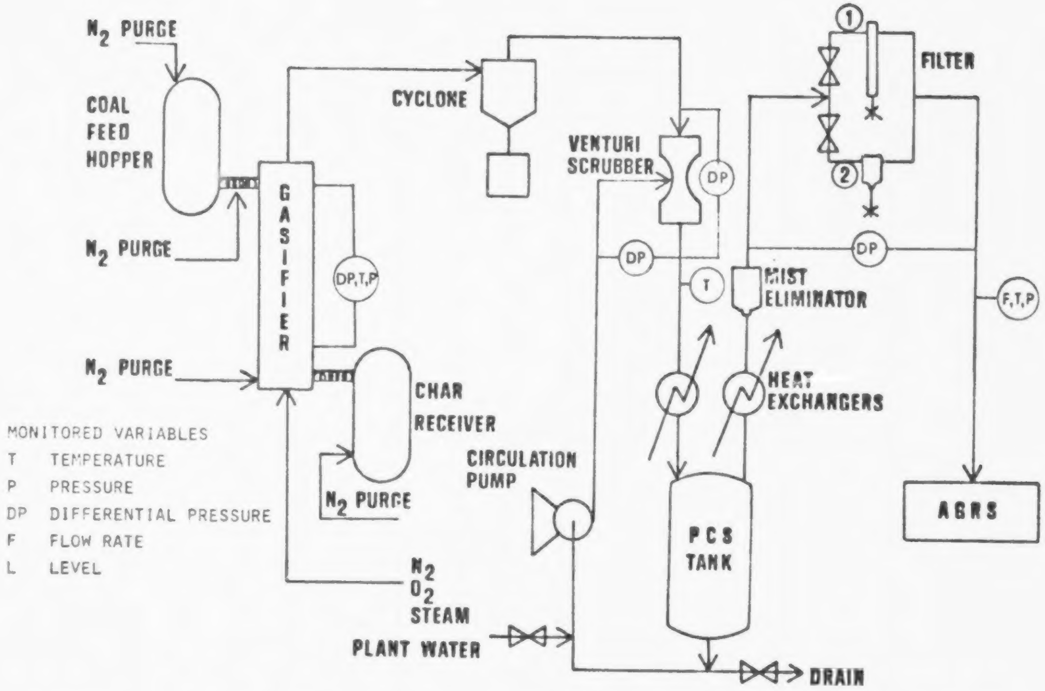
N_2 PURGE
COAL FEED HOPPER
N_2 PURGE
N_2 PURGE
GASIFIER
DP,T,P
CHAR RECEIVER
N_2 PURGE
N_2 O_2 STEAM
PLANT WATER
CYCLONE
VENTURI SCRUBBER
DP
DP
T
CIRCULATION PUMP
PCS TANK
DRAIN
MIST ELIMINATOR
HEAT EXCHANGERS
①
②
FILTER
DP
F,T,P
AGRS
MONITORED VARIABLES
T TEMPERATURE
P PRESSURE
DP DIFFERENTIAL PRESSURE
F FLOW RATE
L LEVEL

Figure 7.1 GASIFIER AND PARTICULATE, CONDENSABLES AND SOLUBLES (PCS) REMOVAL SYSTEM SHOWING PROCESS VARIABLE MONITORING POINTS

liquid samples are obtained from the PCS tank; and gas samples are obtained from a gas sampling port located between the cyclone and the venturi scrubber.

7.2 Elemental Balances

Major, minor, and trace element material balances have been made for Run GO-15, carried out on April 3, 1979. The run consisted of the steam-oxygen gasification of Western Kentucky No. 11 coke of 10x80 mesh size.

Nominal operating conditions for the reactor were 100 psig and 1800°F with a char feed rate of 25 lb/hr, a steam feed rate of 25 lb/hr, and a bed height of 38 inches. A carbon conversion of approximately 42% and a make gas flow rate at the PCS system exit of 11.2 SCFM were obtained. The principal operating variables of the run, selected output variables, and major element material balances are evaluated and logged with an existing data logging and analysis program. The program output is shown in Table 7.1.

All material balances correspond to the steady state portion of the run. Key process variables are shown in Figure 7.2. The data plotted were taken from a printed log made during the run and are actual values of the variables as computed and logged by a computer-based data acquisition system.

Table 7.1 Operating Variables for GO-15

```
                              ******************************************
                              *                                        *
                              * NCSU DEPARTMENT OF CHEMICAL ENGINEERING *
                              *                                        *
                              * FLUIDIZED BED COAL GASIFICATION REACTOR *
                              *                                        *
                              ******************************************

RUN GO-15          9/3/79,  5:15-6:45  RUN #4 ON EXPTL PLAN

          REACTOR SPECIFICATIONS                                SOLID FEED PROPERTIES

   PRESSURE    = 100.8 PSIG ( 7.86 ATM , 796.3 KPA)      WESTERN KENTUCKY #11 COAL CHAR, 10X80 MESH
   TEMPERATURE = 1790.0 DEG.F ( 976.7 DEG.C)             PARTICLE DENSITY          = 112.2 LB/FT**3 (1.797 G/CM**3)
   BED HEIGHT  = 38.0 IN. (0.97 METERS)                  SETTLED BED DENSITY       =  46.2 LB/FT**3 (0.740 G/CM**3)
   BED DIAMETER=  6.0 IN. (0.152 METERS)                 AVERAGE PARTICLE DIAMETER = 494.07 MICRONS
   ESTIMATED BED VOIDAGE = 0.79                          A-R MOISTURE CONTENT      = 0.0098
   BED EXPANSION FACTOR  = 1.92
   ESTIMATED LEAK RATE   = 0.78 SCFM

       PROXIMATE ANALYSIS OF COAL FEED                         ULTIMATE ANALYSES

                                                          COAL FEED   SPENT CHAR   CYCLONE DUST

        FIXED CARBON    = 0.842                  CARBON     0.815        0.758        0.800
        VOLATILE MATTER = 0.016                  HYDROGEN   0.016        0.038        0.004
        MOISTURE        = 0.010                  OXYGEN     0.001        0.001        0.018
        ASH             = 0.132                  NITROGEN   0.010        0.008        0.008
                                                 SULFUR     0.025        0.025        0.026
                                                 ASH        0.132        0.170        0.144

              FEED RATES                                  FEED RATIOS AND CONDITIONS

   COAL      = 25.55 LB/HR AT   70.0 DEG.F       STEAM/COAL = 1.14 LB STEAM/LB COAL(MAF)
             = 11.59 KG/HR AT   21.1 DEG.C                  = 1.19 LB STEAM/LB CARBON

   STEAM     = 24.88 LB/HR AT  365.3 DEG.F       O2/COAL    = 0.40 LB O2/LB COAL(MAF)
             = 11.29 KG/HR AT  185.2 DEG.C                  = 0.42 LB O2/LB CARBON

   OXYGEN    =  8.82 LB/HR AT   76.9 DEG.F       N2/O2      = 0.86 MOLES N2/MOLE O2
             =  4.00 KG/HR AT   24.9 DEG.C
             =  1.65 SCFM                        COMBINED GAS FEED TEMPERATURE = 1000.0 DEG.F
                                                                               =  537.8 DEG.C

   NITROGEN  =  6.67 LB/HR AT   79.0 DEG.F       SUPERFICIAL GAS VELOCITY IN REACTOR = 0.56 FT/S
             =  3.03 KG/HR AT   26.1 DEG.C                                           = 0.17  M/S
             =  1.43 SCFM
   PURGE N2  =  9.76 LB/HR (4.43 KG/HR , 2.08 SCFM)   VS/V(MIN.FLUIDIZATION) =  2.6 (VMF = 0.213 FT/S)
```

Reproduced from
best available copy.

Table 7.1 continued

Output Variables And Material Balances For GO-15

Reproduced from
best available copy.

```
RUN GO-15          4/3/79,  5115-6145  RUN #4 ON EXPTL PLAN

                  CONTROL VARIABLES                                       OUTPUT VARIABLES

      TEMPERATURE                 = 1790.0 DEG.F        PRESSURE DROP OVER 20 IN.  =  7.8 IN.H2O ( 0.280 PSI)
      H2/O2 MOLAR FEED RATIO      = 0.86                                           =  1.9 KPA
      STEAM PARTIAL PRESSURE      = 44.17 PSI           PCS GAS FLOW RATE          =  1.88 LB-MOLE/HR (11.24 SCFM)
      BED HEIGHT                  = 3.17 FT                                        =  1.87 LB-MOLE/HR(DRY BASIS)
      SOLID SPACE TIME            = 35.2 MIN            CYCLONE-GAS FLOW RATE      =  2.67 LB-MOLE/HR (16.00 SCFM)
      GAS SPACE TIME              = 5.65 S                                         =  1.87 LB-MOLE/HR(DRY BASIS)
                                                                                   =  1.21 KMOL/HR
                                                        SOLID HOLDUP               =  15.0 LB ( 6.8 KG)

               PRODUCT FUEL PROPERTIES                                  CONVERSION VARIABLES

   CO  = 25.0% (MOLAR BASIS)                                  CARBON CONVERSION = 41.9%
       = 0.486 LB  CO PRODUCED/LB COAL(MAF)                   STEAM CONVERSION  = 42.7%
   H2  = 35.5% (MOLAR BASIS)                                  SULFUR CONVERSION = 35.2%
       = 0.052 LB  H2 PRODUCED/LB COAL(MAF)
   CH4 =  0.7% (MOLAR BASIS)                                   SOLID MATERIAL BALANCE
       = 0.008 LB CH4 PRODUCED/LB COAL(MAF)

   HEATING VALUE OF MAKE GAS  =  3468.5 BTU/LB          COAL FED                  = 216.0 LB
                              =   214.1 BTU/SCF         SPENT CHAR COLLECTED      = 123.0 LB = 56.9% OF FEED
                              =  8061.0 KJ/KG           CYCLONE DUST COLLECTED    =   7.0 LB =  3.2% OF FEED
                                                        COAL GASIFIED             =  86.0 LB = 39.8% OF FEED
   HEATING VALUE OF SWEET GAS =  6117.7 BTU/LB
                              =   274.1 BTU/SCF         SPENT CHAR REMOVAL RATE    = 14.0 LB/HR
                              = 14217.9 KJ/KG           CHAR RATE FOR MASS BALANCE = 16.9 LB/HR


  CYCLONE EXIT GAS ANALYSIS     PCS EXIT GAS ANALYSIS            ELEMENTAL MATERIAL BALANCES : FLOWS IN LB/HR
        %WET   %DRY  LBMOL/HR    %WET   %DRY  LBMOL/HR
                                                                      MASS     C      H      O      N      S
  CO   14.23  20.32   0.380     20.25  20.32   0.380
  H2   20.23  28.69   0.541     28.79  28.89   0.541            COAL  25.5  20.83   0.40   0.03   0.26  0.644
  CH4   0.42   0.60   0.011      0.60   0.60   0.011           GASES  50.1   0.0    2.78  30.91  16.43  0.0
  CO2  12.21  17.43   0.326     17.37  17.43   0.326     TOTAL INPUT  75.7  20.83   3.19  30.94  16.69  0.644
  N2   22.67  32.38   0.606     32.26  32.33   0.606
  H2S   0.23   0.32   0.006      0.32   0.32   0.006            CHAR  14.0  10.62   0.53   0.02   0.12  0.353
  COS   0.03   0.05   0.001      0.05   0.05   0.001            DUST   0.8   0.64   0.00   0.01   0.01  0.021
  H2O  29.98          0.802      0.35          0.007           GASES  58.0   8.64   2.76  29.37  16.98  0.224
                                                          WASTEWATER   0.0   0.0    0.0    0.0    0.0   0.0
  H2S = 3240.0 PPM(DRY)                                 TOTAL OUTPUT  72.8  19.89   3.29  29.41  17.10  0.598
  COS =  495.0 PPM(DRY)
                                                        % DIFFERENCE -3.8%  -4.5%   3.4%  -5.0%   2.4%  -7.1%
```

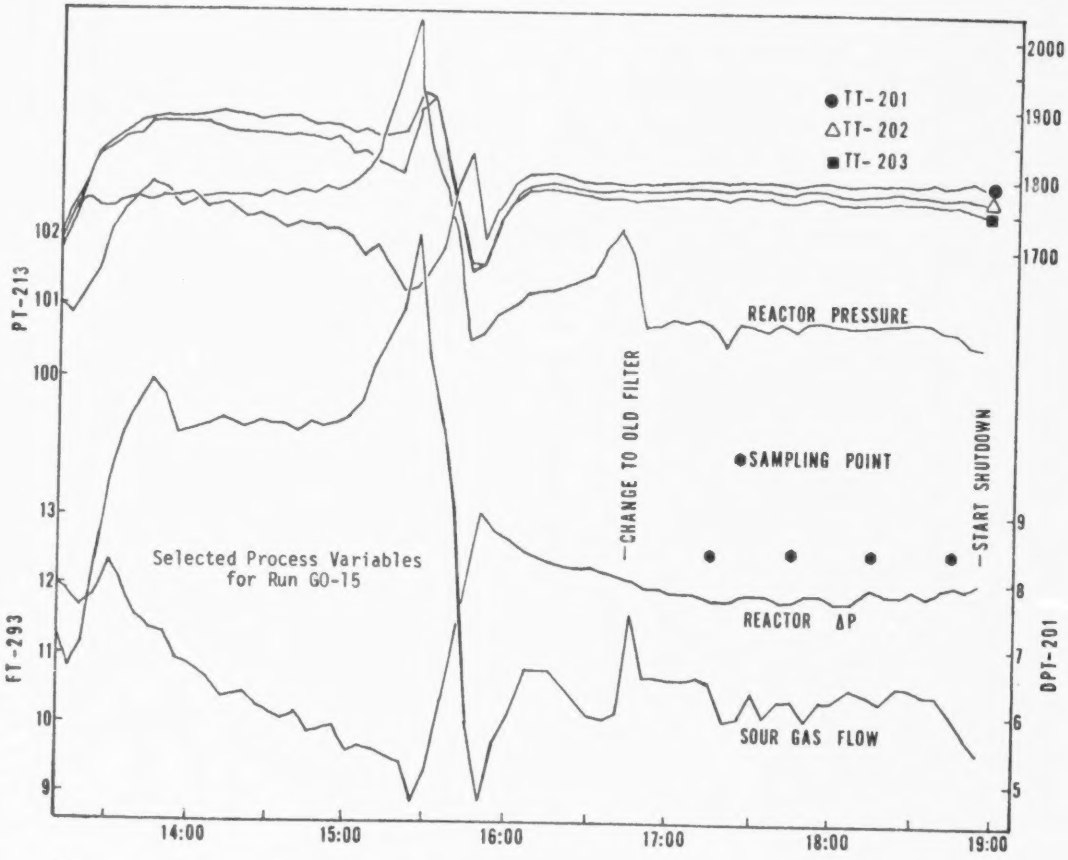

Figure 7.2 GO-15 Run Summary

Gas samples were obtained at each sampling time shown in Figure 7.2. Water samples were obtained at the first and the last sampling times. Solid samples were obtained before and after the run. A special sampling device was used to obtain feed coke, char, and cyclone fines samples corresponding to the steady state portion of the run.

A summary of the solid sample analyses is shown in Table 7.2. All the analyses shown in this table, except that for sulfur, were carried out using ASTM standard procedures. Sulfur was analyzed using a Fisher Model 470 sulfur analyzer.

The results of minor and trace element analyses are shown in Table 7.3.

Trace and minor element balances around the gasifier-PCS system are calculated as follows:

Basis: 1.5 hours at steady state

$$TE_C = TE_H + TE_F + TE_{PCS} + TE_G \qquad (7\text{-}1)$$

where TE_C = weight of element entering in feed coke

TE_H = weight of element leaving in spent char

TE_F = weight of element leaving in cyclone fines

TE_{PCS} = weight of element accumulated in PCS tank during steady state

TE_G = weight of element leaving PCS in the gas.

Table 7.2 Summary of Solid Sample Analyses

Sieve and Moisture Analysis

Sample	Moisture % As Received	Weight Retained on Sieve No.									
		12	20	30	40	60	80	100	200	235	PAN
Feed Coke	0.977 ± 0.003	2.7	28.3	13.6	14.1	20.1	9.5	4.0	5.2	1.7	0.8
Spent Char	0.278 ± 0.001	0.2	14.0	14.2	20.7	32.0	11.0	3.7	3.0	0.4	0.4
Cyclone Fines	1.69 ± 0.02	0	0	0	0	0.4	1.0	3.6	33.2	36.8	24.6
Method/Instrument	ASTM-D-3173	U. S. Standard Sieves, Mechanical Sieve Shaker									

Proximate Analysis

Sample	% Moisture	% Ash	% Volatile Matter	% Fixed Carbon
Feed Coke	0.995 ± 0.005	13.30 ± 0.02	1.62 ± 0.07	84.09
Spent Char	0.234 ± 0.001	17.71 ± 0.07	1.62 ± 0.04	80.44
Cyclone Fines	2.00 ± 0.02	14.33 ± 0.14	1.64 ± 0.04	82.03
Method/Instrument	ASTM-D-3173	ASTM-D-3174	ASTM-D-3175	

Ultimate Analysis

Sample	% Carbon	% Hydrogen	% Nitrogen	% Sulfur	% Oxygen
Feed Coke	81.87 ± 0.93	1.59 ± 0.11	1.03 ± 0.00	2.54 ± 0.005	0.0
Spent Char	78.93 ± 0.10	0.392 ± 0.10	0.868 ± 0.003	2.62 ± 0.04	0.0
Cyclone Fines	79.76 ± 0.05	0.436 ± 0.02	0.829 ± 0.001	2.63 ± 0.07	2.0
Method/Instrument	ASTM-D-3178	ASTM-D-3178	ASTM-D-3179	Fisher Model 470	

Table 7.3 Summary of Trace Element Analyses

Element	Measured Trace Element Concentrations (μg/g) or (μg/ml)				
	Food Coke	Spent Char	Cyclone Fines	NSS WW	SS WW
As[a]	9.60 ± 0.40	12.40 ± 0.40	16.80 ± 0.40	0.019	0.020
Be	6.83 ± 0.06	8.75 ± 0.05	7.59 ± 0.05	0.00115	0.00118
Cr	69.60 ± 0.60	75.00 ± 0.60	72.80 ± 0.60	0.055	0.066
Hg	0.11 ± 0.01	0.08 ± 0.01	0.07 ± 0.01	0.0005	0.0009
Ni	32.30 ± 0.80	131.50 ± 1.50	120.20 ± 2.00	0.06	0.06
Pb	11.90 ± 1.46	11.90 ± 1.46	48.00 ± 1.46	0.065	0.051
Sb[a]	0.78 ± 0.01	0.55 ± 0.02	0.85 ± 0.01	0.092	0.108
V	44.00 ± 0.60	57.00 ± 1.00	71.00 ± 0.60	0.098	0.011
Sm	2.03 ± 0.20	2.58	2.24	0.0019	0.0018
Ce	63.57 ± 1.49	36.14	68.68	0.098	0.142
U	2.23 ± 0.24	3.10	2.99	<0.05	<0.05
Se	<5	<5	<5	0.072	0.046
Th	2.39 ± 0.28	3.42	2.52	<0.05	<0.05
Cr	67.57 ± 1.26	108.75	61.13	1.98	1.79
La	29.29 ± 1.48	16.23	36.09	0.074	0.089
Sb[n]	0.64 ± 0.05	0.63	0.63	0.027	0.018
Br	<5	4.83	<5	<0.5	<0.5
Se	5.53 ± 0.16	8.40	5.99	0.0021	0.0020
Ru	17.84 ± 4.54	36.56	16.83	<0.5	<0.5
Fe	43083 ± 793	51693	31656	7.33	7.24
Co	7.85 ± 0.21	12.60	8.25	<0.5	<0.5
Eu	0.29 ± 0.08	0.38	0.31	<0.1	<0.1
As[n]	8.05	8.50	8.78	<0.015	<0.020

[a] atomic absorbtion analysis
[n] neutron activation analysis

Only TE_G was not measured in this run; it will be assumed to be zero.

The following operating variable values are obtained for Table 7.1 and run data:

Coke Feed Rate = 11.59 kg/hr
Char Removal Rate = 7.67 kg/hr
Cyclone Collection Rate = 0.38 kg/hr
Volume of water in PCS tank = 617 liters

These values are used with the trace element analyses to calculate the terms in equation (7-1).

The results of the trace and minor element mass balances are shown in Table 7.4.

7.3 Evaluation of the Data

It is evident from inspection of Table 7.1 that major element balances can be made with a high degree of accuracy. Such results are comparable to those published for other coal gasification pilot plants (e.g., Gasior, 1978).

Examination of the data shown in Table 7.2 reveals that, as expected, the percentages of moisture, carbon, hydrogen, and nitrogen are smaller in the spent char, while the ash content has increased significantly. The size distributions of the spent char and, to a much greater extent, the cyclone fines are shifted toward smaller particle sizes.

Table 7.4 Trace Element Mass Balance

Basis: 1.5 hours (SS)

Element mg	ΣIN Feed TE_C	Out Char TE_H	Out Fines TE_F	Acc. PCS TE_{PCS}	ΣOut	Alg. Sum.	% Recovery
As[a]	166.90	142.66	9.58	0.62	152.86	14.04	92
Be	118.74	100.67	4.33	0.02	105.02	13.72	88
Cr	1210.00	862.88	41.50	6.79	911.17	298.83	75
Hg	1.91	0.92	0.04	0.25	1.21	0.70	63
Ni	561.54	1512.91	68.51	0.00	1581.42	-1019.88	282
Pb	206.88	136.91	27.36	-8.64	164.27	45.61	79
Sb[a]	13.56	6.33	0.48	9.88	16.69	-3.13	123
V	764.94	655.79	40.47	-53.70	696.26	68.68	91
Sm	35.29	29.68	1.28	-.06	30.96	4.33	88
Ce	1105.16	415.79	39.15	27.16	482.10	623.06	44
U	38.77	35.67	1.70	0.00	37.37	1.40	96
Se			BELOW DETECTION LIMIT				
Th	41.55	39.35	1.44	0.00	40.79	0.76	98
Cr	1174.70	1251.17	34.84	-117.28	1286.01	-111.31	109
La	509.21	186.73	20.57	9.26	216.56	292.65	43
Sb[n]	11.13	7.25	.36	-5.56	7.61	3.52	68

Table 7.4 continued

Element mg	ΣIN Feed TE_C	Out Char TE_H	Out Fines TE_F	Acc. PCS TE_{PCS}	ΣOut	Alg. Sum.	% Recovery
Br			BELOW DETECTION LIMIT				
Sc	96.14	96.64	3.41	-.06	100.05	-3.91	104
Ru	310.15	420.62	9.59	0.00	430.21	-120.06	139
Fe	748998	594728	18044	-55.56	612772	136226	82
Co	136.47	144.96	4.70	0.00	149.66	-13.19	110
Eu	5.04	4.37	0.18	0.00	4.55	0.49	90
As[n]	139.95	97.79	5.00	3.09	105.88	34.07	76

[a] analyzed by AA

[n] analyzed by NAA

It is of interest to determine whether the ash tracer method can provide good estimates of carbon conversion in this gasification system, or if, as in the LFR experiments, ash losses bias the results low. The carbon conversion calculated by the ash tracer method (using equations (4-50) and (6-6)) is 27.7%. The true carbon conversion, calculated from a carbon mass balance, is 41.9% as shown in Table 7.1. The large discrepancy indicates that a significant amount of ash was removed from the char and left the reactor with the gas. The ash was not trapped in the cyclone, as shown by the low ash content of the cyclone fines, which indicates that the ash particles leaving the reactor must be relatively small. It is thought that those small ash particles are trapped in the PCS system. This is supported by the large amount of total residue (typically 0.3 kg) found in the PCS tank at the end of a run.

Based on the discussion presented in Section 6.1.2, the cyclone fines were expected to show a slight increase in ash content. Since such is not the case, the relative weight loss of the spent char particles can be compared to that of the cyclone fines using ash as a tracer. Equation 4-52 yields $\%\Delta W_H^+ = 24.9$ for the char and $\%\Delta W_F^+ = 7.2$ for the fines. This calculation appears to show that the cyclone fines had a smaller residence time in the reactor, and therefore did not react to a large extent.

One of the most important findings of this research is that sulfur appears to be released at approximately the same rate as volatile matter during pyrolysis. This also appears to be the case during the steam-oxygen gasification of coke. The data in Table 7.2 shows that the sulfur mass fraction in the char and cyclone fines remain fairly close to the mass fraction in the feed coke despite a 32% sulfur loss (calculated using equations (4-43), (4-48), and (4-49)). Since the d.a.f. weight loss (calculated with equation (4-47)) is 31%, it appears that equation (5-7) may also be used to estimate the release of sulfur from coal during steam-oxygen gasification.

The trace element analyses show that the spent char is enriched in most trace elements analyzed. Elements depleted in the spent char include Hg, Sb, Ce, and La. Based on the results of the trace and minor element mass balances, it can be concluded that most of the elements analyzed are released from the coke in significant quantities. Furthermore comparison of the elemental mass fractions with the normalized mass fractions calculated by the ash tracer method (equation (6-5)) indicate that for several elements (e.g., V, U, and Eu), the mode of transport out of the coal particles appears to be escape with the ash; volatile elements (e.g., Hg) are released faster, while a few (e.g., Sc) are released slower than the ash. The normalized mass fractions are shown in

Table 7.5 (see Section 6.1 for the discussion that leads to these conclusions). These results are generally consistent with the LFR results discussed in Section 6.

The erratic results of the PCS water analyses have been found to be due to sampling error due to settling or unevenly dispersed ash in the PCS tank. Trace and minor element concentrations determined by NAA in well shaken waste water samples (i.e., including their residue) are an order of magnitude higher than concentrations found in waste water samples where the residue was allowed to settle before the analysis sample was pipetted. Another complication is due to the small steady state sampling interval. The small concentrations of trace elements in the PCS tank cannot be expected to increase dramatically in 1.5 hours when coke is gasified. To overcome these problems in future studies, separate analyses will be made of the filtered PCS water and the residue which will be collected in filters placed between the tank and the drain. A water sampling train has been installed between the cyclone and the venturi scrubber. Its use will permit the obtention of undiluted steam condensate and ash samples.

Finally, the discrepancies observed between the AA and NAA analyses can probably be attributed to sample inhomogeneity and to differences in the sensitivities of the two techniques for the different elements analyzed. A more complete discussion of these problems is presented in Appendix C.

Table 7.5 ψ_A^+ Values in Spent Char

Element	ψ_A^+
As[a]	9.31
Be	6.57
Cr[a]	56.3
Hg	0.06
Ni	98.8
Pb	8.9
Sb	0.41
V	43
Sm	1.94
Ce	27.14
U	2.33
Th	2.57
Cr[b]	81.57
La	12.19
Sb[b]	0.47
Sc	6.31
Ru	36.56
Fe	38821
Co	9.46
Eu	0.29
As[b]	6.38

[a] analyzed by atomic absorption

[b] analyzed by neutron activation

8. CONCLUSIONS

The objectives of this research project were to derive data on equilibrium retentions and kinetics of the release of trace and minor constituents of coal. The principal conclusions are summarized below. In addition, some conclusions are drawn on volatile yields and kinetics of devolatilization at low to medium temperatures, and on some aspects of the experimental methodology explored in the research.

8.1 Trace and Minor Element Release

In the chars produced in batch pyrolysis experiments with nitrogen over a temperature range of 25 to 1200°C: Sm, Cr, Th, Sc, Fe, and Co are retained completely; As, Se, and perhaps La, exhibit intermediate volatility (<50% release); S, Pb, Hg, and Cl are highly volatile (>50% release). Mercury and chlorine show losses greater than 70% at temperatures below 700°C, and more than 75% of the lead is released at temperatures above 1000°C. These results apply to coals with ranks ranging from lignite to anthracite.

Fe, Co, Sc, Na, Ce, and V are completely retained in the LFR chars. C, H, S, As, Se, Pb, La, and Hg are released in significant quantities during fast pyrolysis with the release occurring within a few tenths of a second. In addition, some elements (e.g., Sm and Mn) appear to be released with the ash expelled from the coal particles.

The equilibrium release (or retention) of As, Se, S, Cl, Pb, and Hg has been successfully modeled (see Section 5.2). The model employed has three parameters: T_C, the temperature at which the trace element release begins; ΔW_e, the asymptotic elemental release at high temperatures; and b, a fitted constant. This model was found to describe elemental retentions in lignitic, subbituminous, bituminous, and anthracitic coals for all elements studied except sulfur in anthracite. The model should provide good engineering estimates of the equilibrium extent of volatile trace and minor element release as a function of temperature during the devolatilization stage of any gasification process.

The kinetics of sulfur release from lignitic and subbituminous coals have been modeled with fair results. The bias and imprecision of the retentions of other volatile trace elements made the determination of their kinetic parameters difficult. A first-order model coupled with the equilibrium release (batch) model was used. The sulfur modeling results suggest that improvements in the trace and minor element data could yield the proper Arrhenius parameters for the model, which could then be used to predict the elemental release as a function of time and temperature.

Sulfur was found to be released in direct proportion to the dry ash-free coal weight loss, regardless of coal rank and pyrolysis conditions (temperature, residence time, and heating rate), thereby providing a simple model for sulfur release during pyrolysis.

As would be expected, the mass fractions of nonvolatile elements in the chars tend to be positively correlated with one another over a wide temperature range. The mass fractions of volatile elements tend to be negatively correlated with those of nonvolatile elements but not with one another, indicating that volatile elements are released in different proportions as the temperature increases.

8.2 Volatile Yields and Kinetics of Devolatilization

The volatile yields of five coals ranging in rank from lignitic to anthracitic exhibit similar behavior during slow heating (5-45°C/sec). All coals exhibit a dramatic increase in weight loss between 400 and 600°C, and equilibrium is reached much more rapidly at the higher temperatures. The equilibrium volatile yields exhibit the expected dependence on rank, with lignite showing the highest and anthracite the lowest yields. The equilibrium weight loss data show the characteristic devolatilization behavior of coals pyrolyzed in batch reactors. Moisture evolution occurs at 100°C; devolatilization begins at about 350°C, and most of the weight loss occurs between 400 and 750°C.

Bituminous and anthracitic coals exhibit higher equilibrium volatile yields when pyrolyzed in shallow beds than in deep beds. Lower rank coals do not show such an effect. This conclusion is consistent with the findings of Kobayashi (1976).

The fast pyrolysis devolatilization rates found in this study agree reasonably well with those found in other studies. Nonisothermal pyrolysis models correlate fast pyrolysis weight loss data in laminar flow reactors significantly better than isothermal models. Kobayashi's (1976) two-parallel first-order reactions model predicts pyrolysis weight losses reasonably well for temperatures ranging from 300 to 900°C and residence times ranging from 150 to 1500 msec. However, the best correlation of the data was obtained with a first-order model featuring temperature dependent asymptotic weight loss.

8.3 Experimental Methodology

Laminar flow reactor data are subject to several sources of error, including uncertainties in particle temperature and residence time. The largest source of scatter in the data is caused by variation in particle heating rates (due to changes in coal feed rates and/or feeder gas flow rates). In addition, the char collection devices tend to make the chars inhomogeneous. As discussed previously, the weight loss of coal in the LFR should be determined gravimetrically. The ash tracer technique leads to underestimation of weight losses and hence should not be used to study the kinetics of trace and minor elements during pyrolysis. Ash tracer losses can be corrected to some extent by using in the weight loss calculations the feed coal ash content after it has been subjected to a room temperature run and by increasing the apparent ash content of the chars by about 5%. However, such a procedure is not precise enough for the study of the kinetics of trace and minor element release from coal.

9. RECOMMENDATIONS

The results of this research indicate that the study of the kinetics of trace and minor elements during coal pyrolysis, and coal gasification in general, is feasible. However, considerable refinement of the methods and techniques used is necessary.

Specifically, it was found that the largest source of scatter in the weight loss data was the variation in coal feed rates. This problem can be avoided through more careful operation of the feeder system and frequent recalibration of the feeder valve. It is also recommended that higher main gas and suction flow rates be used to improve the particle collection efficiency such that only a negligible fraction of the coal particles are lost. Finally, a much smaller feeder tip should be used. The resulting higher feeder gas velocities will reduce the particle heating times and make the particle heating time constant less sensitive to variations in feeder gas velocity.

The weight loss of coal pyrolyzed in the LFR should be determined gravimetrically. The ash tracer technique should not be used to study the kinetics of trace and minor element release. In order to ensure that all the coal particles enter the water-cooled collector and thus ensure complete char recovery, it is recommended that the main gas and suction flow rates be increased and the diameter of the reaction tube be decreased. The first two changes should also improve the collection efficiency of the cyclones. The suction flow rate should be increased well above the isokinetic rate; the added uncertainty in the residence time estimates should be amply compensated by the improved reliability in the weight loss estimates. The velocity of the coal particles (and thus their residence time) could be measured with a laser doppler anemometer; the added cost and complexity of the apparatus would not be justified until other more important improvements are made, however.

It is obvious that tars condensed on the surface of the quenched particles. The amount of tar deposited quite likely depends on the size of the particles, and is probably a significant source of sample inhomogeneity and of bias in the devolatilization weight loss estimation. One solution to this problem may be the use of air or boiling water as the coolant in the collector instead of cold water. An increase in reaction time would result, but the added uncertainty in the reaction time due to the slower particle quenching would probably not be as significant as the uncertainty now present in the results due to tar condensation.

Coal and char samples must be made more homogeneous before analysis. The chars produced in the batch and LFR experiments showed the formation of fused lumps. It is possible that the lumps may be enriched or depleted in some elements. In general, the LFR chars showed more scatter than the batch reactor chars. In order to overcome sample inhomogeneity problems, the samples should be ground to a very fine powder and mixed thoroughly in a roller mixer. One drawback of this procedure is that the likelihood of sample contamination is greatly increased by the handling of all samples for trace element analysis. Proper care should render that problem minimal, however. Also, the largest possible sample size should be used in order to "average out" sample inhomogeneities , and several replicate runs should be made at each set of conditions.

Finally, it is recommended that future work be focused on the volatile elements determined in this study, particularly Hg and Pb. More data is needed at low temperatures for the equilibrium release model; such data should allow better estimation of critical temperatures. Future work with the LFR should be carried out exclusively at temperatures above 800°C. Trace/minor element release below that temperature appears to be small and errors in the weight loss determinations appear to be larger than at higher temperatures. Future studies should focus on one coal; North Barber No. 8 from New Mexico is recommended because of its high volatiles content and the ease with which it can be handled in the coal feeder. This study has shown that results obtained with one coal are applicable to most other coals.

LITERATURE CITATIONS

Agreda, V.H., Coal Gasification Project Internal Technical Report No. 10., "Design and Operation of an LFR and a Batch Pyrolysis Reactor", Department of Chemical Engineering, North Carolina State University, Raleigh, NC, 1979.

Anderson, G.L., A.H. Hill, and D.K. Fleming, "Predictions on the Disposition of Select Trace Constituents in Coal Gasification Processes." Paper presented at Environmental Aspects of Fuel Conversion Technology Symposium, Hollywood, FL, April, 1979.

Anthony, D.B., Sc.D. Thesis, Massachusetts Institute of Technology, Cambridge, MS, 1974.

Anthony, D.B., J.B. Howard, H.C. Hottel, and H.P. Meissner, "Rapid Devolatilization of Pulverized Coal," Fifteenth International Symposium on Combustion, p. 1313, The Combustion Institute, Pittsburg, PA, 1975.

Anthony, D.B., J.B. Howard, H.C. Hottel, and H.P. Meissner, "Rapid Devolatilization and Hydrogasification of Bituminous Coal," Fuel, 55, 121, 1976.

Attari, A., A.H. Corcoran, and G.S. Gibson, "Transformation of Sulfur Functional Groups during Pyrolysis of Coal," in Proceedings of 172nd National Meeting of the American Chemical Society, Division of Fuel Chemistry, Vol. 21, pp. 106-111, American Chemical Society, Washington, DC, 1976.

Attari, A., J. Pau, and M. Mensinger, Fate of Trace and Minor Constituents of Coal During Gasification, U.S. Environmental Protection Agency Publication EPA-600/2-76-258, September, 1976.

Babu, S.P., (Ed.), Trace Elements in Fuel, Advances in Chemistry Series 141, Washington, DC, 1975.

Badzioch, S. and P.G.W. Hawksley, "Kinetics of Thermal Decomposition of Pulverized Coal Particles," Ind. Eng. Chem. Process Design Develop., 9, 521, 1970.

Badzioch, S., R.B. Sainsbury, and P.G.W. Hawksley, BCURA Member's Circular, No. 340 , 1968.

Bennett, W.S., "WESCO Coal Gasification Plant: Navajo Considerations," Los Alamos Scientific Laboratory Report No. LA-6247-MS, February, 1976.

Bird, R.B., W.E. Steward, and E.N. Lightfoot, Transport Phenomena, John Wiley & Sons, New York, NY ,1960.

Chukhanov, Z.F., Izv. Akad. SSSR, Otd. Tekh, Nauk, 8, 7, 1954.

Dryden, I.G.C., "Chemical Constitution and Reactions of Coal," in Chemistry of Coal Utilization, Supplementary Volume, H.H. Lowry, ed., John Wiley & Sons, New York, NY, 1962.

Duck, N.W. and G.W. Himus, "On Arsenic in Coal and its Mode of Occurrence," Fuel, 30, 367-71, 1951.

Duhne, C.R., "Calculating the Approach to Equilibrium," Chem. Eng., 84, No. 18, August 29, 1977.

Eddinger, R.T., L.D. Friedman, and E. Rau, "Devolatilization of Coal in a Transport Reactor," Fuel, 45, 245, 1966.

Ferrell, J.K., R.M. Felder, R.W. Rousseau, and D.W. Alexander, "A Coal Gasification-Gas Cleaning Test Facility," Paper presented at the U.S. EPA Symposium Environmental Aspects of Fuel Conversion Technology, III, Miami, FL, September, 1977a.

Ferrell, J.K., R.M. Felder, R.W. Rousseau, and D.W. Alexander, "A Coal Gasification-Gas Cleaning Pilot Plant at North Carolina State University," Paper presented at the Miami International Conference on Alternative Energy Sources, Miami, FL, December, 1977b.

Fiene, F.L., J.K. Kuhn, and H.J. Gluskoter, "Mineralogic Affinities of Trace Elements in Coal," Presented at U.S. EPA Symposium on Coal Cleaning to Achieve Energy and Environmental Goals, in Hollywood, FL, September, 1978.

Forney, A.J., W.P. Haynes, S.J. Gasior, R.M. Karnosky, C.E. Schmidt, and A.G. Sharkey, Trace Element and Major Component Balances Around the Synthane PDU Gasifier, U.S. Energy Research and Development Administration Publication PERC/TPR-75/1, August 1975.

Gasior, S.J., R.G. Lett, J.P. Strakey, and W.P. Haynes, "Major, Minor and Trace Element Balances for the Synthane PDU Gasifier: Illinois No. 6 Coal," Paper presented at the 175th National ACS Meeting, Anaheim, CA, 1978.

Given, P.H., "The Distribution of Hydrogen in Coals and its Relation to Coal Structure," Fuel, 39, 147, 1960.

Gluskoter, H.J., R.R. Ruch, W.H. Miller, R.A. Cahill, G.E. Dreher, and J.K. Kuhn, Trace Elements in Coal: Occurrence and Distribution, U.S. Environmental Protection Agency Publication EPA-600/7-77-064, June, 1977.

Goldschmidt, V.M., "Rare Elements in Coal Ashes," Industrial and Engineering Chemistry, 27, No. 9, p. 1100-1102, 1935.

Goldstein, S., Modern Developments in Fluid Dynamics, 2, p. 599, Dove Publishers, New York, NY, 1965.

Gould, R.F. (Ed.), Fuel Gasification, Advances in Chemistry Series, No. 69, Am. Chem. Soc., Washington, DC, 1967.

Henry, J.P., and B.M. Louks, "An Economic Study of Pipeline Gas Production from Coal," Chem. Tech., p. 237-247, April, 1971.

Hirsh, P.B., "Conclusions from X-Ray Scattering Data on Vitrain Coal," Proc. Conf, Science in the Use of Coal, p. A29, Inst. Fuel, London, England, 1958.

Horton, M.D., "Fast Pyrolysis," in L.D. Smoot and D.T. Pratt, Eds., Pulverized-Coal Combustion and Gasification, Plenum Press, New York, NY, 1979.

Horton, M.D. and L.D. Smoot, "Exploratory Studies of Flames and Explosion Quenching," Interim Report No. 3, U.S. Bureau of Mines, Contract No. HO122052, Chemical Engineering Department, Brigham Young University, Provo, UT, 1975.

Horton, N. and K.V. Aubrey, "The Distribution of Minor Elements in Vitrain: Three Vitrains from the Barnsley seam," London, Journal of the Society of Chemical Industries, 69, Suppl. No. 1, p. 541-548, (revised), 1950.

Hottel, H.C. and J.B. Howard, "New Energy Technology," M.I.T. Press, Cambridge, MS, 1971.

Howard, J.B., "Mechanism of Ignition and Combustion in Flames of Pulverized Bituminous Coal," Ph.D. Thesis, Pennsylvania State Univeristy, University Park, PA, 1965.

Howard, J.B. and Essenhigh, R.H., "Pyrolysis of Coal Particles in Pulverized Fuel Flames," Ind. Eng. Chem. Process Design Develop. 6, 74, 1967.

Jahnig, C.E., R.R. Bertrand, and E.M. Magee, "Control Technology Research and Development Needs," (Gov. Res. Lab., Exxon Research and Eng. Co., Linden, NJ), U.S. Environ. Prot. Agency, Off. Res. Dev., Rep. EPA 1976, EPA-600/2-76-149, Symp. Proc.: Environ. Aspects Fuel Convers. Technol., II, 1975; PB-257 182, 259-65.

Jensen, G.A. and G.T. Austin, "Iron From Coal Minerals," Ind. Eng. Chem. Process Design Develop., 16, (1), 44, 1977.

Kaakinen, J.W., "Trace Elemental Behavior in Coal-Firec Power Plants," Environ. Sci. Technol., 9, 862-869, 1975.

Karn, F.S., R.A. Friedel, and A.G. Sharkey, "Mechanism of Gas Flow through Coal," Fuel, 54, 279, 1975.

Kaskan, W.E., "The Dependence of Flame Temperature on Mass Burning Velocity," Sicth Symposium (International) on Combustion, The Combustion Institute, p. 34, 1956.

Kimber, G.M. and M.D. Gray,""Measurements of Thermal Decomposition of Low and High Rank Non-Swelling Coals at MHD Temperatures," BCURA Document, No. MHD 32, January, 1976.

Klein, D.H., "Pathways of Thirty-Seven Trace Elements Through Coal-Fired Power Plants," Environ. Sci. Technol., 9, 973-979, 1975.

Kobayashi, H., "Rapid Decomposition Mechanism of Pulverized Coal Particles," M.S. Thesis, Department of Aeronautics and Astronautics, Massachusetts Institute of Technology, Cambridge, MS, 1972.

Kobayashi, H., Sc.D. Thesis, Department of Mechanical Engineering, Massachusetts Institute of Technology, Cambridge, MS, 1976.

Kuhn, J.K., D. Kidd, J. Thomas Jr., R. Cahill, D. Dickerson, R. Shiley, C. Kruse, and N.F. Shimp. EPA Contract No. 68022130, 1979.

Kuhn, J.K., D. Kidd, J. Thomas Jr., R. Cahill, D. Dickerson, R. Shiley, C. Kruse, and N.F. Shimp, "Volatility of Coal and its By-products," paper presented at the Third Annual EPA Symposium, Environmental Aspects of Fuel Conversion Technology, Hollywood, FL, September, 1977.

Langhaar, H.C., ASME Trans. Vol. 64, 1942.

Lewellen, P.C., "Product Decomposition Effects in Coal Pyrolysis," M.S. Thesis, Chemical Engineering Department, Massachusetts Institute of Technology, Cambridge, MS, 1975.

Littlejohn, R.F., "Mineral Matter and Ash Distribution in 'As-Fired' Samples of Pulverized Fuels," J. Inst. Fuel, 59, February 1966.

Loison, R. and Chauvin, F., "Pyrolyse Rapide Du Charbon," Chem. Ind. (Paris), 91, 269, 1964 (Reviewed by Badzioch, S., BCURA Monthly Bulletin, 31, 1967).

Loran, B.I. and J.B. O'Hara, "Specific Environmental Aspects of Fisher-Tropsh Coal Conversion Technology," Third Symposium on Environmental Aspects of Fuel Conversion Technology, Hollywood, FL, September 15, 1977.

Lowry, H.H., ed. Chemistry of Coal Utilization, Supplementary Volume, John Wiley & Sons, New York, NY, 1963.

Lukesh, J.S., "Thermal Decomposition of Arseno-pyrite," Am. Mineral, 25, 539-42, 1940.

Lyon, W.S., Trace Element Measurements at the Coal Fired Steam Plant, CRC Press, Cleveland, OH, 1977.

Malte, P.C. and D.P. Rees, "Pulverized-Coal Reaction: Pollutant Formation," in Pulverized-Coal Combustion and Gasification, L.D. Smoot and D.T. Prat, Eds., Plenum Press, New York, NY, 1979.

Marquardt, D.W., "An Algorithm for Least Squares Estimation of Non-Linear Parameters," J. Soc. Ind. App. Math., 11 (2), 431-441, 1963.

Massey, L.G., (Ed.), Coal Gasification, Advances in Chemistry Series 131, Washington, D.C., 1974.

McAdams, W.H., Heat Transmission, Third Edition, pp. 202 et seq., McGraw-Hill Book Co., New York, NT , 1964.

McCabe, W.L. and J.C. Smith, Unit Operations of Chemical Engineering, Second Edition, McGraw-Hill Book Co., New York, NY, 1967.

Menster, M., "Devolatilization of Coal by Rapid Heating," in, L.G. Massey (Ed.), Coal Gasification, Advances in Chemistry Series 131, Washington, DC, 1974.

Morgans, W.T.A. and N.B. Terry, "Measurements of the Static and Dynamic Elastic Moduli of Coal," Fuel, 37, 201, 1958.

Nsakala, N., "Characteristics of Chars Produced by Pyrolysis Following Rapid Heating of Pulverized Coal," Ph.D. Thesis, Pennsylvania State University, University Park, PA, 1976.

O'Gorman, J.W. and P.L. Walker, Jr., "Mineral Matter Characteristics of American Coals of Various Rank," Report to the Office of Coal Research, United States Department of Interior, July 1, 1969.

Padia, A.S., "The Behavior of Ash in Pulverized Coal Under Simulated Combustion Conditions," Sc.D. Thesis, Massachusetts Institute of Technology, Cambridge, MS, 1976.

Page, G.C., "Fate of Pollutants in Industrial Gasifiers," paper presented at the Third Annual EPA Symposium, Environmental Aspects of Fuel Conversion Technology, Hollywood, FL, September 1977.

Pai, S.I., Fluid Dynamics of Jets, pp. 120 147, D. Van Nostrant Co., Inc., New York, NY , 1954.

Pohl, J.H. "Fate of Fuel Nitrogen," Sc.D. Thesis, Massachusetts Institute of Technology, Cambridge, MS, April, 1976.

Pohl, J.H. and A.F. Sarofim, "Devolatilization and Oxidation of Coal Nitrogen," in Sixteenth Symposium (International on Combustion, pp. 491-501, The Combustion Institute, Pittsburg, PA, 1977.

Reidelbach, H. and J. Algermissen, "Theoretical Studies of Coal Pyrolysis in an Entrained Bed Flow Reactor," J. Soc. Auto. Eng. pp. 469-475, 1978.

Reidelbach, H. and M. Summerfield, "Kinetic Model for Coal Pyrolysis Optimization," Amer. Chem. Soc., Div. Fuel Chem., 20, 1, 161, 1975.

Robertson, C.A. in Sainsbury et al. (1966).

Sainsbury, R.B., P.C. Yellow, S. Badzioch, and P.G.W. Hawksley, BCURA Member's Circular, No. 309, 1966.

Sass, A., "Garrett's Coal Pyrolysis Process," Chem. Eng. Progress, 70, No. 1, 1974.

Sevenster, P.G., "Studies of Some Physical Properties of South African Coal," J. South Afr. Chem. Inst., 7, 41, 1954.

Shapatina, E., V.V. Kalyuzhnyi, and Z.F. Chukhanov, "Tehcnological Utilization of Fuel for Energy ,1-Thermal Treatment of Fuels," 1960 (reviewed by Badzioch, S., BCURA Monthly Bulletin, 25, 285, 1961).

Shiley, R., J. Kuhn, R. Cahill, D. Kidd, and D. Dickerson, "Volatile Inorganic Elements From Coal Pyrolysis," in Neil F. Shimp, Characterization of Coal and Coal Residue, EPA Contract No. 68022130, 1978.

Snedecor, G.W. and W.G. Cochran, Statistical Methods, Sixth edition, Iowa State University Press, Ames, IA, p. 557, 1967.

Soloman, P.R., The Evolution of Pollutants During the Rapid Devolatilization of Coal, Report R 76-952588-2, United Technologies Research Center, East Hartford, CN, 1977.

Spackman, W., "The Nature of Coal and Coal Seams," in Short Course in Coal Characteristics and Coal Conversion Processes, Pennsylvania State University, University Park, PA, May 19-23, 1975.

Stickler, D.B., R.E. Gannon, and H. Kobayashi, "Rapid Devolatilization Modeling of Coal," Technical Meeting, Eastern Section of the Combustion Institute, November, 1974.

Stinett, S.J., D.P. Harrison, and R.W. Pike, "Fuel Gasification Prediction of Sulfur Species by Free Energy Minimization," Env. Sci. Technol. 8, 441, 1974.

Suuberg, M., W.A. Peters, and J.B. Howard, "Product Composition and Kinetics of Lignite Pyrolysis," Ind. Eng. Chem. Process Design Develop., 17, 1, 1978.

Tran, D.Q., "Kinetic Modeling of Pyrolysis and Hydrogasification of Carbonaceous Material," Ph.D. Thesis, Department of Mineral Engineering, University of Wyoming, Laramie, WY, 1978.

van Krevelen, D.W. and J. Schuyer, Coal Science, Elsevier, Amsterdam, Holland, 1957.

van Krevelen, D.W., Coal, Elsevier, Amsterdam, Holland, 1961.

Vestal, M.L. and W.H. Johnson, "Desulfurization Kinetics of Ten Bituminous Coals," SRI Corporation, Report No. SRIC 69-10, June 1969.

Wen, C.Y., C.T. Li, S.H. Tscheng, and W.S. O'Brien, "Comparison of Alternative Coal Gasification Processes," 65th Annual AIChE Meeting, New York, NY, November 26-10, 1972.

Wiser, W.H., G.R. Hill, and N.J. Kertamus, "Kinetic Study of the Pyrolysis of High-Volatile Bituminous Coal," Ind. Eng. Chem. Process Design Develop., 6, 133, 1967.

Yurovskii, A.Z., V.S. Kaminskii, and A.L. Rubinstein, Khim. i Tekhnol. Tapliva i Masel, 7, 20-3, 1957.

Zubovic, P., "Geochemistry of Trace Elements in Coal," in, Ayer, F.A., compiles, Symposium Proceedings, Environmental Aspects of Fuel Conversion Technology, II: (December, 1975), Washington DC, Environmental Protection Agency, Environmental Protection Technology Series EPA-600/2-76-149, 1976.

APPENDICES

APPENDICES

Appendix A (Data analysis computer programs) and Appendix B (Data, calculated results, and statistical analysis of data) have been omitted in this report. They are included in the Ph.D. dissertation of Victor H. Agreda*, copies of which may be obtained from University Microfilms, Inc.

---

*Agreda, V.H., "Devolatilization Kinetics and Elemental Release in the Pyrolysis of Pulverized Coal," N.C. State University, 1979.

APPENDIX C

Chemical Analyses

Proximate, ultimate, and trace/minor element analyses were carried out on the coals and chars used and produced in this study. Every effort was made to ensure the accuracy and precision of the analyses and to eliminate any bias in the data due to instrument drift or analyst bias. All samples were analyzed as blind samples, i.e., with a neutral label that did not identify the source of the sample, and in random order. Furthermore, certified standards were run concurrently with the samples. This was done for almost every analyte. If the analysis of the standard did not agree with the certified value, the entire lot of analyses was discarded and new analyses made.

C.1 Proximate Analysis

Moisture in the coal and char samples was determined by establishing the loss in weight of 0.5 g of sample heated to 104-110°C for 1 hour in a moisture oven with bone air circulation. ASTM-D-3173 method was followed.

The ash content was determined by weighing the residue remaining after burning 0.5 g of coal at 950°C in a muffle furnace. The same sample used for moisture analysis was used. ASTM-D-3174 method was followed. Certified standards were run concurrently with the analysis samples.

The volatile matter of the samples was determined by establishing the loss in weight resulting from heating 1.0 g of sample for 6.0 minutes at 550 ± 20°C and 6.0 more minutes at 950 ± 20°C in volatile matter furnaces. ASTM-D-3175 method for sparking coals was used. Certified standards were run concurrently with the analysis samples.

C.2 Ultimate Analysis

The determination of carbon and hydrogen was made by burning 100 mg of sample in a combustion train and fixing the products of combustion in an absorption train after complete oxidation and purification from interfering substances. ASTM-D-3178 method for total carbon and hydrogen was followed. This method gives the total percentages of carbon and hydrogen in the coal as analyzed, and includes the carbon in carbonates and the hydrogen in the moisture and in the water of hydration of silicates. The results for hydrogen were corrected, such that the hydrogen in the moisture would not be included, using the equation: $\%H = \%H - 0.1119x(\%M)$. Benzoic acid samples were used to test the accuracy of the analyses.

Sulfur analyses were carried out with a Fisher Sulfur Analyzer Model 470. The analyzer combusts the sulfur in the samples and detects the sulfur dioxide produced through and amperometric technique. This analyzer is extremely accurate and precise in the analysis of sulfur in coal and coke. However, the analyzer does not detect sulfate sulfur which occurs in small quantities in most coals. Certified coal standards were used to calibrate the analyzer and to check its accuracy periodically.

C.3 Trace/Minor Element Analyses

The majority of the minor/trace element analyses were done by neutron activation. Atomic absorption was used for the analysis of a smaller number of elements. In both cases, NBS certified standards were run concurrently to ensure the accuracy of the analysis.

C.3.1 Neutron Activation Analysis

Neutron activation analysis is an analytical technique dependent on the measurement of the number and energy of γ- and X-rays emitted by the radioactive isotopes produced in the sample matrix by irradiation with thermal neutrons from a nuclear reactor.

All neutron activation analyses reported in this thesis were done by the Activation Analysis Laboratory, Department of Nuclear Engineering, North Carolina State University.

Typical parameters used are: 2 to 4.5 hours irradiation time at $1.5x10^3$ n/cm^2-sec. The decay was monitored for 200 to 1200 seconds with the counting done on an Ortec 24% GeLi and an Ortec 16 mm LEPD coupled to a computerized ND6620 system.

The estimated instrumental error for each element analyzed by this technique is shown in Table C.1. The computer does a convergiance, (1) of pipeting errors (usually <0.2%), (2) weighing errors (usually <0.1%), and (3) counting statistics errors on standards and unknowns (ranging from 0.1 to 100% depending on the element). These error estimates do not include sampling and char inhomogeneity effects.

C.3.2 Atomic Absorption Analysis

These analyses were carried out using a Perkin Elmer 603 Atomic Absorption Spectrophotometer, an HGA-2200 graphite furnace, and a cold vapor mercury analysis system. Ramp heating was used for the drying and charring steps, and normal, temperature controlled, or time controlled heating was used during atomization depending on the volatility of the element. Deuterium background correction was used in all cases except in the analysis of mercury. Electrodeless discharge lamps were used in all cases except in the analysis of Cd, V, Be, and Bi where hollow cathode lamps were used.

F

Table C.1 Percent Error (Instrumental) NAA in Coals

Element	Percent Error
Samarium	± 1%
Uranium	± 6%
Lanthanum	± 1%
Arsenic (<1 ppm)	±5-10%
Arsenic (2-10 ppm)	±2- 5%
Antimony	± 2%
Bromine	± 3%
Sodium	± 2%
Potassium	±10%
Titanium	± 5%
Manganese	± 1%
Copper (<100 ppm)	±25%
Vanadium	± 3%
Aluminum	± 1%
Mercury (<0.10 ppm)	±10%
Cerium	± 5%
Selenium	± 5%
Thorium	± 2%
Chromium	± 5%
Scandium	± 1%

Table C.1 continued

Element	Percent Error
Europium	± 2%
Rubidium	± 5%
Iron	± 2%
Cobalt	± 1%
Zinc (<100 ppm)	±20%
Cesium	± 5%

The waste water samples were digested by evaporative reflux with nitric acid for the analysis of all elements of interest except mercury. Raw waste water samples were analyzed directly for mercury. The solid samples were prepared by two methods: oxygen bomb combustion, and low temperature ashing followed by acid bomb digestion. The liquor obtained from the oxygen bomb combustion was used for the analysis of Hg, Pb, As, Sb, and Cd. A LFE-LTA-504 Low Temperature Plasma Asher was used for the oxidation of the samples intended for the analysis of Cr, B, Be, Ni, P, and optionally Pb and Cd. The low temperature ashes were then digested in teflon lined acid bombs. All acid liquors were then diluted to volume. Typical sample weight to solution volume ratios were 0.5 gram to 100 ml. Waste water samples were typically concentrated from 150 to 50 ml.

Analysis for each element was basically the same. Standard linearity was established for the range the samples fell in, if possible. Generally, if the standards showed curvature, the samples were diluted, or a less sensitive set of parameters was used. All AA and HGA parameters (shown in Table C.2) were optimized to give the best signal to noise ratio. Direct calibration methods were used for the analysis of Hg, Ni, P, Sb, Be, Cr, and V. The method of standard additions was used for the analysis of Pb and As. Nickel complexation was used to allow high temperature charring during the analysis of As. The method described

Table C.2 Summary of Atomic Absorption Analysis Parameters

Element	$\frac{\text{Dry Temp-Time}}{\text{Ramp Time}}$ $\frac{{}^{o}\text{C-Sec}}{\text{Sec}}$	$\frac{\text{Char Temp-Time}}{\text{Char Time}}$ $\frac{{}^{o}\text{C-Sec}}{\text{Sec}}$	Atom. Temp-Time ^{o}C-Sec	Wavelength* nm	Slit nm
Cr	$\frac{125-40}{10}$	$\frac{1100-34}{10}$	2700-8	357.9	(4) 0.7
V	$\frac{125-42}{10}$	$\frac{1700-32}{10}$	2800-8	318.4	(3) 0.2
Be	$\frac{125-42}{10}$	$\frac{1200-30}{10}$	2800-8	234.9	(4) 0.7
Pb	$\frac{125-40}{10}$	$\frac{600-34}{10}$	2300-8	217.0	(4) 0.7
Ni	$\frac{125-41}{10}$	$\frac{1000-30}{10}$	2700-8	232.0	(3) 0.2
As	$\frac{125-30}{10}$	$\frac{1000-30}{10}$	2700-8	253.5	(4) 0.7
Hg		Cold Vapor Analysis		253.5	(4) 0.7

*AA seems to be off by one nanometer

by R.D. Ediger, A.R. Knott, G.E. Peterson and R.D. Beaty ("The Determination of Phosphorus by Atomic Absorbtion Using the Graphite Furnace," Atomic Absorption Newsletter Vol. 17, No. 1, 28 , Jan-Feb, 1978) was followed for the analysis of phosphorus. The correlation coefficients of all the calibration and standard addition lines were greater than 0.94.

The most serious problem encountered in these analyses was interferences from the coal's ash matrix. This problem was particularly acute in the analysis of Pb in MRS coal of 325x400 mesh size. Otherwise, the results of the analyses were satisfactory.

C.3.3 Assessment of Trace Analyses

Comparisons of the behavior of different elements under gasification conditions must be made with caution. Very often the large scatter in the data is not due to sample inhomogeneity but to the small concentration of the element or to the low sensitivity of the analytical technique used. It is well known that the sensitivity and detection limits of NAA and AA vary widely for different elements. A discussion of those variations among the elements studied in this research is beyond the scope of this thesis. The reader is referred to standard texts and manuals in atomic absorption and neutron activation for that purpose.

The analytical techniques must be refined. The same coal or char analyzed several times by NAA and by AA show small but significant differences. However, all analyses made by the same method always appear to be internally consistent. For that reason, elements analyzed by two different methods are reported separately according to the method used. However, the overall accuracy and precision of the chemical analyses used in this research are good and quite comparable with results reported by other researchers (see Sections 2.2.5 and 2.2.6 for references).

U.S. ENVIRONMENTAL PROTECTION AGENCY
Office of Research and Development
Center for Environmental Research Information
Cincinnati, Ohio 45268

OFFICIAL BUSINESS
PENALTY FOR PRIVATE USE. $300
AN EQUAL OPPORTUNITY EMPLOYER

POSTAGE AND FEES PAID
U.S. ENVIRONMENTAL PROTECTION AGENCY
EPA-335

If your address is incorrect, please change on the above label tear off; and return to the above address.
If you do not desire to continue receiving these technical reports, CHECK HERE ☐; tear off label, and return it to the above address,

Publication No. EPA-600/7-79-241

B76/9